ADVANCEMENT IN CANCER STEM CELL BIOLOGY AND PRECISION MEDICINE

EDITED BY: Nikhil Baban Ghate, Eliza Chakraborty and Vicky Yamamoto
PUBLISHED IN: Frontiers in Cell and Developmental Biology and
Frontiers in Genetics

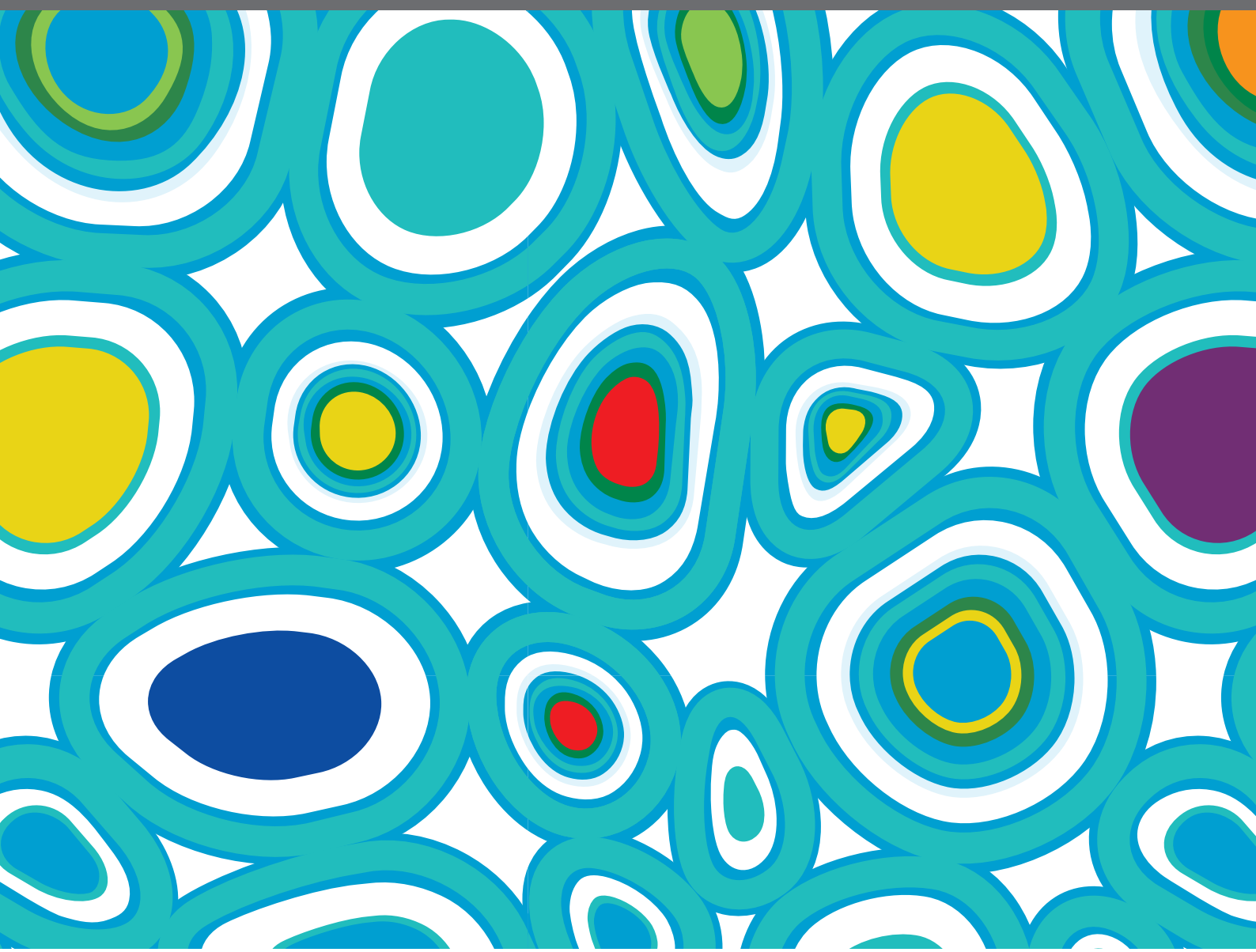

frontiers Research Topics

ISSN 1664-8714
ISBN 978-2-88974-944-7
DOI 10.3389/978-2-88974-944-7

About Frontiers

Frontiers is more than just an open-access publisher of scholarly articles: it is a pioneering approach to the world of academia, radically improving the way scholarly research is managed. The grand vision of Frontiers is a world where all people have an equal opportunity to seek, share and generate knowledge. Frontiers provides immediate and permanent online open access to all its publications, but this alone is not enough to realize our grand goals.

Frontiers Journal Series

The Frontiers Journal Series is a multi-tier and interdisciplinary set of open-access, online journals, promising a paradigm shift from the current review, selection and dissemination processes in academic publishing. All Frontiers journals are driven by researchers for researchers; therefore, they constitute a service to the scholarly community. At the same time, the Frontiers Journal Series operates on a revolutionary invention, the tiered publishing system, initially addressing specific communities of scholars, and gradually climbing up to broader public understanding, thus serving the interests of the lay society, too.

Dedication to Quality

Each Frontiers article is a landmark of the highest quality, thanks to genuinely collaborative interactions between authors and review editors, who include some of the world's best academicians. Research must be certified by peers before entering a stream of knowledge that may eventually reach the public - and shape society; therefore, Frontiers only applies the most rigorous and unbiased reviews.
Frontiers revolutionizes research publishing by freely delivering the most outstanding research, evaluated with no bias from both the academic and social point of view. By applying the most advanced information technologies, Frontiers is catapulting scholarly publishing into a new generation.

What are Frontiers Research Topics?

Frontiers Research Topics are very popular trademarks of the Frontiers Journals Series: they are collections of at least ten articles, all centered on a particular subject. With their unique mix of varied contributions from Original Research to Review Articles, Frontiers Research Topics unify the most influential researchers, the latest key findings and historical advances in a hot research area! Find out more on how to host your own Frontiers Research Topic or contribute to one as an author by contacting the Frontiers Editorial Office: frontiersin.org/about/contact

ADVANCEMENT IN CANCER STEM CELL BIOLOGY AND PRECISION MEDICINE

Topic Editors:
Nikhil Baban Ghate, University of Southern California, United States
Eliza Chakraborty, University of California, Los Angeles, United States
Vicky Yamamoto, University of Southern California, United States

Citation: Ghate, N. B., Chakraborty, E., Yamamoto, V., eds. (2022). Advancement in Cancer Stem Cell Biology and Precision Medicine. Lausanne: Frontiers Media SA. doi: 10.3389/978-2-88974-944-7

Table of Contents

frontiers in Cell and Developmental Biology

EDITORIAL
published: 25 March 2022
doi: 10.3389/fcell.2022.890129

Editorial: Advancement in Cancer Stem Cell Biology and Precision Medicine

Nikhil Baban Ghate[1]*, *Vicky Yamamoto*[2,3,4,5]* and *Eliza Chakraborty*[6]*

[1]Department of Biochemistry and Molecular Medicine, Norris Comprehensive Cancer Center, University of Southern California, Los Angeles, CA, United States, [2]Society for Brain Mapping and Therapeutics (SBMT), Los Angeles, CA, United States, [3]Brain Mapping Foundation (BMF), Los Angeles, CA, United States, [4]The USC Caruso Department of Otolaryngology-Head and Neck Surgery, USC Keck School of Medicine, Los Angeles, CA, United States, [5]USC-Norris Comprehensive Cancer Center, Los Angeles, CA, United States, [6]Department of Biotechnology, DST-FIST Center, Meerut Institute of Engineering and Technology, Meerut, India

Keywords: cancer stem cell, metastasis, head and neck cancer, tumor microenvionment, squamous cell carcinama

Editorial on the Research Topic

Advancement in Cancer Stem Cell Biology and Precision Medicine

Cancer Stem Cells (CSCs) are small subpopulation of cells within tumors with capabilities of self-renewal, differentiation, and tumorigenicity. The clinical relevance of CSCs has been strengthened by emerging evidence suggesting that CSCs are thought to cause treatment resistance, recurrence, and metastasis (Yu et al., 2012). Hence, targeting CSCs for understanding the root-cause of tumorigenesis and development of anticancer therapies can be considered as effective strategy to improve cancer outcomes. CSCs can also be targeted for the development of diagnostic biomarkers to develop personalized oncology approaches. For instance, in glioma patients, precision diagnosis and prognostic prediction can be obtained by checking the expression level of ETV2 gene. ETV2 is found to be involved in the invasion, migration, and epithelial-mesenchymal transition process of glioma. The selection of this gene for diagnosis and prognosis purpose was based on stemness subtype-related risk score model and nomogram. To construct this model RNA-seq data were analysed and 86 mRNA expression-based stemness index-related differentially expressed genes were obtained and combined with weighted gene correlation network analysis (Tan et al.). In another study, Ban et al. calculated the stemness index for samples of multiple myeloma and found that mRNA expression-based stemness index (mRNAsi) was an independent prognostic factor of multiple myeloma. The study also built 34-gene based classifier for predicting prognosis and potential strategies for stemness treatment. However, in case of head and neck squamous cell carcinoma where distinct intratumoral and intertumoral heterogeneity has hindered both the identification of specific biomarkers as well as the establishment of targeted therapies. Hence there is an urgent need for finding strategies for personalized therapeutic options in head and neck cancer patients. In one of the reviews, authors discussed the different approaches in implementing three-dimensional (3D) head and neck cancer *in vitro* and *in vivo* tumor models like spheroid, 3D co-culture, bioprinting, CSC-enriched, and patient-derived explant models for the development of stable biomarkers and for therapeutic efficacy testing in clinical studies (Affolter et al.). In these efforts, to establish a new *in vitro* model having potential value on personalized cancer therapies, Dong et al. propose a cell-culture based technique of conditional reprogramming (CR) of laryngeal and hypopharyngeal squamous cell carcinoma. In this model, the patient-derived CR cells could be transformed to xenograft and organoid and they show similar drug responses compared to clinical studies. In another interesting study, authors have found the presence of hematopoietic stem cell (HSC) transcriptome in human fetal kidney cortex for the first time. Previously, this was only

OPEN ACCESS

Edited and reviewed by:
Valerie Kouskoff,
The University of Manchester, United Kingdom

***Correspondence:**
Nikhil Baban Ghate
nikhs15188@gmail.com
Vicky Yamamoto
vyamamot@med.usc.edu
Eliza Chakraborty
eliza.chakraborty@gmail.com

Specialty section:
This article was submitted to Stem Cell Research, a section of the journal Frontiers in Cell and Developmental Biology

Received: *05 March 2022*
Accepted: *11 March 2022*
Published: *25 March 2022*

Citation:
Ghate NB, Yamamoto V and Chakraborty E (2022) Editorial: Advancement in Cancer Stem Cell Biology and Precision Medicine. Front. Cell Dev. Biol. 10:890129. doi: 10.3389/fcell.2022.890129

observed in zebrafish kidneys. The authors have identified the presence of cells expressing HSC specific marker RUNX1 because it plays a major role in HSC generation (Hwang et al.). Non-coding RNAs (ncRNAs) were initially dubbed as "junk RNAs" but increasing evidence indicates that ncRNAs, such as microRNAs (miRNAs) and long non-coding RNAs (lncRNAs) regulate cancer cell stemness and help maintain CSC populations. In another detailed review on osteosarcoma, authors discussed the role of miR-26a, miR-29b, miR-34a, miR-133a, miR-143, miR-335, miR-382, miR-499a, miR-1247, and let-7d miRNAs in targeting CSCs. They also highlighted the functions of lncRNAs in regulating CSCs in osteosarcoma, such as B4GALT1-AS1, DANCR, DLX6-AS1, FER1L4, HIF2PUT, LINK-A, MALAT1, SOX2-OT, and THOR. The authors believed that targeting these ncRNAs in osteosarcoma might be an effective and novel strategy to eradicate CSCs for osteosarcoma therapy (Liu et al.). Head and neck cancer is one of the cancers in which its 5-years survival has not improved much in the past several decades. Heft-Neal et al. offered a comprehensive review of how the tumor-microenvironment (TME) plays important role in maintaining cancer stem cell niche as well as in treatment resistance. Unlike most reviews on the similar subject, the review also focused on the TME's involvement in tumor heterogeneity in head and neck cancer, which is thought to be the major cause of treatment resistance. Understanding the mechanisms of how heterogeneity arises could lead to effective personalized cancer therapy.

The review by Man et al. highlighted the importance of hematopoietic stem cell (HSC) niche, which is the microenvironment for the maintenance of stem cells, namely, the cellular components and cytokines in the bone marrow (BM) environment. Understanding the BM niche's role in maintaining normal HSCs is essential in understanding how blood cancer develops and in developing effective treatments. This review also provided the roles of BM niche in successful HSC transplantation, which is a life-saving procedure for many hematologic diseases, including leukemia as well as potentially effective therapeutic targets for leukemia.

Finally, Lv et al. reviewed mechanisms of liver cancer stem cell (LCSC) maintenance and survival from over 150 + articles. This comprehensive review covers from important signaling pathways, niche composition, the origin of LCSC to new developments in therapeutics targeting LCSCs. Liver cancer, notably hepatocellular carcinoma, is the leading cause of cancer-related deaths worldwide without effective treatments. Many of the important signaling pathways described in the article, including Wnt, STAT3, TGF-b, Notch, Hedgehog, and BMI1 are known to play important roles during embryonic development and normal physiology. The review underscored the similarity between the normal and cancer stem cell and the complexity of CSC biologic property that we still have much to learn.

While some progress has been made in the treatment for leukemia and solid tumors, such as breast cancer, we still have unmet challenges in improving overall survival and outcomes for common cancers, especially when diagnosed late, such as lung, colon, liver, brain, and head and neck cancers. These articles highlight the emerging evidence that stem cell-like or cancer stem cells may play important roles in cancer development, progression, metastasis, and treatment resistance. The next challenge for scientists investigating cancer stem cells is to delineate the differences between normal stem cells and cancer stem cells, which may enable scientists and clinicians to develop more effective cancer diagnostics and therapeutics.

AUTHOR CONTRIBUTIONS

NG, VY and EC wrote the manuscript. All authors read and approved the final manuscript.

REFERENCE

Yu, Z., Pestell, T. G., Lisanti, M. P., and Pestell, R. G. (2012). Cancer Stem Cells. *Int. J. Biochem. Cell Biol.* 44 (12), 2144–2151. doi:10.1016/j.biocel.2012.08.022

Conflict of Interest: The authors declare that the research was conducted in the absence of any commercial or financial relationships that could be construed as a potential conflict of interest.

frontiers in Cell and Developmental Biology

REVIEW
published: 22 January 2021
doi: 10.3389/fcell.2021.621214

Hematopoietic Stem Cell Niche During Homeostasis, Malignancy, and Bone Marrow Transplantation

*Yan Man[1,2], Xiangmei Yao[1,2], Tonghua Yang[1,2] and Yajie Wang[1,2]**

[1] Department of Hematology, National Key Clinical Specialty of Hematology, Yunnan Blood Disease Clinical Medical Center, Yunnan Blood Disease Hospital, The First People's Hospital of Yunnan Province, Kunming, China, [2] Kunming University of Science and Technology, Kunming, China

Self-renewal and multidirectional differentiation of hematopoietic stem cells (HSCs) are strictly regulated by numerous cellular components and cytokines in the bone marrow (BM) microenvironment. Several cell types that regulate HSC niche have been identified, including both non-hematopoietic cells and HSC-derived cells. Specific changes in the niche composition can result in hematological malignancies. Furthermore, processes such as homing, proliferation, and differentiation of HSCs are strongly controlled by the BM niche and have been reported to be related to the success of hematopoietic stem cell transplantation (HSCT). Single-cell sequencing and *in vivo* imaging are powerful techniques to study BM microenvironment in hematological malignancies and after HSCT. In this review, we discuss how different components of the BM niche, particularly non-hematopoietic and hematopoietic cells, regulate normal hematopoiesis, and changes in the BM niche in leukemia and after HSCT. We believe that this comprehensive review will provide clues for further research on improving HSCT efficiency and exploring potential therapeutic targets for leukemia.

Keywords: hematopoietic stem cells, hematopoietic stem cell niche, niche cells, hematologic malignancy, hematopoietic stem cell transplantation

OPEN ACCESS

Edited by:
Vicky Yamamoto, University of Southern California, United States

Reviewed by:
Jody Jonathan Haigh, University of Manitoba, Canada
Takahiko Hara, Tokyo Metropolitan Institute of Medical Science, Japan

***Correspondence:**
Yajie Wang
kbb165wyj@sina.com

Specialty section:
This article was submitted to Stem Cell Research, a section of the journal Frontiers in Cell and Developmental Biology

Received: *25 October 2020*
Accepted: *04 January 2021*
Published: *22 January 2021*

Citation:
Man Y, Yao X, Yang T and Wang Y (2021) Hematopoietic Stem Cell Niche During Homeostasis, Malignancy, and Bone Marrow Transplantation. Front. Cell Dev. Biol. 9:621214. doi: 10.3389/fcell.2021.621214

INTRODUCTION

The concept of hematopoietic stem cell (HSC) niche was first proposed by Schofield (1978), who proposed that a physical niche of stem cells exists in the bone marrow (BM). The niche consists of a variety of cells that make the microenvironment for the maintenance of stem cells. Based on his theory, advances in imaging techniques, single-cell sequencing, and molecular biology have resulted in a better understanding of HSC heterogeneity (Tikhonova et al., 2019; Christodoulou et al., 2020). As an important exogenous regulation, the BM microenvironment regulates the functional characteristics of HSCs, such as self-renewal (S), maturation (M), apoptosis (A), resting (R), and trafficking (T), together known as "SMART" properties (Cheng, 2008). The blood vessels (Chanavaz, 1995) and nerves (Maryanovich et al., 2018a) entering and exiting the BM cavity form a HSC regulatory network with non-hematopoietic cells and HSC-derived cells via mutual contact or signal transduction (**Figure 1**). Therefore, the loss of specific niche factors may have harmful effects on other niches.

Leukemic stem cells (LSCs) are responsible for drug resistance and relapse of leukemia (Felipe Rico et al., 2013). Leukemia cells can gradually modify the normal hematopoietic

microenvironment into a leukemic microenvironment, thus contributing to disease progression (Duarte et al., 2018; Mendez-Ferrer et al., 2020). In a leukemic niche, the proliferation of normal hematopoietic stem and progenitor cells (HSPCs) is inhibited and most HSCs enter into the quiescent stage, whereas hematopoietic progenitor cells (HPCs) overproliferate and are gradually exhausted (Hu et al., 2009). For instance, Cheng et al. (2015) demonstrated that Egr3, a transcription factor, can maintain HSCs in the G0 phase, thus blocking HSC differentiation. Surprisingly, the inhibitory effect on normal hematopoiesis in leukemia is reversible (Cheng et al., 2015), implying that niche factors govern the malignant characteristics.

Hematopoietic stem cell transplantation (HSCT) is one of the most effective methods for treating hematologic malignancy. However, the occurrence of several complications, such as poor graft function (PGF), graft-vs.-host disease (GVHD), and relapse are roadblocks in improving HSCT efficiency. Moreover, total body irradiation (TBI) and chemotherapy before HSCT can damage recipient's BM microenvironment, subsequently exerting a negative "bystander effect" on transplanted donor HSCs (Shen et al., 2012). Therefore, repairing the BM hematopoietic microenvironment would benefit leukemia treatment and prevent related complications. A recent study based on single-cell sequencing reported that transplanted HSCs decreased gradually within 1 week in myeloablated recipients, and the potential to differentiate into myeloid and erythroid lineages enhanced in some of the remaining HSCs (Dong et al., 2020). Erythropoietin (EPO) and granulocyte colony-stimulating factor (G-CSF) are key hematopoietic factors involved in erythroid and myeloid differentiation, respectively. The data showed that the concentration of EPO and G-CSF increased significantly in the microenvironment after irradiation, which could lead to the rapid differentiation of cells into these lineages (Dong et al., 2020). An in-depth study of changes in the BM microenvironment before and after HSCT is required to explore potential therapeutic targets for leukemia.

REGULATION BY NON-HEMATOPOIETIC CELLS

Osteolineage Cells

Osteolineage cells are the earliest discovered niche cells that regulate HSPC (Taichman et al., 1996; Nilsson et al., 2001). Morrison (Ding and Morrison, 2013) reported that the deletion of CXCL12 from osteoblasts significantly reduced the number of early lymphoid progenitor cells, with no significant effect on HSCs and myeloid progenitor cells. The function of N-cadherin, which regulates HSCs by mediating the adhesion of homologous molecules between osteoblasts and HSCs, is also controversial (Hosokawa et al., 2010; Bromberg et al., 2012). Osteoblasts express a variety of hematopoietic regulatory molecules, including thrombopoietin (TPO) (Qian et al., 2007), angiopoietin 1 (ANGPT1) (Arai et al., 2004) and osteopontin, which negatively regulate stem cell pool size (Nilsson et al., 2005). Altogether, these studies suggest that osteoblasts do not directly regulate HSCs, at least not via CXCL12 or stem cell factor (SCF). However, osteolineage cells are speculated to support the maintenance of early lymphoid progenitors.

A previous study reported that leukemia cells initially homed and localized on the surface of osteoblasts in the epiphysial region, the most active site for the proliferation of leukemia cells (Ninomiya et al., 2007). Scadden and group (Raaijmakers et al., 2010) reported that osteoblastic progenitor cells could not differentiate into osteoblasts when Dicer1 was deleted in the mouse. Moreover, the integrity of the hematopoietic function was destroyed, eventually leading to myelodysplastic syndrome (MDS) and acute myeloid leukemia (AML). Activating mutations in β-catenin in osteoblasts can stimulate the expression of Notch ligand Jagged-1, subsequently activating Notch signaling in HSPCs and changing the differentiation potential of myeloid and lymphoid progenitor cells to induce AML (Kode et al., 2014). Ptpn11 is a positive regulator of the RAS signaling pathway in osteogenic progenitor cells. Activating mutation in Ptpn11 has been reported to overproduce chemokine CCL3 and recruit monocytes to the site of HSCs. Monocytes can produce inflammatory molecules to stimulate HSC differentiation and proliferation, causing juvenile chronic myelomonocytic leukemia (JMML) (Dong et al., 2016). The above researches proved that elimination or mutation of osteoblasts is the predisposing factor for hematological malignancies (**Table 1**).

Osteoclasts play a crucial role in establishing the HSC niche. The HSC clonal expansion requires a physical area having a percentage of osteoblasts to osteoclasts of 25–75% (Christodoulou et al., 2020). Therefore, using traditional methods to characterize the HSC niche as an endosteal niche or vascular niche may be insufficient. One mechanism of multiple myeloma (MM) is the imbalance between bone formation and resorption. In MM, osteoclasts can directly inhibit proliferative $CD4^+$ and $CD8^+$ T cells by upregulating immune checkpoint molecules such as programmed death ligand 1 (PD-L1), CD38, and Galectin-9, thus establishing the immunosuppressive microenvironment to protect myeloma cells (An et al., 2016). MM relapse is associated with dormant myeloma cells. Evidence shows that the dormant state is reversible, and dormant myeloma cells can be reactivated by osteoclasts remodeling the endosteal niche (Lawson et al., 2015). Thus, reactivating dormant myeloma cells by promoting bone resorption and combining it with targeted therapies could help achieve MM long-term remission or even cure.

Perivascular Cells

Perivascular cells, principally pericytes, have been identified in several human organs, they are tissue-specific precursors of MSCs (Yianni and Sharpe, 2019). The combined expression of signaling lymphocytic activation molecule family (Kiel et al., 2005), and new genetic markers, which including CTNAL1 (Acar et al., 2015) and HOXB5 (Chen et al., 2016), suggest that HSCs primarily exist in the perisinusoidal niches (Kiel et al., 2005; Acar et al., 2015; Chen et al., 2016). Interestingly, small arteries surrounded by rare $NG2^+$ pericytes are associated with dormant HSCs, whereas sinusoid-associated leptin receptor$^+$ ($LepR^+$) cells are associated with less quiescent HSCs (Kunisaki et al., 2013). CXCL12-abundant reticular (CAR)

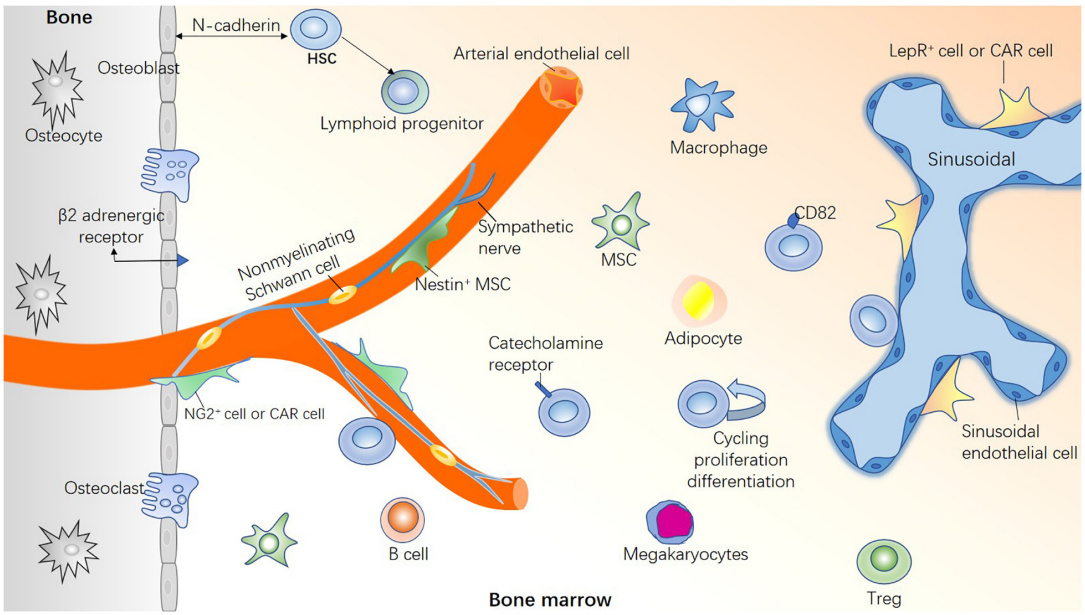

FIGURE 1 | Healthy bone marrow microenvironment. If HSCs are compared to "seed," the BM microenvironment is the "soil" for HSC survival. A healthy BM microenvironment is crucial for regulating the functional characteristics of HSCs, such as proliferation and differentiation, homing and colonization, migration and apoptosis, and maintaining steady hematopoiesis. HSCs are highly heterogeneous, with different types of HSCs located in different niches. Bone marrow microenvironment is composed of a variety of hematopoietic cells and non-hematopoietic cells, in addition, blood vessels and nerve fibers play a pivotal role.

cell subpopulations are differentially localized on the surface of sinusoids and arterioles and secrete specific cytokines to establish a perivascular niche (Baccin et al., 2020). CXCR4 is a specific receptor of stromal cell-derived factor 1 (SDF-1, also known as CXCL12), which functions in HSC homing (Lai et al., 2014). After HSCT, blocking the interaction of CXCR4/SDF-1 with the CXCR4 antagonist AMD3100 can recover hematopoietic function by inducing HSC proliferation (Green et al., 2016).

Mesenchymal stem cells (MSCs) are the precursor cells of BM stromal cells and have been widely used in treating immune-related diseases. In leukemia, MSC interact with leukemia cell. AML cells induced osteogenic differentiation in MSCs. Schepers et al. (2013) demonstrated that leukemic myeloid cells stimulated MSCs to overproduce functionally altered osteoblasts to form BM fibrosis in myeloproliferative neoplasia (MPN) and remodel the endosteal BM niche into a tumor microenvironment. Subsequent studies revealed that following co-culturing with leukemic cell lines, MSCs overexpress early stage osteoblast markers, including OSX and RUNX2 (Battula et al., 2017). Furthermore, mechanistic studies have identified that AML cells upregulated the expression of connective tissue growth factor (CTGF) in BM-MSCs, and activated Smad1/5 signaling, inducing BM-MSCs to differentiate into committed osteoprogenitors, but not mature osteoblasts (Hanoun et al., 2014; Battula et al., 2017). There is report has shown increased adipogenic potential of MSC in AML, decreasing expression of SOX9 and EGR2 increased adipogenic potential of AML-MSCs and enhanced their ability to support AML progenitor cells (Azadniv et al., 2020). Leukemia microenvironment reduces the proliferation and differentiation potential of MSCs. The development of NRAS mutant leukemia is accompanied by gradual functional degeneration of BM MSCs (Xia et al., 2020). *In situ* infusion of healthy donor-derived BM MSCs into the BM cavity can reprogram host macrophages to Arg1-positive phenotype with rapid tissue repair, thereby remodeling the leukemia BM microenvironment and inhibiting leukemia development (Xia et al., 2020). Moreover, impaired MSCs inhibit the generation of HPCs. As a negative regulator of osteoclast function, osteoprotegerin (OPG) can support the function of T-ALL MSCs and promote the proliferation of HPCs via the p38/ERK pathway (Lim et al., 2016). Exosomes are known to mediate intercellular communication. In MM, BM-MSC-derived exosomes with high levels of oncogenic proteins and cytokines are transferred to MM cells to promote MM tumor growth (Roccaro et al., 2013). These studies highlight the contribution of BM-MSCs to disease progression.

The conditioning regimen is a key step in HSC implantation to inactivate the recipient's immune system before transplantation. Moreover, it destroys the BM microenvironment. Numerous studies have validated the function of MSCs in enhancing the efficiency of HSCT (Ball et al., 2007; Peng et al., 2015). According to studies, chemotherapy, used to induce remission, will not inhibit the function of MSCs; however, conditioning regimen can seriously compromise the proliferation characteristics of MSCs (Shipounova et al., 2017). For example, Ding et al. (2014) reported that the number of BM MSCs decreased sharply in the early stage after HSCT, the surviving MSCs supported hematopoiesis *in vitro* and inhibited lymphocyte proliferation. Surprisingly, donor-derived MSCs are not detected in the MSCs after HSCT (Ding et al., 2014), indicating that the

TABLE 1 | Contribution of hematopoietic and non-hematopoietic cells to hematopoietic homeostasis, hematologic malignancies, and after HSCT.

Cell population	Hematopoietic homeostasis		Hematologic malignancies		After HSCT
	Quiescence	Mobilization	Disease	Contribution or pathway	
Osteoblasts	Maintenance of early lymphoid progenitors (Ding and Morrison, 2013)		MDS AML	Deletion of Dicer1 (Raaijmakers et al., 2010)	–
			AML	Mutation of β-catenin (Kode et al., 2014)	
	Hematopoietic regulation [TPO (Qian et al., 2007), ANGPT1 (Arai et al., 2004) and osteopontin (Nilsson et al., 2005)]		JMML	Mutation of Ptpn11 (Dong et al., 2016)	
			MPN	Functionally altered osteoblast (Schepers et al., 2013)	
Osteoclasts	Induction of osteoblasts development		MM	Protection of myeloma cells (PD-L1, CD38) (An et al., 2016)	–
Perivascular cells	NG2$^+$ pericytes (Kunisaki et al., 2013)	Lepr$^+$ pericytes (Kunisaki et al., 2013)	Leukemia	Inhibition of leukemia (reprogram macrophages) (Xia et al., 2020)	Recipient MSCs decreased and reconstruction of BM niche (Ding et al., 2014)
			MM	Promotion of MM growth (MSC-derived exosomes) (Roccaro et al., 2013)	
Endothelial cells	Regulation of HSPCs (Winkler et al., 2012) and Maintenance of hematopoietic (Poulos et al., 2013)		–	LSC engraftment (E-selectin and CXCL12) (Krause et al., 2014)	EPCs decreased and dysfunction (Kong et al., 2013; Cao et al., 2018)
			AML	Chemoresistance to cytarabine (IL-8)	Reconstruction of hematopoietic function (Chute et al., 2007; Hooper et al., 2009; Himburg et al., 2016)
			AML	Inhibition of megakaryocytosis (IL-4) (Gao et al., 2019)	Reduction of GVHD (infuse EPCs) (Zeng et al., 2012)
Adipocytes	Negative regulators of HSC (Yokota et al., 2000; Naveiras et al., 2009)		AML	Energy for leukemia cells (Shafat et al., 2017)	–
			AML	Remodeling the BM adipocytes (GDF15) (Yang et al., 2019)	
	Positive regulators of HSC (Zhou et al., 2017)		AML	Deficiency of erythropoiesis (Boyd et al., 2017)	
			–	Drug resistance of leukemia cells (Behan et al., 2009; Sheng et al., 2016, 2017)	
Regulatory T cells	Maintenance of B cell lymphopoiesis (IL-7) (Pierini et al., 2017)		–	Immune privilege for malignant cells (Wang et al., 2020)	Immune privilege for Allo-HSC (Hirata et al., 2018)
					Prevention of GVHD (Mancusi et al., 2019; Riegel et al., 2020)
Macrophages	CD234/DARC (Hur et al., 2016)	CD169$^+$ Macrophages (Chow et al., 2013)	AML	Polarization of macrophages to M2 phenotype (arginine enzyme) (Mussai et al., 2013)	–
	HSPC homing (ITGA4-dependent) (Li et al., 2018)		ALL	Polarization of macrophages to M2 phenotype (BMP4) (Valencia et al., 2019)	
			CLL	Polarization of macrophages to M2-phenotype (Galletti et al., 2016)	
Megakaryocytes	Secretion TGFβ and TPO		AML	Inhibition of MEP (IL-4) (Gao et al., 2019)	HSC engraftment (PDGF-BB) (Olson et al., 2013)
				Inhibition of HSPCs proliferation (Egr3) (Gong et al., 2018)	HSC expansion (Zhao et al., 2014)

MDS, myelodysplastic syndromes; AML, acute myelocytic leukemia; CML, chronic myeloid leukemia; ALL, acute lymphoblastic leukemia; MPN, myeloproliferative neoplasm; JMML, juvenile chronic myelomonocytic leukemia; MM, multiple myeloma; LSC, leukemia stem cells; CSF1, colony-stimulating factor-1; SCF, stem cell factor; TGF-β,transforming growth factor-β; MSCs, mesenchymal stem cells; THPO, thrombopoietin; ANGPT1, angiopoietin1; IL-8, interleukin-8; Gfi1, growth factor-independent 1; GDF15, growth differentiation factor 15; BMP4, bone morphogenetic protein 4; –, not mentioned in the article or unreported.

recipient MSCs are mainly involved in reconstructing the BM microenvironment after HSCT.

Endothelial Cells

BM endothelial cells (ECs) include arteriolar endothelial cells (AECs) and sinusoid endothelial cells (SECs). AECs secrete nearly all detectable endothelial-derived SCF in the BM (Xu et al., 2018), whereas SECs play indispensable roles in regulating HSC by secreting CXCL12 and a little SCF (Ding et al., 2012), and exclusively expressing adhesion molecule E-selectin (Winkler et al., 2012). Endothelial-specific angiocrine factor Jagged-1 can sustain hematopoietic homeostasis in a Notch-dependent manner by balancing the rate of self-renewal and differentiation of HSPCs (Poulos et al., 2013). In addition, endothelial cell-specific transcription factor Klf6 can directly regulate the expression of chemokine CCL25b and HSC expansion through CCL25b/CCR7 chemotactic signals (Xue et al., 2017).

ECs mediate leukemic stem cell (LSC) homing and engraftment. Sipkins et al. (2005) reported that leukemic cells preferably localize in vascular regions rich in E-selectin and CXCL12 where HSPCs home to. E-selectins and their ligands are required for LSC engraftment in the BM niche (Krause et al., 2014). Activated ECs are considered as potential mediators of leukemia relapse. Specifically, AML-induced activation of ECs stimulates interleukin-8 (IL-8) secretion, leading to a significant proliferation of non-adherent AML cells and chemoresistance to cytarabine (Vijay et al., 2019). Moreover, BM endothelial cells overproduce IL-4 to inhibit megakaryocytosis in AML. A combination of induction chemotherapy and inhibition of IL-4 not only recovers the platelet count but also prolongs the remission time in AML mice (Gao et al., 2019). These studies elucidate the link between endothelial cells and leukemia in the BM (**Figure 2**), thereby offering a potential therapeutic target in leukemia.

It was reported more than 25 years ago that damaged biomarkers of ECs, such as soluble thrombomodulin and von Willebrand factor (vWF), are increased significantly both before and after transplantation (Richard et al., 1996). Intercellular adhesion molecule-1, which represents activated ECs, was remarkably increased 3 weeks after transplantation (Richard et al., 1996). However, these markers have no diagnostic or prognostic value for complications related to transplants (Palomo et al., 2010). Subsequent studies have proved that circulating endothelial cells and endothelial progenitor cells (EPCs) can serve as endothelial damage markers during HSCT, with the potential to predict and diagnose several complications after HSCT (Almici et al., 2017; Ruggeri et al., 2018). A combined infusion of EPCs with HSCT can effectively repair BM micro-vessels, promote hematopoietic and immune reconstruction, reduce the occurrence of GVHD and other related complications (Zeng et al., 2012). After allogeneic hematopoietic stem cell transplantation (also HSCT), the number of EPCs decreased with dysfunction in patients with PGF and aGVHD, manifested as decreased migration and angiogenesis, and increased reactive oxygen levels and apoptosis. The damage degree of EPCs is positively correlated with the level of reactive oxygen species and apoptosis (Kong et al., 2013; Cao et al., 2018).

Hematopoietic recovery after lethal irradiation requires a complete vasculature. In traditional concepts, new blood vessels in the embryo will only be produced when the ECs divide. Plein et al. (2018) found that erythro-myeloid progenitors (EMPs) can differentiate into ECs, these ECs are recruited into pre-existing vasculature to repair damaged blood vessels and generate new blood vessels. This discovery will promote further research on using stem cells to repair damaged blood vessels after HSCT. The function of SECs is inhibited after HSCT, because they are highly sensitive to radiotherapy and chemotherapy. The regeneration of SECs, mediated by the VEGFR2 signaling pathway, is crucial for hematopoietic function reconstruction (Chute et al., 2007; Hooper et al., 2009; Himburg et al., 2016). In addition, AEC-derived SCF can promote HSC recovery after BM cell clearance (Xu et al., 2018). The Notch signaling pathway is involved in irradiation-induced BM injury, such that conditional disruption of Notch signaling increases the sensitivity to irradiation. Human Delta-like 1 (DLL1) fused with an RGD motif acts as an endothelium-targeted soluble Notch DLL1 ligand. As a new Notch activator, it can rescue severe myelosuppression caused by radiation injury and chemical drugs, and greatly promote hematopoiesis reconstruction after transplantation (Tian et al., 2016).

Adipocytes

Previous studies have reported adipocytes as negative regulators of HSCs in the BM (Yokota et al., 2000; Naveiras et al., 2009). After chemotherapy or transplantation, the administration of peroxisome proliferator-activated receptor γ (PPAR-γ) antagonist, which inhibits adipogenesis, can enhance hematopoietic recovery (Naveiras et al., 2009; Zhu et al., 2013). However, recent studies have revealed that BM adipocytes (BMAs) positively regulate HSC regeneration under stress conditions. After radiotherapy or chemotherapy, physiological HSC nests are temporarily destroyed, MSCs initiate adipogenic differentiation urgently, and newly generated adipocytes form a temporary HSC niche to maintain the body's basic hematopoietic function and promote HSC regeneration by secreting SCF. The "fat niche" is gradually replaced by physiological stem cell nests after BM reconstruction (Zhou et al., 2017). Recently, a study based on single-cell sequencing supported the above finding (Tikhonova et al., 2019). It was found that after 5-fluorouracil treatment, the expression of fat-related genes was upregulated in LepR + cell populations, whereas ontogenesis-related genes was downregulated (Tikhonova et al., 2019). Therefore, BMAs may have a dual role in HSC regulation.

BMAs release a series of inflammatory adipokines (leptin, TNF-α, and IL-6), as well as an anti-inflammatory adipokine (adiponectin) to regulate the proliferation and migration of leukemic cells (Beaulieu et al., 2011; Johrer et al., 2015; Ketterl et al., 2018). In contrast, leukemic blasts can program BMAs to support malignant cells. Leukemia cells can activate hormone-sensitive lipase to induce lipolysis. As an oxidative substrate, fatty acid-binding protein-4 carries fatty acids into the AML mitochondria and provides energy to leukemia cells (Shafat et al., 2017). It has been reported that AML cells differentiate the residual BMAs into small adipocytes by secreting growth

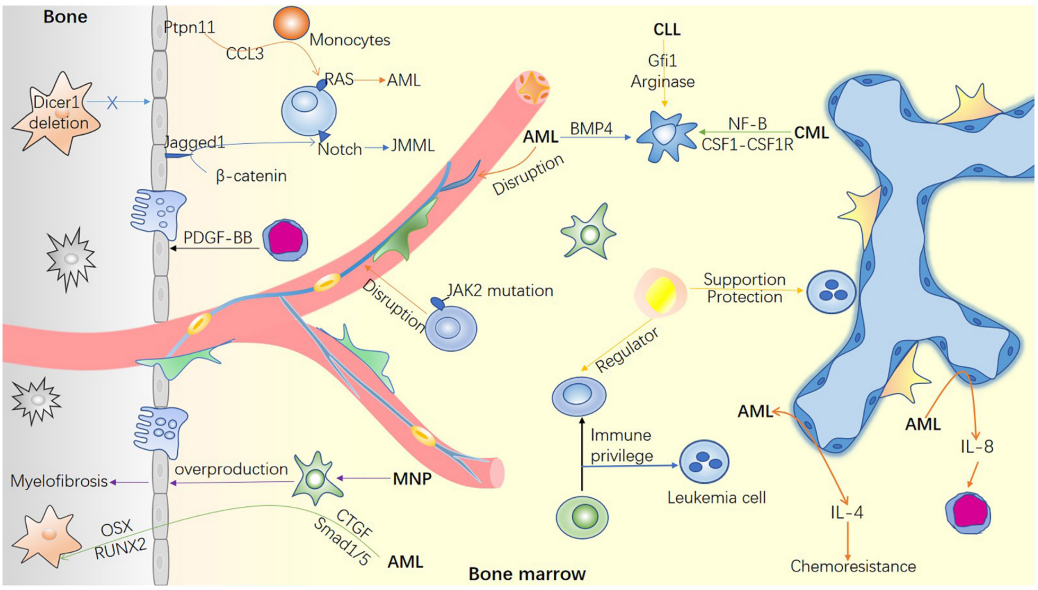

FIGURE 2 | Bone marrow microenvironment in hematological malignancies. The mutation of microenvironment cells can induce hematological malignancies. Simultaneously, malignant cells invade and remold the blood microenvironment to facilitate their survival and inhibit the function of normal hematopoietic cells. The remodeled microenvironment can not only guide the homing of LSC, but also promote the immune escape of tumor cells and resistance to chemotherapy through various mechanisms.

differentiation factor 15 (GDF15). Moreover, transient receptor potential vanilloid 4 mediates GDF15-induced remodeling of BM adipocytes (Yang et al., 2019). A recent study revealed that in patients with AML during complete remission, chemotherapy drugs indirectly blocked MSC adipogenesis, enhanced the efficacy of consolidated chemotherapy, and prevented relapse by promoting GDF15 secretion from BM mononuclear cells (Liu et al., 2018). In addition, AML cells inhibited BMAs, resulting in erythropoiesis deficiency; this effect was reversed by the administration of PPAR-γ agonists *in vivo* (Boyd et al., 2017). In the end, BMAs can protect leukemic cells from drug- or radiation-induced oxidative stress (Sheng et al., 2016), prevent chemotherapy-induced apoptosis, increase the expression of pro-survival signals (Behan et al., 2009), absorb and metabolize chemotherapeutic drugs (Sheng et al., 2017), thus reducing the cytotoxicity of chemotherapeutic drugs and leading to cellular drug resistance of leukemia (Behan et al., 2009; Sheng et al., 2016, 2017; **Figure 2**). Targeting lipolysis may be an effective strategy for leukemia treatment and preventing drug resistance.

Neural Regulation

Nerve fibers regulate HSCs through various signal transduction pathways (**Figure 1**). Early studies found that HSCs dynamically express catecholamine receptors (Spiegel et al., 2007). Sympathetic nerves transmit the adrenergic circadian rhythm signal, mediate the periodic release of HSPCs from BM to blood, by regulating the ability of BM stromal cells to secrete CXCL12 (Mendez-Ferrer et al., 2008). Osteoblasts express β2-adrenergic receptors and sympathetic nerves can inhibit osteoblast activity, it is necessary for G-CSF-induced HSPC mobilization (Asada et al., 2013). The loss of sympathetic nerves or adrenoreceptor β3 signaling is a potent driver of aging of the HSC niche, associated with the development of blood disorders (Maryanovich et al., 2018b). Evidence shows that neuropathy is associated with the progression of myeloproliferative neoplasms (MPNs). Nestin$^+$ MSCs are in close contact with adrenergic nerves (Mendez-Ferrer et al., 2010), and the removal of sympathetic nerve fibers leads to reduced Nestin$^+$ MSC cells, which in turn promotes HSC expansion and MPN development (Baryawno and Scadden, 2014). In addition, β3 adrenergic agonists restored the sympathetic regulation of Nestin$^+$ MSC cells and prevented the progression of MPN. Remarkably, AML induces the sympathetic neuropathy at infiltrated sites, reduces the density of sympathetic nervous system network, expands Nes-GFP$^+$ cells committed to differentiate to the osteoblast lineage, eventually promoting leukemia progression (Hanoun et al., 2014).

In addition to the catecholamine signals emitted by neurons, non-myelinated Schwann cells, which ensheathed the sympathetic nerves, can activate TGF-β produced by several cells in the microenvironment to maintain HSC quiescence (Yamazaki et al., 2011). Arranz et al. (2014) confirmed that HSCs with JAK2 mutation produced IL-1β to trigger BM nerve injury and Schwann cell death, whereas the administration of neuroprotective drugs or sympathomimetic drugs prevented the expansion of mutant HSCs. Furthermore, BM is innervated by parasympathetic nerves. Few studies have proved the role and mechanism of parasympathetic signals in regulating HSCs. Muscarinic receptor type-1 (Chrm1) is one of the acetylcholine receptors in the hypothalamus. Chrm1 signaling is from the central nervous system, initiated by glucocorticoid hormonal

in the hypothalamus–pituitary–adrenal axis, can promote G-CSF-induced mobilization of HSCs (Pierce et al., 2017).

REGULATION BY HSC DESCENDANTS

Regulatory T Cells

Regulatory T cells (Tregs) play a vital role in building immune tolerance and preventing GVHD after allo HSCT. FoxP3$^+$ Treg cells can maintain B cell lymphopoiesis by controlling the production of physiological IL-7 (Pierini et al., 2017). Niche-associated Tregs prevented malignant cells from immune attacks. Therefore, activated T cells were accumulated in the leukemic hematopoietic microenvironment, contributing to the progression of the disease (Wang et al., 2020). Tregs co-localize on the endosteal surface with allo HSCs after transplantation (Fujisaki et al., 2011), they can establish an immune-privileged "sanctuary" for donor-derived HSCs. Allo HSCs are rapidly lost after the depletion of FoxP3$^+$ Treg cells (Fujisaki et al., 2011). Further, BM CD150^{high} Treg cells, located in the HSC niche, prevent allo HSC rejection, and facilitate allo HSC engraftment through adenosine (Hirata et al., 2018). Tregs are more susceptible to both intrinsic and extrinsic apoptotic pathways than the conventional T cells (Matsuoka et al., 2010; Weiss et al., 2011). Mitochondrial apoptotic priming of Tregs increased significantly in patients with mild and moderate chronic GVHD after HSCT (Murase et al., 2014). However, increased "priming" of all T-cell subsets reversed in patients with severe GVHD with typical lymphopenia, who received more intensive immunosuppressive therapy (Murase et al., 2014). Based on the characteristics of Tregs, adoptive Tregs transfer has prevented and treated GVHD (Mancusi et al., 2019; Riegel et al., 2020).

Two major subsets of T lymphocytes express CD4 and CD8 molecules, respectively, known as T-helper cell (Th) and T killer cell (Tc). Tc1 cells can produced perforin and granzyme, induced abnormal MK maturation, and destroyed PLT. Th1 and Th17 cells can secreted related cytokines to induce cytotoxic T cells and macrophage activation. The imbalance between T-helper cell 1 (Th1)/Th2, T killer cell 1 (Tc1)/Tc2, and Th17/Treg changes the level of cytokines and is associated with several complications. For example, Kong (Wang et al., 2016) found that as compared with good graft function (GGF) and healthy donors, the percentage of Th1 and Tc1 cells producing IFN-γ increased in patients with PGF after allo HSCT, whereas the percentage of Th2 and Tc2 cells that produce IL-4 decreased, resulting in an increased proportion of Th1/Th2 and Tc1/Tc2. This finding indicated that both CD4$^+$ and CD8$^+$ T cells were polarized toward type I immune response in patients with PGF. Another study found that the ratio of Th17/Treg in the BM of patients with PGF was significantly higher than in those with GGF (Kong et al., 2017). Therefore, an abnormal T cell response could contribute to the pathogenesis of PGF. Prolonged isolated thrombocytopenia (PT) is an independent risk factor for poor prognosis after allo HSCT (Kim et al., 2006). The proportion of Th1, Tc1, and Th17 cells increased significantly in patients with PT after allo HSCT (Song et al., 2017).

Macrophages

Macrophages are derived from HSCs, they also participate in the formation of the hematopoietic microenvironment (**Figure 1**). In contrast, macrophages can directly regulate HSCs: They express CD234/DARC that interact with CD82 on the surface of LT-HSCs to inhibit cell cycle progression of LT-HSCs (Hur et al., 2016); CD169$^+$ macrophages can promote erythroblast differentiate into reticulocytes and eliminate the aging erythrocyte (Chow et al., 2013); Similarly, VCAM-1$^+$ macrophage-like niche cells interact with HSCs in an ITGA4-dependent manner and direct them homing to a specific niche (Li et al., 2018). The BM macrophages provide the HSC niche indirect support through osteoblasts and Nestin$^+$ MSCs (Chow et al., 2011; Chang et al., 2014), Based on these results, we infer that depleting macrophages could induce HSC mobilization.

Leukemic cells create an immunosuppressive microenvironment for malignant cells by promoting the polarization of macrophages (**Figure 2**). For instance, in AML, the growth factor-independent 1 transcriptional repressor is involved in macrophage polarization (Al-Matary et al., 2016). Similarly, in AML, enzyme arginase enhances arginine metabolism, polarizes monocytes into M2 with immunosuppressive characteristics, and inhibits normal HSPC proliferation and differentiation (Mussai et al., 2013). In addition, interferon regulatory factor 7 promotes the polarization of tumor-related macrophages to M1 by activating the SAPK/JNK pathway. This in turn activates the IRF7-SAPK/JNK pathway to induce more M1-like macrophages and prolonging AML mice survival time (Yang et al., 2018). In acute lymphocytic leukemia (ALL) BM, the proportion of myeloid-derived suppressor cells and M2-like macrophages significantly increased (Hohtari et al., 2019). ALL cells induced the generation of immunosuppressive dendritic cells and M2-like macrophages by expressing bone morphogenetic protein 4 (BMP4) (Valencia et al., 2019). Macrophages in chronic lymphocytic leukemia (CLL) mice demonstrated an M2-like phenotype, and gene expression profiles revealed a high expression of programed death ligand-1 (PD-L1) (Hanna et al., 2016). It has been reported that CLL lymphocytes produce nicotinamide phosphoribosyl transferase after the NF-B signaling pathway is activated and induces M2 phenotype of macrophages (Audrito et al., 2015). Moreover, CLL could induce polarization of M2 macrophages via the colony-stimulating factor-1 (CSF1)-CSF1R pathway, and blocking CSF1R signal transduction can reduce the leukemia cell load (Galletti et al., 2016).

Megakaryocytes

Megakaryocytes (MKs) constitute an integral part of the BM microenvironment (**Table 1**). The hematopoietic differentiation hierarchies are constantly updated, especially the origin of MKs. Adolfsson et al. (2005) proposed a new differentiation model, in which megakaryocyte/erythroid progenitor cells are derived directly from HSCs. In 2018, Frenette demonstrated that platelet and myeloid-based HSCs, marked by vWF expression, are regulated by MKs via CXCL4, whereas lymphoid-based vWF$^-$ HSCs are located in and regulated by NG2 + arteriolar niches

(Pinho et al., 2018). Furthermore, deleting MKs reprogram vWF^+ HSCs from myeloid-based to a balanced lineage after transplantation (Pinho et al., 2018). The hematopoietic process of MKs is regulated by several cytokines and transcription factors, such as TPO and TGF-β. In the bone marrow of AML mice, MKs produced abundant TGFβ1; this overproduced and activated TGFβ1 directly upregulates Egr3 and inhibits the HSC cell cycle (Gong et al., 2018). After chemotherapy or radiotherapy, MKs can temporarily increase the secretion of fibroblast growth factor-1 and inhibit the TGF-β signal pathway, thus stimulating HSCs to enter the cell cycle and expand (Zhao et al., 2014). Thrombocytopenia is a common and fatal complication in patients with leukemia in clinic. In AML mouse, the number of megakaryocyte progenitor cells decreased sharply and the maturation of MKs was severely damaged too, it was surprising that overproduced IL-4 from bone marrow endothelial cells plays an inhibitory role in the differentiation of MKs (Gao et al., 2019). Host MKs play a novel role in promoting donor HSC implantation and expansion. After TBI, surviving MKs migrate to the endosteal surface of trabecular bone (Olson et al., 2013), secreting platelet-derived growth factor-BB to promote the proliferation of osteoblasts and significantly enhance donor HSC engraftment (Olson et al., 2013).

CONCLUSION AND FUTURE PERSPECTIVES

The precise regulation of HSCs by the BM microenvironment is extremely complex. Further studies are required to check whether other niche cells and new factors exist in the BM. Although available literature focuses on how healthy BM microenvironment and leukemia microenvironment regulate HSCs, it lacks research on changes in the BM microenvironment before and after HSCT. In addition, targeted therapy of leukemia is a breakthrough in clinical treatment; however, problems such as drug resistance of targeted therapy, toxicity superposition of combined therapy, and lack of effective targets exist as well. In conclusion, there is a need for more novel therapeutic targets.

AUTHOR CONTRIBUTIONS

All authors drafted the manuscript, contributed to manuscript revision, and approved the final version of the manuscript.

FUNDING

This work was supported by the National Natural Science Foundation of China (82070173, 81700164, and 82060810), the Yunnan Applied Basic Research Projects Foundation (2018FB112), the Medical Reserve Talents Cultivation Project of Yunnan Province (H2017012), the Science and Technology Department of Yunnan Province-Kunming Medical University Applied Basic Research Joint Special Fund Young Doctor Project [2018FE001(-156)], the Doctor Research Fund of Yunnan First People's Hospital (KHBS-2020-007), the Open Project of Yunnan Blood Clinical Medical Center (2019LCZXKF-XY02, 2019LCZXKF-XY14 and 2019LCZXKF-XY11).

REFERENCES

Acar, M., Kocherlakota, K. S., Murphy, M. M., Peyer, J. G., Oguro, H., Inra, C. N., et al. (2015). Deep imaging of bone marrow shows non-dividing stem cells are mainly perisinusoidal. *Nature* 526, 126–130. doi: 10.1038/nature15250

Adolfsson, J., Mansson, R., Hultquist, A., Liuba, K., Jensen, C. T., and Bryder, D. (2005). Identification of Flt3+ lympho-myeloid stem cells lacking erythro-megakaryocytic potential a revised road map for adult blood lineage commitment. *Cell* 121, 295–306. doi: 10.1016/j.cell.2005.02.013

Al-Matary, Y. S., Botezatu, L., Opalka, B., Hones, J. M., Lams, R. F., Thivakaran, A., et al. (2016). Acute myeloid leukemia cells polarize macrophages towards a leukemia supporting state in a growth factor independence 1 dependent manner. *Haematologica* 101, 1216–1227. doi: 10.3324/haematol.2016.143180

Almici, C., Skert, C., Bruno, B., Bianchetti, A., Verardi, R., Neva, A., et al. (2017). Circulating endothelial cell count: a reliable marker of endothelial damage in patients undergoing hematopoietic stem cell transplantation. *Bone Marrow Transpl.* 52, 1637–1642. doi: 10.1038/bmt.2017.194

An, G., Acharya, C., Feng, X., Wen, K., Zhong, M., Zhang, L., et al. (2016). Osteoclasts promote immune suppressive microenvironment in multiple myeloma: therapeutic implication. *Blood* 128, 1590–1603. doi: 10.1182/blood-2016-03-7

Arai, F., Hirao, A., Ohmura, M., Sato, H., Matsuoka, S., Takubo, K., et al. (2004). Tie2/angiopoietin-1 signaling regulates hematopoietic stem cell quiescence in the bone marrow niche. *Cell* 118, 149–161. doi: 10.1016/j.cell.2004.07.004

Arranz, L., Isern, J., Langa, X., Tzankov, A., Lundberg, P., Muntion, S., et al. (2014). Neuropathy of haematopoietic stem cell niche is essential for myeloproliferative neoplasms. *Nature* 512, 78–81. doi: 10.1038/nature13383

Asada, N., Katayama, Y., Sato, M., Minagawa, K., Wakahashi, K., Kawano, H., et al. (2013). Matrix-embedded osteocytes regulate mobilization of hematopoietic stem/progenitor cells. *Cell Stem Cell* 12, 737–747. doi: 10.1016/j.stem.2013.05.001

Audrito, V., Serra, S., Brusa, D., Mazzola, F., Arruga, F., Vaisitti, T., et al. (2015). Extracellular nicotinamide phosphoribosyltransferase (NAMPT) promotes M2 macrophage polarization in chronic lymphocytic leukemia. *Blood.* 125, 111–123. doi: 10.1182/blood-2014-07-589069

Azadniv, M., Myers, J. R., McMurray, H. R., Guo, N., Rock, P., Coppage, M. L., et al. (2020). Bone marrow mesenchymal stromal cells from acute myelogenous leukemia patients demonstrate adipogenic differentiation propensity with implications for leukemia cell support. *Leukemia* 34, 391–403. doi: 10.1038/s41375-019-0568-568

Baccin, C., Velten, L., Helbling, P. M., Grunschlager, F., Steinmetz, L. M., and Trumpp, A. (2020). Combined single-cell and spatial transcriptomics reveal the molecular, cellular and spatial bone marrow niche organization. *Nat. Cell Biol.* 22, 38–48. doi: 10.1038/s41556-019-0439-436

Ball, L. M., Bernardo, M. E., Roelofs, H., Lankester, A., Cometa, A., Egeler, R. M., et al. (2007). Cotransplantation of ex vivo expanded mesenchymal stem cells accelerates lymphocyte recovery and may reduce the risk of graft failure in haploidentical hematopoietic stem-cell transplantation. *Blood* 110, 2764–2767. doi: 10.1182/blood-2007-04-087056

Baryawno, N., and Scadden, D. T. (2014). Blood loses it when nerves go bad. *Cell Res.* 24, 1151–1152. doi: 10.1038/cr.2014.98

Battula, V. L., Le, P. M., Sun, J. C., Nguyen, K., Yuan, B., Zhou, X., et al. (2017). AML-induced osteogenic differentiation in mesenchymal stromal cells supports leukemia growth. *JCI Insight* 2:36. doi: 10.1172/jci.insight.90036

Beaulieu, A., Poncin, G., Humblet, C., Bogdanovic, G., Lognay, G., and Boniver, J. (2011). Leptin reverts pro-apoptotic and antiproliferative effects of alpha-linolenic acids in BCR-ABL positive leukemic cells: involvement of PI3K pathway. *PLoS One* 6:e25651. doi: 10.1371/journal.pone.0025651

Behan, J. W., Yun, J. P., Proektor, M. P., Ehsanipour, E. A., Arutyunyan, A., Moses, A. S., et al. (2009). Adipocytes impair leukemia treatment in mice. *Cancer Res.* 69, 7867–7874. doi: 10.1158/0008-5472.CAN-09-0800

Boyd, A. L., Reid, J. C., Salci, K. R., Aslostovar, L., Benoit, Y. D., and Shapovalova, Z. (2017). Acute myeloid leukaemia disrupts endogenous myelo-erythropoiesis by compromising the adipocyte bone marrow niche. *Nat. Cell Biol.* 19, 1336–1347. doi: 10.1038/ncb3625

Bromberg, O., Frisch, B. J., Weber, J. M., Porter, R. L., Civitelli, R., and Calvi, L. M. (2012). Osteoblastic N-cadherin is not required for microenvironmental support and regulation of hematopoietic stem and progenitor cells. *Blood* 120, 303–313. doi: 10.1182/blood-2011-09-377853

Cao, X. N., Kong, Y., Song, Y., Shi, M. M., Zhao, H. Y., Wen, Q., et al. (2018). Impairment of bone marrow endothelial progenitor cells in acute graft-versus-host disease patients after allotransplant. *Br. J. Haematol.* 182, 870–886. doi: 10.1111/bjh.15456

Chanavaz, M. (1995). Anatomy and histophysiology of the periosteum: quantification of the periosteal blood supply to the adjacent bone with 85Sr and gamma spectrometry. *J. Oral Implantol.* 21, 214–219.

Chang, K. H., Sengupta, A., Nayak, R. C., Duran, A., Lee, S. J., and Pratt, R. G. (2014). p62 is required for stem cell/progenitor retention through inhibition of IKK/NF-kappaB/Ccl4 signaling at the bone marrow macrophage-osteoblast niche. *Cell Rep.* 9, 2084–2097. doi: 10.1016/j.celrep.2014.11.031

Chen, J. Y., Miyanishi, M., Wang, S. K., Yamazaki, S., Sinha, R., Kao, K. S., et al. (2016). Hoxb5 marks long-term haematopoietic stem cells and reveals a homogenous perivascular niche. *Nature* 530, 223–227. doi: 10.1038/nature16943

Cheng, H., Sha, H., Yanfeng, L., Yakun, P., Shihui, M., and Fang, D. (2015). Leukemic marrow infiltration reveals a novel role for Egr3 as a potent inhibitor of normal hematopoietic stem cell proliferation. *Blood* 126, 1302–1313. doi: 10.1182/blood-2015-01-623645

Cheng, T. (2008). Toward 'SMART' stem cells. *Gene Ther.* 15, 67–73. doi: 10.1038/sj.gt.3303066

Chow, A., Huggins, M., Ahmed, J., Hashimoto, D., Lucas, D., Kunisaki, Y., et al. (2013). CD169(+) macrophages provide a niche promoting erythropoiesis under homeostasis and stress. *Nat. Med.* 19, 429–436. doi: 10.1038/nm.3057

Chow, A., Lucas, D., Hidalgo, A., Hashimoto, D., Scheiermann, C., Battista, M., et al. (2011). Bone marrow CD169+ macrophages promote the retention of hematopoietic stem and progenitor cells in the mesenchymal stem cell niche. *J. Exp. Med.* 208, 261–271. doi: 10.1084/jem.20101688

Christodoulou, C., Spencer, J. A., Yeh, S. A., Turcotte, R., Kokkaliaris, K. D., Panero, R., et al. (2020). Live-animal imaging of native haematopoietic stem and progenitor cells. *Nature* 578, 278–283. doi: 10.1038/s41586-020-1971-z

Chute, J. P., Muramoto, G. G., Salter, A. B., Meadows, S. K., Rickman, D. W., Chen, B., et al. (2007). Transplantation of vascular endothelial cells mediates the hematopoietic recovery and survival of lethally irradiated mice. *Blood* 109, 2365–2372. doi: 10.1182/blood-2006-05-022640

Ding, L., and Morrison, S. J. (2013). Haematopoietic stem cells and early lymphoid progenitors occupy distinct bone marrow niches. *Nature* 495, 231–235. doi: 10.1038/nature11885

Ding, L., Saunders, T. L., Enikolopov, G., and Morrison, S. J. (2012). Endothelial and perivascular cells maintain haematopoietic stem cells. *Nature* 481, 457–462. doi: 10.1038/nature10783

Ding, L., Zhu, H., Yang, Y., Wang, Z. D., Zheng, X. L., Yan, H. M., et al. (2014). Functional mesenchymal stem cells remain present in bone marrow microenvironment of patients with leukemia post-allogeneic hematopoietic stem cell transplant. *Leuk. Lymphoma* 55, 1635–1644. doi: 10.3109/10428194.2013.858815

Dong, F., Hao, S., Zhang, S., Zhu, C., Cheng, H., and Yang, Z. (2020). Differentiation of transplanted haematopoietic stem cells tracked by single-cell transcriptomic analysis. *Nat. Cell Biol.* 22, 630–639. doi: 10.1038/s41556-020-0512-511

Dong, L., Yu, W. M., Zheng, H., Loh, M. L., Bunting, S. T., Pauly, M., et al. (2016). Leukaemogenic effects of Ptpn11 activating mutations in the stem cell microenvironment. *Nature* 539, 304–308. doi: 10.1038/nature20131

Duarte, D., Hawkins, E. D., Akinduro, O., Ang, H., Kong, I. Y., Haltalli, M., et al. (2018). Inhibition of endosteal vascular niche remodeling rescues hematopoietic stem cell Loss in AML. *Cell Stem Cell* 22, 64–77.e6. doi: 10.1016/j.stem.2017.11.006

Felipe Rico, J., Hassane, D. C., and Guzman, M. L. (2013). Acute myelogenous leukemia stem cells: from bench to bedside. *Cancer Lett.* 338, 4–9. doi: 10.1016/j.canlet.2012.05.034

Fujisaki, J., Wu, J., Carlson, A. L., Silberstein, L., Putheti, P., Larocca, R., et al. (2011). In vivo imaging of Treg cells providing immune privilege to the haematopoietic stem-cell niche. *Nature* 474, 216–219. doi: 10.1038/nature10160

Galletti, G., Scielzo, C., Barbaglio, F., Rodriguez, T. V., Riba, M., Lazarevic, D., et al. (2016). Targeting macrophages sensitizes chronic lymphocytic leukemia to apoptosis and inhibits disease progression. *Cell Rep.* 14, 1748–1760. doi: 10.1016/j.celrep.2016.01.042

Gao, A., Gong, Y., Zhu, C., Yang, W., Li, Q., Zhao, M., et al. (2019). Bone marrow endothelial cell-derived interleukin-4 contributes to thrombocytopenia in acute myeloid leukemia. *Haematologica* 104, 1950–1961. doi: 10.3324/haematol.2018.214593

Gong, Y., Mei, Z., Wanzhu, Y., Ai, G., Xiuxiu, Y., and Linping, H. (2018). Megakaryocyte-derived excessive transforming growth factor β1 inhibits proliferation of normal hematopoietic stem cells in acute myeloid leukemia. *Exper. Hematol.* 60, 40–46.e2. doi: 10.1016/j.exphem.2017.12.010

Green, M. M., Chao, N., Chhabra, S., Corbet, K., Gasparetto, C., Horwitz, A., et al. (2016). Plerixafor (a CXCR4 antagonist) following myeloablative allogeneic hematopoietic stem cell transplantation enhances hematopoietic recovery. *J. Hematol. Oncol.* 9:71. doi: 10.1186/s13045-016-0301-302

Hanna, B. S., McClanahan, F., Yazdanparast, H., Zaborsky, N., Kalter, V., Rossner, P. M., et al. (2016). Depletion of CLL-associated patrolling monocytes and macrophages controls disease development and repairs immune dysfunction in vivo. *Leukemia* 30, 570–579. doi: 10.1038/leu.2015.305

Hanoun, M., Zhang, D., Mizoguchi, T., Pinho, S., Pierce, H., Kunisaki, Y., et al. (2014). Acute myelogenous leukemia-induced sympathetic neuropathy promotes malignancy in an altered hematopoietic stem cell niche. *Cell Stem Cell* 15, 365–375. doi: 10.1016/j.stem.2014.06.020

Himburg, H. A., Sasine, J., Yan, X., Kan, J., Dressman, H., and Chute, J. P. (2016). A Molecular profile of the endothelial cell response to ionizing radiation. *Radiat. Res.* 186, 141–152. doi: 10.1667/RR14444.1

Hirata, Y., Furuhashi, K., Ishii, H., Li, H. W., Pinho, S., Ding, L., et al. (2018). CD150(high) bone marrow tregs maintain Hematopoietic stem cell quiescence and immune privilege via adenosine. *Cell Stem Cell* 22, 445–453.e5. doi: 10.1016/j.stem.2018.01.017

Hohtari, H., Bruck, O., Blom, S., Turkki, R., Sinisalo, M., Kovanen, P. E., et al. (2019). Immune cell constitution in bone marrow microenvironment predicts outcome in adult ALL. *Leukemia* 33, 1570–1582. doi: 10.1038/s41375-018-0360-361

Hooper, A. T., Butler, J. M., Nolan, D. J., Kranz, A., Iida, K., Kobayashi, M., et al. (2009). Engraftment and reconstitution of hematopoiesis is dependent on VEGFR2-mediated regeneration of sinusoidal endothelial cells. *Cell Stem Cell* 4, 263–274. doi: 10.1016/j.stem.2009.01.006

Hosokawa, K., Arai, F., Yoshihara, H., Iwasaki, H., Nakamura, Y., and Gomei, Y. (2010). Knockdown of N-cadherin suppresses the long-term engraftment of hematopoietic stem cells. *Blood* 116, 554–563. doi: 10.1182/blood-2009-05-224857

Hu, X., Shen, H., Tian, C., Yu, H., Zheng, G., XuFeng, R., et al. (2009). Kinetics of normal hematopoietic stem and progenitor cells in a Notch1-induced leukemia model. *Blood* 114, 3783–3792. doi: 10.1182/blood-2009-06-227843

Hur, J., Choi, J. I., Lee, H., Nham, P., Kim, T. W., Chae, C. W., et al. (2016). CD82/KAI1 maintains the dormancy of long-term Hematopoietic stem cells through interaction with DARC-expressing macrophages. *Cell Stem Cell* 18, 508–521. doi: 10.1016/j.stem.2016.01.013

Johrer, K., Ploner, C., Thangavadivel, S., Wuggenig, P., and Greil, R. (2015). Adipocyte-derived players in hematologic tumors: useful novel targets?. *Expert. Opin. Biol. Ther.* 15, 61–77. doi: 10.1517/14712598.2015.970632

Ketterl, T. G., Chow, E. J., Leisenring, W. M., Goodman, P., Koves, I. H., Petryk, A., et al. (2018). Adipokines, inflammation, and adiposity in Hematopoietic cell transplantation survivors. *Biol. Blood Marrow Transpl.* 24, 622–626.

Kiel, M. J., Yilmaz, O. H., Iwashita, T., Yilmaz, O. H., Terhorst, C., and Morrison, S. J. (2005). SLAM family receptors distinguish hematopoietic stem and progenitor cells and reveal endothelial niches for stem cells. *Cell* 121, 1109–1121. doi: 10.1016/j.cell.2005.05.026

Kim, D. H., Sohn, S. K., Baek, J. H., Kim, J. G., Lee, N. Y., Won, D. I., et al. (2006). Clinical significance of platelet count at day +60 after allogeneic peripheral blood stem cell transplantation. *J. Korean Med. Sci.* 21, 46–51. doi: 10.3346/jkms.2006.21.1.46

Kode, A., Manavalan, J. S., Mosialou, I., Bhagat, G., Rathinam, C. V., Luo, N., et al. (2014). Leukaemogenesis induced by an activating beta-catenin mutation in osteoblasts. *Nature* 506, 240–244. doi: 10.1038/nature12883

Kong, Y., Chang, Y. J., Wang, Y. Z., Chen, Y. H., Han, W., Wang, Y., et al. (2013). Association of an impaired bone marrow microenvironment with secondary poor graft function after allogeneic hematopoietic stem cell transplantation. *Biol. Blood Marrow Transpl.* 19, 1465–1473. doi: 10.1016/j.bbmt.2013.07.014

Kong, Y., Wang, Y. T., Cao, X. N., Song, Y., Chen, Y. H., Sun, Y. Q., et al. (2017). Aberrant T cell responses in the bone marrow microenvironment of patients with poor graft function after allogeneic hematopoietic stem cell transplantation. *J. Transl. Med.* 15:57. doi: 10.1186/s12967-017-1159-y

Krause, D. S., Lazarides, K., Lewis, J. B., von Andrian, U. H., and Van Etten, R. A. (2014). Selectins and their ligands are required for homing and engraftment of BCR-ABL1+ leukemic stem cells in the bone marrow niche. *Blood* 123, 1361–1371. doi: 10.1182/blood-2013-11-538694

Kunisaki, Y., Bruns, I., Scheiermann, C., Ahmed, J., Pinho, S., and Zhang, D. (2013). Arteriolar niches maintain haematopoietic stem cell quiescence. *Nature* 502, 637–643. doi: 10.1038/nature12612

Lai, C. Y., Yamazaki, S., Okabe, M., Suzuki, S., Maeyama, Y., Iimura, Y., et al. (2014). Stage-specific roles for CXCR4 signaling in murine hematopoietic stem/progenitor cells in the process of bone marrow repopulation. *Stem Cells* 32, 1929–1942. doi: 10.1002/stem.1670

Lawson, M. A., McDonald, M. M., Kovacic, N., Terry, R. L., Down, J., Kaplan, W., et al. (2015). Osteoclasts control reactivation of dormant myeloma cells by remodelling the endosteal niche. *Nat. Commun.* 6:8983. doi: 10.1038/ncomms9983

Li, D., Xue, W., Li, M., Dong, M., Wang, J., Wang, X., et al. (2018). VCAM-1(+) macrophages guide the homing of HSPCs to a vascular niche. *Nature* 564, 119–124. doi: 10.1038/s41586-018-0709-707

Lim, M., Pang, Y., Ma, S., Hao, S., Shi, H., Zheng, Y., et al. (2016). Altered mesenchymal niche cells impede generation of normal hematopoietic progenitor cells in leukemic bone marrow. *Leukemia* 30, 154–162. doi: 10.1038/leu.2015.210

Liu, H., Zhai, Y., Zhao, W., Wan, Y., Lu, W., Yang, S., et al. (2018). Consolidation chemotherapy prevents relapse by indirectly regulating bone marrow adipogenesis in patients with acute myeloid leukemia. *Cell Physiol. Biochem.* 45, 2389–2400. doi: 10.1159/000488225

Mancusi, A., Piccinelli, S., and Velardi, A. A. (2019). CD4(+)FOXP3(+) regulatory T cell therapies in HLA haploidentical hematopoietic transplantation. *Front. Immunol.* 10:2901. doi: 10.3389/fimmu.2019.02901

Maryanovich, M., Takeishi, S., and Frenette, P. S. (2018a). Neural regulation of bone and bone marrow. *Cold Spring Harb. Perspect. Med.* 8:a031344. doi: 10.1101/cshperspect.a031344

Maryanovich, M., Zahalka, A. H., Pierce, H., Pinho, S., Nakahara, F., Asada, N., et al. (2018b). Adrenergic nerve degeneration in bone marrow drives aging of the hematopoietic stem cell niche. *Nat. Med.* 24, 782–791. doi: 10.1038/s41591-018-0030-x

Matsuoka, K., Kim, H. T., McDonough, S., Bascug, G., Warshauer, B., Koreth, J., et al. (2010). Altered regulatory T cell homeostasis in patients with CD4+ lymphopenia following allogeneic hematopoietic stem cell transplantation. *J. Clin. Invest.* 120, 1479–1493. doi: 10.1172/JCI41072

Mendez-Ferrer, S., Bonnet, D., Steensma, D. P., Hasserjian, R. P., Ghobrial, I. M., and Gribben, J. G. (2020). Bone marrow niches in haematological malignancies. *Nat. Rev. Cancer* 20, 285–298. doi: 10.1038/s41568-020-0245-242

Mendez-Ferrer, S., Lucas, D., Battista, M., and Frenette, P. S. (2008). Haematopoietic stem cell release is regulated by circadian oscillations. *Nature* 452, 442–447. doi: 10.1038/nature06685

Mendez-Ferrer, S., Michurina, T. V., Ferraro, F., Mazloom, A. R., Macarthur, B. D., and Lira, S. A. (2010). Mesenchymal and haematopoietic stem cells form a unique bone marrow niche. *Nature* 466, 829–834. doi: 10.1038/nature09262

Murase, K., Kim, H. T., Bascug, O. R., Kawano, Y., Ryan, J., and Matsuoka, K. (2014). Increased mitochondrial apoptotic priming of human regulatory T cells after allogeneic hematopoietic stem cell transplantation. *Haematologica* 99, 1499–1508. doi: 10.3324/haematol.2014.104166

Mussai, F., De Santo, C., Abu-Dayyeh, I., Booth, S., Quek, L., Qureshi, A., et al. (2013). Acute myeloid leukemia creates an arginase-dependent immunosuppressive microenvironment. *Blood* 122, 749–758. doi: 10.1182/blood-2013-01-480129

Naveiras, O., Nardi, V., Wenzel, P. L., Hauschka, P. V., Fahey, F., and Daley, G. Q. (2009). Bone-marrow adipocytes as negative regulators of the haematopoietic microenvironment. *Nature* 460, 259–263. doi: 10.1038/nature08099

Nilsson, S. K., Johnston, H. M., and Coverdale, J. A. (2001). Spatial localization of transplanted hemopoietic stem cells: inferences for the localization of stem cell niches. *Blood* 97, 2293–2299. doi: 10.1182/blood.v97.8.2293

Nilsson, S. K., Johnston, H. M., Whitty, G. A., Williams, B., Webb, R. J., and Denhardt, D. T. (2005). Osteopontin, a key component of the hematopoietic stem cell niche and regulator of primitive hematopoietic progenitor cells. *Blood* 106, 1232–1239. doi: 10.1182/blood-2004-11-4422

Ninomiya, M., Abe, A., Katsumi, A., Xu, J., Ito, M., Arai, F., et al. (2007). Homing, proliferation and survival sites of human leukemia cells in vivo in immunodeficient mice. *Leukemia* 21, 136–142. doi: 10.1038/sj.leu.2404432

Olson, T. S., Caselli, A., Otsuru, S., Hofmann, T. J., Williams, R., Paolucci, P., et al. (2013). Megakaryocytes promote murine osteoblastic HSC niche expansion and stem cell engraftment after radioablative conditioning. *Blood* 121, 5238–5249. doi: 10.1182/blood-2012-10-463414

Palomo, M., Diaz-Ricart, M., Carbo, C., Rovira, M., Fernandez-Aviles, F., and Martine, C. (2010). Endothelial dysfunction after hematopoietic stem cell transplantation: role of the conditioning regimen and the type of transplantation. *Biol. Blood Marrow Transpl.* 16, 985–993. doi: 10.1016/j.bbmt.2010.02.008

Peng, Y., Chen, X., Liu, Q., Zhang, X., Huang, K., Liu, L., et al. (2015). Mesenchymal stromal cells infusions improve refractory chronic graft versus host disease through an increase of CD5+ regulatory B cells producing interleukin 10. *Leukemia* 29, 636–646. doi: 10.1038/leu.2014.225

Pierce, H., Zhang, D., Magnon, C., Lucas, D., Christin, J. R., Huggins, M., et al. (2017). Cholinergic signals from the CNS Regulate G-CSF-mediated HSC mobilization from bone marrow via a glucocorticoid signaling relay. *Cell Stem Cell* 20, 648–658.e4. doi: 10.1016/j.stem.2017.01.002

Pierini, A., Nishikii, H., Baker, J., Kimura, T., Kwon, H. S., Pan, Y., et al. (2017). Foxp3(+) regulatory T cells maintain the bone marrow microenvironment for B cell lymphopoiesis. *Nat. Commun.* 8:15068. doi: 10.1038/ncomms15068

Pinho, S., Marchand, T., Yang, E., Wei, Q., Nerlov, C., and Frenette, P. S. (2018). Lineage-biased hematopoietic stem cells are regulated by distinct niches. *Dev. Cell* 44, 634–641.e4. doi: 10.1016/j.devcel.2018.01.016

Plein, A., Fantin, A., Denti, L., Pollard, J. W., and Ruhrberg, C. (2018). Erythro-myeloid progenitors contribute endothelial cells to blood vessels. *Nature* 562, 223–228. doi: 10.1038/s41586-018-0552-x

Poulos, M. G., Guo, P., Kofler, N. M., Pinho, S., Gutkin, M. C., Tikhonova, A., et al. (2013). Endothelial jagged-1 is necessary for homeostatic and regenerative hematopoiesis. *Cell Rep.* 4, 1022–1034. doi: 10.1016/j.celrep.2013.07.048

Qian, H., Buza-Vidas, N., Hyland, C. D., Jensen, C. T., Antonchuk, J., and Mansson, R. (2007). Critical role of thrombopoietin in maintaining adult quiescent hematopoietic stem cells. *Cell Stem Cell* 1, 671–684. doi: 10.1016/j.stem.2007.10.008

Raaijmakers, M. H., Mukherjee, S., Guo, S., Zhang, S., Kobayashi, T., Schoonmaker, J. A., et al. (2010). Bone progenitor dysfunction induces myelodysplasia and secondary leukaemia. *Nature* 464, 852–857. doi: 10.1038/nature08851

Richard, S., Seigneur, M., Blann, A., Adams, R., Renard, M., Puntous, M., et al. (1996). Vascular endothelial lesion in patients undergoing bone marrow transplantation. *Bone Marrow Transpl.* 18, 955–959.

Riegel, C., Boeld, T. J., Doser, K., Huber, E., Hoffmann, P., and Edinger, M. (2020). Efficient treatment of murine acute GvHD by in vitro expanded donor regulatory T cells. *Leukemia* 34, 895–908. doi: 10.1038/s41375-019-0625-623

Roccaro, A. M., Sacco, A., Maiso, P., Azab, A. K., Tai, Y. T., and Reagan, M. (2013). BM mesenchymal stromal cell-derived exosomes facilitate multiple

myeloma progression. *J. Clin. Invest.* 123, 1542–1555. doi: 10.1172/JCI 66517

Ruggeri, A., Paviglianiti, A., Volt, F., Kenzey, C., Rafii, H., and Rocha, V. (2018). Endothelial and circulating progenitor cells in hematological diseases and allogeneic hematopoietic stem cell transplantation. *Curr. Med. Chem.* 25, 4535–4544. doi: 10.2174/0929867324666171012110244

Schepers, K., Pietras, E. M., Reynaud, D., Flach, J., Binnewies, M., Garg, T., et al. (2013). Myeloproliferative neoplasia remodels the endosteal bone marrow niche into a self-reinforcing leukemic niche. *Cell Stem Cell* 13, 285–299. doi: 10.1016/j.stem.2013.06.009

Schofield, R. (1978). The relationship between the spleen colony-forming cell and the haemopoietic stem cell. *Blood Cells* 4, 7–25.

Shafat, M. S., Oellerich, T., Mohr, S., Robinson, S. D., Edwards, D. R., and Marlein, C. R. (2017). Leukemic blasts program bone marrow adipocytes to generate a protumoral microenvironment. *Blood* 129, 1320–1332. doi: 10.1182/blood-2016-08-734798

Shen, H., Yu, H., Liang, P. H., Cheng, H., XuFeng, R., Yuan, Y., et al. (2012). An acute negative bystander effect of gamma-irradiated recipients on transplanted hematopoietic stem cells. *Blood* 119, 3629–3637. doi: 10.1182/blood-2011-08-373621

Sheng, X., Parmentier, J. H., Tucci, J., Pei, H., Oberley, M. J., Neely, M., et al. (2017). Adipocytes sequester and metabolize the chemotherapeutic daunorubicin. *Mol. Cancer Res.* 15, 1704–1713. doi: 10.1158/1541-7786.MCR-17-0338

Sheng, X., Tucci, J., Parmentier, J. H., Ji, L., Behan, J. W., and Heisterkamp, N. (2016). Adipocytes cause leukemia cell resistance to daunorubicin via oxidative stress response. *Oncotarget* 7, 73147–73159. doi: 10.18632/oncotarget.12246

Shipounova, I. N., Petinati, N. A., Bigildeev, A. E., Drize, N. J., Sorokina, T. V., and Kuzmina, L. A. (2017). Alterations of the bone marrow stromal microenvironment in adult patients with acute myeloid and lymphoblastic leukemias before and after allogeneic hematopoietic stem cell transplantation. *Leuk. Lymphoma* 58, 408–417. doi: 10.1080/10428194.2016.1187277

Sipkins, D. A., Wei, X., Wu, J. W., Runnels, J. M., Cote, D., Means, T. K., et al. (2005). In vivo imaging of specialized bone marrow endothelial microdomains for tumour engraftment. *Nature* 435, 969–973. doi: 10.1038/nature03703

Song, Y., Shi, M. M., Zhang, Y. Y., Mo, X. D., Wang, Y., Zhang, X. H., et al. (2017). Abnormalities of the bone marrow immune microenvironment in patients with prolonged isolated thrombocytopenia after allogeneic Hematopoietic stem cell transplantation. *Biol. Blood Marrow Transpl.* 23, 906–912. doi: 10.1016/j.bbmt.2017.02.021

Spiegel, A., Shivtiel, S., Kalinkovich, A., Ludin, A., Netzer, N., Goichberg, P., et al. (2007). Catecholaminergic neurotransmitters regulate migration and repopulation of immature human CD34+ cells through Wnt signaling. *Nat. Immunol.* 8, 1123–1131. doi: 10.1038/ni1509

Taichman, R. S., Reilly, M. J., and Emerson, S. G. (1996). Human osteoblasts support human hematopoietic progenitor cells in vitro bone marrow cultures. *Blood* 87, 518–524.

Tian, D. M., Liang, Y. M., and Zhang, Y. Q. (2016). Endothelium-targeted human Delta-like 1 enhances the regeneration and homing of human cord blood stem and progenitor cells. *J. Transl. Med.* 14:5. doi: 10.1186/s12967-015-0761-760

Tikhonova, A. N., Dolgalev, I., Hu, H., Sivaraj, K. K., Hoxha, E., Pinho, S., et al. (2019). The bone marrow microenvironment at single-cell resolution. *Nature* 569, 222–228. doi: 10.1038/s41586-019-1104-1108

Valencia, J., Fernandez-Sevilla, M. L., Fraile-Ramos, A., Sacedon, R., Jimenez, E., and Vicente, A. (2019). Acute lymphoblastic leukaemia cells impair dendritic cell and macrophage differentiation: role of BMP4. *Cells* 8:722. doi: 10.3390/cells8070722

Vijay, V., Miller, R., Vue, G. S., Pezeshkian, M. B., Maywood, M., Ast, A. M., et al. (2019). Interleukin-8 blockade prevents activated endothelial cell mediated proliferation and chemoresistance of acute myeloid leukemia. *Leuk. Res.* 84:106180. doi: 10.1016/j.leukres.2019.106180

Wang, R., Feng, W., Wang, H., Wang, L., Yang, X., Yang, F., et al. (2020). Blocking migration of regulatory T cells to leukemic hematopoietic microenvironment delays disease progression in mouse leukemia model. *Cancer Lett.* 469, 151–161. doi: 10.1016/j.canlet.2019.10.032

Wang, Y. T., Kong, Y., Song, Y., Han, W., Zhang, Y. Y., Zhang, X. H., et al. (2016). Increased Type 1 immune response in the bone marrow immune microenvironment of patients with poor graft function after allogeneic hematopoietic stem cell transplantation. *Biol. Blood Marrow Transpl.* 22, 1376–1382. doi: 10.1016/j.bbmt.2016.04.016

Weiss, E. M., Schmidt, A., Vobis, D., Garbi, N., Lahl, K., Mayer, C. T., et al. (2011). Foxp3-mediated suppression of CD95L expression confers resistance to activation-induced cell death in regulatory T cells. *J. Immunol.* 187, 1684–1691. doi: 10.4049/jimmunol.1002321

Winkler, I. G., Barbier, V., Nowlan, B., Jacobsen, R. N., Forristal, C. E., Patton, J. T., et al. (2012). Vascular niche E-selectin regulates hematopoietic stem cell dormancy, self renewal and chemoresistance. *Nat. Med.* 18, 1651–1657. doi: 10.1038/nm.2969

Xia, C., Wang, T., Cheng, H., Dong, Y., Weng, Q., Sun, G., et al. (2020). Mesenchymal stem cells suppress leukemia via macrophage-mediated functional restoration of bone marrow microenvironment. *Leukemia* 34, 2375–2383. doi: 10.1038/s41375-020-0775-3

Xu, C., Gao, X., Wei, Q., Nakahara, F., Zimmerman, S. E., and Mar, J. (2018). Stem cell factor is selectively secreted by arterial endothelial cells in bone marrow. *Nat. Commun.* 9:2449. doi: 10.1038/s41467-018-04726-4723

Xue, Y., Lv, J., Zhang, C., Wang, L., Ma, D., and Liu, F. (2017). The vascular niche regulates hematopoietic stem and progenitor cell lodgment and expansion via klf6a-ccl25b. *Dev. Cell* 42, 349–362.e4. doi: 10.1016/j.devcel.2017.07.012

Yamazaki, S., Ema, H., Karlsson, G., Yamaguchi, T., Miyoshi, H., and Shioda, S. (2011). Nonmyelinating Schwann cells maintain hematopoietic stem cell hibernation in the bone marrow niche. *Cell* 147, 1146–1158. doi: 10.1016/j.cell.2011.09.053

Yang, S., Lu, W., Zhao, C., Zhai, Y., Wei, Y., Liu, J., et al. (2019). Leukemia cells remodel marrow adipocytes via TRPV4-dependent lipolysis. *Haematologica* 105:225763. doi: 10.3324/haematol.2019.225763

Yang, X., Feng, W., Wang, R., Yang, F., Wang, L., Chen, S., et al. (2018). Repolarizing heterogeneous leukemia-associated macrophages with more M1 characteristics eliminates their pro-leukemic effects. *Oncoimmunology* 7:e1412910. doi: 10.1080/2162402X.2017.1412910

Yianni, V., and Sharpe, P. T. (2019). Perivascular-derived mesenchymal stem cells. *J. Dent. Res.* 98, 1066–1072. doi: 10.1177/0022034519862258

Yokota, T., Oritani, K., Takahashi, I., Ishikawa, J., Matsuyama, A., Ouchi, N., et al. (2000). Adiponectin, a new member of the family of soluble defense collagens, negatively regulates the growth of myelomonocytic progenitors and the functions of macrophages. *Blood* 96, 1723–1732.

Zeng, L., Chen, C., Song, G., Yan, Z., Xu, S., Jia, L., et al. (2012). Infusion of endothelial progenitor cells accelerates hematopoietic and immune reconstitution, and ameliorates the graft-versus-host disease after hematopoietic stem cell transplantation. *Cell Biochem. Biophys.* 64, 213–222. doi: 10.1007/s12013-012-9387-9385

Zhao, M., Perry, J. M., Marshall, H., Venkatraman, A., Qian, P., He, X. C., et al. (2014). Megakaryocytes maintain homeostatic quiescence and promote post-injury regeneration of hematopoietic stem cells. *Nat. Med.* 20, 1321–1326. doi: 10.1038/nm.3706

Zhou, B. O., Yu, H., Yue, R., Zhao, Z., Rios, J. J., and Naveiras, O. (2017). Bone marrow adipocytes promote the regeneration of stem cells and haematopoiesis by secreting SCF. *Nat. Cell Biol.* 19, 891–903. doi: 10.1038/ncb3570

Zhu, R. J., Wu, M. Q., Li, Z. J., Zhang, Y., and Liu, K. Y. (2013). Hematopoietic recovery following chemotherapy is improved by BADGE-induced inhibition of adipogenesis. *Int. J. Hematol.* 97, 58–72. doi: 10.1007/s12185-012-1233-1234

Conflict of Interest: The authors declare that the research was conducted in the absence of any commercial or financial relationships that could be construed as a potential conflict of interest.

frontiers in Genetics

ORIGINAL RESEARCH
published: 01 March 2021
doi: 10.3389/fgene.2021.616507

Molecular Subtypes Based on the Stemness Index Predict Prognosis in Glioma Patients

Jun Tan[1], Hecheng Zhu[2], Guihua Tang[3], Hongwei Liu[1,4], Siyi Wanggou[1,4], Yudong Cao[1], Zhaoqi Xin[1], Quanwei Zhou[1], Chaohong Zhan[1], Zhaoping Wu[1], Youwei Guo[1], Zhipeng Jiang[1], Ming Zhao[2], Caiping Ren[5], Xingjun Jiang[1] and Wen Yin[1]**

[1]Department of Neurosurgery, Xiangya Hospital, Central South University, Changsha, China, [2]Changsha Kexin Cancer Hospital, Changsha, China, [3]Department of Clinical Laboratory, Hunan Provincial People's Hospital (First Affiliated Hospital of Hunan Normal University), Changsha, China, [4]Hunan International Scientific and Technological Cooperation Base of Brain Tumor Research, Xiangya Hospital, Central South University, Changsha, China, [5]Key Laboratory for Carcinogenesis of Chinese Ministry of Health, School of Basic Medical Science, Cancer Research Institute, Central South University, Changsha, China

OPEN ACCESS

Edited by:
Nikhil Baban Ghate,
University of Southern California,
United States

Reviewed by:
Arijita Sarkar,
University of Southern California,
United States
Ying Zhang,
Capital Medical University, China

***Correspondence:**
Xingjun Jiang
jiangxj@csu.edu.cn
Wen Yin
silver-88@163.com

Specialty section:
This article was submitted to Stem Cell Research, a section of the journal Frontiers in Genetics

Received: 12 October 2020
Accepted: 08 February 2021
Published: 01 March 2021

Citation:
Tan J, Zhu H, Tang G, Liu H, Wanggou S, Cao Y, Xin Z, Zhou Q, Zhan C, Wu Z, Guo Y, Jiang Z, Zhao M, Ren C, Jiang X and Yin W (2021) Molecular Subtypes Based on the Stemness Index Predict Prognosis in Glioma Patients. Front. Genet. 12:616507. doi: 10.3389/fgene.2021.616507

Glioma is the common histological subtype of malignancy in the central nervous system, with high morbidity and mortality. Glioma cancer stem cells (CSCs) play essential roles in tumor recurrence and treatment resistance. Thus, exploring the stem cell-related genes and subtypes in glioma is important. In this study, we collected the RNA-sequencing (RNA-seq) data and clinical information of glioma patients from The Cancer Genome Atlas (TCGA) and Chinese Glioma Genome Atlas (CGGA) databases. With the differentially expressed genes (DEGs) and weighted gene correlation network analysis (WGCNA), we identified 86 mRNA expression-based stemness index (mRNAsi)-related genes in 583 samples from TCGA RNA-seq dataset. Furthermore, these samples from TCGA database could be divided into two significantly different subtypes with different prognoses based on the mRNAsi corresponding gene, which could also be validated in the CGGA database. The clinical characteristics and immune cell infiltrate distribution of the two stemness subtypes are different. Then, functional enrichment analyses were performed to identify the different gene ontology (GO) terms and pathways in the two different subtypes. Moreover, we constructed a stemness subtype-related risk score model and nomogram to predict the prognosis of glioma patients. Finally, we selected one gene (ETV2) from the risk score model for experimental validation. The results showed that ETV2 can contribute to the invasion, migration, and epithelial-mesenchymal transition (EMT) process of glioma. In conclusion, we identified two distinct molecular subtypes and potential therapeutic targets of glioma, which could provide new insights for the development of precision diagnosis and prognostic prediction for glioma patients.

Keywords: molecular subtypes, stemness index, glioma, prognostic signature, immune infiltration

INTRODUCTION

Gliomas are the most common primary malignant tumor of the central nervous system (Ostrom et al., 2014). Therapeutic strategies, including surgery, chemotherapy, and radiotherapy, have been widely applied, but the overall outcome of glioma patients is still unsatisfactory (Bush et al., 2017; Nabors et al., 2017). The heterogeneity of glioma is an account of the poor prognosis (Klughammer et al., 2018). Thus, exploring the molecular mechanism of glioma may facilitate the identification of prognostic biomarkers and potential targets for the treatment of glioma.

Cancer stem cells (CSCs) are a subset of cancer cells with characteristics such as the ability to self-renew long-term, differentiate into defined progenies, and sustain tumor growth (Vlashi and Pajonk, 2015; Clarke, 2019). CSCs contribute to glioma recurrence, radioresistance, and chemoresistance through multiple molecular mechanisms (Prieto-Vila et al., 2017; Schulz et al., 2019). Therefore, a further understanding of the biological behavior of glioma stem cells may facilitate to changes in the treatment dilemma of glioma. Recently, the mRNA expression-based stemness index (mRNAsi), which represents the transcriptomic stemness expression, has been applied to assess CSC characteristics (Malta et al., 2018). In some cancers, such as bladder, lung, breast, or endometrial carcinoma, it has been reported that mRNAsi is a credible marker and is associated with tumor stage (Pan et al., 2019; Liu et al., 2020; Pei et al., 2020). However, its roles in glioma are rare known.

In this study, we collected the RNA-sequencing (RNA-seq) data and clinical information of glioma patients from The Cancer Genome Atlas (TCGA) and Chinese Glioma Genome Atlas (CGGA) databases. We found that glioma patients could be divided into two significant stemness subtypes (S1 and S2 groups) based on mRNAsi-related genes. We identified that the clinical characteristics, such as age, IDH status, and WHO grades, were different in the S1 and S2 groups. The tumor microenvironments in the two groups were also different. Furthermore, based on differentially expressed genes (DEGs) between the two stemness subtypes, a prognostic prediction model was constructed and could effectively divide patients into different prognoses in both TCGA and CGGA datasets. Finally, we selected one gene (ETV2) from the risk score model for further experimental validation. The results showed that ETV2 was more highly expressed in glioma and contributed to the invasion, migration, and epithelial-mesenchymal transition (EMT) process of glioma. Thus, our study provides novel molecular subtypes based on the stemness index to predict prognosis in glioma patients who may promote the clinical diagnosis and treatment of glioma.

MATERIALS AND METHODS

Data Preparation

Figure 1 shows the workflow of data analysis. The RNA-seq data and corresponding clinical data of glioma (lower-grade glioma, LGGs and glioblastoma, GBM) and normal samples in TCGA database were downloaded from the UCSC Xena database[1] (dataset ID: TCGA.GBMLGG.sampleMap/HiSeqV2). In addition, another glioma dataset (RNA-seq and clinical data) was downloaded from the CGGA[2] (dataset ID: mRNAseq_693). The mRNAsi indices of glioma in TCGA were obtained from a previous study (Malta et al., 2018). The tumor purity of glioma is calculated based on the Estimation of STromal and Immune cells in MAlignant Tumors using Expression data (ESTIMATE) algorithm, which can predict the level of infiltrating stromal and immune cells and then infer the tumor purity of tumor tissue (Yoshihara et al., 2013).

Differentially Expressed Genes Analysis

The "limma" R package was utilized to perform the DEG analysis between glioma and normal samples in TCGA database. $|\mathrm{Log_2}(\text{Fold change})| > 1$ and false discovery rate (FDR) < 0.05 were considered as the cutoff criteria. The volcano plot was drawn to show the DEGs.

Weighted Gene Correlation Network Analysis

The selected DEGs were used in weighted gene correlation network analysis (WGCNA) by the WGCNA R package (Langfelder and Horvath, 2008). After filtering the outliers in RNA-seq data, a Pearson correlation matrix was constructed for paired genes. Then, we established a weighted adjacency matrix by the power function amn = $|\mathrm{cmn}|^{\beta}$, as a previous study described (Yu et al., 2012). A proper β value was selected to increase the matrix similarity and establish a co-expression network. Next, the adjacency matrix was converted into a topological overlap matrix (TOM) to measure gene connectivity in the network. Based on TOM-based dissimilarity measurements, average linkage hierarchical clustering was performed with a minimum gene dendrogram size over 30. Finally, their dissimilarity was calculated, and module dendrograms were constructed for further analysis.

Gene significance (GS), representing the correlation between genes and sample traits, was calculated for each module. In the principal component analysis of each module, module eigengenes (MEs) were considered as the first principal component of a clustered module representing the gene expression profiles. Module membership (MM) was defined as the correlation between the module genes and gene expression profiles. In our study, mRNAsi and epigenetically regulated mRNAsi (EGER-mRNAsi) were the selected clinical phenotypes for further analysis. When GS and MM were highly correlated (more than 0.7), the module's own genes were considered as significantly correlated with clinical traits.

Consensus Clustering

After finding the genes highly correlated with mRNAsi and EGER-mRNAsi, we performed consensus clustering to divide patients into different stemness subtypes based on these genes. The R package "ConsensusClusterPlus" was adopted to perform

[1]https://xena.ucsc.edu/public
[2]http://www.cgga.org.cn/index.jsp

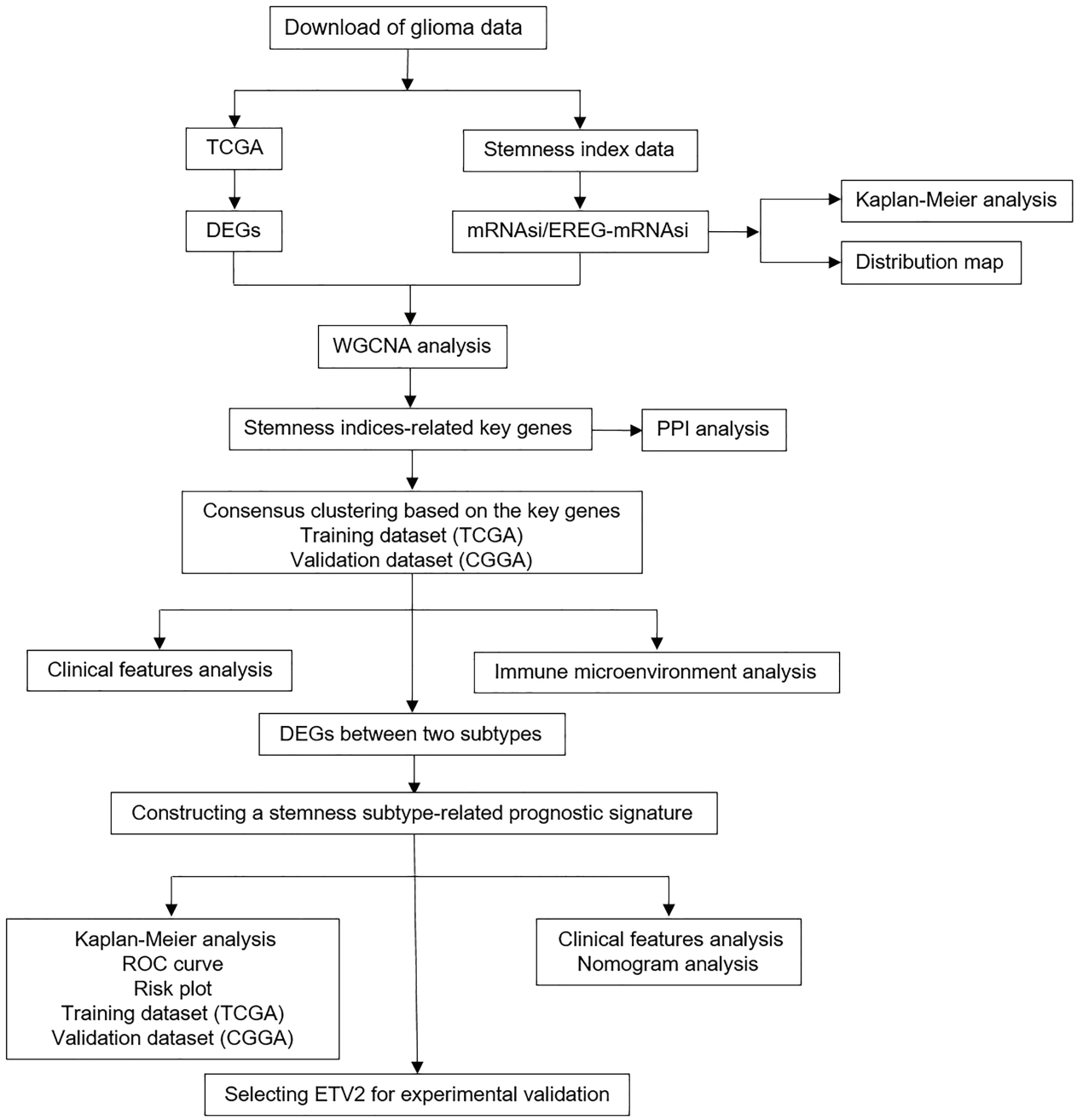

FIGURE 1 | Flowchart presenting the process of analysis.

the consensus clustering (Wilkerson and Hayes, 2010). The optimal number of subgroups was determined by the cumulative distribution function (CDF) and consensus matrices. In addition, the CGGA dataset was used to validate this clustering.

Protein-Protein Interaction Analysis

To explore the protein-protein interaction (PPI) network of the selected genes, they were imported into the STRING database,[3] which is a web tool used to explore the interactions between multiple proteins.

Comparison of Stemness Subtypes

To investigate the difference between the two stemness subtypes in TCGA and CGGA datasets, we used two-sample *t*-tests to

[3]https://string-db.org/

compare different clinical variables such as age, IDH status, and WHO grades in the subtypes. Moreover, stratified survival analysis in different WHO grades was also used to evaluate the prognostic predictive value of the stemness subtypes.

Profiling of Immune Infiltrates in the Two Stemness Subtypes

Becht et al. (2016) designed the microenvironment cell populations-counter (MCP-counter) method, which can robustly quantify the absolute abundance of eight immune (T cells, CD8 T cells, cytotoxic lymphocytes, NK cells, B lineage, monocytic lineage, myeloid dendritic cells, and neutrophils) and two stromal cell (endothelial cells and fibroblasts) populations in heterogeneous tissues from transcriptomic data. The MCPs were analyzed by the "MCPcounter" R package. Based on this package, the proportions of eight tumor-infiltrating immune cells (T cells, CD8 T cells, cytotoxic lymphocytes, NK cells, B lineage, monocytic lineage, myeloid dendritic cells, and neutrophils) and two non-immune cells (endothelial cells and fibroblasts) were calculated based on the normalized RNA-seq data in TCGA and CGGA databases.

Functional Enrichment Analysis

First, DEG analysis between two stemness subtypes was performed. Then, Gene Ontology (GO) and Kyoto Encyclopedia of Genes and Genomes (KEGG) analyses were performed with the Database for Annotation, Visualization and Integrated Discovery (DAVID) to explore the different mechanisms and pathways between the two subtypes (Huang et al., 2009a,b).

Gene set enrichment analysis (GSEA) was performed between the two stemness subtypes with GSEA software. The reference gene set (c2.cp.kegg.v7.1.symbols.gmt) was acquired from the MSigDB database.[4] Only enriched KEGG pathways with a $p < 0.05$ and FDR < 0.25 were considered statistically significant.

Construction and Validation of a Stemness Subtype-Related Prognostic Signature

First, DEG analysis between two stemness subtypes was performed in TCGA dataset as previously described. Then, univariate Cox hazard analysis was performed with $p < 0.05$ as a threshold parameter for the DEGs between the two stemness subtypes. By applying the "glmnet" R package, the least absolute shrinkage and selection operator (LASSO) algorithm was used to construct the stemness subtype-related prognostic signature (Goeman, 2010). This signature was created utilizing Cox regression coefficients to multiply the expression values of the select genes. According to the median of risk score, the patients were divided into high and low-risk groups. In addition, the time-dependent ROC curve and Kaplan-Meier survival curve analyses were used to evaluate the accuracy of the signature. The signature was also validated with CGGA dataset.

[4]http://software.broadinstitute.org/gsea/msigdb/

Nomogram Construction

To evaluate the predictive value of the prognostic signature, univariate and multivariate Cox regression analyses were performed together with the clinical information (grade, age, sex, IDH1, and 1p/19q status). Then, a nomogram was constructed to predict the survival probability by using the "rms" R package (Yin et al., 2020). Calibrations were used to evaluate the accuracy of the nomogram.

Cell Culture, Real-Time Quantitative PCR

HEB, SHG44, and A172 glioma cells were provided by Xiangya Medical School of Central South University, Changsha, China. HEB, A172, and SHG44 cells were cultured in DMEM high glucose medium (Gibco/Thermo Fisher Scientific, Inc.) with 10% fetal bovine serum at 37°C, 5%CO_2. SiRNAs were transfected with Lipofectamine 2000 (Thermo Fisher Scientific) 48 h before analysis. The siRNAs against the ETV2 gene were synthesized by RiboBio Corporation (Product number: siG000002116A-1-5, Guangzhou, China). Total RNA from HEB, SHG44, and A172 cells was extracted by the Trizol lysis method. cDNA synthesis was performed according to the Thermo Scientific RevertAid First Strand cDNA Synthesis Kit (Thermo Scientific, Waltham, MA). The RNA levels of ETV2 were detected by using real-time quantitative PCR (qRT-PCR) according to the manufacturer's protocol. The expression of ETV2 and GAPDH was analyzed by the $2^{-\Delta\Delta Ct}$ method. The primers were obtained from Sangon (Shanghai, China) and the sequences were designed as follows: for ETV2, the forward primer was 5'-CTGGAAAGGTA CAAGCTCATCC-3' and the reverse primer was 5'-AACTTCTG GGTGCAGTAACGC-3'. For GAPDH, the forward primer was 5'-CATTGACCTCAACTACATGGTT-3' and the reverse primer was 5'-CCATTGATGACAAGCTTCCC-3'.

Wound Healing and Transwell assay

Wound healing and transwell assays were performed as previously described (Jia et al., 2018).

Western Blots

A172 and SHG44 cells were lysed with RIPA buffer for half an hour at 4°C. The supernatant was collected and boiled at 95°C for 5–8 min in SDS loading buffer. Then, they were subjected to electrophoresis in 10% SDS-polyacrylamide gels and transferred to the polyvinylidene difluoride membranes. The membranes were blocked with 5% non-fat milk in phosphate-buffered saline (PBS) for 1 h before being incubated with the primary antibody at 4°C overnight. The primary antibodies for western blotting used in this study were GAPDH, ETV2 (ab181847, Abcam), N-cadherin (22018-1-AP, proteintech), and vimentin (10366-1-AP, Proteintech). Then the cells were washed three to four times with 0.1% PBST and incubated with horseradish peroxidase (HRP)-conjugated secondary antibody (1:10,000) for 1 h at room temperature. The membranes were washed in 0.1% PBST four times before exposure. Chemiluminescent HRP substrate was purchased from Millipore (Catalog: WBKLS0500). Images were acquired in a Bio-Rad Universal Hood II machine with Image Lab software.

Immunohistochemistry

These experiments were approved by the Human Ethics Committee of Xiangya Hospital, and informed consent was obtained from all patients. Based on polyformalin-fixed and paraffin-embedded tissues obtained from GBM patients, immunohistochemistry analysis was conducted. The tissue sections were first deparaffinized and hydrated for antigen retrieval. They were then incubated with 0.3% hydrogen peroxide for 10 min at room temperature and washed twice with PBS. After blocking with 5% goat serum for 10 min, the sections were washed with PBS and incubated overnight with a primary antibody against the ETV2 antibody (1:100, Abcam, ab181847) at 4°C. A horseradish peroxidase-labeled secondary antibody (1:400, Abcam, United States) was added dropwise to the sections, and incubation was carried out at 37°C for 30 min. After washing with PBS, the sections were developed using a DAB substrate kit (Sangon Biotech, Shanghai, China) and counterstained with hematoxylin (Sangon Biotech).

Statistical Analysis

The R software (version 3.5.1) and GraphPad Prism (version 7.0.0) were used in statistical analyses, and a $p < 0.05$ was considered significant. The log-rank test was conducted in the Kaplan-Meier survival analysis. The Student's *t*-test was used to compare two groups comparing.

RESULTS

The mRNAsi and Clinical Characteristics in Glioma

mRNA expression-based stemness index is a useful indicator that can estimate the number of CSCs by assessing the similarity and heterogeneity between the tumor cells and stem cells. To explore mRNAsi in glioma, the mRNAsi between normal and glioma samples was calculated using TCGA dataset. However, there was no significant difference of mRNAsi between normal and tumor samples (**Figure 2A**). Next, the correlation between mRNAsi and WHO grades was analyzed. The results showed that different stages of glioma had significantly different mRNAsi values (**Figure 2B**). Furthermore, the predictive potency of mRNAsi for patient survival prediction was also examined. The Kaplan-Meier analysis showed that higher mRNAsi was significantly associated with a better prognosis of glioma patients (**Figure 2C**).

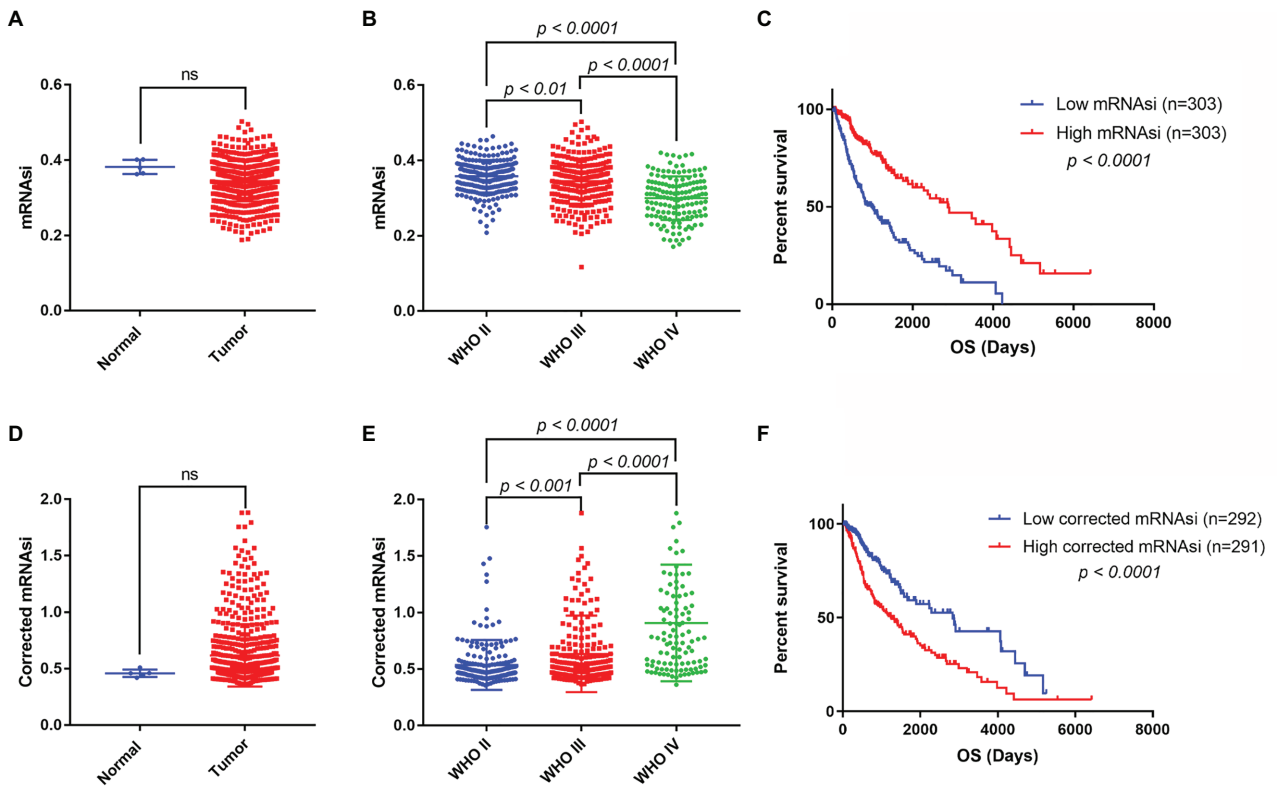

FIGURE 2 | The mRNA expression-based stemness index (mRNAsi), corrected mRNAsi and clinical characteristics in glioma. **(A)** The expression level of mRNAsi in normal (five samples) and tumor (606 samples) tissues. **(B)** Expression level of mRNAsi in gliomas of different WHO grades. **(C)** Kaplan-Meier survival analysis of the relationship between mRNAsi and overall survival (OS). **(D)** The expression level of corrected mRNAsi (mRNAsi/tumor purity) in normal (five samples) and tumor (583 samples) tissues (23 samples cannot calculate the tumor purity). **(E)** The expression level of corrected mRNAsi in glioma of different WHO grades. **(F)** Kaplan-Meier survival analysis of the relationship between corrected mRNAsi and OS.

Because tumor tissues consist of not only tumor cells but also stromal and immune cells, it reminds us that tumor purity is an important factor interfering with the evaluation of mRNAsi in clinical characteristics. To exclude the potential confounding effect of tumor purity on the analysis, the corrected mRNAsi (mRNAsi/tumor purity) was calculated as previously reported (Pan et al., 2019). We reanalyzed the corrected mRNAsi in normal and glioma samples, but still found no significant difference between them (**Figure 2D**). However, we found that the corrected mRNAsi values were positively correlated with WHO grades of glioma (**Figure 2E**). Moreover, we found that patients with higher corrected mRNAsi values had poor prognosis (**Figure 2F**).

Screening of DEGs and Identification of Key Genes-Related to mRNAsi

First, DEG analysis was performed to compare glioma and normal samples. From this analysis, 3,918 DEGs were screened, of which 1,409 were upregulated, and 2,509 were downregulated (**Figure 3A**).

To identify the key genes related to mRNAsi, WGCNA analysis was applied based on the selected DEGs. In total, we identified 11 modules (**Figures 3B,C**), among which the blue and magenta modules exhibited positive correlations with mRNAsi and the red module showed a negative correlation with mRNAsi, with the correlations greater than 0.5 or less than −0.5 (**Figure 3D**). After calculating the correlations between GS and MM of the three modules, we found that the correlations between GS and MM in the red and magenta modules were highly correlated (more than 0.7; **Figures 3E,F**). Therefore, the two modules were chosen for further analyses.

Molecular Subtypes of Glioma Based on mRNAsi-Related Genes

In total, the expression profiling of 86 mRNAsi-related genes in 583 samples from TCGA RNA-seq dataset was obtained. The clinical features of these patients are shown in **Table 1**. Consensus clustering was performed in the 584 samples, and patients could be divided into two significantly different subtypes (S1 and S2 groups; **Figures 4A–C**). The heatmap of the two subtypes is also been shown in **Figure 4D**. Compared with patients in the S1 group, glioma patients in the S2 group showed a shorter overall survival (OS; $p < 0.0001$; **Figure 4E**). The PPI network analysis showed that most of the mRNAsi-related genes were closely correlated and centered on the stemness-related molecules, such as CD44, CD68, IL6, and CXCR4 (Wang et al., 2019; Ma et al., 2020; Osman et al., 2020).

To validate that mRNAsi-related genes could predict prognostic subtypes, the same method with consensus clustering was applied to the CGGA dataset. Interestingly, the patients also could be divide into two distinct subtypes (S1 and S2 groups; **Figures 5A–C**). Patients in the S2 group also had significantly worse OS ($p < 0.0001$; **Figure 5D**).

Clinical Characteristics of Two Stemness Subtypes in the Glioma

To identify the clinical characteristics of the two stemness subtypes, we compared the age, IDH status, and WHO grades of the two stemness subtypes in TCGA dataset. There were significantly more elderly patients (age >= 60) in the S2 group than in the S1 group ($p < 0.0001$; **Figure 6A**). Moreover, we found that the S1 group had more patients with IDH mutantions ($p < 0.0001$; **Figure 6B**). Furthermore, the S1 group had more patients with WHO grade II glioma and fewer patients with WHO IV glioma. However, the S2 group had more patients with WHO grade IV glioma and fewer patients with WHO II glioma ($p < 0.0001$; **Figure 6C**). More importantly, these clinical characteristics of the two stemness subtypes could also be validated in the CGGA dataset (**Figures 6D–F**).

Subsequently, we evaluated the prognostic predictive value of the stemness subtypes in different grades. Considering that almost all the WHO IV glioma patients belong to the S2 group, survival analyses were only performed in patients with WHO grade II and III glioma. Stratified survival analyses showed that patients in the S2 group have a better prognosis than patients in the S1 group in both WHO II and III glioma patients in TCGA database (**Figure 6G**) and CGGA database (**Figure 6H**).

Immunological Microenvironment in Stemness Subtypes of Glioma

The tumor microenvironment consists of the stromal and immune cells and plays a vital role in the aggressiveness of solid tumors. To measure the level of infiltrating immune cells in the tumor microenvironment, we also used MCP-counter estimates to examine the glioma samples in TCGA database. MCP analysis demonstrated that tumor-associated fibroblasts (CAFs) were significantly higher in the S2 group than in the S1 group (**Figures 7A,B**). Moreover, there was a similar finding in the CGGA dataset (**Figures 7C,D**).

Functional Enrichment Analysis Between Two Stemness Subtypes

To explore potential vital molecules and pathways contributing to different subtypes, we performed GO, KEGG, and GSEA analysis between the two stemness subtypes. **Figures 8A–C** shows the top 20 enriched GO terms in biological processes (BP), cellular components (CC), and molecular functions (MF). GO analysis revealed that immune response and cell adhesion were the main terms involved in BP; plasma membrane and extracellular matrix were significantly enriched in CC; calcium ion binding and channel activity were most enriched in MF (**Figures 8A–C**). The results of the KEGG pathway analysis showed that cell adhesion and immunological related pathways were mainly enriched (**Figure 8D**). GSEA showed the significantly enriched hallmark terms, including complement and coagulation cascades, cytokine receptor interaction, intestinal immune network for IgA production, and primary immunodeficiency (**Figure 8E**).

Development and Validation of a Stemness Subtype-Related Prognostic Signature

Among the 3,129 candidate DEGs between the two stemness subtypes in TCGA dataset, 3,118 were identified as being independently associated with OS in univariate Cox regression analysis. The top 20 genes were used to perform

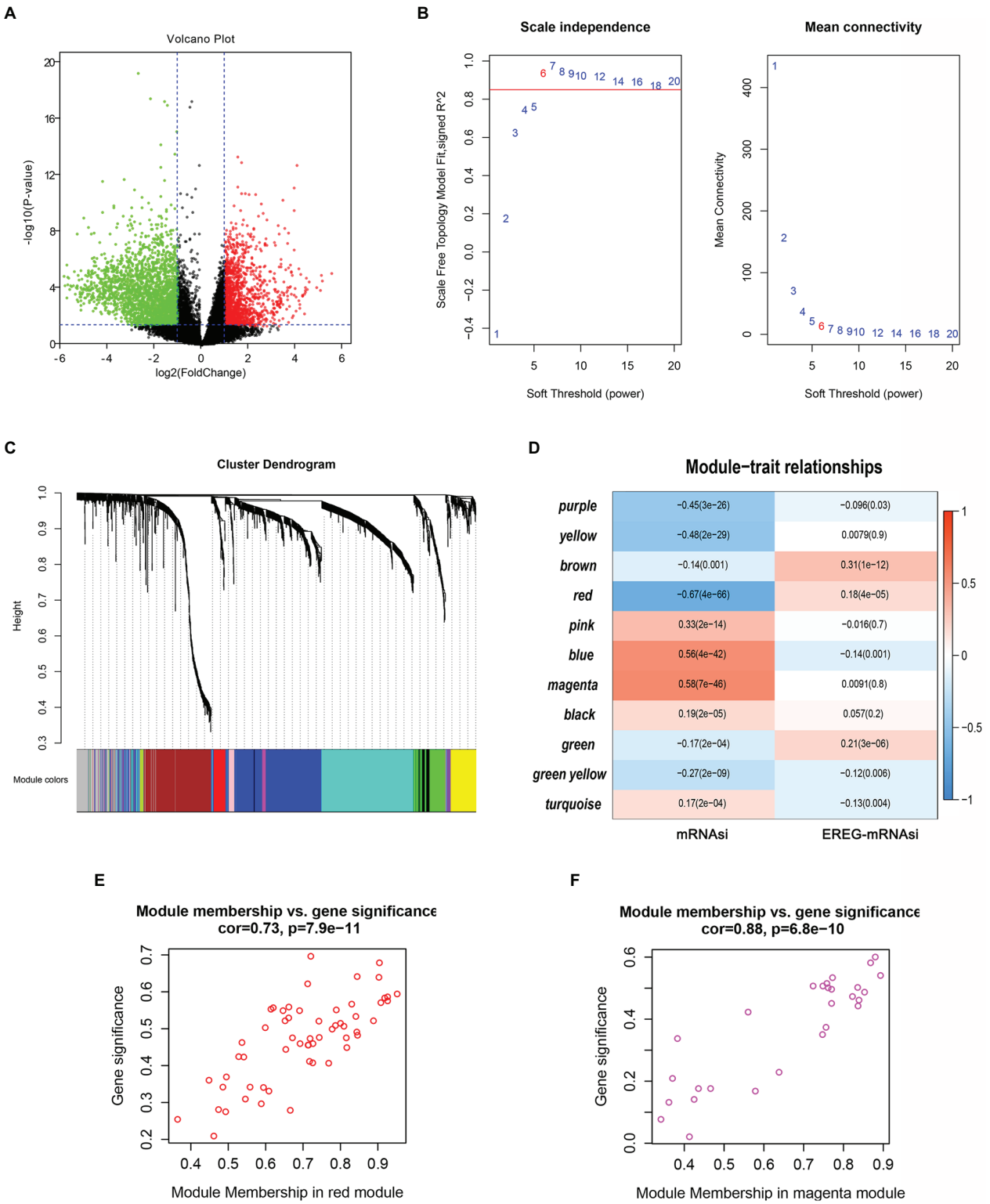

FIGURE 3 | Screening of critical genes related by mRNAsi. **(A)** Volcano plot of differentially expressed genes (DEGs); red represents upregulated genes, and green indicates downregulated genes. **(B,C)** Weighted gene correlation network analysis (WGCNA) of DEGs. Different colors represent different modules. **(D)** Correlation analysis of the modules and clinical traits with mRNAsi or EREG-mRNAsi. Scatter plot analysis of modules in the red **(E)** and magenta **(F)** modules.

multivariate Cox analysis. Based on the results of LASSO Cox regression analysis, a stemness subtype-related prognostic signature was developed. The risk score was calculated as follows: [Expression of PTRF × 0.08845 + Expression of ELF4 × 0.01153 + Expression of ELF5 × 0.2005 + Expression of BTN2A2 × 0.06099 + Expression of HMX1 × (−0.04178) + Expression level of FAAH × (−0.13481) + Expression of RGS16 × 0.10462 + Expression of IL4I1 × 0.12804 + Expression of LUZP2 × (−0.08583) + Expression of PLAT × 0.2138 + Expression of ETV2 × 0.15523].

TABLE 1 | Clinical characteristics of 583 glioma patients from The Cancer Genome Atlas (TCGA) cohort included in this study.

Variables	Number (%)
Vital status	
Alive	370 (63.46%)
Dead	213 (36.54%)
Age	
<60	460 (78.90%)
≥60	123 (21.10%)
Sex	
Female	248 (42.54%)
Male	335 (57.46%)
Tumor grade	
WHO II	224 (38.42%)
WHO III	238 (40.82%)
WHO IV	121 (20.76%)
Molecular subtypes	
IDH mutant and 1p/19q codeletion (LGG)	145 (24.87%)
IDH mutant and 1p/19q non-codel (LGG)	234 (40.14%)
IDH wildtype (LGG)	80 (13.73%)
IDH mutant (GBM)	7 (1.20%)
IDH wildtype (GBM)	101 (17.32%)
Others	16 (2.74%)

LGG, lower-grade glioma; GBM, glioblastoma.

In this prognostic signature, eight genes were negatively associated with OS, and three were positively associated with OS (**Figure 9A**). Based on this prognostic signature, the risk score for each patient was calculated. According to the median cutoff value of risk scores, all patients were divided into high- and low-risk groups in both the training (TCGA dataset) and validation cohorts (CGGA dataset). The distribution of living status and time for each patient in the training and validation cohorts are shown in **Figures 9B,C**. Patients in the high-risk group had a shorter OS than patients in the low-risk group in the training cohort ($p < 0.001$; **Figure 9D**). The time-dependent ROC curve analysis showed that the AUC values of 1, 3, and 5 years were 0.897, 0.892, and 0.826 in the training cohort, respectively ($p < 0.001$; **Figure 9E**). Furthermore, glioma samples (both LGGs and GBM) with an IDH1-mutant type have lower risk scores than IDH1wild-type samples, and the risk scores in LGGs with IDH1-mutant and 1p/19q codeletion samples have lower risk scores than IDH1-mutant and 1p/19q non-codeletion samples (**Figure 9F**). Moreover, we assessed this risk score formula in the CGGA dataset and also found that patients with high-risk scores had poor prognosis in the validation cohort ($p < 0.001$; **Figure 9G**). The time-dependent ROC curve analysis showed that the AUC values of this risk score formula at 1, 3, and 5 years were 0.779, 0.858, and 0.822 in the validation cohort, respectively (**Figure 9H**). The risk scores were also consistent well with the molecular subtypes of glioma (**Figure 9I**).

Development and Evaluation of the Nomogram

In the univariate Cox analysis, the results showed that the risk score, grade, age, IDH status and 1p/19q status were

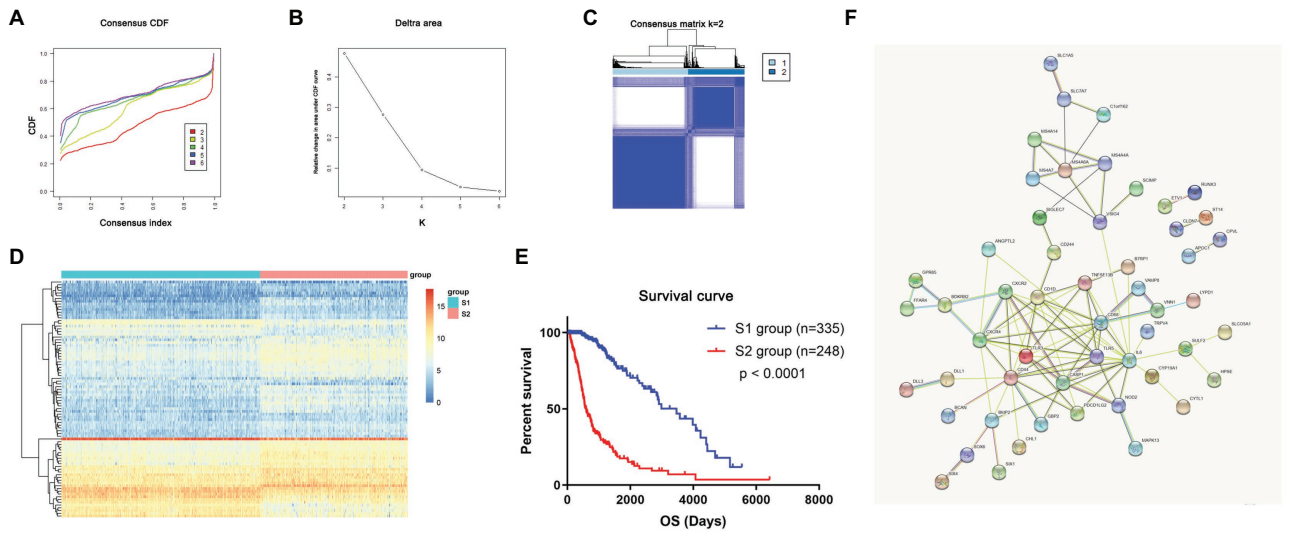

FIGURE 4 | The mRNAsi-related genes could classify glioma into two groups by consensus clustering of TCGA dataset. **(A)** Cumulative distribution function (CDF) for $k = 2$ to $k = 6$. **(B)** Relative change in area under the CDF curve according to different k values. **(C)** Consensus clustering matrix of 583 samples from TCGA dataset for $k = 2$. **(D)** Heatmap of two clusters defined by the expression of mRNAsi genes. **(E)** Survival analysis of patients in the S1 group and S2 group in TCGA cohort. **(F)** Protein-protein interaction (PPI) network of the mRNAsi-related genes.

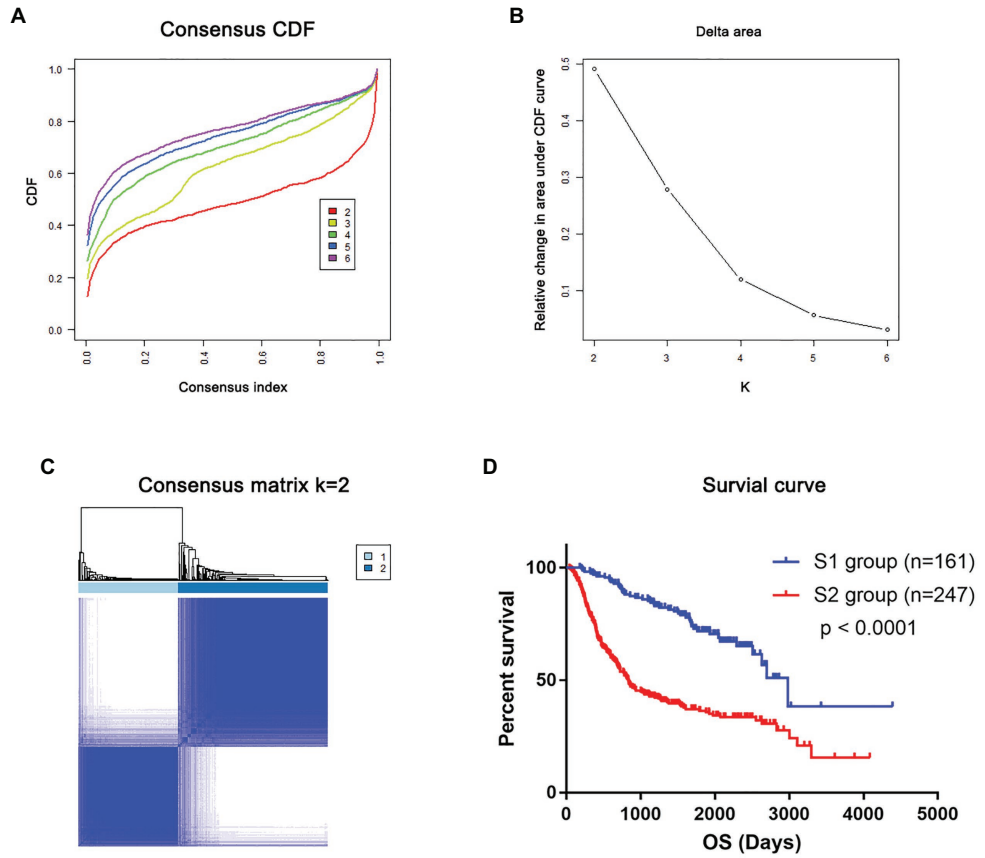

FIGURE 5 | The mRNAsi-related genes could classify glioma into two groups by consensus clustering of the Chinese Glioma Genome Atlas (CGGA) dataset. **(A)** CDF for $k = 2$ to $k = 6$. **(B)** Relative change in area under the CDF curve according to different k values. **(C)** Consensus clustering matrix of 408 samples from TCGA dataset for $k = 2$. **(D)** Survival analysis of patients in the S1 group and S2 group in TCGA cohort.

significantly associated with OS. Then, we performed multivariate Cox regression analyses and the results showed that risk score (HR 1.612; 95% CI 1.258–2.067; p = 1.62E-04), grade (HR 1.488; 95% CI 1.111–1.995; p = 7.76E-03), age (HR 1.035; 95% CI 1.022–1.048; p = 8.85E-08), and 1p/19q status (HR 0.571; 95% CI 0.333–0.980; p = 0.042) were independently related to OS (**Figure 10A**). Based on the risk score and independent prognostic factors (grade, age, and 1p/19q status) in TCGA dataset, we constructed a nomogram model to predict the prognosis of glioma (**Figure 10B**). The calibration plot showed that the predicted values of OS at 1-, 3-, and 5-years for glioma patients had a good correlation with the actual values (**Figure 10C**). Then, the ROC curve analysis of the nomogram also showed a satisfactory evaluation for sensitivity and specificity with a 1-year AUC of 0.909, 3-years AUC of 0.922, and 5-year AUC of 0.874 (**Figure 10D**).

ETV2 Is Involved in the Migration, Invasion, and EMT Process of Glioma Cells

Among the eight genes that were negatively associated with OS, we tested the expression of ETV2 in clinical tissue samples and glioma cell lines. First, we tested the expression of ETV2 in clinical tissue samples with immunohistochemistry. We found that the expression of ETV2 in clinical patients was correlated with WHO grade (**Figure 11A**). We also tested the expression of ETV2 in the SHG44 and A172 cell lines with q-PCR, and the expression of ETV2 in glioma cell lines (SHG44 and A172) was higher than that in the normal human cell line (HEB; **Figure 11B**). Next, we evaluated the effect of ETV2 on glioma cancer cell migration and invasion. Our results revealed that ETV2 knockdown dramatically impaired the cell migration ability of SHG44 and A172 cells relative to the control (**Figures 11C,D**). In *in vitro* invasion assays, the invasion potential was obviously suppressed due to the depletion of ETV2 (**Figures 11E,F**). These findings showed that ETV2 was a significant oncogene associated with the metastatic phenotypes of glioma cells.

EMT may promote the increased migratory capacity and invasiveness of tumor cells (Zhang et al., 2020b). Therefore, we investigated whether ETV2 mediates EMT in glioma. Considering the reduction in epithelial cells, E-cadherin was poorly expressed in glioma, so we tested the expression of vimentin and N-cadherin to analyze the EMT process in

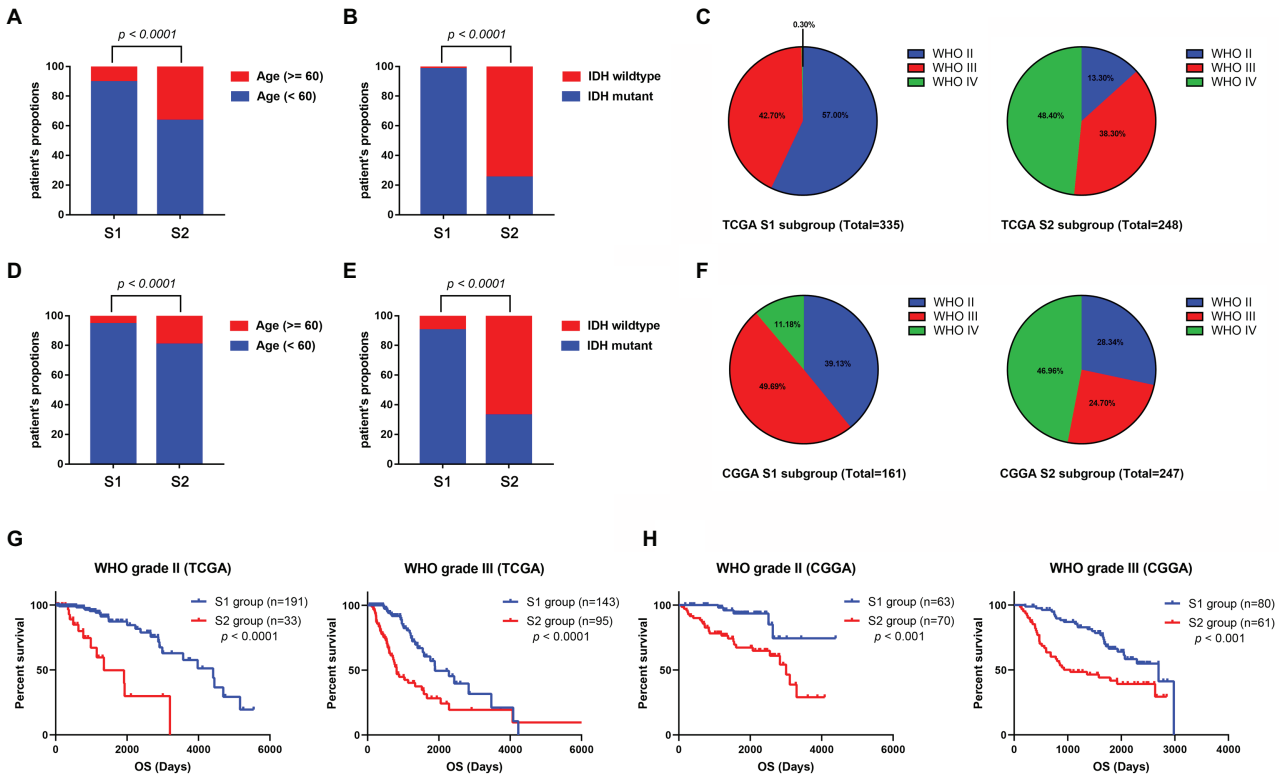

FIGURE 6 | Comparison of the clinical characteristics between the two subtypes using TCGA and CGGA datasets. Histograms to showing that the S2 group of TCGA dataset had significantly more elderly patients **(A)** and more patients with IDH wild-type **(B)**. **(C)** Pie charts show that the S2 group of TCGA datasets has more patients with WHO grade IV glioma and fewer patients with WHO II glioma than the S1 group ($p < 0.001$). Histograms to show that the S2 group of CGGA dataset has significantly more elder patients **(D)** and more patients with IDH wild-type **(E)**. **(F)** Pie charts show that the S2 group of TCGA datasets has more patients with WHO grade IV glioma and fewer patients with WHO II glioma than the S1 group ($p < 0.001$). **(G)** Kaplan-Meier survival curve of S1 and S2 group in different WHO grades (TCGA dataset). **(H)** Kaplan-Meier survival curve of S1 and S2 group in different WHO grades (TCGA dataset).

glioma (Liu et al., 2019). The expression of a mesenchymal marker, N-cadherin, decreased after ETV2 knockdown *via* siRNA. Vimentin is an intermediate filament protein that plays key roles in the integration of cytoskeletal functions and cellular migration. N-cadherin was also decreased after ETV2 knockdown both in both SHG44 and A172 cells. These results indicated that ETV2 is required for the EMT process of glioma.

DISCUSSION

Glioma is the most common and invasive primary brain tumor in adults. Tumor recurrence and treatment resistance are the obstacles to the treatment of glioma. CSCs play essential roles in these processes. Investigating the characteristics of CSCs may facilitate diagnosis, treatment, and prognostic prediction (Chai et al., 2018). In this study, we found that novel molecular subtypes, which based on the stemness index, could effectively predict prognosis in glioma patients. Moreover, the clinical characteristics (age, IDH status, and WHO grades) and tumor microenvironment of the two stemness subtypes are different. This typing could also be validated by the external dataset. Based on the DEGs of the two subtypes, we established a risk score model and a nomogram that could effectively predict the OS of glioma patients. Finally, we selected one gene (ETV2) from the risk score model for experimental validation. To our knowledge, this is the first study to provide a new type of glioma based on the mRNAsi-related genes.

Cancer stemness signatures, which are based on gene expression differences, have been applied to assess the clinical prognosis of some types of tumors (Ben-Porath et al., 2008; Eppert et al., 2011; Pinto et al., 2015). In 2018, Malta et al. (2018) proposed the conception of mRNAsi, which is considered as a more comprehensive index to uncover the characteristics of CSCs. Subsequently, mRNAsi was widely applied to reveal the stemness-related characteristics of different cancers, such as lung cancer (Qin et al., 2020; Zhang et al., 2020a), bladder cancer (Pan et al., 2019), endometrial carcinoma (Liu et al., 2020), medulloblastoma (Lian et al., 2019), and breast cancer (Pei et al., 2020). Moreover, mRNAsi was also used to identify the prognostic biomarkers and therapeutic targets associated with CSC characteristics of glioma (Lvu et al., 2020; Xia et al., 2020). Compared with a previous study, we performed the consensus clustering and identified novel molecular subtypes

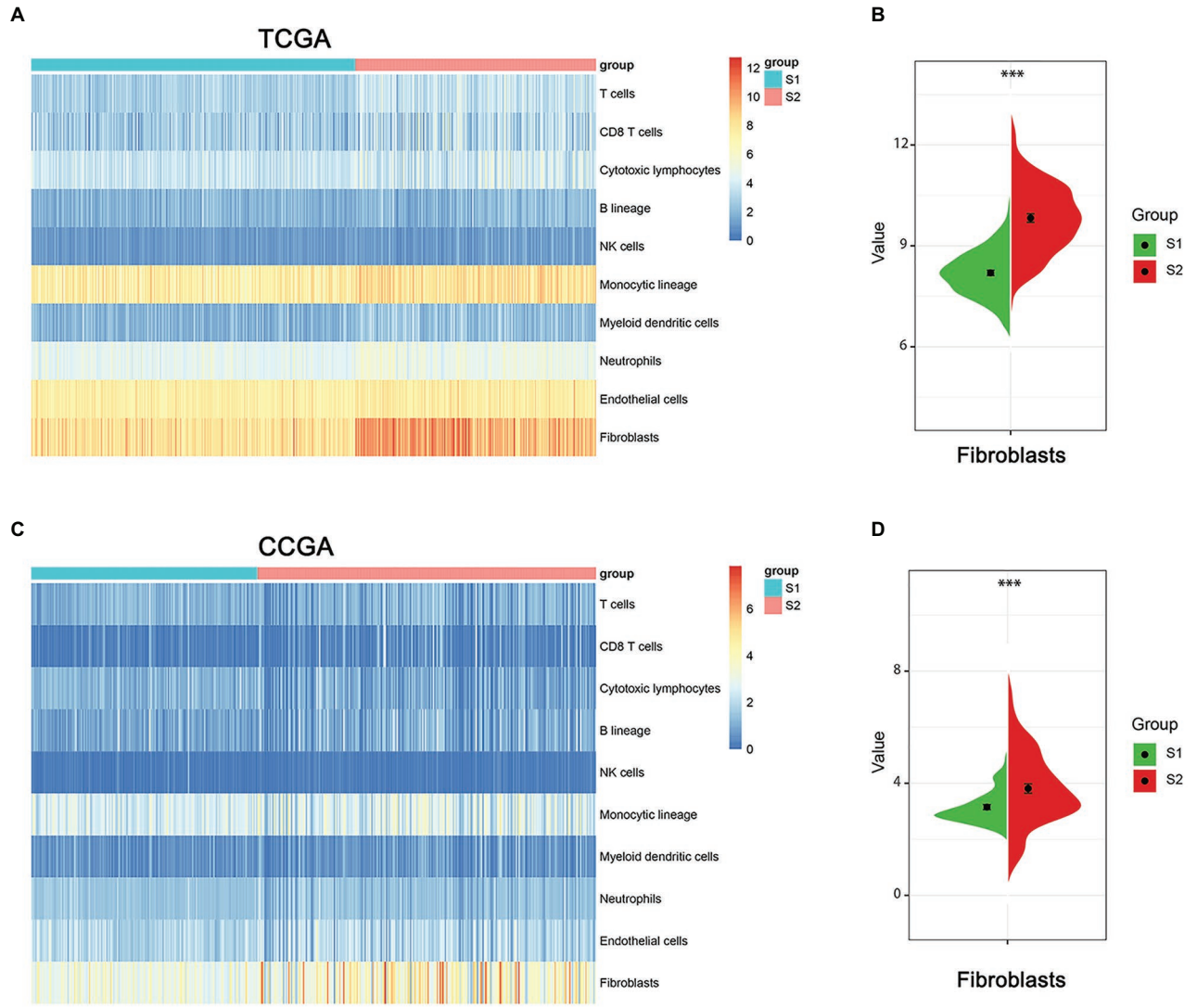

FIGURE 7 | The immune cell infiltrate distribution of the two stemness subtypes. **(A)** Heatmap of immune infiltration cells in the two stemness subtypes of TCGA dataset. **(B)** The proportion of cancer-related fibroblasts in S1 and S2 group of TCGA dataset. ***represents *p* value of less than 0.001. **(C)** Heatmap of immune infiltration cells in the two stemness subtypes of CGGA dataset. **(D)** The proportion of cancer-related fibroblasts in S1 and S2 group of CCGA dataset. ***represents *p* value of less than 0.001.

(S1 and S2 group) of glioma based on mRNAsi-related genes. We also constructed a nomogram model to predict the prognosis of glioma, which has potential for clinical application. More importantly, we performed some *in vitro* experiments to confirm the function of ETV2 in glioma cells.

Gliomas are the most frequent intrinsic tumors of the central nervous system. In the revised fourth edition of the WHO classification of CNS tumors published in 2016, the status of IDH and 1p/19q codeletion was applied in classification (Zhang et al., 2013). In our study, patients in subtype I (S1 group) were younger, more likely to have IDH-mutant status, lower WHO grades and poor prognosis than those in the subtype II (S2 group). Based on our risk score model, we found that glioma samples (both LGGs and GBM) with an IDH1-mutant type have lower risk scores than IDH1wild-type samples, and the risk scores in LGGs with IDH1-mutant and 1p/19q codeletion samples have lower risk scores compared with than IDH1-mutant and 1p/19q non-codeletion samples. The immunological microenvironments between the two subtypes were also different. Gliomas in subtype II (S2 group) are more likely to have a higher proportion of tumor-related immune and stromal cells, especially CAFs. CAFs, one of the main cellular components of the tumor microenvironment, play an important role in promoting cancer cell invasion and dissemination (Hurtado et al., 2020). These results indicated that this new typing could provide novel mechanistic and clinical insights for the diagnosis, treatment, and prognostic prediction of glioma patients.

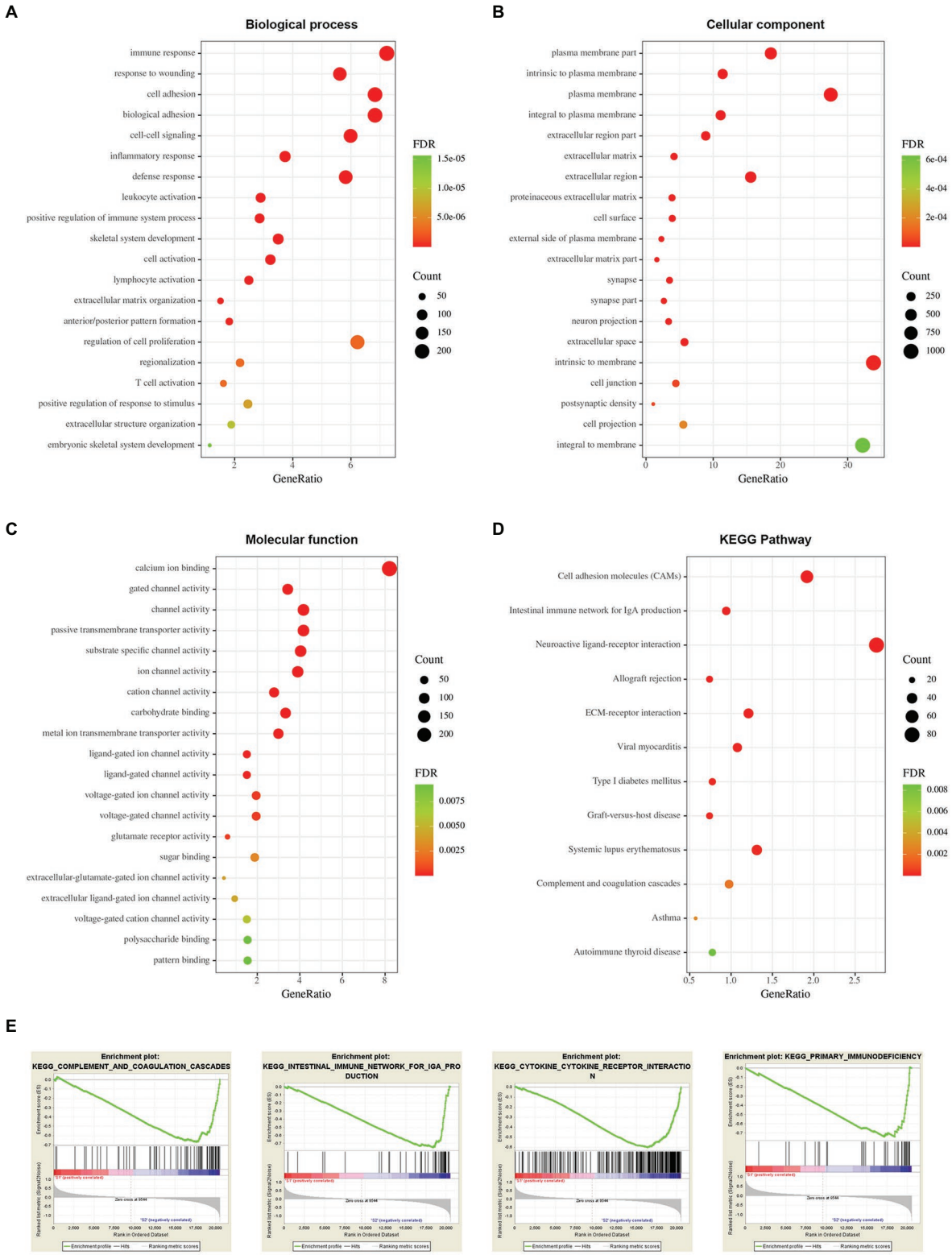

FIGURE 8 | Functional enrichment analysis between two stemness subtypes of TCGA dataset. **(A)** The top 20 terms of biological processes (BP) in DEGs of two stemness subtypes. **(B)** The top 20 terms of cellular components (CC). **(C)** The top 20 terms of molecular functions (MF). **(D)** The Kyoto Encyclopedia of Genes and Genomes (KEGG) pathway in DEGs of two stemness subtypes. **(E)** The top four significantly enriched pathways of gene set enrichment analysis (GSEA).

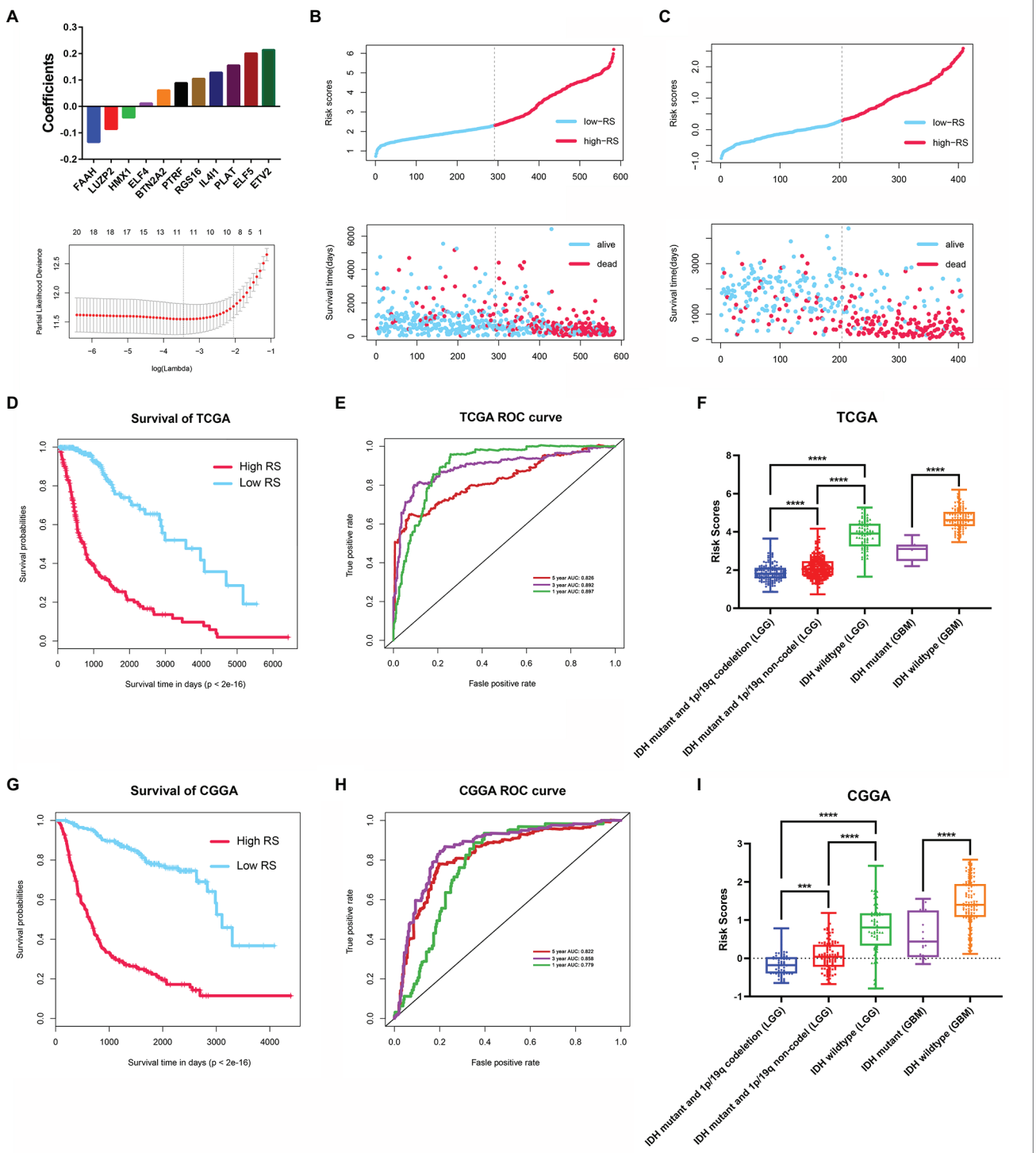

FIGURE 9 | Construction and validation of the stemness subtype-related risk score model. **(A)** The 11 genes were selected by least absolute shrinkage and selection operator (LASSO) Cox analysis in TCGA dataset. Risk scores and living status for each patient in the training cohort **(B)** and the validation cohort **(C)**. **(D)** Kaplan-Meier curves of the OS of each patient in the training cohort. **(E)** Time-dependent ROC curve analysis of the risk score model in the training cohort (TCGA dataset). **(F)** The risk score distributions in different molecular subtypes of glioma (TCGA dataset). **(G)** Kaplan-Meier curves of the OS of each patient in the validation cohort (CCGA dataset). **(H)** Time-dependent ROC curve analysis of the risk score model in the validation cohort (CCGA dataset). **(I)** The risk score distributions in different molecular subtypes of glioma (CGGA dataset). ***$p < 0.001$ and ****$p < 0.0001$.

A

Characteristics	Univariate		Multivariate	
	HR (95%CI)	p-value	HR (95%CI)	p-value
RS	2.717 (2.404-3.071)	**1.34E-57**	1.612 (1.258-2.067)	**1.62E-04**
Grade	4.493 (3.625-5.569)	**8.26E-43**	1.488 (1.111-1.995)	**7.76E-03**
Age	1.066 (1.055-1.077)	**1.25E-32**	1.035(1.022-1.048)	**8.85E-08**
Gender	0.815 (0.614-1.081)	0.155		
IDH status	0.113 (0.084-0.152)	**2.86E-47**	0.767 (0.434-1.357)	0.362
1p/19q status	0.242 (0.151-0.388)	**4.01E-09**	0.571 (0.333-0.980)	**0.042**

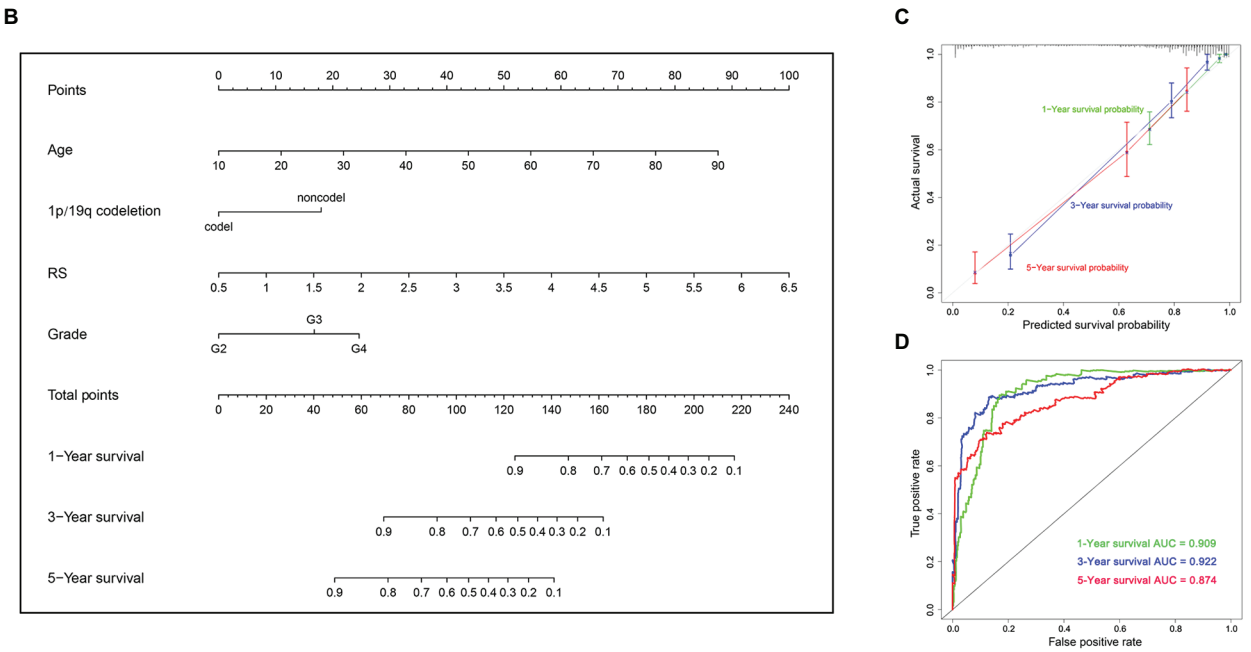

FIGURE 10 | The nomogram based on TCGA dataset for survival prediction in glioma patients. **(A)** Univariate and multivariate Cox regression analysis of clinical features. **(B)** Development a nomogram for the quantitative prediction of 1-, 3-, and 5-years survival for LGG patients. **(C)** The calibration curves for predicting glioma patient 1-, 3-, 5-years survival. **(D)** The 1-, 3-, and 5-year time-dependent ROC curves of the nomogram.

Functional enrichment analysis of the DEGs between two stemness subtypes showed that immune and ECM-related GO terms and pathways were mainly enriched. This implied that the immunological microenvironment and ECM components might have a close relationship with the stemness characteristics of glioma. Previous studies have shown that glioma stem cells interact with immune cells and simulate the early microenvironment during tumorigenesis (Zhai et al., 2020). CSCs can protect cancer cells from immune attack by producing immune inhibitory factors to communicate with tumor microenvironment components (Khosravi et al., 2020). Moreover, CSCs contribute to glioma invasiveness, which is closely correlated with the extracellular matrix (Ortensi et al., 2013). These findings were in accordance with our findings.

In the present study, we also developed a stemness subtype-related prognostic signature. There were 11 essential prognostic genes in this signature, which have not been reported in previous glioma stemness index related publications (Lvu et al., 2020; Xia et al., 2020). Our results are a good supplement to the existing research about the prognosis prediction of patients with glioma. Among the three prognostic genes that were positively associated with OS, LUZP2 is a protein limitedly

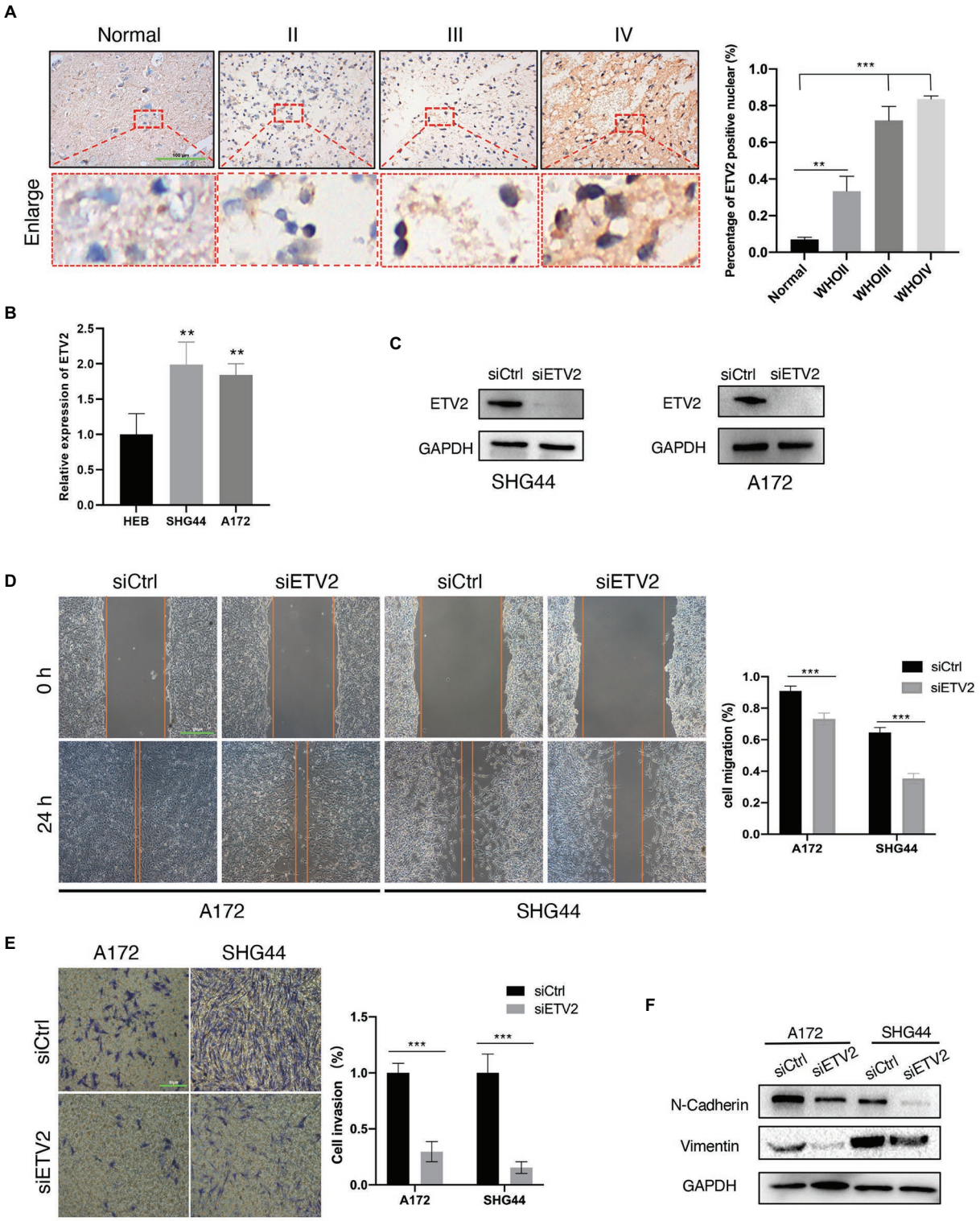

FIGURE 11 | ETV2 is involved in the migration, invasion, and epithelial-mesenchymal transition (EMT) process of glioma cells. **(A)** Expression of ETV2 in IHC stained images of glioma tissues compared with adjacent non-tumor tissues was showed. For quantification, three para-cancerous tissues and five glioma sample for tumor groups were counted, mean values with SD are given, *p*-value is calculated by unpaired *t*-test, $^{**}p < 0.01$ and $^{***}p < 0.001$. **(B)** q-PCR showed the relative

(Continued)

FIGURE 11 | expression of ETV2 in HEB, SHG44, and A172 cells. **(C)** Western blot showed the ETV2 siRNA knockdown efficiency in SHG44 and A172 cells. **(D)** Wound healing assay showed that ETV2 knockdown led to profound impairment in cell migration ability of A172 and SHG44 relative to the control. **(E)** Invasion assays showed that ETV2 depletion resulted in suppression of A172 and SHG44 cell invasion capability. **(F)** Vimentin and N-cadherin levels were detected by western blot analysis in A172 and SHG44 cells after ETV2 knockdown with siRNA. For **(D,E)** mean values with SD form three independent experiments are given. *p*-value is calculated by unpaired *t*-test, ***$p < 0.001$.

expressed in the brain and spinal cord. A recent study showed that low LUZP2 expression independently predicted poor OS in LGG (Li et al., 2020). Fatty-acid amide hydrolase (FAAH), an intracellular serine hydrolase, plays an important role in the inhibition of stem cell migration (Wollank et al., 2015). Among the eight genes that were negatively associated with OS, ETV2, ELF5, IL4I1, and BTN2A2 were novel prognostic biomarkers for glioma, which have not yet been reported yet. ETV2 is a critical factor for vascular development and regeneration, which may contribute to tumorigenesis (Baltrunaite et al., 2017; Choi, 2018). In GBM, ETV2 is sufficient and necessary for the trans-differentiation of GBM stem cells to an endothelial lineage (Humm and Sylvia, 1965). In our study, we found that ETV2 is negatively associated with OS. The expression of ETV2 is closely associated with WHO grade. More importantly, *in vitro* experiment revealed that ETV2 is involved in the migration, invasion, and EMT process of glioma cells. ELF5 is an epithelial-specific member of the E26 transforming sequence (ETS) transcription factor family, which plays critical roles in malignancy, particularly in basal-like and endocrine-resistant forms of breast cancer (Piggin et al., 2016; Singh et al., 2020). IL4I1 and BTN2A2 are both involved in the regulation of the immunologic microenvironment in different tumors (Smith et al., 2010; Sarter et al., 2016; Molinier-Frenkel et al., 2019; Sadik et al., 2020). However, what is their roles in tumorigenesis and progression of glioma are still need further investigation.

There were some limitations in our study. First, there were only very limited normal samples (only five normal samples) included in our study, which might lead to there being no difference in mRNAsi between normal and tumor samples. Second, DEG analysis might neglect some potential mRNAs that were closely related to the mRNAsi. Third, this study is a retrospective study, and the stemness-related typing of glioma should be further confirmed by prospective studies. Finally, the underlying mechanisms of the selected genes in the model affecting the prognosis of glioma should be elucidated by more experiments *in vivo*.

In this study, we identified two distinct stemness-related molecular subtypes of glioma, which could provide new insights for the development of precision diagnosis and prognostic prediction for glioma patients. Moreover, we developed a stemness subtype-related prognostic signature that could effectively predict the prognosis of glioma patients.

DATA AVAILABILITY STATEMENT

The original contributions presented in the study are included in the article/supplementary material, further inquiries can be directed to the corresponding authors.

AUTHOR CONTRIBUTIONS

XJ and WY conceived and designed the study. JT and WY wrote the manuscript. YC, ZX, QZ, and CZ analyzed the results. GT, HL, SW, YG, and ZJ performed the image visualization. JT, HZ, MZ, and CR performed the validation experiment. All authors contributed to the article and approved the submitted version.

FUNDING

This study was supported by the National Natural Science Foundation of China (no. 81472355) and the Hunan Provincial Science and Technology Department (no. 2014FJ6006).

REFERENCES

Baltrunaite, K., Craig, M. P., Palencia Desai, S., Chaturvedi, P., Pandey, R. N., Hegde, R. S., et al. (2017). ETS transcription factors Etv2 and Fli1b are required for tumor angiogenesis. *Angiogenesis* 20, 307–323. doi: 10.1007/s10456-017-9539-8

Becht, E., Giraldo, N. A., Lacroix, L., Buttard, B., Elarouci, N., Petitprez, F., et al. (2016). Estimating the population abundance of tissue-infiltrating immune and stromal cell populations using gene expression. *Genome Biol.* 17:218. doi: 10.1186/s13059-016-1070-5

Ben-Porath, I., Thomson, M. W., Carey, V. J., Ge, R., Bell, G. W., Regev, A., et al. (2008). An embryonic stem cell-like gene expression signature in poorly differentiated aggressive human tumors. *Nat. Genet.* 40, 499–507. doi: 10.1038/ng.127

Bush, N. A., Chang, S. M., and Berger, M. S. (2017). Current and future strategies for treatment of glioma. *Neurosurg. Rev.* 40, 1–14. doi: 10.1007/s10143-016-0709-8

Chai, R., Zhang, K., Wang, K., Li, G., Huang, R., Zhao, Z., et al. (2018). A novel gene signature based on five glioblastoma stem-like cell relevant genes predicts the survival of primary glioblastoma. *J. Cancer Res. Clin. Oncol.* 144, 439–447. doi: 10.1007/s00432-017-2572-6

Choi, K. (2018). ETS transcription factor ETV2/ER71/Etsrp in haematopoietic regeneration. *Curr. Opin. Hematol.* 25, 253–258. doi: 10.1097/MOH.0000000000000430

Clarke, M. F. (2019). Clinical and therapeutic implications of cancer stem cells. *N. Engl. J. Med.* 380, 2237–2245. doi: 10.1056/NEJMra1804280

Eppert, K., Takenaka, K., Lechman, E. R., Waldron, L., Nilsson, B., van Galen, P., et al. (2011). Stem cell gene expression programs influence clinical outcome in human leukemia. *Nat. Med.* 17, 1086–1093. doi: 10.1038/nm.2415

Goeman, J. J. (2010). L1 penalized estimation in the cox proportional hazards model. *Biom. J.* 52, 70–84. doi: 10.1002/bimj.200900028

Huang, W. D., Sherman, B. T., and Lempicki, R. A. (2009a). Systematic and integrative analysis of large gene lists using DAVID bioinformatics resources. *Nat. Protoc.* 4, 44–57. doi: 10.1038/nprot.2008.211

Huang, W. D., Sherman, B. T., and Lempicki, R. A. (2009b). Bioinformatics enrichment tools: paths toward the comprehensive functional analysis of large gene lists. *Nucleic Acids Res.* 37, 1–13. doi: 10.1093/nar/gkn923

Humm, D. G., and Sylvia, A. L. (1965). Soluble proteins of a melanoma and normal skin from the swordtail, platyfish, and their hybrids. *Science* 150, 635–636. doi: 10.1126/science.150.3696.635

Hurtado, P., Martínez-Pena, I., and Piñeiro, R. (2020). Dangerous liaisons: circulating tumor cells (CTCs) and cancer-associated fibroblasts (CAFs). *Cancer* 12:2861. doi: 10.3390/cancers12102861

Jia, W., Jiang, X., Liu, W., Wang, L., Zhu, B., Zhu, H., et al. (2018). Effects of three-dimensional collagen scaffolds on the expression profiles and biological functions of glioma cells. *Int. J. Oncol.* 52, 1787–1800. doi: 10.3892/ijo.2018.4330

Khosravi, N., Mokhtarzadeh, A., Baghbanzadeh, A., Hajiasgharzadeh, K., Shahgoli, V. K., Hemmat, N., et al. (2020). Immune checkpoints in tumor microenvironment and their relevance to the development of cancer stem cells. *Life Sci.* 256:118005. doi: 10.1016/j.lfs.2020.118005

Klughammer, J., Kiesel, B., Roetzer, T., Fortelny, N., Nemc, A., Nenning, K. H., et al. (2018). The DNA methylation landscape of glioblastoma disease progression shows extensive heterogeneity in time and space. *Nat. Med.* 24, 1611–1624. doi: 10.1038/s41591-018-0156-x

Langfelder, P., and Horvath, S. (2008). WGCNA: an R package for weighted correlation network analysis. *BMC Bioinformatics* 9:559. doi: 10.1186/1471-2105-9-559

Li, Y., Deng, G., Qi, Y., Zhang, H., Jiang, H., Geng, R., et al. (2020). Downregulation of LUZP2 Is correlated with poor prognosis of low-grade glioma. *Biomed. Res. Int.* 2020:9716720. doi: 10.1155/2020/9716720

Lian, H., Han, Y. P., Zhang, Y. C., Zhao, Y., Yan, S., Li, Q. F., et al. (2019). Integrative analysis of gene expression and DNA methylation through one-class logistic regression machine learning identifies stemness features in medulloblastoma. *Mol. Oncol.* 13, 2227–2245. doi: 10.1002/1878-0261.12557

Liu, N., Wang, Z., Liu, D., and Xie, P. (2019). HOXC13-AS-miR-122-5p-SATB1-C-Myc feedback loop promotes migration, invasion and EMT process in glioma. *OncoTargets Ther.* 12, 7165–7173. doi: 10.2147/OTT.S220027

Liu, J., Wu, Z., Sun, R., Nie, S., Meng, H., Zhong, Y., et al. (2020). Using mRNAsi to identify prognostic-related genes in endometrial carcinoma based on WGCNA. *Life Sci.* 258:118231. doi: 10.1016/j.lfs.2020.118231

Lvu, W., Fei, X., Chen, C., and Zhang, B. (2020). In silico identification of the prognostic biomarkers and therapeutic targets associated with cancer stem cell characteristics of glioma. *Biosci. Rep.* 40:BSR20201037. doi: 10.1042/BSR20201037

Ma, X., Chen, J., Liu, J., Xu, B., Liang, X., Yang, X., et al. (2020). IL-8/CXCR2 mediates tropism of human bone marrow-derived mesenchymal stem cells toward CD133(+) /CD44(+) colon cancer stem cells. *J. Cell. Physiol.* 236, 3114–3128. doi: 10.1002/jcp.30080

Malta, T. M., Sokolov, A., Gentles, A. J., Burzykowski, T., Poisson, L., Weinstein, J. N., et al. (2018). Machine learning identifies stemness features associated with oncogenic dedifferentiation. *Cell* 173, 338.e15–354.e15. doi: 10.1016/j.cell.2018.03.034

Molinier-Frenkel, V., Prévost-Blondel, A., and Castellano, F. (2019). The IL4I1 enzyme: a new player in the immunosuppressive tumor microenvironment. *Cells* 8:757. doi: 10.3390/cells8070757

Nabors, L. B., Portnow, J., Ammirati, M., Baehring, J., Brem, H., Butowski, N., et al. (2017). NCCN guidelines insights: central nervous system cancers, version 1.2017. *J. Natl. Compr. Cancer Netw.* 15, 1331–1345. doi: 10.6004/jnccn.2017.0166

Ortensi, B., Setti, M., Osti, D., and Pelicci, G. (2013). Cancer stem cell contribution to glioblastoma invasiveness. *Stem Cell Res. Ther.* 4:18. doi: 10.1186/scrt166

Osman, A., Oze, M., Afify, S. M., Hassan, G., El-Ghlban, S., Nawara, H. M., et al. (2020). Tumor-associated macrophages derived from cancer stem cells. *Acta Histochem.* 122:151628. doi: 10.1016/j.acthis.2020.151628

Ostrom, Q. T., Bauchet, L., Davis, F. G., Deltour, I., Fisher, J. L., Langer, C. E., et al. (2014). The epidemiology of glioma in adults: a "state of the science" review. *Neuro Oncol.* 16, 896–913. doi: 10.1093/neuonc/nou087

Pan, S., Zhan, Y., Chen, X., Wu, B., and Liu, B. (2019). Identification of biomarkers for controlling cancer stem cell characteristics in bladder cancer by network analysis of transcriptome data stemness indices. *Front. Oncol.* 9:613. doi: 10.3389/fonc.2019.00613

Pei, J., Wang, Y., and Li, Y. (2020). Identification of key genes controlling breast cancer stem cell characteristics via stemness indices analysis. *J. Transl. Med.* 18:74. doi: 10.1186/s12967-020-02260-9

Piggin, C. L., Roden, D. L., Gallego-Ortega, D., Lee, H. J., Oakes, S. R., and Ormandy, C. J. (2016). ELF5 isoform expression is tissue-specific and significantly altered in cancer. *Breast Cancer Res.* 18:4. doi: 10.1186/s13058-015-0666-0

Pinto, J. P., Kalathur, R. K., Oliveira, D. V., Barata, T., Machado, R. S., Machado, S., et al. (2015). StemChecker: a web-based tool to discover and explore stemness signatures in gene sets. *Nucleic Acids Res.* 43, W72–W77. doi: 10.1093/nar/gkv529

Prieto-Vila, M., Takahashi, R. U., Usuba, W., Kohama, I., and Ochiya, T. (2017). Drug resistance driven by cancer stem cells and their niche. *Int. J. Mol. Sci.* 18:2574. doi: 10.3390/ijms18122574

Qin, S., Long, X., Zhao, Q., and Zhao, W. (2020). Co-expression network analysis identified genes associated with cancer stem cell characteristics in lung squamous cell carcinoma. *Cancer Invest.* 38, 13–22. doi: 10.1080/07357907.2019.1697281

Sadik, A., Somarribas Patterson, L. F., Öztürk, S., Mohapatra, S. R., Panitz, V., Secker, P. F., et al. (2020). IL4I1 is a metabolic immune checkpoint that activates the AHR and promotes tumor progression. *Cell* 182, 1252.e34–1270.e34. doi: 10.1016/j.cell.2020.07.038

Sarter, K., Leimgruber, E., Gobet, F., Agrawal, V., Dunand-Sauthier, I., Barras, E., et al. (2016). Btn2a2, a T cell immunomodulatory molecule coregulated with MHC class II genes. *J. Exp. Med.* 213, 177–187. doi: 10.1084/jem.20150435

Schulz, A., Meyer, F., Dubrovska, A., and Borgmann, K. (2019). Cancer stem cells and radioresistance: DNA repair and beyond. *Cancer* 11:862. doi: 10.3390/cancers11060862

Singh, S., Kumar, S., Srivastava, R. K., Nandi, A., Thacker, G., Murali, H., et al. (2020). Loss of ELF5-FBXW7 stabilizes IFNGR1 to promote the growth and metastasis of triple-negative breast cancer through interferon-γ signalling. *Nat. Cell Biol.* 22, 591–602. doi: 10.1038/s41556-020-0495-y

Smith, I. A., Knezevic, B. R., Ammann, J. U., Rhodes, D. A., Aw, D., Palmer, D. B., et al. (2010). BTN1A1, the mammary gland butyrophilin, and BTN2A2 are both inhibitors of T cell activation. *J. Immunol.* 184, 3514–3525. doi: 10.4049/jimmunol.0900416

Vlashi, E., and Pajonk, F. (2015). Cancer stem cells, cancer cell plasticity and radiation therapy. *Semin. Cancer Biol.* 31, 28–35. doi: 10.1016/j.semcancer.2014.07.001

Wang, J., Li, X., Wu, H., Wang, H., Yao, L., Deng, Z., et al. (2019). EMP1 regulates cell proliferation, migration, and stemness in gliomas through PI3K-AKT signaling and CD44. *J. Cell. Biochem.* 120, 17142–17150. doi: 10.1002/jcb.28974

Wilkerson, M. D., and Hayes, D. N. (2010). ConsensusClusterPlus: a class discovery tool with confidence assessments and item tracking. *Bioinformatics* 26, 1572–1573. doi: 10.1093/bioinformatics/btq170

Wollank, Y., Ramer, R., Ivanov, I., Salamon, A., Peters, K., and Hinz, B. (2015). Inhibition of FAAH confers increased stem cell migration via PPARα. *J. Lipid Res.* 56, 1947–1960. doi: 10.1194/jlr.M061473

Xia, P., Li, Q., Wu, G., and Huang, Y. (2020). Identification of glioma cancer stem cell characteristics based on weighted gene prognosis module co-expression network analysis of transcriptome data stemness indices. *J. Mol. Neurosci.* 70, 1512–1520. doi: 10.1007/s12031-020-01590-z

Yin, W., Jiang, X., Tan, J., Xin, Z., Zhou, Q., Zhan, C., et al. (2020). Development and validation of a tumor mutation burden-related immune prognostic model for lower-grade glioma. *Front. Oncol.* 10:1409. doi: 10.3389/fonc.2020.01409

Yoshihara, K., Shahmoradgoli, M., Martínez, E., Vegesna, R., Kim, H., Torres-Garcia, W., et al. (2013). Inferring tumour purity and stromal and immune cell admixture from expression data. *Nat. Commun.* 4:2612. doi: 10.1038/ncomms3612

Yu, G., Wang, L. G., Han, Y., and He, Q. Y. (2012). clusterProfiler: an R package for comparing biological themes among gene clusters. *OMICS* 16, 284–287. doi: 10.1089/omi.2011.0118

Zhai, Y., Li, G., Li, R., Chang, Y., Feng, Y., Wang, D., et al. (2020). Single-cell RNA-sequencing shift in the interaction pattern between glioma stem cells

and immune cells during tumorigenesis. *Front. Immunol.* 11:581209. doi: 10.3389/fimmu.2020.581209

Zhang, C., Bao, Z., Zhang, W., and Jiang, T. (2013). Progress on molecular biomarkers and classification of malignant gliomas. *Front. Med.* 7, 150–156. doi: 10.1007/s11684-013-0267-1

Zhang, Y., Tseng, J. T., Lien, I. C., Li, F., Wu, W., and Li, H. (2020a). mRNAsi index: machine learning in mining lung adenocarcinoma stem cell biomarkers. *Genes* 11:257. doi: 10.3390/genes11121395

Zhang, Q., Yang, L., Guan, G., Cheng, P., Cheng, W., and Wu, A. (2020b). LOXL2 upregulation in gliomas drives tumorigenicity by activating autophagy to promote TMZ resistance and trigger EMT. *Front. Oncol.* 10:569584. doi: 10.3389/fonc.2020.569584

Conflict of Interest: The authors declare that the research was conducted in the absence of any commercial or financial relationships that could be construed as a potential conflict of interest.

frontiers in Cell and Developmental Biology

ORIGINAL RESEARCH
published: 11 June 2021
doi: 10.3389/fcell.2021.668833

Detection of Hematopoietic Stem Cell Transcriptome in Human Fetal Kidneys and Kidney Organoids Derived From Human Induced Pluripotent Stem Cells

*Jin Wook Hwang[1,2], Christophe Desterke[1,2], Julien Loisel-Duwattez[3], Frank Griscelli[1,2,4,5], Annelise Bennaceur-Griscelli[1,2,4,5] and Ali G. Turhan[1,2,4,5]**

[1] INSERM U935/UA09, Université Paris-Saclay, Villejuif, France, [2] ESTeam Paris Sud, Université Paris Sud, Villejuif, France, [3] INSERM U1195, AP-HP, Service de Neurologie, Faculté de Médecine, Hôpital Bicêtre, Université Paris-Saclay, Le Kremlin-Bicêtre, France, [4] INGESTEM National IPSC Infrastructure, Villejuif, France, [5] Division of Hematology, AP-HP Paris Saclay, Le Kremlin-Bicêtre, France

OPEN ACCESS

Edited by:
Nikhil Baban Ghate,
University of Southern California,
United States

Reviewed by:
Hengbin Wang,
University of Alabama at Birmingham,
United States
Louis Charles Penning,
Utrecht University, Netherlands

***Correspondence:**
Ali G. Turhan
turviv33@gmail.com

Specialty section:
This article was submitted to Stem Cell Research, a section of the journal Frontiers in Cell and Developmental Biology

Received: 17 February 2021
Accepted: 12 May 2021
Published: 11 June 2021

Citation:
Hwang JW, Desterke C, Loisel-Duwattez J, Griscelli F, Bennaceur-Griscelli A and Turhan AG (2021) Detection of Hematopoietic Stem Cell Transcriptome in Human Fetal Kidneys and Kidney Organoids Derived From Human Induced Pluripotent Stem Cells. Front. Cell Dev. Biol. 9:668833. doi: 10.3389/fcell.2021.668833

Background: In mammalians, hematopoietic stem cells (HSCs) arise in the dorsal aorta from the hemogenic endothelium, followed by their migration to the fetal liver and to the bone marrow. In zebrafish, the kidney is the site of primary hematopoiesis. In humans, the presence of HSCs in the fetal or adult kidney has not been established.

Methods: We analyzed the presence of HSC markers in the human fetal kidneys by analysis of single-cell datasets. We then analyzed in kidney organoids derived from induced pluripotent stem cells (iPSCs) the presence of hematopoietic markers using transcriptome analyses.

Results: Twelve clusters were identified as stromal, endothelial, and nephron cell type-specific markers in the two fetal stage (17 weeks) kidney datasets. Among these, the expression of hematopoietic cells in cluster 9 showed an expression of primitive markers. Moreover, whole transcriptome analysis of our iPSC-derived kidney organoids revealed induction of the primitive hematopoietic transcription factor RUNX1 as found in the human fetal kidney cortex.

Conclusion: These finding support the presence of cells expressing HSC transcriptome in the human kidney. The mechanisms of the appearance of the cells with the same transcriptional features during iPSC-derived kidney organoid generation require further investigation.

Keywords: hematopoietic stem cell, fetal kidney, IPSC, organoid, transcriptome

INTRODUCTION

Hematopoietic stem cells (HSCs) are characterized by their capacity of both self-renewal and differentiation into blood and immune cell lineages throughout the life of the individual in a stem cell-regulating microenvironment, or HSC niche. HSC-niche interactions in the bone marrow, liver, and kidney have been extensively studied using vertebrate animal models, including mice,

frogs, zebrafish, and chickens (Mikkola and Orkin, 2006; Gao et al., 2018). During mammalian hematopoiesis, the most primitive hematopoietic cells migrate from the aorta–gonad–mesonephros (AGM) region to the fetal liver and to the bone marrow, which is the site of adult hematopoiesis (Gao et al., 2018). However, the persistence of some degree of hematopoietic activity in adult tissues is possible, as this has been suggested by the discovery of donor-derived chimeric hematopoiesis after liver transplantation showing the contribution of donor-derived cells to hematopoiesis (Taniguchi et al., 1996). To our knowledge, there has been no study analyzing the possibility of donor-derived hematopoiesis after kidney transplantation. It should be reminded that in the majority of cases, kidney transplants are performed using kidneys from deceased donors (Stachura et al., 2009; Butler et al., 2018). HSC-kidney niche interactions have been studied in many reports. For example, zebrafish kidney stromal cell lines can support and maintain early hematopoietic precursors and differentiation of lymphoid, myeloid, and erythroid precursors (Stachura et al., 2009).

Recent advances in single-cell RNA sequencing technology are leading to new discoveries and validation in fetal organs and organoids (Butler et al., 2018; Menon et al., 2018; Park et al., 2018). Here, we first analyzed the presence of transcriptional markers of HSCs in fetal kidneys through analysis of a single-cell dataset described by Butler et al. (2018), Lindström et al. (2018), Menon et al. (2018), and Park et al. (2018). We then performed a transcriptome analysis of induced pluripotent stem cell (iPSC)-derived kidney organoids. We show that HSC-related markers can be detected in both fetal kidneys and the human iPSC-derived kidney organoids.

RESULTS

Human Fetal Kidney Cortex Harbors Cells Expressing Hematopoietic Transcripts

Single-cell transcriptome is a powerful technology to investigate cell heterogeneity in a tissue. Butler et al. (2018), Lindström et al. (2018), Menon et al. (2018), and Park et al. (2018) performed these experiments in cortex tissues isolated from two human fetal kidneys (17 weeks) by 10× genomics technology. This work allowed us to perform *in silico* analyses. To this end, we merged and analyzed with Seurat package the 2 respective MTX files generated by cell ranger in order to suppress batch error and to perform downstream unsupervised analysis. To build the common matrix of the two samples, genes that were found expressed in a minimum of five cells by sample were conserved. After the data from the two kidney samples were merged, the Seurat digital matrix comprised 7,860 cells for 18,119 transcripts. During batch correction with canonical correlation, we observed that the two kidney samples were found well superposed in first factorial map of canonical correlation (**Supplementary Figure 1A**) and the shared correlation strength decreases on the 30 components of canonical correlation (**Supplementary Figure 1B**). t-Distributed stochastic neighbor embedding (tSNE) analysis on the common variable genes on the 40 principal components of the principal component analysis allowed to identify 12 clusters (**Figure 1A**) reproducible in both kidneys (**Supplementary Figure 1C**). Majority of the tSNE central cells comprising clusters 3, 2, 0, and 1 expressed mesoderm transcription factor TCF21 (**Figure 1A** and **Supplementary Figure 2**); also, an expression of TCF21 is positive in cells from cluster 6, which highly expressed matrix molecules such as lumican (LUM) (**Figure 1A** and **Supplementary Figure 2**), decorin (DCN), and collagens (COL3A1, COL1A1, and COL1A2) (**Figure 1B**). In cluster 4, cells were found to be positive for KDR (**Figure 1A**) and CD34 (data not shown), suggesting an expression profile corresponding to endothelial cells. Cells identified in cluster 7 have a high expression of downstream NOTCH pathway transcription factor HEY1 such as cells from cluster 0, which are central proximal from this position during tSNE analysis (**Figure 1A**). Some clusters of cells that are left eccentric (clusters 8 and 11) expressed tubular markers such as FXYD2 (**Figure 1A** and **Supplementary Figure 2**), encoding the sodium/potassium-transporting ATPase subunit gamma. Cluster of cells number 10, also left eccentric during tSNE analysis expressed some podocyte markers such as Protein Tyrosine Phosphatase Receptor Type O (PTPRO) (**Figure 1A** and **Supplementary Figure 2**), but also SOST (Sclerostin and PODXL: podocalyxin like) (**Figure 1B**). Cluster of cells number 5 expressed specifically the renin molecule a well-known renal molecule (**Figure 1A** and **Supplementary Figure 2**). These results suggest that tSNE analysis performed post canonical analysis in these two merged samples reflect the cell diversity compatible with kidney organ at this stage of development described in the original paper (Lindström et al., 2018). Surprisingly, in unsupervised tSNE analysis of the human kidney cortex, we found the left-top eccentric cluster number 9 (**Figure 1A**), which is principally defined by the specific expression of serglycin (SRGN) (**Figures 1A**, **2A** and **Supplementary Table 1**). SRGN is known to be a hematopoietic cell granule proteoglycan. In this cluster of cells, there is also a specific expression of hematopoietic cluster of differentiation such as PTPRC alias CD45 and CD44 (**Figure 2B**). Some molecules such as CD74 and HLA-DRA implicated in antigen-presenting cell functionalities are also expressed in this cluster of cells (**Figure 2C**). Interestingly, a fraction of cells from cluster 9 also expressed primitive hematopoietic transcription factors such as SPI1 (alias PU.1) and RUNX1 (**Figure 2D**). Some of the cells from the same cluster also expressed CXCR4 receptor, which is well known to be expressed on primitive human hematopoietic cells for their homing function. These original results on cluster 9 suggest the presence of cells with hematopoietic transcriptome with some of them expressing primitive markers in the human kidney cortex at fetal stage (17 weeks).

Generation and Characterization of Induced Pluripotent Stem Cell-Derived Kidney Organoids

Human iPSC-derived kidney organoids have been generated as previously described (Hwang et al., 2019). Briefly, iPSC

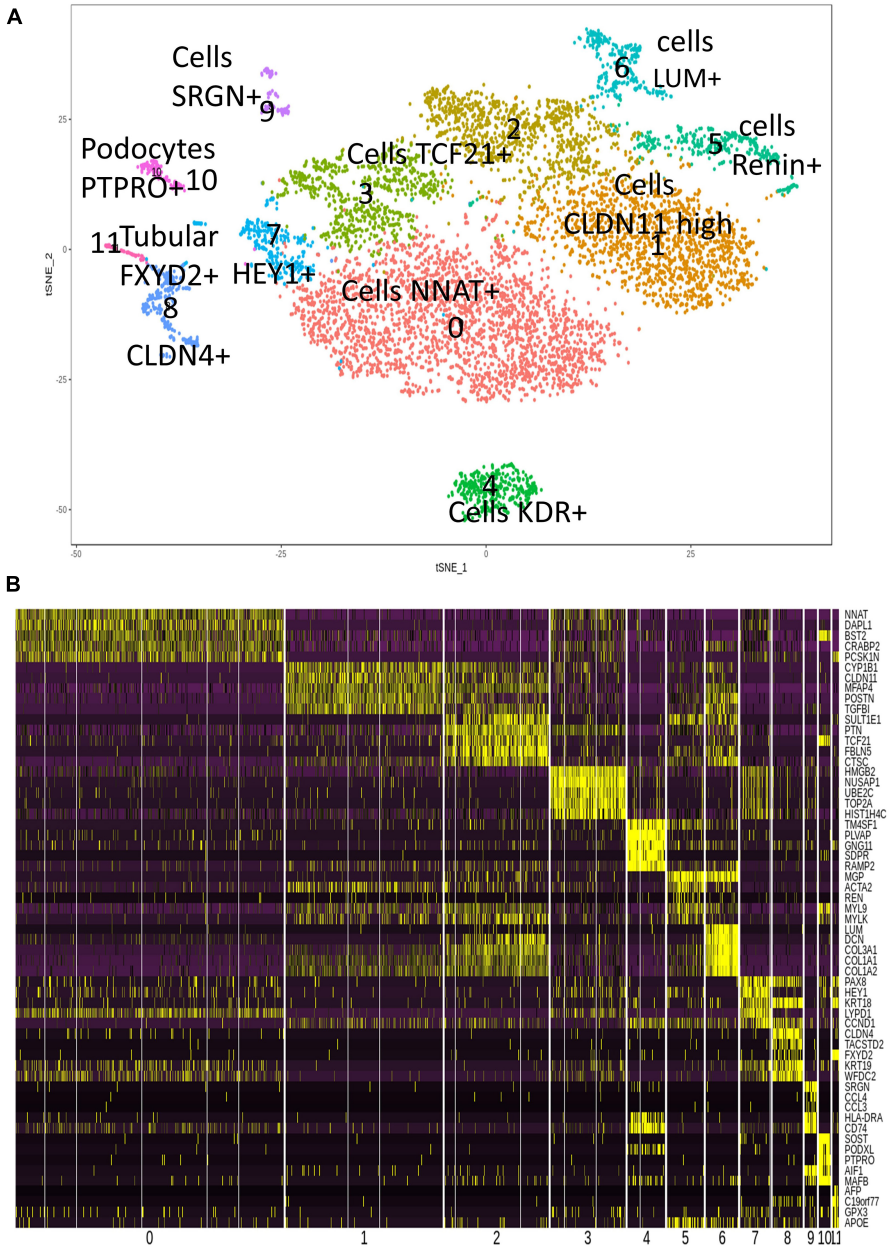

FIGURE 1 | Cell heterogeneity in human fetal kidney cortex by single-cell transcriptome. **(A)** t-Distributed stochastic neighbor embedding (tSNE) plot with 11 cell clusters from the combined analysis of the merged fetal kidney cortex (two human kidneys, 17 weeks; 7,860 cells) after canonical correlation. **(B)** Heatmap with the expression pattern of the top five cluster-specific genes in 11 clusters identified in human fetal kidney cortex.

aggregates were generated in E8 media and Geltrex matrix leading to spontaneous formation of complex kidney organoids at days 12–14 of the culture (**Figure 3A**). We characterized iPSC-derived kidney organoids using whole-mounting staining with confocal imaging. As can be seen in **Figure 3B**, glomeruli-like structures, which contained cells stained for the nephron marker Nephrin, were easily identified (Ruotsalainen et al., 2000). Moreover, ultrastructure analyses revealed cell–cell junctions and the podocyte foot process formation in kidney organoids (**Figure 3C**).

Detection of a Hematopoietic Transcriptome Program Induced Pluripotent Stem Cell-Derived Kidney Organoids

We performed, in duplicate, whole transcriptome analysis of iPSC-derived kidney organoids as compared with native iPSC with Clariom S human technology. After Robust Multi-array Average (RMA) normalization, we identified 3,546 differentially expressed genes (DEGs) with LIMMA

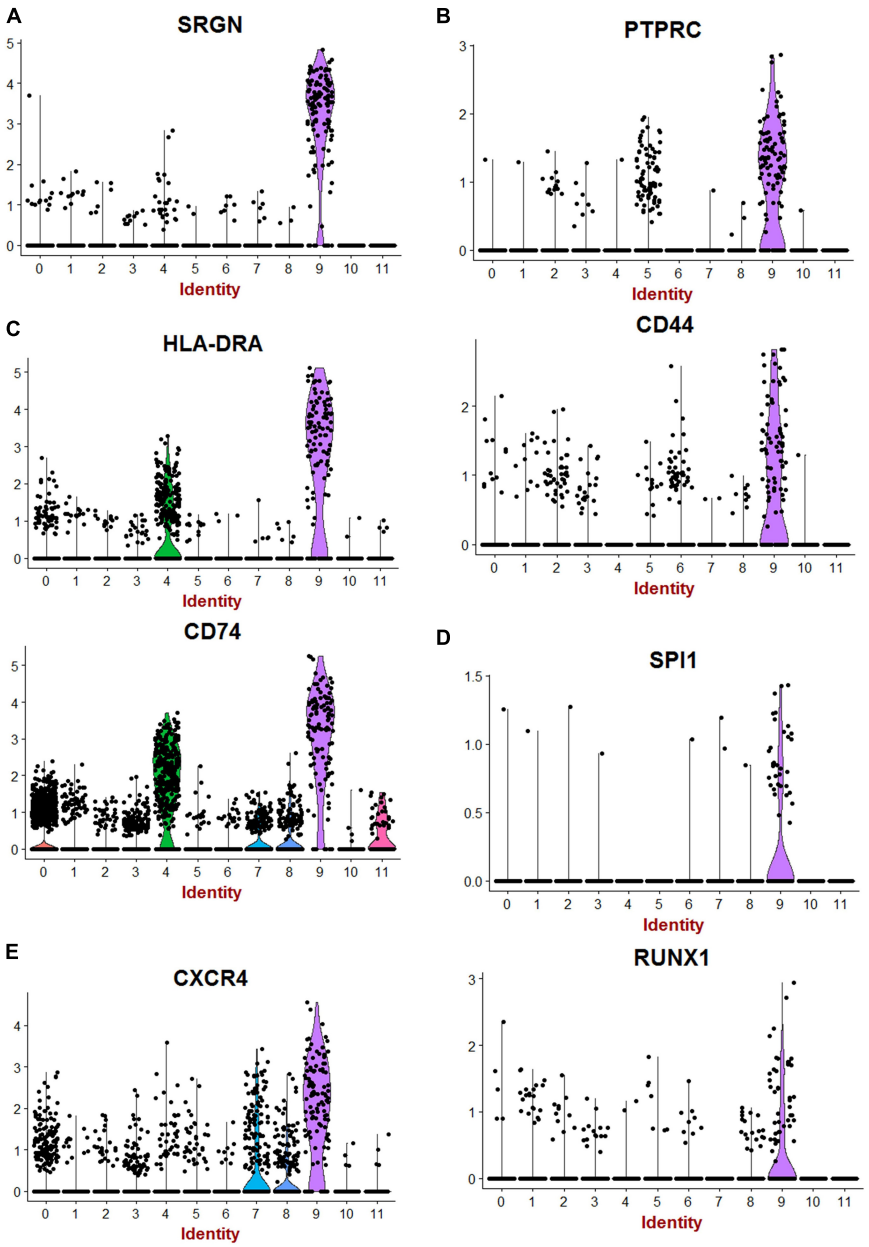

FIGURE 2 | Hematopoietic transcripts detected in human fetal kidney cortex by single-cell RNA sequencing. **(A)** Violin plot of serglycin (SRGN) expression. **(B)** Violin plot of hematopoietic clusters of differentiation (PTPRC Alias CD45). **(C)** Violin plot of expression of transcripts of differentiated hematopoietic cells (HLA-DRA:HLA-DR Alpha). **(D)** Violin plot of expression of SPI1 (PU.1) and RUNX1. **(E)** Violin plot of expression for CXCR4 receptor.

algorithm (**Figure 4A**) comprising 1,432 upregulated genes. This DEG profile allowed to discriminate experimental sample groups by unsupervised classification (**Figure 4B**). After functional enrichment on WikiPathways database, we identified a hematopoietic program in iPSC-derived kidney organoids. Especially, we uncovered an upregulation of RUNX1 and CD34 corresponding to genes expressed in HSCs and that of FLI1, CXCR4, and MXI1 downstream at erythrocyte and megakaryocyte progenitor levels. There was also a repression of MYB megakaryocytic repressor (**Figure 4C**). These results suggest the implication of a hematopoietic transcriptional program in our iPSC-derived kidney organoids and especially induction of the primitive hematopoietic transcription factor RUNX1, which was also detectable at the single-cell level (**Figure 2D**) in human *ex vivo* fetal kidney cortex.

Transcriptome data of iPSCs and organoids have been submitted on National Center for Biotechnology Information (NCBI) Gene Expression Omnibus (GEO) data repository under GEO accession number Series GSE172319.

DISCUSSION

The involvement of kidney in hematopoiesis has been clearly demonstrated in zebrafish (Ej and Li, 2010). In humans, the most primitive hematopoietic cells arise from mesodermal lineage in AGM through hemogenic endothelium (Dzierzak and Speck, 2008). Kidney is also a tissue developed from mesoderm, but the presence of cells with HSC transcriptome has not been studied. Here, we first analyzed the HSC markers in fetal kidney through analysis of fetal kidney single-cell dataset analyses. In human fetal kidney cortex, we found some cells expressing RUNX1 in a cluster of cells that harbored expression hematopoietic markers (cluster 9 on **Figures 1A,B**). In cluster 9 of human fetal kidney sc-RNAseq, a high expression of hematopoietic markers was confirmed by the presence of SRGN-positive cells (**Figure 2A**) as well as cells expressing PTPRC alias CD45 Leukocyte Common Antigen and CD44 (receptor of hyaluronic acid) (**Figure 2B**). SRGN (alias hematopoietic proteoglycan core protein) is a protein found in secretory granules of myeloid cells as well as in platelets. Our analysis showed also the presence of cells positive for MHC class II molecule HLA-DRA and CD74 (**Figure 2C**) and, most interestingly, cells expressing of hematopoietic transcription factors SPI1 and RUNX1 (**Figure 2D**). Finally, in this cluster 9 of fetal kidney, we found a higher expression of CXCR4 receptor of CXCL12 implicated in migration properties of HSCs (**Figure 2E**). All these results allowed to suggest the presence of cells harboring hematopoietic transcriptome in human fetal kidney.

We then analyzed the transcriptome of iPSC-derived kidney organoids and performed differential expression analysis of the kidney organoid versus parental iPSCs. Microarray analysis revealed important regulation of transcriptional program of these cells during their differentiation (**Figure 4A**). This differentially expressed program allowed to discriminate group samples by unsupervised classification (**Figure 4B**). After functional enrichment performed on upregulated genes during the differentiation process of the iPSC-derived kidney organoids, we observed the induction of HSC markers such as RUNX1 and CD34 (**Figure 4C**). It is well established that RUNX1 along with a *cis*-regulatory elements integrating the GATA, ETS, and SCL transcriptional networks plays a major role in HSC generation (Nottingham et al., 2007). We also found induction of FLI1 during the differentiation of iPSC-derived kidney organoid. SPI1 (alias PU.1), the main target downstream RUNX1 (Imperato et al., 2015), is also a master regulator of hematopoiesis, as it prevents excessive HSC division and exhaustion by controlling the transcription of multiple cell-cycle regulators (Staber et al., 2013). Association of SPI1 and RUNX1 is comprised a combination of seven transcription factors, which are sufficient to convert hemogenic endothelium into hematopoietic stem and progenitor cells that engraft myeloid, B, and T cells in primary and secondary mouse recipients (Sugimura et al., 2017). In transcriptome analyses of iPSC-derived kidney organoids, we found an upregulation of MYB, which is known to participate to cell fate decisions between erythropoiesis and megakaryopoiesis in human hematopoiesis (Bianchi et al., 2015). Amongst the hematopoietic transcripts identified in human fetal kidney cortex, we have also detected the expression of which, CXCR4 in relation with its ligand CXCL12, is involved in homing of hematopoietic cells to the bone marrow (Sugiyama et al., 2006).

Our data have some limitations including the fact that we cannot exclude the presence of mesodermal cells undergoing the fate of hematopoietic differentiation during our kidney organoid differentiation. Secondly, we could not identify the presence of cells with HSC functionality (self-renewal; differentiation) in the current experiments. However, these data suggest that at some point during embryonic development, a special "kidney niche" could appear transiently in humans. The identification of such a niche or its molecular counterparts could be of major interest to amplify human HSCs for transplantation purposes, such has been described in zebrafish (Stachura et al., 2009; Wolf et al., 2017). It is known that zebrafish embryonic stromal trunk (ZEST) cells derived from the HSC emergence site are functionally similar to the mammalian AGM niche cells. Moreover, ZEST cells and kidney cell lines have similar signaling properties (Wolf et al., 2017; Mahony and Bertrand, 2019). Our results suggest that a "kidney microenvironmental niche" niche could be of interest to generate conditions for HSC culture and expansion.

MATERIALS AND METHODS

- Key resources table

Reagent or resource	Source	Identifier
Antibodies		
Nephrin	Abcam	ab85379
DAPI	Sigma-Aldrich	D9542
Chemicals, peptides, and recombinant proteins		
Essential 8 basal medium	Thermo Fisher Scientific	A1516901
Essential 8 supplement	Thermo Fisher Scientific	A1517101
Geltrex LDEV-Free Reduced Growth Factor Basement Membrane Matrix	Thermo Fisher Scientific	A1413202
ROCK inhibitor	Global stem	GSR-6102
Reagent or resource	**Source**	**Identifier**
Experimental models: Cell lines		
Human iPSC: PB33	Human	–
Osmium tetroxide solution	Sigma-Aldrich	75632
Glutaraldehyde grade I	Sigma-Aldrich	G5882
Software and algorithms		
ImageJ		

Generation of Induced Pluripotent Stem Cells

The iPSC line used is this study was generated using Sendaï virus-mediated gene transfer of the four "Yamanaka" factors as previously described, using bone marrow mononuclear cells of a normal donor (Hwang et al., 2019).

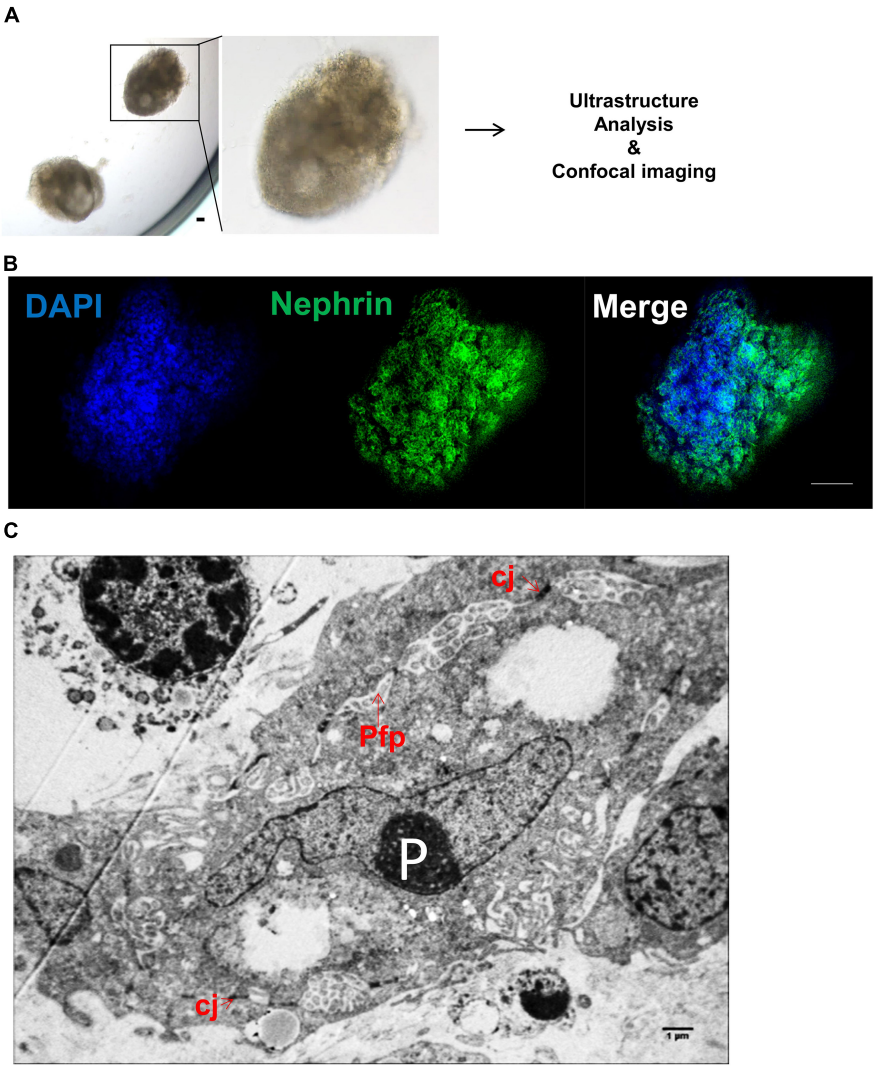

FIGURE 3 | Characterization of human induced pluripotent stem cell (iPSC)-derived kidney organoids. **(A)** Optical image of iPSC-derived kidney organoids at day + 14. Scale bar: 100 μm. **(B)** Confocal analysis and whole-mount staining for Nephrin in iPSC-derived kidney organoids showing nephron vesicles. Scale bar: 50 μm. **(C)** Representative electron microscopy image of podocytes in iPSC-derived kidney organoid at day + 14 showing P, podocytes; Pfp, podocyte foot process; and cj, cell-cell junctions. Scale bar: 1 μm.

Generation of Kidney Organoids

Induced pluripotent stem cells were maintained on Geltrex-coated (STEMCELL Technologies Inc., Vancouver, BC, Canada) flat culture dish in E8 media (STEMCELL Technologies Inc.) according to manufacturer's guidelines. Colonies were manually harvested at 60–80% confluence. Cells were then collected and dissociated into single cells using EDTA. Cells (1×10^6 or 1×10^5/well) were put onto ultra-low attachment 24-well or 96-well plate (Corning Inc., Corning, NY, United States) to allow them to form aggregated in suspension with ROCK inhibitor (2–5 μmol). Cell aggregates were cultured in E8 medium (STEMCELL Technologies) with daily medium change for 6–7 days. Control iPSC-A (iPSC-aggregates) were plated on a Geltrex (STEMCELL Technologies) in 96-well plate or 8-well culture chamber. And then aggregates were treated E8 medium (STEMCELL Technologies) with daily medium change for 12–14 days. Images were taken using a NIKON microscope (Nikon Instruments Inc., Melville, NY, United States).

Whole-Mount Immunostaining of 3D Kidney Organoids

Kidney organoids cultured on 96-well culture dishes were washed with phosphate-buffered saline (PBS), fixed with 4% paraformaldehyde in PBS for 120 min, permeabilized with 0.2% Triton X-100 (Sigma) in PBS, and blocked with 10% serum. For Nephrin staining, the antibody [Nephrin (Cat#ab85379; Abcam), Cambridge, United Kingdom] was diluted in PBS containing 10% serum and washed in PBS. Samples were incubated with secondary antibodies in antibody dilution buffer and then washed in PBS. Nuclei were labeled with DAPI mounting

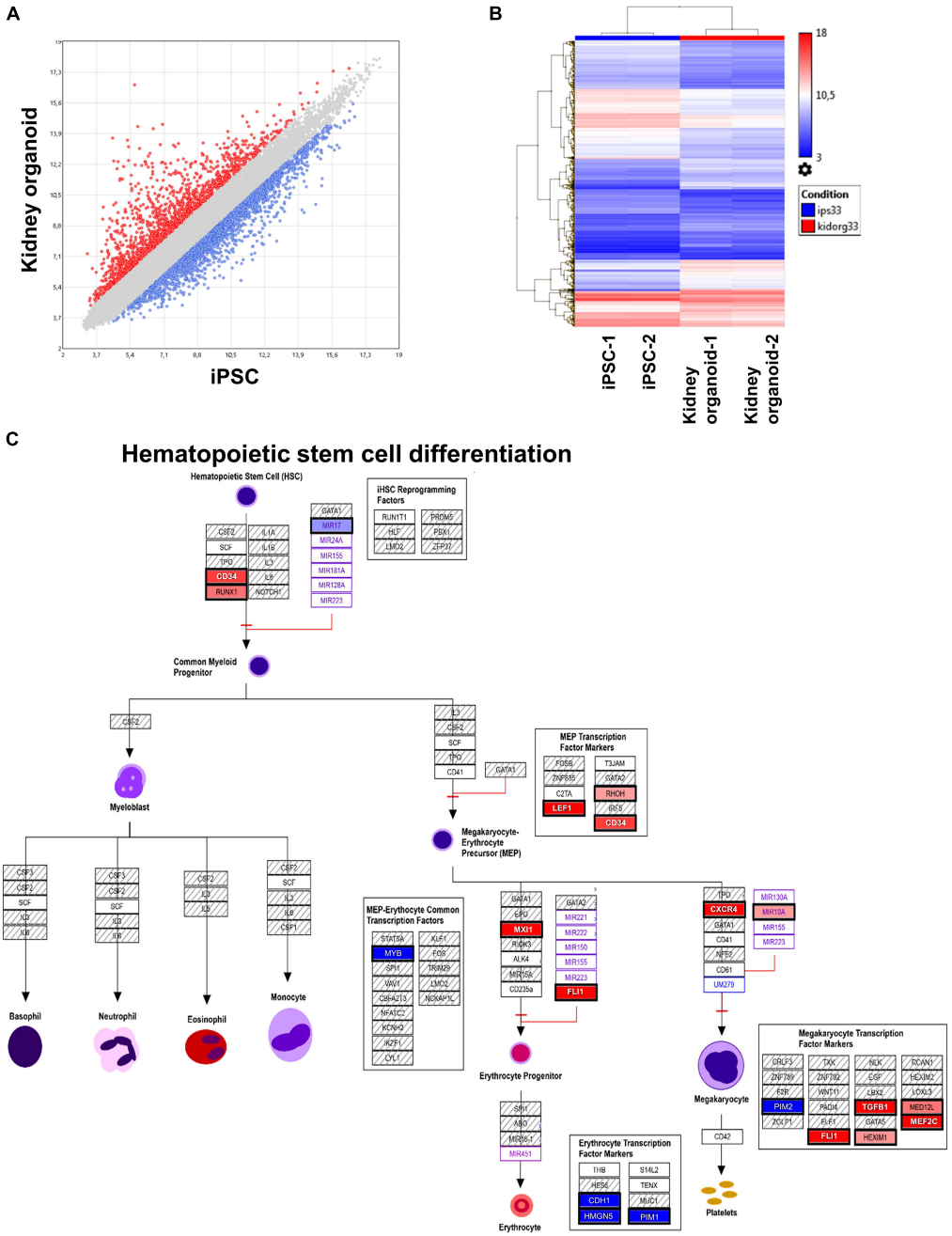

FIGURE 4 | Transcriptional program induced in kidney organoid derived from human induced pluripotent stem cells (iPSCs). **(A)** Scatterplot of differentially expressed genes found in transcriptome of kidney organoid versus iPSC. **(B)** Expression heatmap with unsupervised classification performed on differentially expressed genes induced during kidney organoid differentiation from iPSC. **(C)** Functional enrichment performed on WikiPathway database showing potential implication hematopoietic stem cell function during differentiation of kidney organoid derived from human iPSC.

medium. Visualization and capture were realized with a Zeiss confocal microscope. Negative controls were the experiments with secondary antibodies, yielding no staining (data not shown).

Transmission Electron Microscopy

Kidney organoids were gently centrifuged and pelleted before the TEM process, as follows. The cells were fixed in 2.5% glutaraldehyde in PBS for 1 h at 4°C, washed in PBS, and fixed in 1% osmium tetroxide in PBS for 1 h. They were dehydrated in ascending series of graded ethyl alcohols and then in acetone. Each sample was infiltrated with the resin before being embedded in epoxy resin and polymerized for 72 h. Semi-thin sections of about 0.5–1 μm were obtained and colored with toluidine blue before being examined via a light microscope with an

associated digital camera and hooked to a computer for image processing and editing (Leica DC300, Wetzlar, Germany). Ultra-thin sections of about 60/90 nm were contrasted with heavy metals (uranyl acetate and lead citrate) and were examined using a Jeol 1010 transmission electron microscope at an accelerated voltage of 80 kV. Images were photographed on digital images Gatan Digital Micrograph (brure Erlangen 500 W) and camera and edited by ImageJ and Microsoft Power Point.

Human Fetal Single-Cell Transcriptome Analysis

Dataset GSE112570 of single-cell RNA-sequencing allows to explore cellular heterogeneity of human kidney cortical nephrogenic niche (Lindström et al., 2018). Experiments were performed with technology 10× Genomics single-cell RNA sequencing on two human kidney samples (17 weeks) indexed in GEO database: GSM3073088 and GSM3073089. Molecular index was realized: Chromium Single Cell 3′ v2 single-cell RNA-Seq of poly A selected mRNA kit (10× Genomics), and sequencing was processed on NextSeq 500 (Illumina, San Diego, CA, United States). Bioinformatics base call by bcl2fastq v. 2.17 reads were mapped using STAR 2.5.1b (Genome: GRCh37), and count tables were generated using the Cell Ranger software version 1.3.1. Downstream bioinformatics single-cell transcriptome analyses were performed in R software version 3.4.3. Digital matrix was built with both 10× MTX files and merged in Seurat R-package version 2.3.0 (Butler et al., 2018) with package dependencies of matrix version 1.2-12, cowplot 0.9.2, and ggplot2 version 2.2.1 (Wickham, 2009). Batch correction was performed with canonical correlation on 30 dimensions before mathematical dimension reduction with tSNE algorithm. Also, dplyr library version 0.7.4 was used to generate intermediate table of best genes by cluster. Bioinformatics code to perform these single-cell analyses was deposed at the following web address: https://github.com/cdesterke/hsckidney/.

Kidney Organoid Microarray Analysis

Microarray Clariom S human was done on process total RNA from human wild-type (WT) iPSC and its derived kidney organoids in duplicates (Hwang et al., 2019). Expression matrix was built with CEL files generated on Affymetrix Station and normalized by RMA method with TAC version 4.0 software (Applied Biosystems, Foster City, CA, United States) (Irizarry et al., 2003). DEGs were estimated with linear models for microarray data (LIMMA) algorithm by using a false discovery rate threshold of less 5% (Ritchie et al., 2015). Functional enrichment analysis on DEGs was performed on WikiPathway database.

DATA AVAILABILITY STATEMENT

The data presented in the study are deposited in the Gene Expression Omnibus (GEO) repository, accession number GSE172319.

AUTHOR CONTRIBUTIONS

JH and AT conceived, designed, analyzed the data, and wrote the manuscript. JH performed all organoids experiments and performed confocal laser scanning microscopy with analysis. JL-D performed the TEM. CD analyzed the bioinformatics data. AB-G, FG, and AT analyzed the data and supervised the project. JH, CD, and AT wrote the manuscript. All authors contributed to the article and approved the submitted version.

SUPPLEMENTARY MATERIAL

The Supplementary Material for this article can be found online at: https://www.frontiersin.org/articles/10.3389/fcell.2021.668833/full#supplementary-material

Supplementary Figure 1 | Canonical correlation with batch correction between the two fetal kidneys process in single cell transcriptome. **(A)** Factorial map showing superposition of the cells from the respective kidneys. During normalization of the transcriptome, a canonical correlation normalization was applied between the cells of the 2 kidneys, the factorial map showed that cells from each kidney were well spread on this map with a good overlapping. **(B)** Profile of the shared correlation strength between the respective kidneys (30 dimensions); tSNE plot post canonical correlation on the merged 2 kidneys. **(C)** t-SNE dimension reduction of single cell transcriptome from human fetal kidney after batch correction, cells from each kidney (respectively green and red) are plotted with t-SNE dimension reduction algorithm and their distribution in the map confirmed a good batch correction during the analyses (canonical correlation with Seurat R-package).

Supplementary Figure 2 | Violinplot of cluster markers found in single cell sequencing after merging the fetal cortex of two human kidneys.

Supplementary Table 1 | Table presenting differential expressed genes found in cluster 9 as compared to others clusters in human fetal kidney cortex.

REFERENCES

Bianchi, E., Bulgarelli, J., Ruberti, S., Rontauroli, S., Sacchi, G., Norfo, R., et al. (2015). MYB controls erythroid versus megakaryocyte lineage fate decision through the miR-486-3p-mediated downregulation of MAF. *Cell Death Differ.* 22, 1906–1921. doi: 10.1038/cdd.2015.30

Butler, A., Hoffman, P., Smibert, P., Papalexi, E., and Satija, R. (2018). Integrating single-cell transcriptomic data across different conditions, technologies, and species. *Nat. Biotechnol.* 36, 411–420. doi: 10.1038/nbt.4096

Dzierzak, E., and Speck, N. A. (2008). Of lineage and legacy–the development of mammalian hematopoietic stem cells. *Nat. Immunol.* 9, 129–136. doi: 10.1038/ni1560

Ej, P., and Li, Z. (2010). *Hematopoietic development in the zebrafish. Int. J. Dev. Biol.* Available online at: https://pubmed.ncbi.nlm.nih.gov/20711990/ (accessed Dec 4, 2020).

Gao, X., Xu, C., Asada, N., and Frenette, P. S. (2018). The hematopoietic stem cell niche: from embryo to adult. *Dev. Camb. Engl.* 145:dev139691.

Hwang, J. W., Desterke, C., Féraud, O., Richard, S., Ferlicot, S., Verkarre, V., et al. (2019). iPSC-derived embryoid bodies as models of c-met-mutated

hereditary papillary renal cell carcinoma. *Int. J. Mol. Sci.* 20:4867. doi: 10.3390/ijms20194867

Imperato, M. R., Cauchy, P., Obier, N., and Bonifer, C. (2015). The RUNX1-PU.1 axis in the control of hematopoiesis. *Int. J. Hematol.* 101, 319–329. doi: 10.1007/s12185-015-1762-8

Irizarry, R. A., Bolstad, B. M., Collin, F., Cope, L. M., Hobbs, B., and Speed, T. P. (2003). Summaries of affymetrix GeneChip probe level data. *Nucleic Acids Res.* 31:e15. doi: 10.1093/nar/gng015

Lindström, N. O., De Sena Brandine, G., Tran, T., Ransick, A., Suh, G., Guo, J., et al. (2018). Progressive recruitment of mesenchymal progenitors reveals a time-dependent process of cell fate acquisition in mouse and human nephrogenesis. *Dev. Cell* 45, 651–660.e4.

Mahony, C. B., and Bertrand, J. Y. (2019). How HSCs colonize and expand in the fetal niche of the vertebrate embryo: an evolutionary perspective. *Front. Cell Dev. Biol.* 7:34. doi: 10.3389/fcell.2019.00034

Menon, R., Otto, E. A., Kokoruda, A., Zhou, J., Zhang, Z., Yoon, E., et al. (2018). Single-cell analysis of progenitor cell dynamics and lineage specification in the human fetal kidney. *Dev. Camb. Engl.* 145:dev164038.

Mikkola, H. K. A., and Orkin, S. H. (2006). The journey of developing hematopoietic stem cells. *Development* 133, 3733–3744. doi: 10.1242/dev.02568

Nottingham, W. T., Jarratt, A., Burgess, M., Speck, C. L., Cheng, J.-F., Prabhakar, S., et al. (2007). Runx1-mediated hematopoietic stem-cell emergence is controlled by a Gata/Ets/SCL-regulated enhancer. *Blood* 110, 4188–4197. doi: 10.1182/blood-2007-07-100883

Park, J., Shrestha, R., Qiu, C., Kondo, A., Huang, S., Werth, M., et al. (2018). Single-cell transcriptomics of the mouse kidney reveals potential cellular targets of kidney disease. *Science* 360, 758–763. doi: 10.1126/science.aar2131

Ritchie, M. E., Phipson, B., Wu, D., Hu, Y., Law, C. W., Shi, W., et al. (2015). limma powers differential expression analyses for RNA-sequencing and microarray studies. *Nucleic Acids Res.* 43:e47. doi: 10.1093/nar/gkv007

Ruotsalainen, V., Patrakka, J., Tissari, P., Reponen, P., Hess, M., Kestilä, M., et al. (2000). Role of nephrin in cell junction formation in human nephrogenesis. *Am. J. Pathol.* 157, 1905–1916. doi: 10.1016/s0002-9440(10)64829-8

Staber, P. B., Zhang, P., Ye, M., Welner, R. S., Nombela-Arrieta, C., Bach, C., et al. (2013). Sustained PU.1 levels balance cell-cycle regulators to prevent exhaustion of adult hematopoietic stem cells. *Mol. Cell* 49, 934–946. doi: 10.1016/j.molcel.2013.01.007

Stachura, D. L., Reyes, J. R., Bartunek, P., Paw, B. H., Zon, L. I., and Traver, D. (2009). Zebrafish kidney stromal cell lines support multilineage hematopoiesis. *Blood* 114, 279–289. doi: 10.1182/blood-2009-02-203638

Sugimura, R., Jha, D. K., Han, A., Soria-Valles, C., da Rocha, E. L., Lu, Y.-F., et al. (2017). Haematopoietic stem and progenitor cells from human pluripotent stem cells. *Nature* 545, 432–438.

Sugiyama, T., Kohara, H., Noda, M., and Nagasawa, T. (2006). Maintenance of the hematopoietic stem cell pool by CXCL12-CXCR4 chemokine signaling in bone marrow stromal cell niches. *Immunity* 25, 977–988. doi: 10.1016/j.immuni.2006.10.016

Taniguchi, H., Toyoshima, T., Fukao, K., and Nakauchi, H. (1996). Presence of hematopoietic stem cells in the adult liver. *Nat. Med.* 2, 198–203. doi: 10.1038/nm0296-198

Wickham, H. (2009). *ggplot2: Elegant Graphics for Data Analysis*. Verl, NY: Springer.

Wolf, A., Aggio, J., Campbell, C., Wright, F., Marquez, G., Traver, D., et al. (2017). Zebrafish caudal haematopoietic embryonic stromal tissue (CHEST) cells support haematopoiesis. *Sci. Rep.* 7:44644.

Conflict of Interest: The authors declare that the research was conducted in the absence of any commercial or financial relationships that could be construed as a potential conflict of interest.

frontiers in Cell and Developmental Biology

REVIEW
published: 08 July 2021
doi: 10.3389/fcell.2021.666515

Precision Medicine Gains Momentum: Novel 3D Models and Stem Cell-Based Approaches in Head and Neck Cancer

Annette Affolter, Anne Lammert, Johann Kern, Claudia Scherl and Nicole Rotter*

Department of Otorhinolaryngology, Head and Neck Surgery, University Hospital Mannheim, Medical Faculty Mannheim, Heidelberg University, Mannheim, Germany

Despite the current progress in the development of new concepts of precision medicine for head and neck squamous cell carcinoma (HNSCC), in particular targeted therapies and immune checkpoint inhibition (CPI), overall survival rates have not improved during the last decades. This is, on the one hand, caused by the fact that a significant number of patients presents with late stage disease at the time of diagnosis, on the other hand HNSCC frequently develop therapeutic resistance. Distinct intratumoral and intertumoral heterogeneity is one of the strongest features in HNSCC and has hindered both the identification of specific biomarkers and the establishment of targeted therapies for this disease so far. To date, there is a paucity of reliable preclinical models, particularly those that can predict responses to immune CPI, as these models require an intact tumor microenvironment (TME). The "ideal" preclinical cancer model is supposed to take both the TME as well as tumor heterogeneity into account. Although HNSCC patients are frequently studied in clinical trials, there is a lack of reliable prognostic biomarkers allowing a better stratification of individuals who might benefit from new concepts of targeted or immunotherapeutic strategies. Emerging evidence indicates that cancer stem cells (CSCs) are highly tumorigenic. Through the process of stemness, epithelial cells acquire an invasive phenotype contributing to metastasis and recurrence. Specific markers for CSC such as CD133 and CD44 expression and ALDH activity help to identify CSC in HNSCC. For the majority of patients, allocation of treatment regimens is simply based on histological diagnosis and on tumor location and disease staging (clinical risk assessments) rather than on specific or individual tumor biology. Hence there is an urgent need for tools to stratify HNSCC patients and pave the way for personalized therapeutic options. This work reviews the current literature on novel approaches in implementing three-dimensional (3D) HNSCC *in vitro* and *in vivo* tumor models in the clinical daily routine. Stem-cell based assays will be particularly discussed. Those models are highly anticipated to serve as a preclinical prediction platform for the evaluation of stable biomarkers and for therapeutic efficacy testing.

Keywords: head and neck cancer, 3D cell culture, cancer stem cell models, bioprinting, personalized therapy

OPEN ACCESS

Edited by:
Nikhil Baban Ghate, University of Southern California, United States

Reviewed by:
Debashish Das, Narayana Nethralaya, India
Petros Papagerakis, University of Saskatchewan, Canada

****Correspondence:***
Annette Affolter
annette.affolter@umm.de

Specialty section:
This article was submitted to Stem Cell Research, a section of the journal Frontiers in Cell and Developmental Biology

Received: *10 February 2021*
Accepted: *30 April 2021*
Published: *08 July 2021*

Citation:
Affolter A, Lammert A, Kern J, Scherl C and Rotter N (2021) Precision Medicine Gains Momentum: Novel 3D Models and Stem Cell-Based Approaches in Head and Neck Cancer. Front. Cell Dev. Biol. 9:666515. doi: 10.3389/fcell.2021.666515

CONVENTIONAL TREATMENT STRATEGIES AND NEW THERAPEUTIC CONCEPTS IN HEAD AND NECK CANCER

Head and neck squamous cell carcinoma (HNSCC) is a heterogeneous tumor entity with varying clinical presentation and prognosis. Current treatment options for the disease have limited success particularly in recurrent or metastatic stage. For early stage disease, surgery and radiotherapy (RT) are the main pillars. Concurrent platinum-based chemotherapy with irradiation is standard-of-care for locoregionally advanced tumors, both in an adjuvant or primary setting. However, especially the present non-surgical standard-of-care treatment with concurrent high-dose cisplatin (100 mg/m^2) every 3 weeks and RT (70 Gy over 6–7 weeks) entails severe acute and late toxicities (Denis et al., 2003) as well as functional deficits resulting in a reduced quality of life. For patients who are not eligible for cisplatin-based chemotherapy, the anti-epidermal growth factor receptor (EGFR) monoclonal antibody cetuximab is an option and can be administered in combination with RT. So far, cetuximab is the only EMA-approved targeted therapy agent for HNSCC. In the case of recurrent or metastatic (R/M) disease, platinum-based chemotherapy is the mainstay of therapy, and the addition of cetuximab to standard cytotoxic chemotherapy offers some benefit in the first-line setting, but at the cost of increased toxic effects. Unfortunately, there is no biomarker currently available to be able to predict whether HNSCC patients will benefit from EGFR blockade or not (Egloff and Grandis, 2009). A new combination of cetuximab with another agent that has been recently presented is the taxane-based TPEx scheme which has been demonstrated to exert lower toxicity along with a reduced duration of therapy (Guigay et al., 2019) in a palliative setting.

Over a long period, there was no standard second-line therapy for advanced R/M HNSCC after platinum-based chemotherapy. Two immune checkpoint inhibitors (CPI), nivolumab, and pembrolizumab targeting programmed cell death protein 1 recently got approval for mono- or combination therapy (Ferris et al., 2016; Burtness et al., 2019). Immune CPI are amongst the central developments in oncology in the last decade, but the response is very heterogeneous for many entities, including HNSCC. However, despite encouraging results, the overall response rates of these agents only range from 13 to 18% (Ferris et al., 2016; Larkins et al., 2017). Primary resistance against CPI is seen in up to 60% of all patients, including HNSCC (Topalian et al., 2012).

The combination of immune CPI with established therapies (irradiation, chemotherapy, and cetuximab) is currently being tested in several clinical studies (Seliger, 2019), however up to now the effect of such conventional treatments on immune checkpoints remains unclear. Considering that serious immune-associated toxicity can occur during immunotherapy, it is absolutely necessary to identify predictive biomarkers to predict the response of the tumor to checkpoint blockade (Bai et al., 2020). In addition to the immunohistochemical evaluation of the presence of PD-L1, immune cell infiltration, the mutation load of the tumor or the expression profile of immune-associated genes are currently being investigated (Partlová et al., 2015; Mandal et al., 2016; Chen X. et al., 2018; Hanna et al., 2018; Oliva et al., 2019; Wang et al., 2019). However, no valid predictive markers for HNSCC have been established so far.

Newly developed technologies, such as high-throughput sequencing might be essential to determine differences in genetic, epigenetic, biological, and immunological properties of HNSCC. Furthermore, etiological risk factors such as tobacco and alcohol abuse as well as infection with human papillomavirus (HPV) have a great impact on the treatment outcome. The rapid increase in the incidence of HPV-positive oropharyngeal cancer in younger patients and the more favorable prognosis observed in this subgroup (Ang et al., 2010) have led to the concept of treatment de-escalation for HPV-driven cancers, as recently reviewed by Mehanna et al. (2020). Several de-escalation studies worldwide have been initiated over the past decade. Strategies include a dose reduction of RT as well as decreasing dosages of systemic therapy or omitting platinum based chemotherapy (Mehanna et al., 2020). These studies aimed to improve quality of life by lowering toxic side effects with the same probability of survival. It is important to notice, that the biological basis for de-escalation remains unclear. Also the first trials DE-ESCALATE and RTOG1016 did not identify successful de-escalation strategies.

Some studies report an improvement to salvage chemotherapy (SCT) after exposure to immune CPI for different tumor entities that exposure to ICI improves response to SCT (Schvartsman et al., 2017; Rossi et al., 2018; Szabados et al., 2018). Saleh et al. (2019) confirm this finding for HNSCC and an increased response rate to chemotherapy (30%) administered after progression on ICI in patients with R/M SCCHN. However, this finding has to be confirmed in additional cohorts and prospective clinical trials and needs to be optimized. The prognosis for HNSCC patients who progress on CPI is dismal, a situation providing the rationale for the identification of new (targeted) treatments.

VALUE OF PRECISION MEDICINE: CURRENT STATE OF PREDICTIVE MARKERS

The future of cancer therapy may lie in treatments designed precisely for a specific type of cancer. Individualized targeted therapies might inhibit local and distant tumor growth by interfering with the molecular pathways that cause cancer cells to proliferate and survive.

The term "precision medicine" refers to different approaches: targeted therapy, immunotherapy, or genomics. However, all these concepts have the aim to align medical care with molecular and possibly also environmental and lifestyle factors of certain patient groups. Optimizing the success rates of modern therapies with less adverse effects is the main aim in precision medicine. Biomarker-supported therapy is an

essential sub-discipline of precision medicine. Biomarkers are DNA-, mRNA-, or protein-based and comprise driver mutations, protein expression, mRNA, MSI (microsatellite instability), tumor mutational burden (TMB), and epigenetic biomarkers, e.g., specific methylation patterns of DNA.

The only targeted therapy approved in R/M HNSCC is the antibody against EGFR, cetuximab (Licitra et al., 2011, 2013), pembrolizumab (Seiwert et al., 2016), and nivolumab (Ferris et al., 2016) targeting PD-1 examples for immune-CPI. Remarkably, the decision to administer these therapeutic compounds is not biomarker-based (Malone and Siu, 2018).

Although EGFR overexpression is observed in > 90% of HNSCC (Dassonville et al., 1993; Rubin Grandis et al., 1996) and is associated with an unfavorable clinical outcome (Rubin Grandis et al., 1998; Ang et al., 2004) the correlation with response to treatment is inconsistent (Vermorken et al., 2007). So far, no molecular marker has been identified to correlate with HNSCC response to EGFR-targeting in patients. Tumor EGFR copy number did not turn out as a predictive biomarker for the efficacy of cetuximab plus platinum/5-FU as first-line therapy for patients with R/M HNSCC (Licitra et al., 2011).

Immunotherapeutic anti-PD-1 agents have achieved to become standard-of-care for platinum-refractory R/M HNSCC as they have proven to show evidence of survival benefit and long-term responses. However, appropriate stratification of patients who will benefit from immunotherapy is crucial due to response rates below 20% (Ferris et al., 2016; Larkins et al., 2017). Research is currently focusing on the identification of CPI response predictors. The issue whether PD-L1 expression is a reliable biomarker of response in HNSCC has been recently addressed in different studies. There is a general tendency of PD-L1 expressing tumors to show superior response rates to CPI compared to PD-L1 negative tumors (Hansen and Siu, 2016). This observation has been endorsed by the KEYNOTE-040 and -048 trials in R/M HNSCC where survival in PD-L1 expressing cases was significantly increased (Burtness et al., 2019; Cohen et al., 2019). Interestingly, no significant association between PD-L1 levels and response to nivolumab or survival were found in the CHECKMATE-141 trial (Ferris et al., 2016, 2018). These diverging findings might be due to differences in the assays when determining the PD-L1 status on the one hand. On the other hand, there is evidence that PD-L1 is regulated by multiple signaling pathways that are frequently altered and known as survival pathways in HNSCC such as PI3K/Akt, or MAPK (Lui et al., 2013; Lawrence et al., 2015).

These molecular interactions and furthermore their varying expression over time between first diagnosis and progression, metastases or recurrence, after acquiring therapy resistance or during treatment have demonstrated the dynamics of PD-L1 in multiple tumor entities (Gadiot et al., 2011; Darb-Esfahani et al., 2016; Han et al., 2016; Ock et al., 2017). It is worth mentioning that, in a smaller percentage, PD-L1 negative tumors also respond to CPI. The success of immunotherapy is guided by various other factors such as association with HPV, the infiltration of the tumor with immune cells, or TMB. So far, it has been demonstrated that response to immune CPI is correlated with increased TMB. This might imply that prior therapy with DNA damaging compounds may enhance sensitivity to CPI due to increased TMB. In HNSCC indeed one study demonstrated that prior treatment with chemotherapy was associated with increased overall survival relative to patients with prior surgery or radiation therapy in an observational study of patients with head and neck squamous cell carcinoma (HNSCC) treated with anti-programmed cell death 1 ligand 1 (anti-PD-L1) (Hanna et al., 2018). Yet, this thesis was not substantiated in other cancer entities (Pulte and Brenner, 2010; Reck et al., 2016; Forde et al., 2018) or further studies. It has to be taken into account that prior chemotherapy may as well enhance subclonal mutations and intratumoral heterogeneity, features that are discussed to negatively correlate with sensitivity to CPI.

Currently, additional biomarkers of response to anti-PD-1/PD-L1 agents in HNSCC have been proposed. The oral and intestinal microbiota is discussed as a candidate marker as this ecosystem correlates microenvironment and tumor microenvironment (TME) as they may regulate environmentally induced immune responses and ultimately impact on therapeutic efficacy Its composition has not only shown an impact on PD-L1 efficacy but is also correlated with response to treatment in different cancers. This is in line with studies suggesting an association with other tumoral features such as progression or recurrence (Oliva et al., 2019).

Recently published studies on patients with HNSCC indicate that the level of PD-1 expression by CD8 + T cells is associated with cell functionality and overall survival of the patient. Kansy et al. found a higher frequency of PD-1 expression that was upregulated on TIL in HPV-positive patients with a significantly better clinical outcome. In a murine HPV+ model treated with anti-PD-1 mAb where PD-$1^{high/low}$ populations were differentially modified. Different PD-1 expression levels lead to the interpretation of PD-1 expression as a marker of competent tumor reactive T cells while PD-1^{high} expression was interpreted as an indicator of exhaustion of dysfunctional cells negatively impacting on the TME. For validation, baseline PD-1 levels need to be correlated with patient responder status (Kansy et al., 2017).

Why are there currently no validated biomarkers predicting response that are comprehensively applicable to all HNSCC patients? Oliva et al. explain this issue by the fact that most investigations on HNSCC biomarkers have been performed retrospectively by using baseline archival tumor material, which does not mirror spatial and tumoral heterogeneity. They claim that it is not sufficient to separately evaluate potential predictors. To take account of the complexity of immune responses, markers should always be analyzed in the context with other factors, and interactions, especially between the immune system and the TME, should be thoroughly considered (Oliva et al., 2019).

ENVIRONMENTAL AND LIFE-STYLE DETERMINANTS OF HNSCC

For disease prevention or control, the recognition of main social and behavioral variables and implementation into appropriate programs and policies is mandatory. Addressing of these variables would reduce the risk of serious diseases such as cancer thereby improving popular health (Allam and Windsor, 2013).

In HNSCC, most approaches refer to oral cancer. Tobacco and alcohol usage, tobacco chewing and dietary malnutrition are the most important downstream social determinants (Llewellyn et al., 2001). Hobdell et al. (2003) published an association between socioeconomic status (SES) variables and oral health. They observed a distinct gradient between the most highly and least socio-economically developed countries and the incidence of oral diseases including cancer, dental caries, and destructive periodontal disease. Attributable risk factors also comprise diet deficiencies. Fresh food contains antioxidants and anti-carcinogenic agents which might help oppose the damaging influence of carcinogens such as smoking, alcohol drinking or tobacco chewing (Bosetti et al., 2003; Boccia et al., 2008). Employment in certain sectors can enhance the risk for oral malignancies i.e., by exposure to formaldehyde, or by working in painting and printing, textile and electronic factory jobs (Allam and Windsor, 2013). Vučičević Boras et al. compared the environmental and behavioral risk factors living environment, occupational exposure, education, residence, family cancer, diet, smoking, and alcohol consumption parameters in patients with head and neck cancer (HNC) with a control group. They discussed smoking and low education as significant risk factors for HNC regardless of gender. Family HNC and breast cancer were significant risk predictors (Vučičević Boras et al., 2019). Omics-based approaches might offer novel tools for diagnosis and treatment of head and neck malignancies in the field of precision health (Adeola et al., 2019). Omics technologies comprehensively screen for early changes in DNA, RNA, protein, and metabolite expression (Rai et al., 2018) and may contribute to the clearly needed early detection of oral cancer. Disruption of the circadian clock was recently linked to head and neck pathologies, such as oral cancer and Sjögren syndrome (Matsumoto et al., 2016; Adeola et al., 2019). Nearly half of all protein encoding genes are subject to circadian rhythms in transcription, mostly organ-unspecifically (Zhang et al., 2014). Hence, circadian variations in multi-omics analyses, recently called circadiOmics are discussed as a relevant step toward unbiased precision health (Ceglia et al., 2018).

CANCER STEM CELL MARKERS AS PROGNOSTICATORS IN HNSCC

In solid tumors, in addition to the main tumor mass consisting of well-differentiated cells, a subpopulation of immature tumor cells called cancer stem cells (CSCs) exists. CSC show unlimited proliferative capacity, have the ability for self-renewal, differentiation, and tumor invasion, and are capable of DNA damage repair. CSC-related factors as well as the TME both contribute to radioresistance and reveal new therapeutic approaches (Albers et al., 2012; Arnold et al., 2020).

CD44+, a cell membrane-bound glycoprotein that occurs in several isoforms, is considered as a marker for the CSC phenotype (Zhang et al., 2012). These isoforms are generated by alternative splicing of a region of variable exons. They differ in their amino acid sequence and their amount of N- and O-glycosylation (Franzmann et al., 2007), whereby their apparent molecular weight varies between 85 and 250 kilo Dalton (kD) (Saito et al., 1998). At least 20 variants of CD44 have been reported. They arise through alternative splicing of 10 exons, which encode the proximal part of the respective extracellular domain (Screaton et al., 1993; Ponta et al., 1998). For the first time, CD44 was described as a receptor on circulating lymphocytes, where it conveys homing, cell adherence and migration (Stamenkovic et al., 1989). Prince et al. (2007) showed that CD44+ tumor cells, which typically make up < 10% of all HNSCC cells, were able to develop a new primary *in vivo*, while CD44 – cells were not. Günthert et al. (1991) demonstrated that the expression of CD44 caused metastatic potential in a non-metastatic cell line in the rat model. Since then, various analyses have been initiated that imply the correlation between CD44 expression and tumor progression, metastasis, and prognosis. Such associations exist in several epithelial tumor entities, besides HNSCC in colorectal carcinoma (Thenappan et al., 2009), breast carcinoma (Park et al., 2010), and different types of gastric carcinoma (Okayama et al., 2009).

Previously we observed CD44 in human HNSCC tumor tissue samples by immunofluorescence (Faber et al., 2011). Other research groups used flow cytometry (Prince et al., 2007), immunohistochemistry or microarray technology (Han et al., 2009) to verify CD44+ cells in HNSCC. The results consistently postulate the presence of CD44 in HNSCC tumors at both protein and gene levels. Prince et al. (2007) published that CD44+ tumor cells usually make up < 10% of all cells in the entirety of HNSCC. The percentage of CD44+ cells within HNSCC is subject to inter-individual fluctuations. Here, the proportion of CD44+ cells varied from 4% to over 90% (Pries et al., 2008). A possible explanation for these extreme variations is the fact that different methods (FACS analyzes versus immunohistochemistry) have been used in these studies.

We and others (Herold-Mende et al., 1996; Han et al., 2009) described a surface staining pattern of CD44 in HNSCC cell lines and tissue samples (Faber et al., 2011), an observation that indicates its role as an adhesion molecule during tumor survival and progression. CD44 is supposed to attach the cells to the extracellular matrix (ECM). The adherence of malignant cells must be alternated in order to be able to detach from the primary tumor and to form metastases elsewhere (Schirrmacher, 1985). In various tumor cell lines and human tumors the extracellular portion of CD44 serves as a substrate for proteolytic cleavage processes by metalloproteinases (MMPs) (Okamoto et al., 2002). Remarkably, CD44 expression could be found mainly in the area of the tumor invasive front, which is in direct contact with the stromal cells surrounding the tumor and forms the tumor stem cell niche in HNSCC (Faber et al., 2013a).

Already in 2010, Joshua et al. suggested that flow cytometric measurements of the frequency of Lin-CD44þ cells may provide a prognostic test for patients with HNSCC. They observed a correlation between a high frequency of Lin-CD44þ cells with tumor aggressiveness represented by factors such as advanced T classification and recurrence (Joshua et al., 2012). Chen et al. (2014) suggested that CD44 is related to worse T category, N category, tumor grade and prognosis in pharyngeal and laryngeal cancer, but no clear association was revealed between CD44

expression and oral cancer. Jakob et al. (2020) recommend testing for CSC markers in patients with advanced or late stage HNSCC, as they observed correlations between CSC markers ALDH1, BCL11B, BMI-1, and CD44 and prognosis.

ALDH1 is a human aldehyde dehydrogenase that can be used to identify both physiological stem cells and CSC (Ma and Allan, 2011). The expression of ALDH1 is associated with an increased incidence of metastases (Kim et al., 2015). In contrast, ALDH1 is associated with tumor malignancy and cell self-renewal potential in head and neck tumors, but there is no significant correlation with the 5-year survival rate of the patients examined. Although ALDH1 has been shown to play a role in the maintenance of CSC in HNSCC, there is no correlation whatsoever with the occurrence of lymph node metastases. Furthermore, stem cell properties in HNSCC were interrelated with other surface markers such as Sox2 and OCT3 for the first time (Huang et al., 2014; Yu and Cirillo, 2020). ALDH1 is associated with squamous cell carcinomas in other locations than head and neck. The marker was primarily found in the invasive front and in metastatic lesions of esophageal carcinomas (Yang et al., 2014) exhibiting a more aggressive potential for invasion and metastasis.

In HNSCC, ALDH1 expression is not relevant for therapeutic decisions, although it was shown to be associated lymph node metastases (Michifuri et al., 2012; Yu and Cirillo, 2020). A meta-analysis by Dong et al. from 2017 summarized 14 studies with a total of 1258 patients regarding the effect of ALDH1 in HNSCC. They demonstrated a significant correlation of ALDH1 with tumor differentiation and reduced overall survival (Dong et al., 2017). According to Leinung et al. CD44 is found more ubiquitously in HNSCC compared to ALDH1. As a result, ALDH1 seems to be more suitable to identify a certain CSC subpopulation. However, the authors state that neither CD44 nor ALDH1 alone or in combination is suitable to detect CSC separately in HNSCC (Leinung et al., 2015). Besides CD44 and ALDH1, several other stem cell markers have been described for HNSCC, such as Bmi-1, CD133, Nanog, Oct-4, and SOX2 (Satpute et al., 2013; Patel et al., 2014; Qian et al., 2015) and

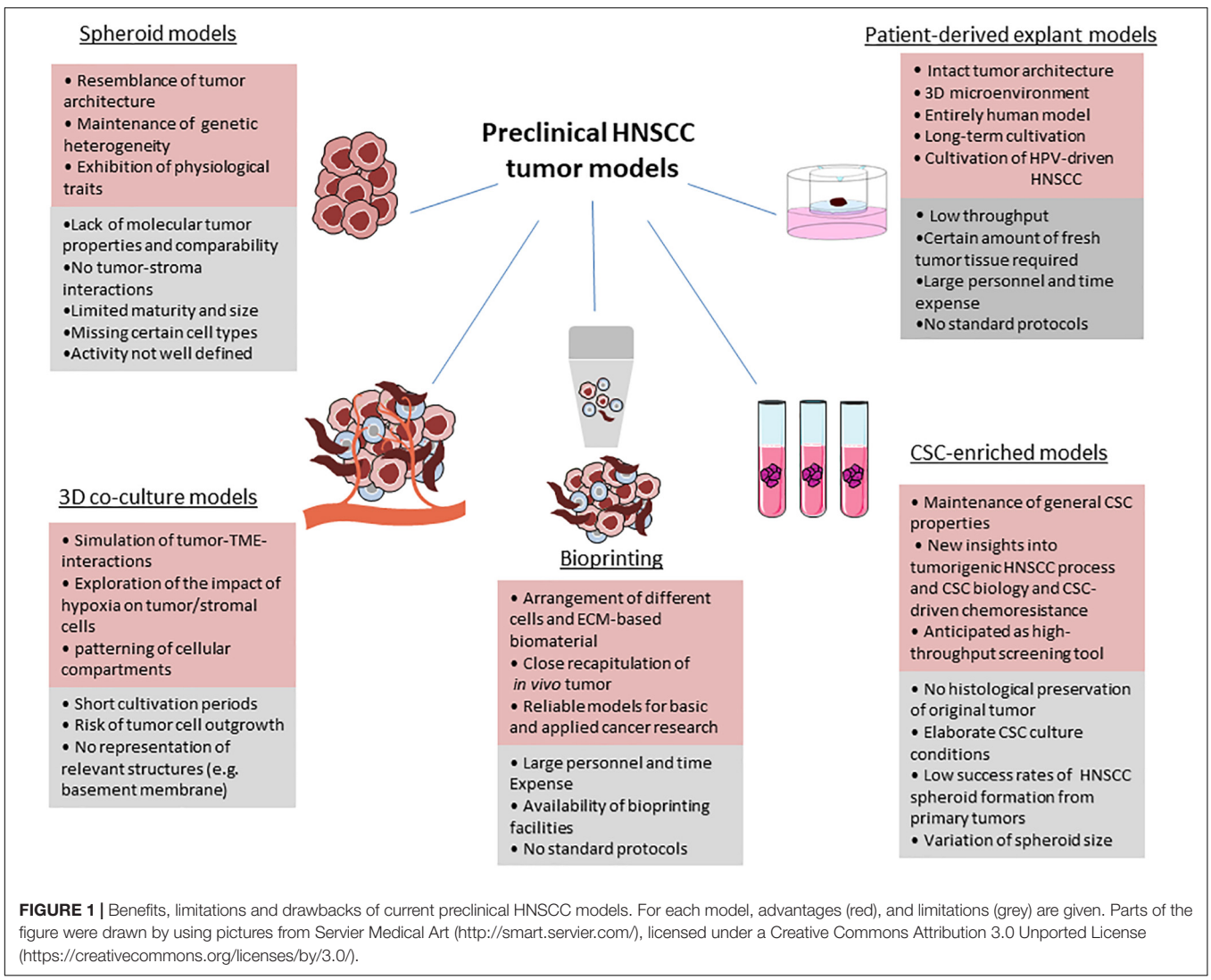

FIGURE 1 | Benefits, limitations and drawbacks of current preclinical HNSCC models. For each model, advantages (red), and limitations (grey) are given. Parts of the figure were drawn by using pictures from Servier Medical Art (http://smart.servier.com/), licensed under a Creative Commons Attribution 3.0 Unported License (https://creativecommons.org/licenses/by/3.0/).

those have partly been associated with prognosis (Chen et al., 2014; Dong et al., 2014; Zhou and Sun, 2014). However, as methodology, patient cohorts, and sample quality in studies are not standardized yet, the role of stem cell markers in HNSCC remains unclear and the prognostic value is discussed controversially (Fan et al., 2017). Some studies link CD133 to lymph node metastases in HNSCC (Mannelli et al., 2015). However, this observation was based only on a small HNSCC sample number. If detectable, CD133 seems to be associated with a tendency to metastasize (Tang et al., 2013; Mannelli et al., 2015).

Some groups have recently suggested further molecular stem cell markers in squamous cell carcinoma, including SOX2, where, in particular, a co-expression of ALDH1 and SOX2 was found (Huang et al., 2014). The SOX2 gene encodes for a transcription factor that is responsible for maintaining the self-renewal capacity in physiological stem cells and neural progenitor cells (Adachi et al., 2010). It has only recently been associated with stem cell properties in malignant cells (Huang et al., 2014).

In summary, it can be stated that there is no single tumor stem cell marker and no combination of markers currently established in HNSCC. Features of malignancy, such as susceptibility to metastasis and recurrence were related to varying expression levels of various stem cell markers.

Immune CPI are one of the central developments in oncology during the last decade. Unfortunately, as has been mentioned above the response is very heterogeneous in many tumor entities, including HNSCC. The efficacy of CPI is limited by the capacity of tumor cells to escape the immune system. CSCs are supposed to play a crucial role in this process as they are known to contribute to the formation of metastases and recurrences. However, the informative value of stem cell markers as predictors may be limited due to the distinct intratumoral heterogeneity as well as tumor/metastasis heterogeneity in HNSCC. Expression levels may be subject to variability within the tumor and during tumor progression (Ihler et al., 2018). To be able to take all these aspects into consideration, innovative preclinical tumor models need to be established and standardized.

ENVIRONMENTAL AND LIFE-STYLE INFLUENCES IN CSC BEHAVIOR

As many other cell types, CSC are also regulated by a variety of extrinsic microenvironmental stimuli and adapt to changing environmental conditions such as hypoxia or nutrient deficiency (Peitzsch et al., 2019a,b). Under the exposure of specific stimuli, stem cells are capable of acquiring a specific phenotype. Stem cell behavior can be influenced by various factors such as oxygen concentrations. Adult stem cells have the ability to shift toward an oxidative metabolism once remain in a state of quiescence in their specialized niche until external signals induce a metabolic shift toward an oxidative metabolism (Kumar et al., 2017).

One critical extrinsic factor is nicotine. Yu et al. suggest by their data that this noxious agent may play a critical role in the development of tobacco-induced cancers by regulating CSC features, and that these effects are likely mediated through pathways that promote epithelial-mesenchymal transition (EMT). Nicotine promotes the CSC phenotype thereby enhancing the tumor-propagating capability of HNSCC cells (Yu et al., 2012). In NSCLC cells it has also been shown that nicotine can induce expression of Sox2 as well as mesenchymal markers and enhance migration and stemness (Schaal et al., 2018). Alcohol has also been proposed as another key factor for the development of HNSCC as there is evidence that alcohol increases CSC population, thereby promoting aggressiveness, recurrence, and therapy resistance of cancers.

Activation of signaling compounds such as MAPK, Wnt/GSK3β/β-catenin, and TLR4/Nanog, and alterations of the TME induced by alcohol cause the promotion of CSC. These environmental factors, which frequently apply to HNSCC patients may reveal novel therapeutic approaches targeting the respective multi-components/cascades regulating characteristics of CSC (Xu and Luo, 2017). Based on the results from preclinical *in vitro* and *in vivo* studies it is likely that combining chemotherapy with CSC-targeting agents may help to overcome resistance against conventional chemotherapy. A variety of compounds targeting CSC differentiation and cell death cascades in combination with chemotherapy are currently being investigated in clinical trials (Li et al., 2017). After completion, new insights about safety and efficacy of these combination schemes are expected.

PRECLINICAL TUMOR MODELS FOR HNSCC

Preclinical models that precisely predict clinical outcomes are urgently needed in the field of cancer drug discovery and development (**Figure 1**).

Under optimal conditions, tumor tissue can be kept in culture over a period of sufficient length to be able to investigate short- and long-term effects of therapy. By testing different treatment strategies, the outcome of the individual patient can be analyzed before starting treatment and will help assign patients to their optimal therapy. Due to the existent progression in the development of new therapy regimens such as targeted therapies and immunotherapies, cell culture techniques also attained increasing prominence, in particular those that grow in three-dimensional (3D) architecture (Demers et al., 2020) (**Table 1**).

Three-Dimensional Culture Models/Spheroids

Spheroids have widely gained popularity because they reflect the tumor architecture more precisely compared to 2D systems or monolayer cultures. A tumor grows in a 3D spatial array therefore cells incorporated in these tumor formations are not evenly exposed to nutrients and oxygen as well as to cellular stress factors. The TME varies between the single regions of a 3D tumor construct. It is clear that in a 2D assay all tumor cells are exposed to oxygen and nutrients in an equal manner. Thus, in this system the factual situation in cancer is misrepresented and is only suitable to assess a minor fraction of HNSCC molecular biology aspects. The impact of cell-cell contacts on therapeutic

TABLE 1 | Preclinical 3D models for HNSCC.

Tumor Derivation	HNSCC
Spheroids	Köpf-Maier and Zimmermann, 1991 Eke et al., 2009 Storch et al., 2010 Eke et al., 2013 Hagemann et al., 2017 Hagemann et al., 2018 Melissaridou et al., 2019 Driehuis et al., 2019
Co-cultures	Hoffmann et al., 2009 Sawant et al., 2016 Young et al., 2018 Huang et al., 2019 Dean et al., 2020
CSC-enriched spheroid models	Lim et al., 2011 Goričan et al., 2020 Melissaridou et al., 2019
Patient-derived explant models *-in vitro-* *-in vivo-*	Robbins et al., 1994 Au et al., 1993 Pathak et al., 2007 Gerlach et al., 2014 Suzuki et al., 2015 Freudlsperger et al., 2015 Donnadieu et al., 2016 Affolter et al., 2016 Peria et al., 2016 Hickman et al., 2014 Dohmen et al., 2018 Engelmann et al., 2020 Peng et al., 2013 Li et al., 2016 Klinghammer et al., 2015 Facompre et al., 2017 Morton et al., 2016 Stecklum et al., 2020
Tumor on chip	Bhatia and Ingber, 2014 Skardal et al., 2017 Aleman and Skardal, 2019 Carr et al., 2014 Kennedy et al., 2019 Bower et al., 2017 Sylvester et al., 2013
Bioprinting models	Almela et al., 2018
Mathematical modeling for precision medicine	Linxweiler et al., 2016 Panikkanvalappil et al., 2019 Emerick et al., 2013 Enderling et al., 2019 Caudell et al., 2017 Scott et al., 2017

CSC, cancer stem cells; HNSCC, Head and neck squamous cell carcinoma.

response is not depicted in monolayer cultures; the informative value of *in vitro* treatment efficacy studies is limited (**Figure 1**).

When analyzing treatment sensitivity, considerable differences were observed between 2D and 3D HNSCC *in vitro* cultures in response to irradiation (Storch et al., 2010) and EGFR inhibitors or cisplatin (Melissaridou et al., 2019). Interestingly, Melissaridou et al. reported an increased resistance to cisplatin treatment, which might be due to increased expression of CSC-associated proteins Nanog and Sox1 observed in tumor spheroids. They conclude that cells cultured in 3D take on the CSC-like phenotype and that lower sensitivity of cells cultured under 3D conditions may be attributable to this increase expression of genes associated with epithelial-mesenchymal transition (EMT) and stemness (Melissaridou et al., 2019).

Multicellular tumor spheroids (Franko and Sutherland, 1979; Köpf-Maier and Zimmermann, 1991) have been established for various entities including HNC already decades ago. Spheroids have an outer layer of proliferating cells and an inside layer of mainly quiescent cells with necrotic areas in the center and can be further divided into different subpopulations (Carlsson and Nederman, 1989). In 2012, it was demonstrated that there is great similarity of EGFR signaling and radiation response between 3D SCC cultures and HNSCC xenografts compared to cell monolayers (Eke et al., 2013). The authors describe a greater physiological relevance of 3D growth conditions regarding cell morphology, gene and protein expression patterns, protein-protein interactions, and intracellular signaling as well as response to radio/-chemotherapy (Kenny, 2007; Eke et al., 2009; Storch et al., 2010).

These 3D models have been shown to phenocopy the original tumor in a way that *in vitro* drug responses of the model can be traced back to genetic alterations of the primary (Drost and Clevers, 2018). Hagemann et al. (2017, 2018) propose a single spheroid-based *in vitro* assay, which is described as a testing tool for individual therapy susceptibility to current standard and new targeted regimens. Spheroids were generated from single cell suspensions, first from different cell lines including the proprietary PiCa cell line, later from primary human cancer cells derived from fresh tumor biopsies. Spheroids were exposed and incubated with cisplatin or 5-FU, which led to a significant reduction in growth speed over time compared to untreated controls. Spheroids were also irradiated with a dose of 2 Gy significantly reducing the dynamic of cellular growth. They claim their spheroid model to be a useful tool to unveil drug effectiveness and complex drug resistance mechanisms. Factors impacting on radiation response such as DNA repair, apoptosis, oxygen supply and cellular contacts in spheroid cell culture are considered as comparable to *in vivo* tumors (Dubessy et al., 2000; Weiswald et al., 2015). Although 3D cultures such as spheroids have advantages compared to monolayer techniques, the system has inherent limitations. Although spheroids are established for being exposed to different conventional and novel therapies with cell viability and spheroid size as read-outs these experiments and moreover the correlation with clinical data and prognosis are still pending. The model is most likely a straight forward and cost-efficient assay but

it is unclear how predictive it is in terms of correlation with the later response to therapy and with clinical outcome (Hagemann et al., 2017, 2018).

Extensive analyses on and detailed culture conditions for oral mucosal organoids were recently published by Driehuis et al. (2019). They managed to keep a panel of 26 organoids deriving from HNSCC and corresponding normal epithelium in culture for 10–14 days. The organoids showed rapid growth and culture exceeded 65% efficiency. Productive infection of the organoids with herpes simplex virus (HSV) and HPV could be demonstrated which has so far only been described for immortalized cell lines, or primary cells with short cultivation periods. The susceptibility to common drugs such as cetuximab, the PI3K inhibitor alpelisib, and the BRAF inhibitor vemurafenib was also assessed. In summary, the tumor cell phenotype, the tumorigenic potential, and the response to therapy were assessed by the use of the 3D model. Altogether clinical response data of seven HNSCC patients were analyzed. In one case, a correlation between radiation sensitivity of the HNSCC organoids and the clinical response of the corresponding HNSCC patient could be observed. However, the authors define the aim of the study as of establishing optimal conditions as an experimental basis for future prospective investigations of larger tumor cohorts, not to determine the predictive potential of HNSCC-derived organoids in therapeutic guidance.

Cancer stem cell-enriched spheroids incorporate CSC or cells with stem cell traits. The expression of CD44 detected by cell sorting or self-renewing features is used for enriching these CSC. Weiswald et al. (2015) describe tumorospheres as a model of CSC expansion established in a serum-free medium with stem cell media growing under low-adherent conditions. In this model it has to be ensured that the self-renewal capacity of the CSC is depicted. Goričan et al. describe a new HNC stem cell-enriched spheroid model (SCESM) suitable for high-throughput screens of anti-CSC compounds. Advantages are that the model is faster than the traditional culture of free-floating spheres and enables higher CSC enrichment than the multicellular spheroid model (Goričan et al., 2020). Melissandrou et al. found that under 3D culturing conditions cells adapt to a CSC-like phenotype. They observed that results from 3D HNSCC culture differed significantly from monolayer data (Melissaridou et al., 2019). HNSCC-driven sphere-forming cells (referred to as squamospheres) that possess the general properties of CSC, such as self-renewal, stem cell marker expression, aberrant differentiation, tumor-initiating potential, and chemoresistance with increased side population have been reported by Lim et al. (2011) who interpret their model as an aid for new insights into CSC biology in HNSCC.

However, the usability of CSC-enriched spheroids is limited by the fact that the original tumor is not histologically preserved. Furthermore, CSC frequently develop a central necrosis (Demers et al., 2020). Putative CSC or tumor cells exhibiting stem-cell like features for the use of 3D cultures have been obtained from tumors. As CSC cultivation is determined by certain in-depth conditions which these experiments do not necessarily adapt why results from CSC-enriched spheroid cultures should be accepted with reservation (Ishiguro et al., 2017).

The evaluation of self-renewal can be hampered by cell density as the clonal growth conditions are impaired. The comparability of different studies on CSC-enriched spheroids is limited because of the variation of experimental parameters such as sphere size. However, it is anticipated that after refinement of protocols and SOPs tumor-derived cultures will be a useful tool for the identification of CSC-inhibiting molecules. Especially in the light of liquid biopsy approaches, spheroid cultivation of CSC obtained from circulating blood may allow to analyze the original tumor in a non-invasive manner (Ishiguro et al., 2017) (**Figure 1**).

Head and Neck Cancer Models Preserving the TME – 3D Co-culture Tumor Models

There are many benefits from current models such as organoids but although these models have been shown to phenocopy the original tumor in terms of drug susceptibility they lack the preservation of tumor-stroma interactions which are known to be essential for carcinogenesis and even resistance development (Storch et al., 2010; Valkenburg et al., 2018). Sensitivity testing of novel immunotherapeutic approaches is impaired as they require an intact immune system to be effective. Results from co-culture studies (Sawant et al., 2016) give clear evidence that the TME exerts tumor-promoting effects (Curry et al., 2014) which is a strong argument for the establishment and implementation of more advanced 3D tumor models (Tinhofer et al., 2020). Cancer-associated fibroblasts (CAFs), one of the major components in TME, play a critical role in tumorigenesis. On the one hand, there is an active interaction of CAFs with tumor cells, with CAFs promoting survival and invasion properties of cancer (Xu et al., 2014; Young et al., 2018; Rodrigues et al., 2020). CAFs create a tumor-supportive environment but do not only affect tumor cells but also immune cells through direct and indirect mechanisms (Takahashi et al., 2016; Huang et al., 2019). However, more interrelations need to be extensively studied to better understand the role of CAFs in HNC. For instance, CAFs might play a different role in HPV-driven HNSCC compared to non-HPV driven HNSCC, but these aspects are still unclear. As tumor-associated stromal cells exert either positive or negative effects on tumor growth and propagation, the absence of the stromal components in multicellular tumor spheroid models limits the utility of such models in cancer research (Xu et al., 2014). 3D cell culture models incorporating the tumor in its entirety are therefore clearly needed to illustrate dynamic and reciprocal interactions between the solid tumor and the TME, including immune cells, stromal cells, stromal ECM components, and growth factors (**Figure 1**).

Young et al. propose the TRACER model (Tissue Role for the Analysis of Cellular Environment and Response) as a co-culture protocol simulating interactions between CAF-TME in head and neck tumors. The original basic monoculture TRACER system is a stacked paper tumor model in which cells in a hydrogel matrix are infiltrated into a cellulose scaffold that is rolled onto an aluminum core to reflect a 3D construct. The authors have refined the former monoculture by incorporating both head and neck primary patient CAFs and head and neck tumor cell populations

in order to assess tumor-CAF interrelations. The longest culture time that was assessed for the co-culture TRACER configuration is 48 h as it was assumed that cancer cells would outgrow CAFs in a direct co-culture construct under extended cultivation periods. The authors who were using an immortalized HNSCC cell line (FaDu) speculate that primary cancer cells would be essential to avoid outgrowth and also to reflect heterogeneity of the patient population. The model is considered to be feasible for reflection of migration patterns of tumor cells through the CAFs environment and for mimicking CAFs' influence on tumor cells. However, the authors consider the fact that the system is not entirely suitable to address questions that require real-time imaging. Furthermore, while some features of the TME can be recreated, relevant structures such as a basement membrane and other important cell types are not represented in the platform (Young et al., 2018). The cultivation period is rather short with only 48 h because of the anticipated outgrowth of tumor cells that might cause a disproportionate ratio of the two cell populations. The authors envision that incorporation of primary cancer cells in the system will be necessary for longer cultivation periods and also to reflect heterogeneity of patient tumors. The model was supposed to be valuable for exploring the impact of hypoxia which is known to alter the behavior of stroma and cancer cells toward progression of disease (Brown and Wilson, 2004; Vaupel et al., 2004; Vaupel and Mayer, 2007). Conventional 3D co-culture models are mostly unsuitable to assess questions where spatial organization of different cellular components within the tumor is relevant. The TRACER platform, however, is assumed to be useful for patterning of distinct cellular compartments and cell separation for phenotypic assessment (Young et al., 2018).

Dean et al. expand the TRACER model by co-culturing HNSCC cells with CAFs and found that tumor cell invasion into an acellular collagen layer was enhanced in this co-culture setting. The observation was found to be dependent on the distribution of ECM density within the culture. The platform allowed to mimic density variations of tumors *in vivo* and to reflect the distribution of CAFs within the tumor at different disease stages (Dean et al., 2020).

Hoffmann et al. demonstrated that an anti-EGFR monoclonal antibody induced leukocyte infiltration into EGFR-overexpressing tumor spheroids due to an upregulation of chemokine expression mediated by anti-EGFR signal transduction. The spheroids enabled them to identify molecular mechanisms responsible for anti-EGFR monoclonal antibody-mediated infiltration of immune cells into tumors (Hoffmann et al., 2009).

Patient-Derived Explant Models

Patient-derived explants may be beneficial as those systems retain the original TME including the ECM, and stromal, immune, and vascular cells, thereby reflecting tumor stroma interactions. Powley et al. (2020) claim PDEs to be a potent model of choice for cancer drug and biomarker discovery programs taking tumor heterogeneity into account. However, the application of PDEs has not been implemented in the daily clinical routine yet. We recently described the maintenance of HNSCC tumor explants on a dermal equivalent (DE) for up to 21 days, which is the longest culture duration demonstrated so far (Demers et al., 2020; Engelmann et al., 2020). The DE containing human fibroblasts is used as a scaffold for cultivating vital HNSCC samples. One of the main findings was that the model allowed to classify the tumor samples into different invasion patterns, namely invasive, expansive, and silent. The invasive type shows an infiltrative scattering of detached tumor cell clusters into the scaffold. Expansively growing tumor samples migrate horizontally on top of the DE, while silent type tumors grow without migration or invasion. CAFs and leucocytes could be consistently detected for up to 21 days representing the modeling of an intact TME. The new system allows to mimic fractionated irradiation showing heterogeneous responses within the cohort, measured by expression levels of apoptosis marker cleaved caspase-3 as a read-out. Interestingly, one patient suffering from an early recurrence 17 months after first diagnosis and treatment, with the corresponding 3D-OTC sample displaying invasive growth which might reflect a more aggressive tumor biology. Although it was feasible to maintain HPV-driven HNSCC in culture for up to 21 days the interpretation of results was more challenging, with varying p16INK4a expression levels over time (Engelmann et al., 2020).

Dohmen et al. present a sponge-gel-supported histoculture model, which has been developed for prediction of individual responses to therapy. Tumor fragments were kept in culture for 7 days The proportion of tumor cells could be quantified, tumor viability, proliferation, EGFR expression levels and present immune cells were scored The authors emphasize the sustainability of the microenvironment they found with immune cells still present on day 7 as one of the major advantages of their model. Although it was unclear whether they were still functionally active or viable, based on the morphology the authors believe the immune cells to keep their viability up to day 7. The authors hope that the histoculture model, which comes closer to reality than cell lines or even organoids due the preservation of the heterogeneity and TME may allow for personalized treatment stratification and testing for new treatment strategies in the future (Dohmen et al., 2018).

In the past few years the *ex vivo* tissue culture model was established. The model allowed to prove the increased activation of the ERK/MAPK and PI3K-AKT signaling cascades by irradiation and its modulation by pharmacological inhibition (Freudlsperger et al., 2015; Affolter et al., 2016). A heterogeneous induction of ERK and AKT phosphorylation was found in the tumor tissue cultures suggesting a contextual regulation mode. Due to the small number of cases, correlation with clinical parameters was possible only to a limited extent. However, patients with low basal ERK phosphorylation and postradiogenic induction suffered from a relapse during follow up suggesting that this constellation might be an indicator for an unfavorable outcome (Affolter et al., 2016).

Peria et al. describe the cultivation of explant HNSCC tissue cultures over 48 h in order to immunohistochemically evaluate the expression of Ki-67, AE1, AE3, p40, and CK-5/6 after administration of cetuximab or sorafenib, respectively. During this time frame tumor architecture and cell viability were sustained. Afterward, the tissue increasingly developed necrosis and the effect of treatment with cetuximab based on few remaining proliferating cells could no longer reliably be analyzed.

Clinical patient data were not matched with the results from the explant cultures. This is planned for follow-up studies in bigger cohorts (Peria et al., 2016).

Despite encouraging results described by us and others PDE cultures are limited by the following factors as summarized by Powley et al. (2020): PDEs can only be cultured after extraction of sufficient spare tumor material either by surgical resection of the tumor or tumor biopsies. Fresh tumor tissue for experimental procedures needs to be obtained before the surgical specimen is formalin-fixed for pathologic routine diagnostics. That means, the excision of tumor material for experimental procedures must by no means affect clinical diagnostics. The access and preparation of tumor tissue is dependent on the collaboration with head and neck surgeons, OR staff, and pathologists. Last, if the tumor tissue is not intact anymore, experimental data can be impaired. Therefore, Powley et al. list PDEs as a poor model for invasion and metastases, however, we have recently featured a 3D-organotypic co-culture model for HNSCC as a tool to study different invasion patterns possibly correlated with clinical characteristics and outcome We did not detect any disintegration of the tumor architecture during this period (Engelmann et al., 2020). Peria et al. referred to the currently required relatively large amount of fresh tumor tissue as a disadvantage of short-term assays. In small HNSCC there is a risk of rendering the margins of the specimens unusable for the pathologist when preparing vital tissue cultures. The authors aim to adapt their technique to the use of needle biopsy material to generate higher case numbers (Peria et al., 2016).

Hickman et al. (2014) criticize that a standardization of the manufacturing process could be hampered by the variability of individual steps such as ischemia times of the tissue and time window to start the cutting procedure. Mechanical stress factors in the course of sample processing, such as changes of temperature, the oxygen content, and availability of nutrients, not only determine the tissue quality at the starting point of the cultivation, but are likely to influence both the sensitivity of the tumor cells *ex vivo* on therapeutics as well as their suitability for reliable biochemical analyzes. So far, these issues appear to pare down most of the tissue cultures approaches to short-term experiments (**Figure 1**).

Possible solutions are, on the one hand, combinations of strategies, to achieve longer cultivation times, such as scaffolding the vital tumor explant by distinct matrices as a co-culture model (Engelmann et al., 2020). On the other hand, the comparison of preparation and culture conditions in multicenter validation studies for simplification of processes is a prerequisite to find a broad application in patient stratification for novel, yet to be defined therapy regimens. Once there is a standard protocol, expression analysis of central markers for pathogenesis and for treatment response in HNSCC should be evaluated to test their sensitivity to combination schemes consisting of new and conventional treatments.

Patient-derived xenograft (PDX) models are being applied for various tumor entities including HNSCC (Fichtner et al., 2008; Daniel et al., 2009; Peng et al., 2013; Lin et al., 2014; Li et al., 2016). They are generated by implantation of tumor cells derived from fresh patient tumor tissue subcutaneously, orthotopically, or under the kidney capsule of immunodeficient mice (e.g., NODSCID, NSG mice) (Choi et al., 2014). Conventional xenograft models with established tumor cell lines often show little histological similarity to the original tumor, due to *in vitro* co-cultivation and associated changes in the genetic and epigenetic profiles (Daniel et al., 2009). It is feasible to analyze different compounds and their combinations through passaging and transplantation of the tumor in several mice. It has been observed in several studies that PDX models do predict clinical trial drug responses (Bertotti et al., 2011; Gao et al., 2015; Townsend et al., 2016; Karamboulas et al., 2018).

At least initially, PDX models represent complex biological and molecular interactions between tumor cells and their microenvironment (Garber, 2009; Tentler et al., 2012). Furthermore, phenotypic and molecular characteristics of the original tumor tissue such as chromosomal copy number variants, single nucleotide polymorphisms and gene expression profiles, are mapped (Choi et al., 2014). Cassidy et al. criticize that stromal influences on therapy response as well as immunologic drivers remain underrepresented in the PDX model. In the course of passaging, the PDX parts of the human stroma are replaced by murine equivalents, and it is unclear how precisely mouse fibroblasts mimic their human counterparts (Cassidy et al., 2015). Another main challenge of PDX models is the lack of a functional human immune system to analyze tumor-TME-interactions, especially in terms of immuno-oncological questions. High costs and high personnel expenditure also hinder the widespread use of the model system (Choi et al., 2014). Moreover, the engraftment of HPV-driven HNSCC compared to non-HPV driven HNSCC appears to be complicated as reported in various studies (Klinghammer et al., 2015; Facompre et al., 2017).

A possible solution for the lack of a functional immune system in the PDX model is the humanized mouse model (XactMice model) for HNC (Morton et al., 2016). In this system, human hematopoietic stem and progenitor cells (HSPCs) reconstitute the bone marrow from NSG (NOD/SCID/IL2rg-/-) mice that has previously been suppressed by irradiation. Consecutively, patient-derived tumor tissue is transplanted into the mice. Human HSPCs form immune cells that invade into the xenograft and recreate its natural microenvironment. In consequence, the expression patterns of epithelial, stromal, and immunological genes in XactMice tumors match the patient's tumor to a greater extent than tumors from non-humanized mice. Likewise, iPDX (immune-patient-derived xenograft) models offer the possibility of testing the effects of CPI on the human immune system. In this variation of the conventional PDX platform the experiments are performed during the first passages, before the replacement of human by murine stroma. By systemic administration of monoclonal antibodies to the animals, human TILs in the TME can be targeted. So while it is advantageous to explore the species-specific interaction among human tumor and immune cells, broad clinical applicability is limited by the fact that iPDX only start growing after 1–2 months and the number of mice that can be xenografted per sample is low (Sanmamed et al., 2016). Approaches for HNSCC immune-PDX models have recently been proposed (Stecklum et al., 2020). However, there is no resounding draft for the application of PDX models in the clinical routine so far.

REAL-TIME LIVE IMAGING IN PRECISION MEDICINE

Molecular imaging is a real-time and non-invasive approach for visualization of expression and activity of relevant targets as well as various biological processes, namely hypoxia, angiogenesis, and apoptosis. The ambitious aim is to streamline progress into novel drug development approaches by discovering physiologic or molecular alterations prefiguring cancer at an early stage with better prognosis, and depicting response to cancer therapy in a real-time setting (McDermott and Kilcoyne, 2016). New optical technologies such as confocal laser endomicroscopy (CLE) help to overcome invasive and time-consuming surgical biopsies. CLE enables microscopic visualization of lesions in real-time (optical biopsy) for different cancers, including HNSCC (Linxweiler et al., 2016). From their study on 10 HNSCC tissue samples Shinohara et al. describe a clear difference between cancer and normal mucosa in the uniformity of nuclear size and shape measured by real-time *in vivo* imaging using CLE. The technique could potentially be usable for the distinction of cancerous from non-cancerous tissue without invasive biopsies. Although the authors point out to several limitations, such as the examiner's bias and their improvable double staining method, it is likely that CLE will gain relevance for in real-time classification of regions in the head and neck (Shinohara et al., 2020). Panikkanvalappil et al. describe plasmonically enhanced Raman spectroscopy (PERS) in the real-time monitoring of endogenously generated CO and assessing the dynamics of hemeoxygenase-1 (HO-1) in live HNC cells. Their findings could produce useful insights into the signaling action of CO and HO-1 in tumor progression (Panikkanvalappil et al., 2019). Lee et al. established intravital imaging models to enable real-time observation of cancer cells of the bone marrow environment. In an approach to identify the biologic processes of cancer cells in a real-time manner the distribution and phenotype of cancer cells in bone marrow of a live mouse model could be assessed by two-photon microscopy. The study provided new data about *in vivo* cancer cell biology in bone marrow. In particular, the group identified dormancy and reactivation of cancer cells. Interestingly, after injection of the chemotherapeutic agent gemcitabine, cancer cells appeared to be less affected than normal cells in the bone marrow. However, the technique has certain disadvantages, as the scope to perivascular niche for the cancer cells in the bone marrow environment is limited and wound healing processes as induced by bone marrow transplantation, might impair the results. The model is promising but has to be experimentally validated (Lee et al., 2018). To date, for HNSCC there is no comparable real-time live imaging model.

SENSITIVITY TESTING IN HISTOCULTURE MODELS

Already 25 years ago approaches were taken to assess the correlation between drug sensitivity of sponge-gel-supported histocultures and their corresponding original HNC specimens to cisplatin (Robbins et al., 1991, 1994; Au et al., 1993). The *in vitro*-like maintenance of three-dimensional tissue architecture of the tumors in histoculture was supposed to confer clinical predictivity of drug response of the model (Robbins et al., 1994). The Histoculture Drug Response Assays (HDRA) is a three dimensional native state histoculture assay that simulates the structure of tumor in the body and is used to assay the chemo-responsiveness of the tumor. One major limitation of these HDRA is their comparatively short cultivation period (Robbins et al., 1991, 1994). HNSCC histocultures have been tested for response to various chemotherapeutics, such as cisplatin, 5-FU, and mitomycin C treatment. While there were no apparent differences for cisplatin and mitomycin C, the nodal metastatic tumors seemed to be less sensitive to 5-FU than the primaries (Au et al., 1993). A more recent study by Gerlach et al. tested the response of vital HNSCC slides on membrane culture inserts to cetuximab, cisplatin, and docetaxel and observed cell loss and also an increase of apoptosis reflected by an increase of cleaved caspase 3 after treatment with docetaxel but not with other drugs. The authors concluded that their assay can be used to better understand the mechanisms of tumor resistance by harvesting surviving tumor cells after treatment. However, they did not correlate susceptibility to treatments of the cultured tumor samples to the respective patient's response and clinical outcome yet (Gerlach et al., 2014).

Indeed there was one study in which patients received the same treatment that was tested *in vitro*, by the use of a HDRA (Pathak et al., 2007). Inhibition rates quantified by proliferation assays were taken as a read-out. There was a significant correlation between the *in vitro* chemosensitivity and the clinical response to different chemotherapeutic regimens.

Although these data appear promising, there are various reasons why the HDRA is not taken into routine clinical practice such as the requirement of an in-hospital laboratory to ensure the quick processing of fresh biopsies, large effort of time and personnel and last the lack of sensitivity and specificity when correlating *in vivo* tumor response to *in vitro* HDRA chemosensitivity (Dohmen et al., 2018).

In terms of survival prediction, Suzuki et al. investigated the correlation of overall survival represented by 18F-FDG-uptake with *in vitro* sensitivity data. 18F-FDG-uptake of the primary tumor in PET/CTs, which is considered as a marker of poor OS, and *in vitro* chemosensitivity of cisplatin using HDRA in HNC were correlated. In samples with a high inhibition index of cisplatin in the patient cohort a prolonged OS was significantly associated with a high inhibition index (>50) and a high SUV max (standardized uptake value) validated by PET (Suzuki et al., 2015).

Recently, Driehuis et al. reported a BRAF-mutant organoid line derived from a BRAF-mutant HNSCC to show increased responsiveness to the BRAF inhibitor vemurafenib. However, no correlations between EGFR expression of the organoids and cetuximab response were found when cetuximab was applied or between sensitivity toward PI3K inhibitor alpelisib and organoids harboring a PIK3CA mutation (Driehuis et al., 2019). Donnadieu et al. report the short-term cultivation of HNSCC tumor slices for 48 h. Cultures were exposed to a panel of targeted therapies that are directed against selected oncogenic transduction pathways,

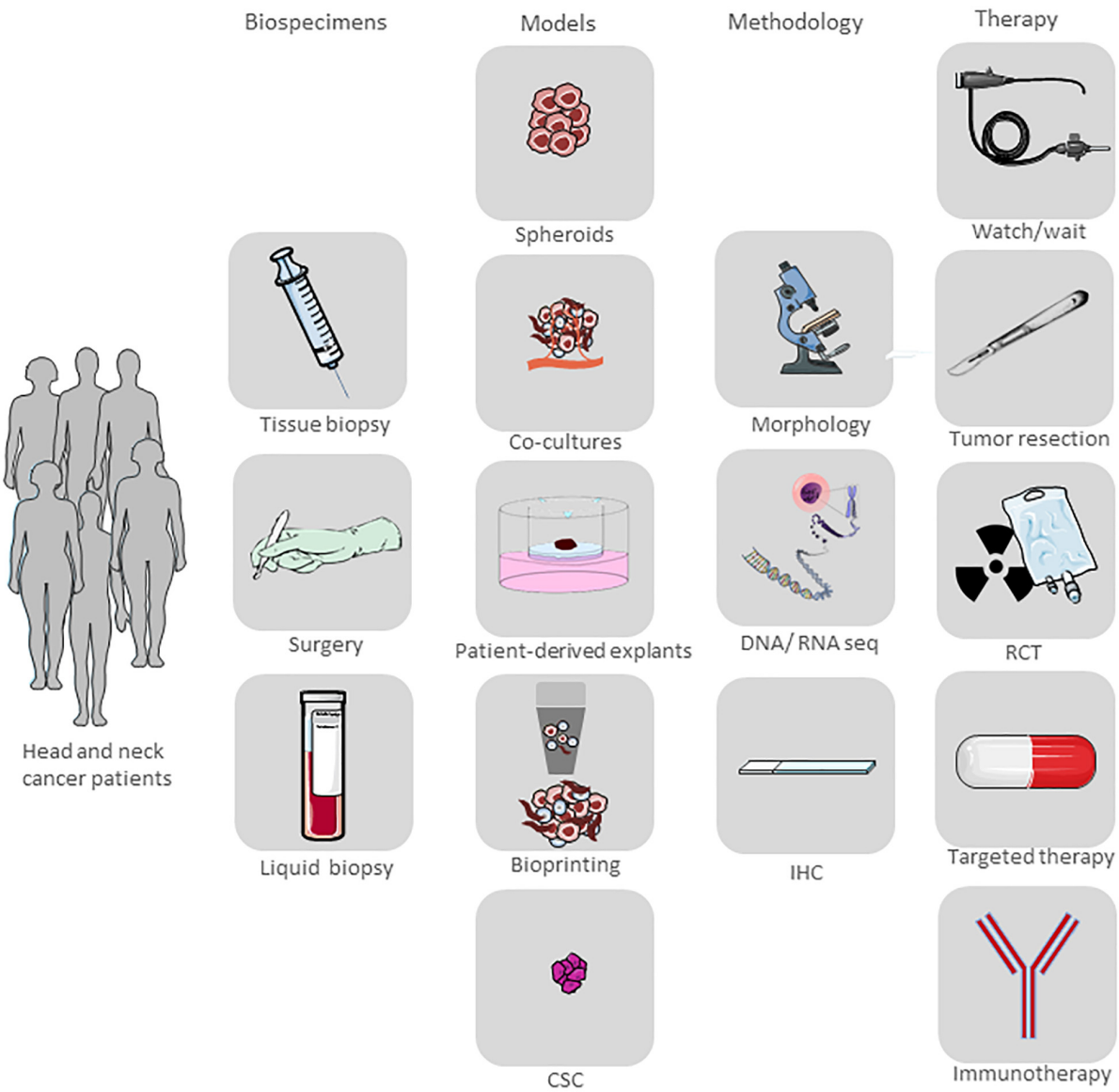

FIGURE 2 | Vision of a translational HNSCC platform. The platform ultimately aims to shorten time to diagnosis and treatment, predict tumor relapse or progress and identify targetable mutations after treatment by analysis of different biospecimen with established and new, innovative technologies. Overall, developing a precision medicine platform for head and neck malignancies will improve survival in patients with a dismal clinical outcome. Parts of the figure were drawn by using pictures from Servier Medical Art (http://smart.servier.com/), licensed under a Creative Commons Attribution 3.0 Unported License (https://creativecommons.org/licenses/by/3.0/).

including EGFR, B-RAF, KIT, HGFR, FGFR, and mTOR. The compounds were in phase II/III trials for the treatment of solid malignancies at the time the study was conducted. The authors observed varying responses to the different treatments in the individual patient samples. Proliferation was impaired by multi-kinase inhibitor sorafenib in 5/14 of the individual patient samples while, interestingly, cetuximab as the only drug approved for HNSCC treatment was only effective in 2/14 tumors. At least one of the eight drugs tested caused a more than 50% inhibition of proliferation in 10/14 tumors (Donnadieu et al., 2016).

PERSONALIZED THERAPEUTIC APPROACHES FOR HNC BASED ON 3D AND STEM CELL MODELS AND IMPLEMENTATION INTO CLINICAL ROUTINE

Why has none of the novel and auspicious efforts made it into the clinical routine so far? Blom et al. discuss the lack of evidence in the form of prospective correlations as a reason. No randomized controlled trials have been performed to compare

assay-led treatment with standard or physician's choice of therapy regarding prolongation of survival (Blom et al., 2017).

Precision medicine initiatives applying small molecule inhibitors (SMIs) and monoclonal antibodies may reveal significant potential for the management of not only HNSCC but also malignancies of the salivary glands. Still, targeted therapy studies have not shown any sweeping success in HNSCC so far (Machiels et al., 2010; Schmitz et al., 2012; Vokes et al., 2015; Kochanny et al., 2020; Seiwert et al., 2020). Preclinical tumor models provide the opportunity to test targeted therapies on patient tissues. However, as mAbs and SMIs except cetuximab are not implemented in the clinical routine treatment of HNSCC yet, the correlation of experimental results with clinical data and outcome is practically impossible. This may be one explanation why the predictive potential of 3D cancer models has not been validated in large patient populations so far.

Different diagnostic tests are routinely used to predict the activity or resistance of some targeted therapies. Molecular profiling of the individual tumors is performed in the frame of biomarker-driven studies but to unveil mechanisms of resistance development is not considered in these studies (Von Hoff et al., 2010; Tsimberidou et al., 2012, 2017; Massard et al., 2017; Harris et al., 2018). Some trials select patients upfront on the basis of genetic alterations which are generally rare, for instance, when treating patients with FGFR-positive recurrent HNC with Infigratinib (BGJ398) (NCT02706691) or screening patients for HRAS mutations to allocate them to treatment with Tipifarnib (NCT03719690). Although the medication arms in these trails seem to yield promising results, the trials bear the risk of a large proportion of screen failures as they assign patients to a very specific therapy for rather small subpopulations harboring those rare mutations.

The EORTC-1559-HNCG (NCT03088059) is an umbrella biomarker-driven study dedicated to recurrent and/or metastatic HNSCC patients for second-line treatments and beyond after platinum-based therapy (Galot et al., 2018). First, NGS and IHC, respectively are carried out on actual biopsy material in order to depict oncogenes and tumor suppressor genes relevant for HNSCC. These findings are the basis for the inclusion of patients to one of the treatment arms or in case of non-eligibility to an immunotherapy cohort (Galot et al., 2018).

So-called window-of-opportunity clinical trials aim to identify biomarkers in tumor samples that have been collected after application of a certain drug for a short period of time and before definitive therapy, while efficacy is not necessarily expected. This period is called a window-of-opportunity situation. It is an advantage that post-treatment samples can be easily collected from the surgically removed specimen. However, window-of-opportunity trials have been rare, especially in HNSCC (Marous et al., 2015; Gougis et al., 2019).

More umbrella and basket trials are currently under way for HNSCC to investigate targeted compounds in monotherapy (Galot et al., 2018; Gougis et al., 2019). However, tumor heterogeneity is one of the most notable features of HNSCC is not taken into account. Hence, translational research focusing on the analysis of liquid biopsies and tumor tissue samples and building bridges between bench and bedside is crucial for identifying resistance mechanisms and subsequently new combinatorial regimens that are potent to overcome them.

In this regard, it should be considered that in HNSCC DNA-guided precision medicine is not the only aspect to be taken into account. The genotype alone may not reliably predict drug responses suggesting that the tissue in which the cancer mutation occurs can be a major factor in determining response to therapy (Cohen and Settleman, 2014; Voest and Bernards, 2016).

As discussed before, sensitivity testing in histoculture models is not novel in HNSCC research. In 2001, Singh et al. already claimed the HDRA to be a strong predictor of survival. There was a significant association between HDRA assessment of chemoresponse and clinical outcome in 41 HNSCC samples treated with cisplatin and 5-fluoruracil. Afterward, cell survival fractions were determined by proliferation assays. A tumor was defined sensitive when the inhibition rate was greater than 30%. Patients whose tumors were sensitive toward one or both of the chemotherapeutic agents had a more favorable outcome in terms of cause-specific survival at 2 year follow up (Singh et al., 2002). In a more recent study, Jamal et al. demonstrate results from a retrospective analysis of 22 HNSCC specimens that underwent testing with the ChemoFx assay (Precision Therapeutics, Inc.). The assay is supposed to determine the response to chemotherapy thereby serving as a prediction tool. Tumor cells were isolated from solid tissue samples and cultured, then exposed to increasing dosages of conventional chemotherapeutic agents. Response was measured in quantifying cell counts and classified as "responsive," "intermediate response," or "non-responsive." Data from 11/21 patients were eventually interpreted. Nine of those showed a predictable chemoresponse assay (81.8% predictability of effective treatment). All 6 patients who had a predictable poor response failed their chemotherapeutic regimen within 6 months and succumbed to their illness after 3 years of follow up, except one patient with an intermediate response in the assay. The authors interpreted the test to having the potential as a useful adjunct for the selection of therapeutic schemes while acknowledging its limitations (Jamal et al., 2017). Although the data are quite promising, this model is certainly limited by the absence of TME cells impacting on treatment response. The patients which were treated with combined surgery and radiochemotherapy (RCT), while cultures were merely treated with cisplatin although it is known that irradiation and cisplatin show synergistic effects with platinum-based compounds functioning as a radiosensitizer (Negi et al., 2016). RT was not modeled in cultures though.

So far, none of the platforms discussed here has made it into the daily routine of HNSCC treatment. In this regard, Blom et al. (2017) point to another challenge of preclinical tumor platforms. They claim that (chemo) sensitivity assays might be a better predictor for therapy resistance than for sensitivity. Complex mechanisms of resistance development *in vivo* may go beyond those at the cellular levels and cannot be modeled *ex vivo*. Consequently, sensitivity is expected to be higher than specificity in these assays.

To achieve an acceptable correlation with clinical treatment schemes, various combinations regimens administered to patients must be diligently imitated *ex vivo* to ensure data

comparability. However, validation of existing tumor models can only be obtained in large prospective trials which are still outstanding to date.

CANCER STEM CELLS IN THERAPY OF HNSCC

Cancer stem cell share properties with somatic stem cells such as the ability to self-renew and differentiate. Furthermore, CSC are thought to be non-responsive to antineoplastic treatments such as chemo- or RT and are therefore clinically decisive. As with somatic stem cells, CSC are thought to reside in a specialized supportive microenvironment called the stem cell niche. Possible strategies in HNSCC-therapy could be affecting functions of the stem cell niche or target CSC themselves. Further factors contributing to CSC therapeutic resistance include the activation of signaling pathways that provoke self-renewal; the presence of multiple drug resistance membrane transporters (e.g., ATP-binding cassette drug transporters) and an immense capacity for DNA repair. All of these targets hold the potential to serve as a therapeutic strategy for different cancer entities including HNSCC.

Targeting the CSC Niche

The interaction between SDF-1 and its receptor CXCR4 could play an important role in the environment of the tumor stem cell niche. SDF-1 is a multifunctional cytokine that is secreted by a wide variety of tissues, including endothelial and stromal cells (Chen and Wang, 2019) 282 nucleotides code for a polypeptide of 93 amino acids. SDF-1 occurs in two isoforms through alternative splicing, SDF-1 alpha (amino acids 24–88) and SDF-1 beta (amino acids 24–93) (De La Luz Sierra et al., 2004; Faber et al., 2013a). SDF-1 alpha is so far the only proven chemokine which is capable to induce migration in hematopoietic progenitor cells (Möhle et al., 1998). Accordingly, it is considered one of the key regulators of hematopoietic progenitor cells in the cell traffic between peripheral blood circulation and bone marrow. We and others previously indicated that SDF-1 alpha induces polarization and directed migration of hematopoietic progenitors and leukemic cells (Möhle et al., 1998; Faber et al., 2007), two requirements for metastasis. The 7-transmembrane receptor CXCR4 was identified as the receptor of SDF-1 alpha. Interactions between SDF-1 alpha and CXCR4 already play a role in embryonic development, especially in the hematopoietic, vascular, and cardiac systems. The signal transduction pathways triggered by the binding of SDF-1 alpha to CXCR4 are not yet fully understood. Mechanisms that are involved here include Gi protein-supported activation of PI3K and the phospholipase C cascade (Petit et al., 2005; Goichberg et al., 2006).

The function of SDF-1 alpha, which is bound to CXCR4, may be mimicked or blocked by small peptide agonists or antagonists (Faber et al., 2007). Affecting signal transduction pathways activated by the SDF-1-CXCR4 axis by peptide agonists (or antagonists) includes a high potential for therapeutic interventions. There is increasing evidence that cell migration along with adhesion to the cellular stem cell niche is important in HNSCC CSCs. To unveil these mechanisms could potentially facilitate novel therapeutic options – e.g., through the use of peptide agonists and antagonists (Faber et al., 2007) for interference with the tumor stem cell niche and the subsequent inhibition or blockade of further tumor invasion and metastasis.

Our own preliminary work has already demonstrated the existence and functionality of this axis in the tumor stem cell niche of HNSCC (Faber et al., 2013b).

Targeting CSC Signaling Pathways

Erroneous signaling pathways can result in formation of CSC populations leading to tumor recurrence or metastasis. Disturbance of physiological pathways that are involved in the regulation of normal stem-cell-renewal, proliferation, and differentiation can promote tumorigenesis. When aberrantly activated, the Hedgehog (HH) signaling pathway, that is essential for stem cell maintenance, has been implicated in the tumorigenesis of various malignancies. Activating mutations in the HH pathway cause a subset of skin (basal cell carcinoma) and brain (medulloblastoma) tumors. Furthermore, the growth of many tumors is supported by HH pathway activity in stromal cells (Ng and Curran, 2011). HH inhibitors, which can be naturally occurring or synthetic, block both intrinsic signaling in cancer cells as well as extrinsic signaling to stromal cells to reduce tumor growth (Yauch et al., 2008). In HNSCC, Gan et al. showed that radiation-induced therapeutic inhibition by increased glioma-associated oncogene GLI1 expression could be partly reversed by HH pathway blockade with cyclopamine which resulted in radiosensitivity of the tumor. They demonstrated that GLI1, that is upregulated at the tumor-stroma intersection in HNSCC, is increased by RT, where it contributes to stroma-mediated resistance, and that HH inhibition offers a rational strategy to reverse this process and to sensitize HNSCC to irradiation (Gan et al., 2014).

The Notch signaling pathway is important for stem cell proliferation, differentiation, and apoptosis (Wang et al., 2008). It is activated through ligand-receptor-interactions (Notch receptors Notch 1–4 and Notch ligands Delta1, 3, 4 and Jagged1, 2) and known to play a role in a variety of malignancies, e.g., breast cancer and glioma (Krishna et al., 2019; Parmigiani et al., 2020). Inhibition of the Notch pathway with specific antibodies directed against Notch-ligands or –receptors has been shown to reduce breast CSC populations and to improve efficacy of chemotherapy in PDXs (Hoey et al., 2009; Qiu et al., 2013). Zhao et al. found elevated levels of Notch1/Hes1 in human HNSCC, especially in tissue post chemotherapy and lymph node metastases. The Notch1-inhibitor DAPT (GSI-IX) significantly reduced CSC populations and tumor-self-renewal ability *in vitro* and *in vivo*. The combined strategy of Notch1-blockade and chemotherapy synergistically attenuated chemotherapy-enriched CSC populations, promising therapeutic potential in future clinical trials (Zhao et al., 2016).

In HNSCC, the Wnt signaling pathways could also comprise therapeutic starting points. The Wnt/beta-catenin pathway is well characterized and there is increasing evidence indicating its role in oncogenesis and tumor development (Takahashi-Yanaga and Kahn, 2010). Wnt pathway activation maintains

CSC phenotype and promotes tumor progression e.g., Wnt activation increases CSC characteristics like sphere formation and invasiveness. Accordingly, Wnt inhibitors significantly reduce growth of HNSCC PDXs and suppress Wnt activation at the tumor epithelial-stromal boundary (Le et al., 2019). These studies suggest targeting Wnt signaling in the TME might offer a promising therapeutic approach.

The transforming growth factor-beta (TGF-β) superfamily of secreted factors comprises more than 30 members including Activins, Nodals, Bone Morphogenetic Proteins (BMPs), and Growth and differentiation factors (GDFs). The TGF-β/activin group includes TGF-β, activin, and Nodal, and the BMP/GDF group includes BMP, GDF, and AMH ligands (Weiss and Attisano, 2013). BMPs govern the intestinal niche homeostasis and balance self-renewal and differentiation (Clevers, 2013; Vermeulen and Snippert, 2014). HNSCC with high baseline BMP-2 protein level are associated with higher rates of local recurrence (Sand et al., 2014). Mulligan et al. indicate that HNSCC CSC upregulate SMURF1 expression to modulate BMP-signaling. This has important implications since non-CSC tumor cells, which display active BMP-signaling, are responsive to current treatments, unlike CSC, which may be more resistant to current therapies and contribute to poor treatment responses. Reactivating BMP-signaling is likely to sensitize CSC to current treatments and improve patient outcomes (Mulligan et al., 2013). Dysregulated TGF-β signaling that functions upstream of Wnt/β-catenin signaling is common in numerous solid tumors, including HNSCC (Bae et al., 2016). The role of TGFβ ligands in HNSCC CSC has not been fully explored. It was demonstrated that TGF-β1 treatment enriches the properties of HNSCC CSC by enhancing sphere formation and increasing self-renewal and stemness-associated gene expression (Oct4 and Sox2) of primary HNSCC CSC. Consecutively, ALDH+ cell population enriched post treatment demonstrating a direct relation between TGF-β signaling and CSC. Following stimulation with TGF-β1, the cells exhibited more resistance to cisplatin and elevated expression of EMT regulators Twist, Snail, and Slug. Bian et al. demonstrated that the loss of TGF-β signaling and PTEN in epithelial cells promotes HNSCC through regulation of both premalignant cells progressing into cancer cells through senescence evasion and the expansion of epithelial stem cells and interactions with the TME in a mouse model. They interpret their findings as significant for the identification of diagnostic biomarkers, as well as for effective treatment strategies targeting both the TGF-β and the PI3K/Akt pathways (Bian et al., 2012). Li K. et al. (2019) showed that TGF-β-induced the activation of AKT rather than ERK1/2 in oral SCC and further illustrated that the non-Smad AKT-FOXO3a axis is essential to regulate the stemness of CSC. There is evidence from the results of different entities such as breast, cervical, and ovarian cancer that the canonical pathway as well as crosstalk of TGF-β are both important factors to regulate the cancer stemness (Chihara et al., 2017; Wu et al., 2017; Matsumoto et al., 2018; Li K. et al., 2019).

The JAK/STAT (Janus kinase/signal transducers and activators of transcription) signaling pathway plays a crucial role in biological processes such as cell proliferation, differentiation, apoptosis, and immune regulation and mediates the cellular response to cytokines. By impairing the pathway, tumor immune surveillance is compromised and tumor formation promoted (Dreesen and Brivanlou, 2007). Besides many other cancer types, aberrant activation of STATs has also been found in HNSCC (Song and Grandis, 2000). JAK/STAT signaling seems to have a functional purpose in survival, self-renewal, and metastasis of CSCs. JAK/STAT signaling in stem cells has been shown to be involved in maintaining embryonic stem cell self-renewal properties, hematopoiesis, and neurogenesis (Chambers, 2004; Stine and Matunis, 2013). In different types of cancer JAK/STAT signaling is aberrantly activated in CSC (Zhou et al., 2007; Birnie et al., 2008). JAK/STAT signaling has been implicated in CSC-mediated metastasis indicating a potential requirement of the pathway for the survival of early metastatic colonies (Calon et al., 2012). In CSC of prostate cancer STAT3 activation by IL-6 or ROS, caused an upregulation of their self-renewal ability (Qu et al., 2013). Growth and survival of CSCs with constitutively activated JAK/STAT were reduced by pharmacologically inhibiting JAK1/2 in an AML model (Cook et al., 2014). As HNSCC is a cancer entity with a high activation level of the JAK/STAT it is most likely that the pathway influences CSC in HNSCC as well. A mechanism which was proposed by Islam et al. (2014) for HNSCC describes that CSC are regulated by RhoC by overexpressing IL-6 and phosphorylation of STAT3. Due to the significance of STAT3 maintaining CSC properties inhibiting the cascade may eliminate CSCs in preventing cancer (Lee et al., 2019).

In humans, the hippo pathway is involved in a multitude of cancer-related physiological and pathophysiological events such as CSC self-renewal, tumorigenesis and anti-cancer drug resistance (Zhao et al., 2011; Moroishi et al., 2015; Zhao and Yang, 2015; Jae Hyung et al., 2018). Expression of genes controlled by the Hippo downstream transcriptional coactivators YAP (Yes-associated protein 1) and TAZ (WWTR1, WW domain containing transcription regulator 1) is widely deregulated in human cancer including HNSCC (Santos-de-Frutos et al., 2019).

Elevated TAZ confers CSC-like properties in diverse cancer contexts (Cordenonsi et al., 2011; Li et al., 2015; Li J. et al., 2019). SOX2 was identified as a direct target of TAZ for the modulation of CSCs self-renewal and maintenance in HNSCC implicating that targeting the TAT/TAZ/TEAD4-SOX2 axis might count as an amenable target for HNSCC therapy (Li J. et al., 2019). Approaches to develop YAP/TAZ inhibitors are currently under investigation (Bae et al., 2016; Shin and Kim, 2020) in the sense of a direct inhibitor between YAP/TAZ and their transcriptional partner TEADs as AP/TAZ signaling might not be as substantial for the normal homeostasis of adult tissues as for neoplastic progression. Another potential strategy is to target the upstream regulators of YAP and TAZ. The molecular program orchestrated by YAP is associated with poor prognosis and tumor progression in HNSCC providing a rationale for developing new therapies targeting the Hippo pathway effector comprising compounds that are already approved for other indications and are currently under preclinical evaluation (Taccioli et al., 2015; Segrelles et al., 2018).

The ErbB family, including EGFR, is known as a key player in cellular processes such as metastasis, tumorigenesis, cell

proliferation, and drug resistance, all features related to CSC. It has been shown that EGFR activation increases the expression of stem cell marker CD44. Blocking EGFR tyrosine kinase domains reduces both stem cell maintenance and EMT, and loss of CD44 down-regulates both total and phosphorylated EGFR (Abhold et al., 2012; Perez et al., 2013). These observations suggest that pharmacological blockade of EGFR signal transduction may affect CSC preservation. The effects of cetuximab and erlotinib on CSC were examined in a HNSCC *in vitro* model (Fernanda Setúbal Destro Rodrigues et al., 2018). The drugs caused a decrease in proliferation for all subpopulations and large cellular shifts between the subpopulations EMT-CSC, Epi-CSC and differentiating cell compartments. Loss of EMT-CSCs reduced cell motility and as a consequence presumably a reduction of invasion and metastasis. EGFR inhibition also induced shifts of Epi-CSCs into the differentiating cell compartment which typically is more chemo/radiation-sensitive. This might be a desired effect to enhance the response of tumor cell populations to adjunctive therapies. Abhold et al. also investigated the potential function of EGFR as a regulator of stemness in HNSCC. After *in vitro* activation of EGFR stem cell markers CD44, BMI-1, Oct-4, NANOG, CXCR4, and SDF-1 as well as increased tumorosphere formation were induced, effects that were reversible by administering the EGFR kinase inhibitor Gefinitib. After pharmacological EGFR blockade, the invasion ability was reduced in CSC and the cells showed an increased response toward to cisplatin-induced death. Targeting CSC by blockade of EGFR potentially prevents relapse and secondary tumors and should be taken into account when scheduling HNSCC treatment (Abhold et al., 2012). Another example for a RTK associated with CSC is MET which was shown to be expressed in HNSCC cells having the capacity for self-renewal (Sun and Wang, 2011). Met(+) HNSCC cells built spherical colonies in contrast to MET(-) cells and increasingly expressed self-renewal pathways. The MET receptor was also responsible for cisplatin resistance, tumor formation and metastatic spread in a mouse model. The authors suggested to gain more evidence about the c-Met(+) HNSCC population which might be relevant for tumor progression.

Targeting CSC Surface Markers

A very specific therapeutic target to point at are CSC surface markers, e.g., CD44 or CD133. Examples for such membrane markers have been introduced above. Specific antibodies targeting these surface markers are currently under investigation. Especially in leukemia, CD44 has been utilized among others to specifically target leukemia stem cells in human AML. In each case, treatment with antibodies against these cell surface markers dramatically decreased malignant potential and eradicated CSCs in mice (Chen et al., 2013). In treating breast cancer, an anti-CD44 antibody-conjugated gold nanorod has been used to target and ablate CD44 positive cells. Using this approach, CD44-targeted cells absorb infrared light resulting in increased local temperature leading to apoptosis (Alkilany et al., 2012). For HNSCC, Su et al. explored a method for preparing anti-CD44 antibody-modified superparamagnetic iron oxide nanoparticles. After co-culturing these with stem cells, the majority of nanoparticles penetrated into the cytoplasm. After alternating magnetic field treatment, the modified nanoparticles induced CSCs to undergo apoptosis. These results demonstrate that CSCs in HNSCC can be eradicated using CD44-targeted magnetic nanoparticles (Su et al., 2019). CD133 was already introduced to play a crucial role in many types of CSCs besides HNSCC, e.g., lung and breast cancer. Treatment with carbon nanotubes conjugated with anti-CD133 monoclonal antibodies followed by radiation with infrared laser light can selectively target CD133 positive glioblastoma cells. Photothermolysis caused by nanotubes specifically eradicates targeted cells (Wang et al., 2011). Kobayashi H and Choyke PL summarized that near-infrared photoimmunotherapy can be applied to any cancer with overexpressed target membrane proteins for which there is a suitable monoclonal antibody. A special remark is made to near-infrared photoimmunotherapy directed at CD44 and CD133, which are not only considered markers of CSCs in breast cancer and glioblastoma but also in HNSCC (Kobayashi and Choyke, 2019).

IMPACT OF CANCER STEM CELLS ON FIELD CANCERIZATION IN HNSCC

The "field cancerization" (FC) concept, first described by Slaughter et al. (1953) is based on the observation that normal mucosa adjacent to the tumor contains certain pre-neoplastic genetic fingerprints, which can consecutively cause the development of local recurrence or second primary tumors after abnormal tissue is still residing after surgery (Willenbrink et al., 2020). Normal mucosa adjacent to the tumor acquires molecular alterations in case of carcinogen exposure, i.e., mutations in oncogenes/tumor suppressors, loss of heterozygosity (LOH), and genomic instability. In a multi-step operation, molecular events transform normal epithelium into cancer cells. In theory, only cells that inhabit the epithelia long enough, such as CSC, might accumulate all these genetic alterations. CSC harbor tumor-propagating features and are among the cells accounting for tumor initiation and development. Therefore, it appears practical that CSC might be capable of orchestrating the development of pre-cancerous cells in areas of FC and their transformation into malignant cells (Simple et al., 2015). Furthermore, CSC are considered to have intra-epithelial migratory capability (Biddle et al., 2011). One major observation is the identification of CSC markers in tumor-adjacent normal epithelium supporting the idea of a relation between CSC and FC (Gallmeier et al., 2011; Suresh et al., 2012). Vice versa, molecular FC markers are detected in CSC such as LOH in certain genetic regions like 3p, 0921, 17p11-12, and 13q, most of them encoding for genes that are related to CSC functions. Simple et al. (2015) propose a model of FC orchestrated by CSC. They assume that CSC stem from de-differentiated tumor cells. Another thesis is that normal stem cells (NSC) transform into CSC which is backed by the fact that NSC inhabit the epithelium long enough to collect crucial genetic alterations. The hypothesis of CSC driving FC is substantiated by cancer-related genetic alterations in chromosome positions 3p, 9p, 8p, and 18q. A hit at 13q where Rb gene is situated

eventually leads to carcinoma development among subclones that have already transformed from NCS into CSC. In summary, the thesis of an involvement of CSC in FC is sustained by the identification of CSC specific markers in the epithelium adjacent to invasive cancers and the characteristic features of CSC such as tumor-promoting initiation and migration.

MATHEMATICAL MODELS FOR PREDICTING SURVIVAL AND FOR CSC PLASTICITY

Mathematical models are becoming increasingly attractive for capturing data from experimental studies in the wider context of tumor growth dynamics. Emerick et al. (2013) introduced a predictive cancer model and web-based calculator, which estimated the risk of death for HNSCC patients. The binary-biological model integrates data on tumor size, lymph node metastases, and further prognostic factors into estimation of dying from cancer. The model is based on equations such as the relationship between tumor size and the risk of death (the SizeOnly equation) and the relationship between size, number of positive nodes, and the risk of death (the Size 1 Nodes equation). Associations between the risk factors and the actual death risk were precisely captured. Between tumor size and risk of cancer death the risk was monotonically increasing with each cm in tumor size across all HNSCC sublocalizations. Enderling et al. (2019) propose a model for predicting patient-specific RT responses in HNC as a tool for customized radiation dose fractionation. The model aims at the integration of biological differences into clinical RT parameters. In the so-called genomic-adjusted radiation dose (GARD) variables such as the individual patient radiosensitivity index, and the radiation dose or fractionation schedule planned for each patient are implemented. The rationale is to increase dosages in case of resistant cancers and decrease complication risk by lowering the dose in case of sensitive tumors. Although it is acknowledged that other measures of radiosensitivity or biological parameters such as hypoxia or immune responses, and cellular processes including proliferation and DNA repair, are not yet considered, the model is an approach to genomically inform radiation dose (Caudell et al., 2017; Scott et al., 2017).

Stochastic process-based methods have also been developed for modeling growth features and sensitivity of CSC. To undergo quiescence is one feature of stem cells. To analyze how the quiescent state influences treatment, Komarova et al. present a stochastic model to assess how quiescence affects colonic growth before and during CML treatment in the absence of mutations, and how the generation of resistant mutants is influenced by therapy. The model predicted a biphasic response upon therapy, with a fast first phase and a slower second phase. The authors concluded that additional clinical data is needed to determine whether alternative response patterns can also be observed (Komarova, 2006). Hence, mathematical models are valuable to describe how therapy changes the tumor milieu. *In silico* simulation of the influence of an environmental context on the expression of stem-like properties might reveal new insights into the association of stemness with niche-related phenotypic plasticity and add to the development of new treatments. Picco et al. (2017) introduce a mathematical model of context-driven CSC plasticity in which stemness continuously varies across a phenotypic spectrum, directly driven by the environment of breast cancer cells. The hypothesis that all cancer cells are able to adapt to an invasive stem-like phenotype showing the capability of cancer initiation and repopulation. The model calculates main features of stemness varying on a scale from the highest stemness (high invasiveness, self-renewal ability) to full differentiation (poor invasion ability, low proliferative activity). The phenotype is directly modulated be the CSC niche, an environment maintaining cancer cells with a high stem cell like degree phenotype. By the use of a hybrid discrete-continuum (HDC) model, first described by Anderson (Anderson and Chaplain, 1998; Anderson et al., 2000) cancer cell phenotypes are defined by their grade of stemness. The model calculates the plasticity of cancer cells by their shifting ability on the scale of differentiation, represented by a degree of differentiation, D^i. D^0 stands for highest stemness, and D^N stands for full differentiation of a cancer cell with poor stemness. N is the total amount of degrees on the scale. Corresponding to each D^i is a specific phenotype that determines the remodeling of the ECM (production and degradation rate) by the respective cell and its proliferation capacity. It is likely that the HDC approach could be transferred from breast cancer to other entities. Although the possibilities of mathematical modeling are manifold, one might take into account that tumorigenesis is a multifactorial process. In a recent review it is discussed that most deterministic models show limitations to predict the last phases of cancer growth and cannot predict long-term tumor growth rate (Tabassum et al., 2019). Brady and Enderling critically discuss the fact that mathematical tumor models frequently lack access to high-resolution cancer biology or oncology data including independent training and validation data sets. The models are limited to being merely academic and not feasible to speculate on optimal therapy. It is mandatory to set up a standard to adequately train and validate the models. The purpose of such models should be up-front subclassified into either "academic" or "translational" to prevent loss of credibility (Brady and Enderling, 2019).

TUMOR ORGAN-ON-CHIP MODELS

Current innovations in microfluidic cell culture technology have led to the generation of human organs-on-chips (or organ chips) that mimic cancer cell behavior within a functional tissue and organ-specific context (Bhatia and Ingber, 2014; Skardal et al., 2017; Aleman and Skardal, 2019; Sontheimer-Phelps et al., 2019; Trujillo-de Santiago et al., 2019).These "organs-on-chips" permit the development of novel *in vitro* disease models, and could eventually help to replace animal models for drug development and toxin testing (Huh et al., 2011). The technology allows to examine vascular perfusion and the effects of medication or microenvironmental factors on cancer cells, either alone or enriched with other cell types as epithelial and endothelial

cells, fibroblasts, immune cells, then visualizing sensitivity and response in real-time (Sontheimer-Phelps et al., 2019). Another advantage of microfluidic systems is that they offer perfusion causing continuous nutrient supply and waste removal, in turn maintaining a more stable culture environment, and will potentially allow to identify physiochemical mediators of mass transport in the tumor ECM (Avendano et al., 2019).

Technical challenges are the separation and isolation of cancer and stromal cells from the individual patient. The cells have to be re-arranged on organ-chips in the appropriate proportions and location to accurately mimic cell-specific features, thereby considering culture condition and isolation protocols for all different cellular subgroups. The technique is supposed to be elaborate and time-consuming and has to be correlated with existing patient outcome and response data before transferred into the clinical applicability. Another potential limitation is the absorption of small molecules such as certain drugs by the most commonly used material for organ chips, PDMS, so the development of further new materials for organ-chips might be required (Sontheimer-Phelps et al., 2019).

In a recent review the application of tumor-on-chip systems in precision or personalized medicine is addressed (Trujillo-de Santiago et al., 2019). The maintenance of vital tumor tissue from biopsies in microfluidic systems, is described as feasible in different cancer types, including HNSCC (Carr et al., 2014; Astolfi et al., 2016). Kennedy et al. describe a robust, easy to use, tumor-on-a-chip platform, which maintains vital HNSCC samples for the purpose of *ex vivo* irradiation. The model mimicked microvascular flow and diffusion by the use of sintered discs to separate the tissue from media. Viability was sustained for 68 hrs. Tumor biopsies showed an adequate response to fractionated IR. The addition of concurrent cisplatin considerably increased the apoptotic cell fraction. The novel platform is described as cost-effective and transferable to other cancer types (Kennedy et al., 2019).

Some recent papers have described the maintenance of portions of real tumorous tissue from biopsies in microfluidic systems (Trujillo-de Santiago et al., 2019). Bower et al. (2017) were able to sustain the tissue integrity of HNSCC samples for 48 h in a simple microfluidic chamber. Sylvester et al. cultivated HNSCC tumor biopsies in a microfluidic device for up to 9 days after surgical removal. The response of HNSCC tissue samples (fresh and fresh-frozen) to standard anticancer drugs (cisplatin, 5-flurouracil or docetaxel) was monitored. Proliferation and showing similar viability and metabolic cell death were statistically similar in frozen and fresh biopsies. Dose-dependent cell deaths seen after administration of all drugs. Cytotoxicity was enhanced by combination of drugs. The results demonstrate that tumor tissue can be cryogenically stored and analyzed at a later (Sylvester et al., 2013). Although highly sophisticated tumor-on-chip systems are not in any event cost-efficient, it is highly likely that its embodiments will be of translational significance. The assessment of responsiveness of individual tumors by using microfluidic cultures and selection of specific therapy schemes could contribute to new insights into HNSCC biology, to customized care and consecutively to improved prognosis.

USAGE OF BIOMATERIALS AS SCAFFOLDS FOR 3D CULTURE MODELS

As presented before, the development of novel 3D cultures is based on a better understanding of TME structure and interactions. To improve cellular functions, various forms of biomaterials are already available serving as a scaffold for 3D cell culture which are comprehensively summarized in recent reviews (Gu and Mooney, 2016; Kamatar et al., 2020; Park et al., 2021). One method is the usage of hydrogels, which can be further divided into synthetic and natural. Another cell-culturing technique is based on solid, namely porous and fibrous scaffolds, which is one of the older techniques in the field (Cheng and Kisaalita, 2010). These scaffolds mainly consist of porous foams or fibrous meshes made from synthetic polymers. Decellularized native tissue preserves the natural environment and recapitulates key ECM components, a major advantage compared with artificial scaffolds. The technique is currently under investigation for advanced bioprocessing into organotypic 3D solid tumor models (Ferreira et al., 2020) and there are trends to derive bioinks from decellularized ECM (Dzobo et al., 2019). The surfaces of ultra-low adherent (ULA) plates are coated with polymers enabling spheroid formation of cells as attachment to the surface of the plates is impaired. For instance, ULA plates have been used for testing anti-CSC compounds in the stem cell-enriched HNSCC tumor model by Goričan et al. (2020).

3D BIOPRINTING MODELS

In addition to the above mentioned methods, a technique developed in the field of tissue engineering emerged in the field of constructing tumor models in the last decade. The development of 3D bioprinting technologies in the biomedical field enabled the construction of artificial tissues with complex structures and various components using different cell types and natural (e.g., collagen, fibrin, etc.) or synthetic (e.g., polyethylene glycol, gelatin-methacrylate, etc.) hydrogels. It is expected that the 3D bioprinting technique will overcome disadvantages of currently existing tumor models like the lack of controllable spatial distribution of tumor cells and ECM compositions (Zhang et al., 2016; Ma et al., 2020). The technical possibilities of 3D bioprinting will allow to arrange different cell types (e.g., cancer cells, CSCs, endothelial cells, CAFs, etc.) and ECM-based biomaterials to generate tumor models that recapitulate the *in vivo* tumor very closely including the architecture of a tumor (Penfornis et al., 2017; Langer et al., 2019) (**Figure 1**). It is expected that 3D bioprinting will pave the way to both, to reliable models to predict the optimal treatment of a cancer patient and to more reliable models for basic and applied cancer research. Currently, protocols for bioprinted tumor models of glioma, liver, breast, ovarian, and cervical cancers are published as mentioned in the review of Ma et al. (2020). Regarding HNCs, in 2018 a study was published by Almela et al. (2018), in which a 3D printed bone mimicking scaffold was used to investigate the bone

invasion of oral squamous cancer cells to develop a cancerous bone oral mucosal model. A protocol to create a bioprinted head and neck tumor model has yet not been published. However, since 3D bioprinting has only emerged in the last decade in the field of constructing tumor models, the authors of this review are convinced that it will become a powerful technique to develop various head and neck tumor models.

ELECTROSPUN NANOFIBRES

Electrospinning is a well-known process to produce fibrous and porous three-dimensional (3D) materials starting from a polymeric solution. This process was first used in the field of tissue engineering but meanwhile it is also applied to engineer 3D cancer models. These fibrous materials are able to mimic the ECM of living tissue (Cavo et al., 2020). The use of different polymers enables the possibility to adapt the properties of the scaffold to the varying properties of ECMs from different tumor entities. A summary of materials used can be found in the review by Chen S. et al. (2018) in which advantages and disadvantages of this technique are also discussed (Chen S. et al., 2018). Such fibrous scaffolds were developed for many tumor types like breast cancer, pancreatic cancer and many more. A comprehensive summary of tumor types for which such models exist can be found in Cavo's review (Cavo et al., 2020). However, such models are currently not published for HNC.

SOFT LITHOGRAPHY AND BIOIMPRINTS

The soft lithography technique is used to produce so-called bioimprints. These bioimprints provide *in vitro* substrates with cell-like features and enables to investigate effects of physical topographies that are similar to those experienced by cells *in vivo* (Tan et al., 2015). Materials used for bioimprints are for example polydimethylsiloxane (PDMS), polystyrene (pST), polymethacrylate (pMA), and some others (Murray et al., 2014; Mutreja et al., 2015; Tan et al., 2015). How such bioimprints are created is well described in the studies of Murray et al. (2014), Tan et al. (2015).

One limitation is that both of the above mentioned techniques lack mimicking the complete microenvironment, including vascularization and immune cells (Chen S. et al., 2018). For HNC cells, this method has not yet been established.

FUTURE CHALLENGES

As summarized in this review article, clinical implementation of chemoresponse assays and biomarkers as well as therapeutic targets will enable patient stratification based on molecular characterization of the tumor and TME by 3D modeling (**Figure 2**). In HNSCC, however, reliable models that are predictive of clinical efficacy remain scarce. So far, no description of a successful translation of chemosensitivity assays or predictive models into the clinical routine has been published for HNSCC. Druggable target components in HNSCC have been identified and more are being discovered due to the development of novel technologies and acquisition of competence in the field of personalized medicine. Despite all these innovations specific tumor-related challenges need to be considered. Due to the frequent development of therapy resistance there is an absolute need to unveil the underlying mechanisms in order to develop strategies for circumvention. Although it has been demonstrated that combinatorial regimens might be advantageous there are still no standardized tumor models available that allow predicting the efficacy of these combinations and testing the individual sensitivity of the tumor to be able to select from an abundance of therapeutic agents. After having identified a suitable therapeutic approach, the tumor ideally should be constantly monitored to discover the outgrowth of resistant clones as early as possible. Also, further characterization of the architecture and physiology of CSC-enriched spheroids in future studies will be crucial for future therapy development.

Optimizing current therapies and developing new therapeutic targets is an ambitious aim in HNSCC research in order to improve its prognosis. The further establishment of suitable 3D cancer models will be an essential in this process.

AUTHOR CONTRIBUTIONS

AA, JK, and NR conceived the topic for this review. All authors listed have made a substantial, direct and intellectual contribution to the work, and approved it for publication.

REFERENCES

Abhold, E. L., Kiang, A., Rahimy, E., Kuo, S. Z., Wang-Rodriguez, J., Lopez, J. P., et al. (2012). EGFR kinase promotes acquisition of stem cell-like properties: a potential therapeutic target in head and neck squamous cell carcinoma stem cells. *PLoS One* 7:e32459. doi: 10.1371/journal.pone.0032459

Adachi, K., Suemori, H., Yasuda, S. Y., Nakatsuji, N., and Kawase, E. (2010). Role of SOX2 in maintaining pluripotency of human embryonic stem cells. *Genes Cells* 15, 455–470.

Adeola, H. A., Papagerakis, S., and Papagerakis, P. (2019). Systems biology approaches and precision oral health: a circadian clock perspective. *Front. Physiol.* 10:399. doi: 10.3389/fphys.2019.00399

Affolter, A., Muller, M. F., Sommer, K., Stenzinger, A., Zaoui, K., Lorenz, K., et al. (2016). Targeting irradiation-induced mitogen-activated protein kinase activation in vitro and in an ex vivo model for human head and neck cancer. *Head Neck* 38(Suppl. 1), E2049–E2061.

Albers, A. E., Chen, C., Köberle, B., Qian, X., Klussmann, J. P., Wollenberg, B., et al. (2012). Stem cells in squamous head and neck cancer. *Crit. Rev. Oncol. Hematol.* 81, 224–240.

Aleman, J., and Skardal, A. (2019). A multi-site metastasis-on-a-chip microphysiological system for assessing metastatic preference of cancer cells. *Biotechnol. Bioeng.* 116, 936–944. doi: 10.1002/bit.26871

Alkilany, A. M., Thompson, L. B., Boulos, S. P., Sisco, P. N., and Murphy, C. J. (2012). Gold nanorods: their potential for photothermal therapeutics and drug

delivery, tempered by the complexity of their biological interactions. *Adv. Drug Deliv. Rev.* 64, 190–199. doi: 10.1016/j.addr.2011.03.005

Allam, E., and Windsor, J. L. J. D. (2013). Social and behavioral determinants of oral cancer. *Dentistry* 4, 1–3.

Almela, T., Al-Sahaf, S., Brook, I. M., Khoshroo, K., Rasoulianboroujeni, M., Fahimipour, F., et al. (2018). 3D printed tissue engineered model for bone invasion of oral cancer. *Tissue Cell* 52, 71–77. doi: 10.1016/j.tice.2018.03.009

Anderson, A. R., and Chaplain, M. A. (1998). Continuous and discrete mathematical models of tumor-induced angiogenesis. *Bull. Math. Biol.* 60, 857–899. doi: 10.1006/bulm.1998.0042

Anderson, A. R. A., Chaplain, M. A. J., Newman, E. L., Steele, R. J. C., and Thompson, A. M. (2000). Mathematical modelling of tumour invasion and metastasis. *J. Theor. Med.* 2:490902.

Ang, K., Zhang, Q., Wheeler, R. H., Rosenthal, D. I., Nguyen-Tan, F., Kim, H., et al. (2010). A phase III trial (RTOG 0129) of two radiation-cisplatin regimens for head and neck carcinomas (HNC): impact of radiation and cisplatin intensity on outcome. *J. Clin. Oncol.* 28, 5507–5507. doi: 10.1200/jco.2010.28.15_suppl.5507

Ang, K. K., Andratschke, N. H., and Milas, L. (2004). Epidermal growth factor receptor and response of head-and-neck carcinoma to therapy. *Int. J. Radiat. Oncol. Biol. Phys.* 58, 959–965.

Arnold, C. R., Mangesius, J., Skvortsova, I.-I., and Ganswindt, U. (2020). The role of cancer stem cells in radiation resistance. *Front. Oncol.* 10:164. doi: 10.3389/fonc.2020.00164

Astolfi, M., Péant, B., Lateef, M. A., Rousset, N., Kendall-Dupont, J., Carmona, E., et al. (2016). Micro-dissected tumor tissues on chip: an ex vivo method for drug testing and personalized therapy. *Lab Chip* 16, 312–325. doi: 10.1039/c5lc01108f

Au, J. L., Wientjes, M. G., Rosol, T. J., Koolemans-Beynen, A., Goebel, E. A., and Schuller, D. E. (1993). Histocultures of patient head and neck tumors for pharmacodynamics studies. *Pharm. Res.* 10, 1493–1499.

Avendano, A., Cortes-Medina, M., and Song, J. W. (2019). Application of 3-D microfluidic models for studying mass transport properties of the tumor interstitial matrix. *Front. Bioeng. Biotechnol.* 7:6. doi: 10.3389/fbioe.2019.00006

Bae, W.-J., Lee, S.-H., Rho, Y.-S., Koo, B.-S., and Lim, Y.-C. (2016). Transforming growth factor β1 enhances stemness of head and neck squamous cell carcinoma cells through activation of Wnt signaling. *Oncol. Lett.* 12, 5315–5320. doi: 10.3892/ol.2016.5336

Bai, R., Lv, Z., Xu, D., and Cui, J. (2020). Predictive biomarkers for cancer immunotherapy with immune checkpoint inhibitors. *Biomark. Res.* 8:34.

Bertotti, A., Migliardi, G., Galimi, F., Sassi, F., Torti, D., Isella, C., et al. (2011). A molecularly annotated platform of patient-derived xenografts ("xenopatients") identifies HER2 as an effective therapeutic target in cetuximab-resistant colorectal cancer. *Cancer Discov.* 1, 508–523. doi: 10.1158/2159-8290.cd-11-0109

Bhatia, S. N., and Ingber, D. E. (2014). Microfluidic organs-on-chips. *Nat. Biotechnol.* 32, 760–772. doi: 10.1038/nbt.2989

Bian, Y., Hall, B., Sun, Z. J., Molinolo, A., Chen, W., Gutkind, J. S., et al. (2012). Loss of TGF-β signaling and PTEN promotes head and neck squamous cell carcinoma through cellular senescence evasion and cancer-related inflammation. *Oncogene* 31, 3322–3332. doi: 10.1038/onc.2011.494

Biddle, A., Liang, X., Gammon, L., Fazil, B., Harper, L. J., Emich, H., et al. (2011). Cancer stem cells in squamous cell carcinoma switch between two distinct phenotypes that are preferentially migratory or proliferative. *Cancer Res.* 71, 5317–5326. doi: 10.1158/0008-5472.can-11-1059

Birnie, R., Bryce, S. D., Roome, C., Dussupt, V., Droop, A., Lang, S. H., et al. (2008). Gene expression profiling of human prostate cancer stem cells reveals a pro-inflammatory phenotype and the importance of extracellular matrix interactions. *Genome Biol.* 9:R83.

Blom, K., Nygren, P., Larsson, R., and Andersson, C. R. (2017). Predictive value of ex vivo chemosensitivity assays for individualized cancer chemotherapy: a meta-analysis. *SLAS Technol.* 22, 306–314. doi: 10.1177/2472630316686297

Boccia, S., Cadoni, G., Sayed-Tabatabaei, F. A., Volante, M., Arzani, D., De Lauretis, A., et al. (2008). CYP1A1, CYP2E1, GSTM1, GSTT1, EPHX1 exons 3 and 4, and NAT2 polymorphisms, smoking, consumption of alcohol and fruit and vegetables and risk of head and neck cancer. *J. Cancer Res. Clin. Oncol.* 134, 93–100. doi: 10.1007/s00432-007-0254-5

Bosetti, C., Gallus, S., Trichopoulou, A., Talamini, R., Franceschi, S., Negri, E., et al. (2003). Influence of the Mediterranean diet on the risk of cancers of the upper aerodigestive tract. *Cancer Epidemiol. Biomarkers Prev.* 12, 1091–1094.

Bower, R., Green, V. L., Kuvshinova, E., Kuvshinov, D., Karsai, L., Crank, S. T., et al. (2017). Maintenance of head and neck tumor on-chip: gateway to personalized treatment? *Future Sci. OA* 3:Fso174. doi: 10.4155/fsoa-2016-0089

Brady, R., and Enderling, H. (2019). Mathematical models of cancer: when to predict novel therapies, and when not to. *Bull. Math. Biol.* 81, 3722–3731. doi: 10.1007/s11538-019-00640-x

Brown, J. M., and Wilson, W. R. (2004). Exploiting tumour hypoxia in cancer treatment. *Nat. Rev. Cancer* 4, 437–447. doi: 10.1038/nrc1367

Burtness, B., Harrington, K. J., Greil, R., Soulières, D., Tahara, M., De Castro, G. Jr., et al. (2019). Pembrolizumab alone or with chemotherapy versus cetuximab with chemotherapy for recurrent or metastatic squamous cell carcinoma of the head and neck (KEYNOTE-048): a randomised, open-label, phase 3 study. *Lancet* 394, 1915–1928.

Calon, A., Espinet, E., Palomo-Ponce, S., Tauriello, D. V., Iglesias, M., Céspedes, M. V., et al. (2012). Dependency of colorectal cancer on a TGF-β-driven program in stromal cells for metastasis initiation. *Cancer Cell* 22, 571–584. doi: 10.1016/j.ccr.2012.08.013

Carlsson, J., and Nederman, T. (1989). Tumour spheroid technology in cancer therapy research. *Eur. J. Cancer Clin. Oncol.* 25, 1127–1133. doi: 10.1016/0277-5379(89)90404-5

Carr, S. D., Green, V. L., Stafford, N. D., and Greenman, J. (2014). Analysis of radiation-induced cell death in head and neck squamous cell carcinoma and rat liver maintained in microfluidic devices. *Otolaryngol. Head Neck Surg.* 150, 73–80. doi: 10.1177/0194599813507427

Cassidy, J. W., Caldas, C., and Bruna, A. (2015). Maintaining tumor heterogeneity in patient-derived tumor xenografts. *Cancer Res.* 75, 2963–2968. doi: 10.1158/0008-5472.can-15-0727

Caudell, J. J., Torres-Roca, J. F., Gillies, R. J., Enderling, H., Kim, S., Rishi, A., et al. (2017). The future of personalised radiotherapy for head and neck cancer. *Lancet Oncol.* 18, e266–e273.

Cavo, M., Serio, F., Kale, N. R., Damone, E., Gigli, G., and Del Mercato, L. L. (2020). Electrospun nanofibers in cancer research: from engineering of in vitro 3D cancer models to therapy. *Biomater. Sci.* 8, 4887–4905. doi: 10.1039/d0bm00390e

Ceglia, N., Liu, Y., Chen, S., Agostinelli, F., Eckel-Mahan, K., Sassone-Corsi, P., et al. (2018). CircadiOmics: circadian omic web portal. *Nucleic Acids Res.* 46, W157–W162.

Chambers, I. (2004). The molecular basis of pluripotency in mouse embryonic stem cells. *Cloning Stem Cells* 6, 386–391. doi: 10.1089/clo.2004.6.386

Chen, D., and Wang, C. Y. (2019). Targeting cancer stem cells in squamous cell carcinoma. *Precis Clin. Med.* 2, 152–165. doi: 10.1093/pcmedi/pbz016

Chen, J., Zhou, J., Lu, J., Xiong, H., Shi, X., and Gong, L. J. B. C. (2014). Significance of CD44 expression in head and neck cancer: a systemic review and meta-analysis. *BMC Cancer* 14:15. doi: 10.1186/1471-2407-14-15

Chen, K., Huang, Y. H., and Chen, J. L. (2013). Understanding and targeting cancer stem cells: therapeutic implications and challenges. *Acta Pharmacol. Sin.* 34, 732–740. doi: 10.1038/aps.2013.27

Chen, S., Boda, S. K., Batra, S. K., Li, X., and Xie, J. (2018). Emerging roles of electrospun nanofibers in cancer research. *Adv. Healthc. Mater.* 7:e1701024.

Chen, X., Yan, B., Lou, H., Shen, Z., Tong, F., Zhai, A., et al. (2018). Immunological network analysis in HPV associated head and neck squamous cancer and implications for disease prognosis. *Mol. Immunol.* 96, 28–36. doi: 10.1016/j.molimm.2018.02.005

Cheng, K., and Kisaalita, W. S. (2010). Exploring cellular adhesion and differentiation in a micro-/nano-hybrid polymer scaffold. *Biotechnol. Prog.* 26, 838–846. doi: 10.1002/btpr.391

Chihara, Y., Shimoda, M., Hori, A., Ohara, A., Naoi, Y., Ikeda, J.-I., et al. (2017). A small-molecule inhibitor of SMAD3 attenuates resistance to anti-HER2 drugs in HER2-positive breast cancer cells. *Breast Cancer Res. Treat.* 166, 55–68. doi: 10.1007/s10549-017-4382-6

Choi, S. Y., Lin, D., Gout, P. W., Collins, C. C., Xu, Y., and Wang, Y. (2014). Lessons from patient-derived xenografts for better in vitro modeling of human cancer. *Adv. Drug Deliv. Rev.* 79-80, 222–237. doi: 10.1016/j.addr.2014.09.009

Clevers, H. J. C. (2013). The intestinal crypt, a prototype stem cell compartment. *Cell* 154, 274–284. doi: 10.1016/j.cell.2013.07.004

Cohen, E. E. W., Soulières, D., Le Tourneau, C., Dinis, J., Licitra, L., Ahn, M. J., et al. (2019). Pembrolizumab versus methotrexate, docetaxel, or cetuximab for recurrent or metastatic head-and-neck squamous cell carcinoma (KEYNOTE-040): a randomised, open-label, phase 3 study. *Lancet* 393, 156–167.

Cohen, R. L., and Settleman, J. (2014). From cancer genomics to precision oncology–tissues still an issue. *Cell* 157, 1509–1514. doi: 10.1016/j.cell.2014.05.027

Cook, A. M., Li, L., Ho, Y., Lin, A., Li, L., Stein, A., et al. (2014). Role of altered growth factor receptor-mediated JAK2 signaling in growth and maintenance of human acute myeloid leukemia stem cells. *Blood* 123, 2826–2837. doi: 10.1182/blood-2013-05-505735

Cordenonsi, M., Zanconato, F., Azzolin, L., Forcato, M., Rosato, A., Frasson, C., et al. (2011). The Hippo transducer TAZ confers cancer stem cell-related traits on breast cancer cells. *Cell* 147, 759–772. doi: 10.1016/j.cell.2011.09.048

Curry, J. M., Sprandio, J., Cognetti, D., Luginbuhl, A., Bar-Ad, V., Pribitkin, E., et al. (2014). Tumor microenvironment in head and neck squamous cell carcinoma. *Semin. Oncol.* 41, 217–234.

Daniel, V. C., Marchionni, L., Hierman, J. S., Rhodes, J. T., Devereux, W. L., Rudin, C. M., et al. (2009). A primary xenograft model of small-cell lung cancer reveals irreversible changes in gene expression imposed by culture in vitro. *Cancer Res.* 69, 3364–3373. doi: 10.1158/0008-5472.can-08-4210

Darb-Esfahani, S., Kunze, C. A., Kulbe, H., Sehouli, J., Wienert, S., Lindner, J., et al. (2016). Prognostic impact of programmed cell death-1 (PD-1) and PD-ligand 1 (PD-L1) expression in cancer cells and tumor-infiltrating lymphocytes in ovarian high grade serous carcinoma. *Oncotarget* 7, 1486–1499. doi: 10.18632/oncotarget.6429

Dassonville, O., Formento, J. L., Francoual, M., Ramaioli, A., Santini, J., Schneider, M., et al. (1993). Expression of epidermal growth factor receptor and survival in upper aerodigestive tract cancer. *J. Clin. Oncol.* 11, 1873–1878. doi: 10.1200/jco.1993.11.10.1873

De La Luz Sierra, M., Yang, F., Narazaki, M., Salvucci, O., Davis, D., Yarchoan, R., et al. (2004). Differential processing of stromal-derived factor-1alpha and stromal-derived factor-1beta explains functional diversity. *Blood* 103, 2452–2459. doi: 10.1182/blood-2003-08-2857

Dean, T., Li, N. T., Cadavid, J. L., Ailles, L., and Mcguigan, A. P. (2020). A TRACER culture invasion assay to probe the impact of cancer associated fibroblasts on head and neck squamous cell carcinoma cell invasiveness. *Biomater. Sci.* 8, 3078–3094. doi: 10.1039/c9bm02017a

Demers, I., Donkers, J., Kremer, B., and Speel, E. J. (2020). Ex vivo culture models to indicate therapy response in head and neck squamous cell carcinoma. *Cells* 9:2527. doi: 10.3390/cells9112527

Denis, F., Garaud, P., Bardet, E., Alfonsi, M., Sire, C., Germain, T., et al. (2003). Late toxicity results of the GORTEC 94-01 randomized trial comparing radiotherapy with concomitant radiochemotherapy for advanced-stage oropharynx carcinoma: comparison of LENT/SOMA, RTOG/EORTC, and NCI-CTC scoring systems. *Int. J. Radiat. Oncol. Biol. Phys.* 55, 93–98. doi: 10.1016/s0360-3016(02)03819-1

Dohmen, A. J. C., Sanders, J., Canisius, S., Jordanova, E. S., Aalbersberg, E. A., Van Den Brekel, M. W. M., et al. (2018). Sponge-supported cultures of primary head and neck tumors for an optimized preclinical model. *Oncotarget* 9, 25034–25047. doi: 10.18632/oncotarget.25244

Dong, Y., Ochsenreither, S., Cai, C., Kaufmann, A. M., Albers, A. E., and Qian, X. (2017). Aldehyde dehydrogenase 1 isoenzyme expression as a marker of cancer stem cells correlates to histopathological features in head and neck cancer: a meta-analysis. *PLoS One* 12:e0187615. doi: 10.1371/journal.pone.0187615

Dong, Z., Liu, G., Huang, B., Sun, J., Wu, D. J. I. J. O. C., and Medicine, E. (2014). Prognostic significance of SOX2 in head and neck cancer: a meta-analysis. *Int. J. Clin. Exp. Med.* 7, 5010–5020.

Donnadieu, J., Lachaier, E., Peria, M., Saidak, Z., Dakpe, S., Ikoli, J. F., et al. (2016). Short-term culture of tumour slices reveals the heterogeneous sensitivity of human head and neck squamous cell carcinoma to targeted therapies. *BMC Cancer* 16:273. doi: 10.1186/s12885-016-2318-x

Dreesen, O., and Brivanlou, A. H. (2007). Signaling pathways in cancer and embryonic stem cells. *Stem Cell Rev.* 3, 7–17.

Driehuis, E., Kolders, S., Spelier, S., Lõhmussaar, K., Willems, S. M., Devriese, L. A., et al. (2019). Oral mucosal organoids as a potential platform for personalized cancer therapy. *Cancer Discov.* 9, 852–871. doi: 10.1158/2159-8290.cd-18-1522

Drost, J., and Clevers, H. (2018). Organoids in cancer research. *Nat. Rev. Cancer* 18, 407–418. doi: 10.1038/s41568-018-0007-6

Dubessy, C., Merlin, J. M., Marchal, C., and Guillemin, F. (2000). Spheroids in radiobiology and photodynamic therapy. *Crit. Rev. Oncol. Hematol.* 36, 179–192. doi: 10.1016/s1040-8428(00)00085-8

Dzobo, K., Motaung, K. S. C. M., and Adesida, A. (2019). Recent trends in decellularized extracellular matrix bioinks for 3D printing: an updated review. *Int. J. Mol. Sci.* 20:4628. doi: 10.3390/ijms20184628

Egloff, A. M., and Grandis, J. R. (2009). Improving response rates to EGFR-targeted therapies for head and neck squamous cell carcinoma: candidate predictive biomarkers and combination treatment with Src inhibitors. *J. Oncol.* 2009:896407.

Eke, I., Leonhardt, F., Storch, K., Hehlgans, S., and Cordes, N. (2009). The small molecule inhibitor QLT0267 Radiosensitizes squamous cell carcinoma cells of the head and neck. *PLoS One* 4:e6434. doi: 10.1371/journal.pone.0006434

Eke, I., Schneider, L., Förster, C., Zips, D., Kunz-Schughart, L. A., and Cordes, N. (2013). EGFR/JIP-4/JNK2 signaling attenuates cetuximab-mediated radiosensitization of squamous cell carcinoma cells. *Cancer Res.* 73, 297–306. doi: 10.1158/0008-5472.can-12-2021

Emerick, K. S., Leavitt, E. R., Michaelson, J. S., Diephuis, B., Clark, J. R., and Deschler, D. G. (2013). Initial clinical findings of a mathematical model to predict survival of head and neck cancer. *Otolaryngol. Head Neck Surg.* 149, 572–578. doi: 10.1177/0194599813495178

Enderling, H., Sunassee, E., and Caudell, J. J. (2019). Predicting patient-specific radiotherapy responses in head and neck cancer to personalize radiation dose fractionation. *Biorxiv* [Preprint]. doi: 10.1101/630806

Engelmann, L., Thierauf, J., Koerich Laureano, N., Stark, H. J., Prigge, E. S., Horn, D., et al. (2020). Organotypic co-cultures as a novel 3D model for head and neck squamous cell carcinoma. *Cancers* 12:2330. doi: 10.3390/cancers12082330

Faber, A., Barth, C., Hörmann, K., Kassner, S., Schultz, J. D., Sommer, U., et al. (2011). CD44 as a stem cell marker in head and neck squamous cell carcinoma. *Oncol. Rep.* 26, 321–326.

Faber, A., Goessler, U. R., Hoermann, K., Schultz, J. D., Umbreit, C., and Stern-Straeter, J. (2013a). SDF-1-CXCR4 axis: cell trafficking in the cancer stem cell niche of head and neck squamous cell carcinoma. *Oncol. Rep.* 29, 2325–2331. doi: 10.3892/or.2013.2380

Faber, A., Hoermann, K., Stern-Straeter, J., Schultz, D. J., and Goessler, U. R. (2013b). Functional effects of SDF-1α on a CD44(+) CXCR4(+) squamous cell carcinoma cell line as a model for interactions in the cancer stem cell niche. *Oncol. Rep.* 29, 579–584. doi: 10.3892/or.2012.2171

Faber, A., Roderburg, C., Wein, F., Saffrich, R., Seckinger, A., Horsch, K., et al. (2007). The many facets of SDF-1alpha, CXCR4 agonists and antagonists on hematopoietic progenitor cells. *J. Biomed. Biotechnol.* 2007:26065.

Facompre, N. D., Sahu, V., Montone, K. T., Harmeyer, K. M., Nakagawa, H., Rustgi, A. K., et al. (2017). Barriers to generating PDX models of HPV-related head and neck cancer. *Laryngoscope* 127, 2777–2783. doi: 10.1002/lary.26679

Fan, Z., Li, M., Chen, X., Wang, J., Liang, X., Wang, H., et al. (2017). Prognostic value of cancer stem cell markers in head and neck squamous cell carcinoma: a meta-analysis. *Sci. Rep.* 7:43008.

Fernanda Setúbal Destro Rodrigues, M., Gammon, L., Rahman, M. M., Biddle, A., Daumas Nunes, F., and Mackenzie, I. C. (2018). Effects of Cetuximab and Erlotinib on the behaviour of cancer stem cells in head and neck squamous cell carcinoma. *Oncotarget* 9, 13488–13500. doi: 10.18632/oncotarget.24416

Ferreira, L. P., Gaspar, V. M., and Mano, J. F. (2020). Decellularized extracellular matrix for bioengineering physiomimetic 3D in vitro tumor models. *Trends Biotechnol* 38, 1397–1414. doi: 10.1016/j.tibtech.2020.04.006

Ferris, R. L., Blumenschein, G. Jr., Fayette, J., Guigay, J., Colevas, A. D., Licitra, L., et al. (2016). Nivolumab for recurrent squamous-cell carcinoma of the head and neck. *N. Engl. J. Med.* 375, 1856–1867.

Ferris, R. L., Blumenschein, G. Jr., Fayette, J., Guigay, J., Colevas, A. D., Licitra, L., et al. (2018). Nivolumab vs investigators choice in recurrent or metastatic squamous cell carcinoma of the head and neck: 2-year long-term survival update of CheckMate 141 with analyses by tumor PD-L1 expression. *Oral Oncol.* 81, 45–51. doi: 10.1016/j.oraloncology.2018.04.008

Fichtner, I., Rolff, J., Soong, R., Hoffmann, J., Hammer, S., Sommer, A., et al. (2008). Establishment of patient-derived non-small cell lung cancer xenografts as models for the identification of predictive biomarkers. *Clin. Cancer Res.* 14, 6456–6468. doi: 10.1158/1078-0432.ccr-08-0138

Forde, P. M., Chaft, J. E., Smith, K. N., Anagnostou, V., Cottrell, T. R., Hellmann, M. D., et al. (2018). Neoadjuvant PD-1 blockade in resectable lung cancer. *N. Engl. J. Med.* 378, 1976–1986.

Franko, A. J., and Sutherland, R. M. (1979). Oxygen diffusion distance and development of necrosis in multicell spheroids. *Radiat. Res.* 79, 439–453. doi: 10.2307/3575173

Franzmann, E. J., Reategui, E. P., Pedroso, F., Pernas, F. G., Karakullukcu, B. M., Carraway, K. L., et al. (2007). Soluble CD44 is a potential marker for the early detection of head and neck cancer. *Cancer Epidemiol. Biomarkers Prev.* 16, 1348–1355. doi: 10.1158/1055-9965.epi-06-0011

Freudlsperger, C., Horn, D., Weißfuß, S., Weichert, W., Weber, K. J., Saure, D., et al. (2015). Phosphorylation of AKT(Ser473) serves as an independent prognostic marker for radiosensitivity in advanced head and neck squamous cell carcinoma. *Int. J. Cancer* 136, 2775–2785. doi: 10.1002/ijc.29328

Gadiot, J., Hooijkaas, A. I., Kaiser, A. D., Van Tinteren, H., Van Boven, H., and Blank, C. (2011). Overall survival and PD-L1 expression in metastasized malignant melanoma. *Cancer* 117, 2192–2201. doi: 10.1002/cncr.25747

Gallmeier, E., Hermann, P. C., Mueller, M. T., Machado, J. G., Ziesch, A., De Toni, E. N., et al. (2011). Inhibition of ataxia telangiectasia- and Rad3-related function abrogates the in vitro and in vivo tumorigenicity of human colon cancer cells through depletion of the CD133(+) tumor-initiating cell fraction. *Stem Cells* 29, 418–429. doi: 10.1002/stem.595

Galot, R., Le Tourneau, C., Guigay, J., Licitra, L., Tinhofer, I., Kong, A., et al. (2018). Personalized biomarker-based treatment strategy for patients with squamous cell carcinoma of the head and neck: EORTC position and approach. *Ann. Oncol.* 29, 2313–2327. doi: 10.1093/annonc/mdy452

Gan, G. N., Eagles, J., Keysar, S. B., Wang, G., Glogowska, M. J., Altunbas, C., et al. (2014). Hedgehog signaling drives radioresistance and stroma-driven tumor repopulation in head and neck squamous cancers. *Cancer Res.* 74, 7024–7036. doi: 10.1158/0008-5472.can-14-1346

Gao, H., Korn, J. M., Ferretti, S., Monahan, J. E., Wang, Y., Singh, M., et al. (2015). High-throughput screening using patient-derived tumor xenografts to predict clinical trial drug response. *Nat. Med.* 21, 1318–1325.

Garber, K. (2009). From human to mouse and back: 'tumorgraft' models surge in popularity. *J. Natl. Cancer Inst.* 101, 6–8. doi: 10.1093/jnci/djn481

Gerlach, M. M., Merz, F., Wichmann, G., Kubick, C., Wittekind, C., Lordick, F., et al. (2014). Slice cultures from head and neck squamous cell carcinoma: a novel test system for drug susceptibility and mechanisms of resistance. *Br. J. Cancer* 110, 479–488. doi: 10.1038/bjc.2013.700

Goichberg, P., Kalinkovich, A., Borodovsky, N., Tesio, M., Petit, I., Nagler, A., et al. (2006). cAMP-induced PKCzeta activation increases functional CXCR4 expression on human CD34+ hematopoietic progenitors. *Blood* 107, 870–879. doi: 10.1182/blood-2005-03-0941

Goričan, L., Gole, B., and Potočnik, U. (2020). Head and neck cancer stem cell-enriched spheroid model for anticancer compound screening. *Cells* 9:1707. doi: 10.3390/cells9071707

Gougis, P., Moreau Bachelard, C., Kamal, M., Gan, H. K., Borcoman, E., Torossian, N., et al. (2019). Clinical development of molecular targeted therapy in head and neck squamous cell carcinoma. *JNCI Cancer Spectr.* 3:kz055.

Gu, L., and Mooney, D. J. (2016). Biomaterials and emerging anticancer therapeutics: engineering the microenvironment. *Nat. Rev. Cancer* 16, 56–66. doi: 10.1038/nrc.2015.3

Guigay, J., Fayette, J., Mesia, R., Lafond, C., Saada-Bouzid, E., Geoffrois, L., et al. (2019). TPExtreme randomized trial: TPEx versus Extreme regimen in 1st line recurrent/metastatic head and neck squamous cell carcinoma (R/M HNSCC). *J. Clin. Oncol.* 37, 6002–6002. doi: 10.1200/jco.2019.37.15_suppl.6002

Günthert, U., Hofmann, M., Rudy, W., Reber, S., Zöller, M., Haussmann, I., et al. (1991). A new variant of glycoprotein CD44 confers metastatic potential to rat carcinoma cells. *Cell* 65, 13–24. doi: 10.1016/0092-8674(91)90403-l

Hagemann, J., Jacobi, C., Gstoettner, S., Welz, C., Schwenk-Zieger, S., Stauber, R., et al. (2018). Therapy testing in a spheroid-based 3D cell culture model for head and neck squamous cell carcinoma. *J. Vis. Exp.* 134:57012.

Hagemann, J., Jacobi, C., Hahn, M., Schmid, V., Welz, C., Schwenk-Zieger, S., et al. (2017). Spheroid-based 3D cell cultures enable personalized therapy testing and drug discovery in head and neck cancer. *Anticancer Res.* 37, 2201–2210. doi: 10.21873/anticanres.11555

Han, J., Kioi, M., Chu, W. S., Kasperbauer, J. L., Strome, S. E., and Puri, R. K. (2009). Identification of potential therapeutic targets in human head & neck squamous cell carcinoma. *Head Neck Oncol.* 1:27. doi: 10.1186/1758-3284-1-27

Han, J. J., Kim, D. W., Koh, J., Keam, B., Kim, T. M., Jeon, Y. K., et al. (2016). Change in PD-L1 expression after acquiring resistance to gefitinib in EGFR-mutant non-small-cell lung cancer. *Clin. Lung Cancer* 17, 263.e2–270.e2.

Hanna, G. J., Lizotte, P., Cavanaugh, M., Kuo, F. C., Shivdasani, P., Frieden, A., et al. (2018). Frameshift events predict anti-PD-1/L1 response in head and neck cancer. *JCI Insight* 3:e98811.

Hansen, A. R., and Siu, L. L. (2016). PD-L1 testing in cancer: challenges in companion diagnostic development. *JAMA Oncol.* 2, 15–16. doi: 10.1001/jamaoncol.2015.4685

Harris, L., Chen, A., O'dwyer, P., Flaherty, K., Hamilton, S., Mcshane, L., et al. (2018). *Abstract B080: Update on the NCI-Molecular Analysis for Therapy Choice (NCI-MATCH/EAY131) Precision Medicine Trial*. Philadelphia: AACR.

Herold-Mende, C., Seiter, S., Born, A. I., Patzelt, E., Schupp, M., Zöller, J., et al. (1996). Expression of CD44 splice variants in squamous epithelia and squamous cell carcinomas of the head and neck. *J. Pathol.* 179, 66–73. doi: 10.1002/(sici)1096-9896(199605)179:1<66::aid-path544>3.0.co;2-5

Hickman, J. A., Graeser, R., De Hoogt, R., Vidic, S., Brito, C., Gutekunst, M., et al. (2014). Three-dimensional models of cancer for pharmacology and cancer cell biology: capturing tumor complexity in vitro/ex vivo. *Biotechnol. J.* 9, 1115–1128. doi: 10.1002/biot.201300492

Hobdell, M. H., Oliveira, E. R., Bautista, R., Myburgh, N. G., Lalloo, R., Narendran, S., et al. (2003). Oral diseases and socio-economic status (SES). *Br. Dent. J.* 194, 91–96. doi: 10.1038/sj.bdj.4809882

Hoey, T., Yen, W. C., Axelrod, F., Basi, J., Donigian, L., Dylla, S., et al. (2009). DLL4 blockade inhibits tumor growth and reduces tumor-initiating cell frequency. *Cell Stem Cell* 5, 168–177. doi: 10.1016/j.stem.2009.05.019

Hoffmann, T. K., Schirlau, K., Sonkoly, E., Brandau, S., Lang, S., Pivarcsi, A., et al. (2009). A novel mechanism for anti-EGFR antibody action involves chemokine-mediated leukocyte infiltration. *Int. J. Cancer* 124, 2589–2596. doi: 10.1002/ijc.24269

Huang, C. F., Xu, X. R., Wu, T. F., Sun, Z. J., and Zhang, W. F. (2014). Correlation of ALDH1, CD44, OCT4 and SOX2 in tongue squamous cell carcinoma and their association with disease progression and prognosis. *J. Oral Pathol. Med.* 43, 492–498. doi: 10.1111/jop.12159

Huang, Y.-H., Chang, C.-Y., Kuo, Y.-Z., Fang, W.-Y., Kao, H.-Y., Tsai, S.-T., et al. (2019). Cancer-associated fibroblast-derived interleukin-1β activates protumor C-C motif chemokine ligand 22 signaling in head and neck cancer. *Cancer Sci.* 110, 2783–2793. doi: 10.1111/cas.14135

Huh, D., Hamilton, G. A., and Ingber, D. E. (2011). From 3D cell culture to organs-on-chips. *Trends Cell Biol.* 21, 745–754. doi: 10.1016/j.tcb.2011.09.005

Ihler, F., Gratz, R., Wolff, H. A., Weiss, B. G., Bertlich, M., Kitz, J., et al. (2018). Epithelial-mesenchymal transition during metastasis of HPV-negative pharyngeal squamous cell carcinoma. *BioMed Res. Int.* 2018:7929104.

Ishiguro, T., Ohata, H., Sato, A., Yamawaki, K., Enomoto, T., and Okamoto, K. (2017). Tumor-derived spheroids: Relevance to cancer stem cells and clinical applications. *Cancer Sci.* 108, 283–289. doi: 10.1111/cas.13155

Islam, M., Sharma, S., and Teknos, T. N. (2014). RhoC regulates cancer stem cells in head and neck squamous cell carcinoma by overexpressing IL-6 and phosphorylation of STAT3. *PLoS One* 9:e88527. doi: 10.1371/journal.pone.0088527

Jae Hyung, P., Ji Eun, S., and Hyun Woo, P. (2018). The role of hippo pathway in cancer stem cell biology. *Mol. Cells* 41, 83–92.

Jakob, M., Sharaf, K., Schirmer, M., Leu, M., Küffer, S., Bertlich, M., et al. (2020). Role of cancer stem cell markers ALDH1, BCL11B, BMI-1, and CD44 in the prognosis of advanced HNSCC. *Strahlenther. Onkol.* 197, 231–245. doi: 10.1007/s00066-020-01653-5

Jamal, B. T., Grillone, G. A., and Jalisi, S. (2017). Chemoresponse assay in head and neck cancer patients: a three-year follow up. *J. Clin. Diagn. Res.* 11, Xc01–Xc03.

Joshua, B., Kaplan, M. J., Doweck, I., Pai, R., Weissman, I. L., Prince, M. E., et al. (2012). Frequency of cells expressing CD44, a head and neck cancer stem cell marker: correlation with tumor aggressiveness. *Head Neck* 34, 42–49. doi: 10.1002/hed.21699

Kamatar, A., Gunay, G., and Acar, H. (2020). Natural and synthetic biomaterials for engineering multicellular tumor spheroids. *Polymers* 12:2506. doi: 10.3390/polym12112506

Kansy, B. A., Concha-Benavente, F., Srivastava, R. M., Jie, H. B., Shayan, G., Lei, Y., et al. (2017). PD-1 status in CD8(+) T cells associates with survival and anti-PD-1 therapeutic outcomes in head and neck cancer. *Cancer Res.* 77, 6353–6364. doi: 10.1158/0008-5472.can-16-3167

Karamboulas, C., Bruce, J. P., Hope, A. J., Meens, J., Huang, S. H., Erdmann, N., et al. (2018). Patient-derived xenografts for prognostication and personalized treatment for head and neck squamous cell carcinoma. *Cell Rep.* 25, 1318.e4–1331.e4.

Kennedy, R., Kuvshinov, D., Sdrolia, A., Kuvshinova, E., Hilton, K., Crank, S., et al. (2019). A patient tumour-on-a-chip system for personalised investigation of radiotherapy based treatment regimens. *Sci. Rep.* 9:6327.

Kenny, P. A. (2007). Three-dimensional extracellular matrix culture models of EGFR signalling and drug response. *Biochem. Soc. Trans.* 35, 665–668. doi: 10.1042/bst0350665

Kim, N., Choung, H. K., Lee, M. J., Khwarg, S. I., and Kim, J. E. (2015). Cancer stem cell markers in eyelid sebaceous gland carcinoma: high expression of ALDH1, CD133, and ABCG2 correlates with poor prognosis. *Invest. Ophthalmol. Vis. Sci.* 56, 1813–1819. doi: 10.1167/iovs.14-15547

Klinghammer, K., Raguse, J. D., Plath, T., Albers, A. E., Joehrens, K., Zakarneh, A., et al. (2015). A comprehensively characterized large panel of head and neck cancer patient-derived xenografts identifies the mTOR inhibitor everolimus as potential new treatment option. *Int. J. Cancer* 136, 2940–2948. doi: 10.1002/ijc.29344

Kobayashi, H., and Choyke, P. L. (2019). Near-infrared photoimmunotherapy of cancer. *Acc. Chem. Res.* 52, 2332–2339.

Kochanny, S. E., Worden, F. P., Adkins, D. R., Lim, D. W., Bauman, J. E., Wagner, S. A., et al. (2020). A randomized phase 2 network trial of tivantinib plus cetuximab versus cetuximab in patients with recurrent/metastatic head and neck squamous cell carcinoma. *Cancer* 126, 2146–2152. doi: 10.1002/cncr.32762

Komarova, N. (2006). Stochastic modeling of drug resistance in cancer. *J. Theor. Biol.* 239, 351–366. doi: 10.1016/j.jtbi.2005.08.003

Köpf-Maier, P., and Zimmermann, B. (1991). Organoid reorganization of human tumors under in vitro conditions. *Cell Tissue Res.* 264, 563–576. doi: 10.1007/bf00319046

Krishna, B. M., Jana, S., Singhal, J., Horne, D., Awasthi, S., Salgia, R., et al. (2019). Notch signaling in breast cancer: from pathway analysis to therapy. *Cancer Lett.* 461, 123–131. doi: 10.1016/j.canlet.2019.07.012

Kumar, A., Placone, J. K., and Engler, A. J. J. D. (2017). Understanding the extracellular forces that determine cell fate and maintenance. *Development* 144, 4261–4270. doi: 10.1242/dev.158469

Langer, E. M., Allen-Petersen, B. L., King, S. M., Kendsersky, N. D., Turnidge, M. A., Kuziel, G. M., et al. (2019). Modeling tumor phenotypes in vitro with three-dimensional bioprinting. *Cell Rep.* 26, 608.e6–623.e6.

Larkins, E., Blumenthal, G. M., Yuan, W., He, K., Sridhara, R., Subramaniam, S., et al. (2017). FDA approval summary: pembrolizumab for the treatment of recurrent or metastatic head and neck squamous cell carcinoma with disease progression on or after platinum-containing chemotherapy. *Oncologist* 22, 873–878. doi: 10.1634/theoncologist.2016-0496

Lawrence, M. S., Sougnez, C., Lichtenstein, L., Cibulskis, K., Lander, E., Gabriel, S. B., et al. (2015). Comprehensive genomic characterization of head and neck squamous cell carcinomas. *Nature* 517, 576–582. doi: 10.1038/nature14129

Le, P. N., Keysar, S. B., Miller, B., Eagles, J. R., Chimed, T. S., Reisinger, J., et al. (2019). Wnt signaling dynamics in head and neck squamous cell cancer tumor-stroma interactions. *Mol. Carcinog.* 58, 398–410. doi: 10.1002/mc.22937

Lee, H., Jeong, A. J., and Ye, S. K. (2019). Highlighted STAT3 as a potential drug target for cancer therapy. *BMB Rep.* 52, 415–423. doi: 10.5483/bmbrep.2019.52.7.152

Lee, S. H., Park, S. A., Zou, Y., Seo, S. U., Jun, C. D., Lee, W. J., et al. (2018). Real-time monitoring of cancer cells in live mouse bone marrow. *Front. Immunol.* 9:1681. doi: 10.3389/fimmu.2018.01681

Leinung, M., Ernst, B., Döring, C., Wagenblast, J., Tahtali, A., Diensthuber, M., et al. (2015). Expression of ALDH1A1 and CD44 in primary head and neck squamous cell carcinoma and their value for carcinogenesis, tumor progression and cancer stem cell identification. *Oncol. Lett.* 10, 2289–2294. doi: 10.3892/ol.2015.3542

Li, H., Wheeler, S., Park, Y., Ju, Z., Thomas, S. M., Fichera, M., et al. (2016). Proteomic characterization of head and neck cancer patient-derived xenografts. *Mol. Cancer Res.* 14, 278–286. doi: 10.1158/1541-7786.mcr-15-0354

Li, J., Li, Z., Wu, Y., Wang, Y., Wang, D., Zhang, W., et al. (2019). The Hippo effector TAZ promotes cancer stemness by transcriptional activation of SOX2 in head neck squamous cell carcinoma. *Cell Death Dis.* 10:603.

Li, K., Yang, L., Li, J., Guan, C., Zhang, S., Lao, X., et al. (2019). TGFβ induces stemness through non-canonical AKT-FOXO3a axis in oral squamous cell carcinoma. *EBioMedicine* 48, 70–80. doi: 10.1016/j.ebiom.2019.09.027

Li, Y., Atkinson, K., and Zhang, T. (2017). Combination of chemotherapy and cancer stem cell targeting agents: preclinical and clinical studies. *Cancer Lett.* 396, 103–109. doi: 10.1016/j.canlet.2017.03.008

Li, Z., Wang, Y., Zhu, Y., Yuan, C., Wang, D., Zhang, W., et al. (2015). The Hippo transducer TAZ promotes epithelial to mesenchymal transition and cancer stem cell maintenance in oral cancer. *Mol. Oncol.* 9, 1091–1105. doi: 10.1016/j.molonc.2015.01.007

Licitra, L., Mesia, R., Rivera, F., Remenár, É, Hitt, R., Erfán, J., et al. (2011). Evaluation of EGFR gene copy number as a predictive biomarker for the efficacy of cetuximab in combination with chemotherapy in the first-line treatment of recurrent and/or metastatic squamous cell carcinoma of the head and neck: EXTREME study. *Ann. Oncol.* 22, 1078–1087. doi: 10.1093/annonc/mdq588

Licitra, L., Störkel, S., Kerr, K. M., Van Cutsem, E., Pirker, R., Hirsch, F. R., et al. (2013). Predictive value of epidermal growth factor receptor expression for first-line chemotherapy plus cetuximab in patients with head and neck and colorectal cancer: analysis of data from the EXTREME and CRYSTAL studies. *Eur. J. Cancer* 49, 1161–1168. doi: 10.1016/j.ejca.2012.11.018

Lim, Y. C., Oh, S. Y., Cha, Y. Y., Kim, S. H., Jin, X., and Kim, H. (2011). Cancer stem cell traits in squamospheres derived from primary head and neck squamous cell carcinomas. *Oral Oncol.* 47, 83–91. doi: 10.1016/j.oraloncology.2010.11.011

Lin, D., Wyatt, A. W., Xue, H., Wang, Y., Dong, X., Haegert, A., et al. (2014). High fidelity patient-derived xenografts for accelerating prostate cancer discovery and drug development. *Cancer Res.* 74, 1272–1283. doi: 10.1158/0008-5472.can-13-2921-t

Linxweiler, M., Kadah, B. A., Bozzato, A., Bozzato, V., Hasenfus, A., Kim, Y. J., et al. (2016). Noninvasive histological imaging of head and neck squamous cell carcinomas using confocal laser endomicroscopy. *Eur. Arch. Otorhinolaryngol.* 273, 4473–4483. doi: 10.1007/s00405-016-4145-8

Llewellyn, C. D., Johnson, N. W., and Warnakulasuriya, K. A. (2001). Risk factors for squamous cell carcinoma of the oral cavity in young people–a comprehensive literature review. *Oral Oncol.* 37, 401–418. doi: 10.1016/s1368-8375(00)00135-4

Lui, V. W., Hedberg, M. L., Li, H., Vangara, B. S., Pendleton, K., Zeng, Y., et al. (2013). Frequent mutation of the PI3K pathway in head and neck cancer defines predictive biomarkers. *Cancer Discov.* 3, 761–769. doi: 10.1158/2159-8290.cd-13-0103

Ma, I., and Allan, A. L. (2011). The role of human aldehyde dehydrogenase in normal and cancer stem cells. *Stem Cell Rev. Rep.* 7, 292–306. doi: 10.1007/s12015-010-9208-4

Ma, L., Li, Y., Wu, Y., Aazmi, A., Zhang, B., Zhou, H., et al. (2020). The construction of in vitro tumor models based on 3D bioprinting. *Bio Design Manuf.* 3, 227–236. doi: 10.1007/s42242-020-00068-6

Machiels, J. P., Henry, S., Zanetta, S., Kaminsky, M. C., Michoux, N., Rommel, D., et al. (2010). Phase II study of sunitinib in recurrent or metastatic squamous cell carcinoma of the head and neck: GORTEC 2006-01. *J. Clin. Oncol.* 28, 21–28.

Malone, E., and Siu, L. L. (2018). Precision medicine in head and neck cancer: myth or reality? *Clin. Med. Insights Oncol.* 12:1179554918779581.

Mandal, R., şenbabaoğlu, Y., Desrichard, A., Havel, J. J., Dalin, M. G., Riaz, N., et al. (2016). The head and neck cancer immune landscape and its immunotherapeutic implications. *JCI Insight* 1:e89829.

Mannelli, G., Magnelli, L., Deganello, A., Busoni, M., Meccariello, G., Parrinello, G., et al. (2015). Detection of putative stem cell markers, CD44/CD133, in primary and lymph node metastases in head and neck squamous cell carcinomas. A preliminary immunohistochemical and in vitro study. *Clin. Otolaryngol.* 40, 312–320. doi: 10.1111/coa.12368

Marous, M., Bièche, I., Paoletti, X., Alt, M., Razak, A. R., Stathis, A., et al. (2015). Designs of preoperative biomarkers trials in oncology: a systematic review of the literature. *Ann. Oncol.* 26, 2419–2428. doi: 10.1093/annonc/mdv378

Massard, C., Michiels, S., Ferté, C., Le Deley, M.-C., Lacroix, L., Hollebecque, A., et al. (2017). High-throughput genomics and clinical outcome in hard-to-treat advanced cancers: results of the MOSCATO 01 trial. *Cancer Discov.* 7, 586–595. doi: 10.1158/2159-8290.cd-16-1396

Matsumoto, C. S., Almeida, L. O., Guimarães, D. M., Martins, M. D., Papagerakis, P., Papagerakis, S., et al. (2016). PI3K-PTEN dysregulation leads to mTOR-driven upregulation of the core clock gene BMAL1 in normal and malignant epithelial cells. *Oncotarget* 7:42393. doi: 10.18632/oncotarget.9877

Matsumoto, T., Yokoi, A., Hashimura, M., Oguri, Y., Akiya, M., and Saegusa, M. (2018). TGF-β-mediated LEFTY/Akt/GSK-3β/Snail axis modulates epithelial-mesenchymal transition and cancer stem cell properties in ovarian clear cell carcinomas. *Mol. Carcinog.* 57, 957–967. doi: 10.1002/mc.22816

McDermott, S., and Kilcoyne, A. (2016). Molecular imaging-its current role in cancer. *Qjm* 109, 295–299. doi: 10.1093/qjmed/hcv141

Mehanna, H., Rischin, D., Wong, S. J., Gregoire, V., Ferris, R., Waldron, J., et al. (2020). De-escalation after DE-ESCALATE and RTOG 1016: a head and neck cancer intergroup framework for future de-escalation studies. *J. Clin Oncol.* 38, 2552–2557. doi: 10.1200/jco.20.00056

Melissaridou, S., Wiechec, E., Magan, M., Jain, M. V., Chung, M. K., Farnebo, L., et al. (2019). The effect of 2D and 3D cell cultures on treatment response, EMT profile and stem cell features in head and neck cancer. *Cancer Cell Int.* 19:16.

Michifuri, Y., Hirohashi, Y., Torigoe, T., Miyazaki, A., Kobayashi, J., Sasaki, T., et al. (2012). High expression of ALDH1 and SOX2 diffuse staining pattern of oral squamous cell carcinomas correlates to lymph node metastasis. *Pathol. Int.* 62, 684–689. doi: 10.1111/j.1440-1827.2012.02851.x

Möhle, R., Bautz, F., Rafii, S., Moore, M. A., Brugger, W., and Kanz, L. (1998). The chemokine receptor CXCR-4 is expressed on CD34+ hematopoietic progenitors and leukemic cells and mediates transendothelial migration induced by stromal cell-derived factor-1. *Blood* 91, 4523–4530. doi: 10.1182/blood.v91.12.4523

Moroishi, T., Hansen, C. G., and Guan, K. L. (2015). The emerging roles of YAP and TAZ in cancer. *Nat. Rev. Cancer* 15, 73–79. doi: 10.1038/nrc3876

Morton, J. J., Bird, G., Keysar, S. B., Astling, D. P., Lyons, T. R., Anderson, R. T., et al. (2016). XactMice: humanizing mouse bone marrow enables microenvironment reconstitution in a patient-derived xenograft model of head and neck cancer. *Oncogene* 35, 290–300. doi: 10.1038/onc.2015.94

Mulligan, M., Khammanivong, A., Gopalakrishnan, R., and Dickerson, E. (2013). "SMURF1 modulates BMP signaling in HNSCC stem cells," in *Proceedings of the IADR/AADR/CADR General Session and Exhibition 2013* (Washington, DC).

Murray, L. M., Nock, V., Evans, J. J., and Alkaisi, M. M. (2014). Bioimprinted polymer platforms for cell culture using soft lithography. *J. Nanobiotechnol.* 12:60.

Mutreja, I., Woodfield, T. B., Sperling, S., Nock, V., Evans, J. J., and Alkaisi, M. M. (2015). Positive and negative bioimprinted polymeric substrates: new platforms for cell culture. *Biofabrication* 7:025002. doi: 10.1088/1758-5090/7/2/025002

Negi, P., Kingsley, P. A., Srivastava, H., and Sharma, S. K. (2016). Three weekly versus weekly cisplatin as radiosensitizer in head and neck cancer: a decision dilemma. *Asian Pac. J. Cancer Prev.* 17, 1617–1623. doi: 10.7314/apjcp.2016.17.4.1617

Ng, J. M., and Curran, T. (2011). The Hedgehog's tale: developing strategies for targeting cancer. *Nat. Rev. Cancer* 11, 493–501. doi: 10.1038/nrc3079

Ock, C. Y., Kim, S., Keam, B., Kim, S., Ahn, Y. O., Chung, E. J., et al. (2017). Changes in programmed death-ligand 1 expression during cisplatin treatment in patients with head and neck squamous cell carcinoma. *Oncotarget* 8, 97920–97927. doi: 10.18632/oncotarget.18542

Okamoto, I., Tsuiki, H., Kenyon, L. C., Godwin, A. K., Emlet, D. R., Holgado-Madruga, M., et al. (2002). Proteolytic cleavage of the CD44 adhesion molecule in multiple human tumors. *Am. J. Pathol.* 160, 441–447. doi: 10.1016/S0002-9440(10)64863-8

Okayama, H., Kumamoto, K., Saitou, K., Hayase, S., Kofunato, Y., Sato, Y., et al. (2009). CD44v6, MMP-7 and nuclear Cdx2 are significant biomarkers for prediction of lymph node metastasis in primary gastric cancer. *Oncol. Rep.* 22, 745–755.

Oliva, M., Spreafico, A., Taberna, M., Alemany, L., Coburn, B., Mesia, R., et al. (2019). Immune biomarkers of response to immune-checkpoint inhibitors in head and neck squamous cell carcinoma. *Ann. Oncol.* 30, 57–67. doi: 10.1093/annonc/mdy507

Panikkanvalappil, S. R., Garlapati, C., Hooshmand, N., Aneja, R., and El-Sayed, M. A. (2019). Monitoring the dynamics of hemeoxygenase-1 activation in head and neck cancer cells in real-time using plasmonically enhanced Raman spectroscopy. *Chem. Sci.* 10, 4876–4882. doi: 10.1039/c9sc00093c

Park, S. Y., Lee, H. E., Li, H., Shipitsin, M., Gelman, R., and Polyak, K. (2010). Heterogeneity for stem cell-related markers according to tumor subtype and histologic stage in breast cancer. *Clin. Cancer Res.* 16, 876–887. doi: 10.1158/1078-0432.ccr-09-1532

Park, Y., Huh, K. M., and Kang, S. W. (2021). Applications of biomaterials in 3D cell culture and contributions of 3D cell culture to drug development and basic biomedical research. *Int. J. Mol. Sci.* 22:2491. doi: 10.3390/ijms22052491

Parmigiani, E., Taylor, V., and Giachino, C. (2020). Oncogenic and tumor-suppressive functions of NOTCH signaling in glioma. *Cells* 9:2304. doi: 10.3390/cells9102304

Partlová, S., Bouček, J., Kloudová, K., Lukešová, E., Zábrodský, M., Grega, M., et al. (2015). Distinct patterns of intratumoral immune cell infiltrates in patients with HPV-associated compared to non-virally induced head and neck squamous cell carcinoma. *Oncoimmunology* 4:e965570. doi: 10.4161/21624011.2014.965570

Patel, S. S., Shah, K. A., Shah, M. J., Kothari, K. C., and Rawal, R. M. (2014). Cancer stem cells and stemness markers in oral squamous cell carcinomas. *Asian Pac. J. Cancer Prev.* 15, 8549–8556. doi: 10.7314/apjcp.2014.15.20.8549

Pathak, K. A., Juvekar, A. S., Radhakrishnan, D. K., Deshpande, M. S., Pai, V. R., Chaturvedi, P., et al. (2007). In vitro chemosensitivity profile of oral squamous cell cancer and its correlation with clinical response to chemotherapy. *Indian J. Cancer* 44, 142–146. doi: 10.4103/0019-509x.39376

Peitzsch, C., Kurth, I., Ebert, N., Dubrovska, A., and Baumann, M. (2019a). Cancer stem cells in radiation response: current views and future perspectives in radiation oncology. *Int. J. Radiat. Biol.* 95, 900–911. doi: 10.1080/09553002.2019.1589023

Peitzsch, C., Nathansen, J., Schniewind, S. I., Schwarz, F., and Dubrovska, A. (2019b). Cancer stem cells in head and neck squamous cell carcinoma: identification, characterization and clinical implications. *Cancer* 11:616. doi: 10.3390/cancers11050616

Penfornis, P., Vallabhaneni, K. C., Janorkar, A. V., and Pochampally, R. R. (2017). Three dimensional tumor models for cancer studies. *Front. Biosci.* 9, 162–173. doi: 10.2741/e793

Peng, S., Creighton, C. J., Zhang, Y., Sen, B., Mazumdar, T., Myers, J. N., et al. (2013). Tumor grafts derived from patients with head and neck squamous carcinoma authentically maintain the molecular and histologic characteristics of human cancers. *J. Transl. Med.* 11:198. doi: 10.1186/1479-5876-11-198

Perez, A., Neskey, D. M., Wen, J., Pereira, L., Reategui, E. P., Goodwin, W. J., et al. (2013). CD44 interacts with EGFR and promotes head and neck squamous cell carcinoma initiation and progression. *Oral Oncol.* 49, 306–313. doi: 10.1016/j.oraloncology.2012.11.009

Peria, M., Donnadieu, J., Racz, C., Ikoli, J. F., Galmiche, A., Chauffert, B., et al. (2016). Evaluation of individual sensitivity of head and neck squamous cell carcinoma to cetuximab by short-term culture of tumor slices. *Head Neck* 38(Suppl. 1), E911–E915.

Petit, I., Goichberg, P., Spiegel, A., Peled, A., Brodie, C., Seger, R., et al. (2005). Atypical PKC-zeta regulates SDF-1-mediated migration and development of human CD34+ progenitor cells. *J. Clin. Invest.* 115, 168–176. doi: 10.1172/jci200521773

Picco, N., Gatenby, R. A., and Anderson, A. R. A. (2017). Stem cell plasticity and niche dynamics in cancer progression. *IEEE Trans. Bio Med. Eng.* 64, 528–537. doi: 10.1109/tbme.2016.2607183

Ponta, H., Wainwright, D., and Herrlich, P. (1998). The CD44 protein family. *Int. J. Biochem. Cell Biol.* 30, 299–305. doi: 10.1016/s1357-2725(97)00152-0

Powley, I. R., Patel, M., Miles, G., Pringle, H., Howells, L., Thomas, A., et al. (2020). Patient-derived explants (PDEs) as a powerful preclinical platform for anti-cancer drug and biomarker discovery. *Br. J. Cancer* 122, 735–744. doi: 10.1038/s41416-019-0672-6

Pries, R., Wittkopf, N., Hasselbacher, K., and Wollenberg, B. (2008). [Constitutive expression of the potential stem cell marker CD44 in permanent HNSCC cell lines]. *HNO* 56, 461–466.

Prince, M. E., Sivanandan, R., Kaczorowski, A., Wolf, G. T., Kaplan, M. J., Dalerba, P., et al. (2007). Identification of a subpopulation of cells with cancer stem cell properties in head and neck squamous cell carcinoma. *Proc. Natl. Acad. Sci. U.S.A.* 104, 973–978. doi: 10.1073/pnas.0610117104

Pulte, D., and Brenner, H. (2010). Changes in survival in head and neck cancers in the late 20th and early 21st century: a period analysis. *Oncologist* 15, 994–1001. doi: 10.1634/theoncologist.2009-0289

Qian, X., Ma, C., Nie, X., Lu, J., Lenarz, M., Kaufmann, A. M., et al. (2015). Biology and immunology of cancer stem (-like) cells in head and neck cancer. *Crit. Rev. Oncol. Hematol.* 95, 337–345.

Qiu, M., Peng, Q., Jiang, I., Carroll, C., Han, G., Rymer, I., et al. (2013). Specific inhibition of Notch1 signaling enhances the antitumor efficacy of chemotherapy in triple negative breast cancer through reduction of cancer stem cells. *Cancer Lett.* 328, 261–270. doi: 10.1016/j.canlet.2012.09.023

Qu, Y., Oyan, A. M., Liu, R., Hua, Y., Zhang, J., Hovland, R., et al. (2013). Generation of prostate tumor-initiating cells is associated with elevation of reactive oxygen species and IL-6/STAT3 signaling. *Cancer Res.* 73, 7090–7100. doi: 10.1158/0008-5472.CAN-13-1560

Rai, V., Mukherjee, R., Ghosh, A. K., Routray, A., and Chakraborty, C. (2018). "Omics" in oral cancer: new approaches for biomarker discovery. *Arch. Oral Biol.* 87, 15–34. doi: 10.1016/j.archoralbio.2017.12.003

Reck, M., Rodríguez-Abreu, D., Robinson, A. G., Hui, R., Csőszi, T., Fülöp, A., et al. (2016). Pembrolizumab versus chemotherapy for PD-L1-positive non-small-cell lung cancer. *N. Engl. J. Med.* 375, 1823–1833.

Robbins, K. T., Connors, K. M., Storniolo, A. M., Hanchett, C., and Hoffman, R. M. (1994). Sponge-gel-supported histoculture drug-response assay for head and neck cancer. Correlations with clinical response to cisplatin. *Arch. Otolaryngol. Head. Neck Surg.* 120, 288–292. doi: 10.1001/archotol.1994.01880270036007

Robbins, K. T., Varki, N. M., Storniolo, A. M., Hoffman, H., and Hoffman, R. M. (1991). Drug response of head and neck tumors in native-state histoculture. *Arch. Otolaryngol. Head Neck Surg.* 117, 83–86. doi: 10.1001/archotol.1991.01870130089022

Rodrigues, J., Heinrich, M. A., Teixeira, L. M., and Prakash, J. (2020). 3D in vitro model (r)evolution: unveiling tumor-stroma interactions. *Trends Cancer* 7, 249–264. doi: 10.1016/j.trecan.2020.10.009

Rossi, C., Gilhodes, J., Maerevoet, M., Herbaux, C., Morschhauser, F., Brice, P., et al. (2018). Efficacy of chemotherapy or chemo-anti-PD-1 combination after failed anti-PD-1 therapy for relapsed and refractory Hodgkin lymphoma: a series from Lysa centers. *Am. J. Hematol.* [Epub ahead of print]. doi: 10.1002/ajh.25154

Rubin Grandis, J., Melhem, M. F., Barnes, E. L., and Tweardy, D. J. (1996). Quantitative immunohistochemical analysis of transforming growth factor-alpha and epidermal growth factor receptor in patients with squamous cell carcinoma of the head and neck. *Cancer* 78, 1284–1292. doi: 10.1002/(sici)1097-0142(19960915)78:6<1284::aid-cncr17>3.0.co;2-x

Rubin Grandis, J., Melhem, M. F., Gooding, W. E., Day, R., Holst, V. A., Wagener, M. M., et al. (1998). Levels of TGF-alpha and EGFR protein in head and neck squamous cell carcinoma and patient survival. *J. Natl. Cancer Inst.* 90, 824–832. doi: 10.1093/jnci/90.11.824

Saito, H., Tsujitani, S., Katano, K., Ikeguchi, M., Maeta, M., and Kaibara, N. (1998). Serum concentration of CD44 variant 6 and its relation to prognosis in patients with gastric carcinoma. *Cancer* 83, 1094–1101. doi: 10.1002/(sici)1097-0142(19980915)83:6<1094::aid-cncr7>3.0.co;2-8

Saleh, K., Daste, A., Martin, N., Pons-Tostivint, E., Auperin, A., Herrera-Gomez, R. G., et al. (2019). Response to salvage chemotherapy after progression on immune checkpoint inhibitors in patients with recurrent and/or metastatic squamous cell carcinoma of the head and neck. *Eur. J. Cancer* 121, 123–129. doi: 10.1016/j.ejca.2019.08.026

Sand, J. P., Kokorina, N. A., Zakharkin, S. O., Lewis, J. S., and Nussenbaum, B. (2014). BMP-2 expression correlates with local failure in head and neck squamous cell carcinoma. *Otolaryngol. Head Neck Surg.* 150, 245–250. doi: 10.1177/0194599813513003

Sanmamed, M. F., Chester, C., Melero, I., and Kohrt, H. (2016). Defining the optimal murine models to investigate immune checkpoint blockers and their combination with other immunotherapies. *Ann. Oncol.* 27, 1190–1198. doi: 10.1093/annonc/mdw041

Santos-de-Frutos, K., Segrelles, C., and Lorz, C. (2019). Hippo pathway and YAP signaling alterations in squamous cancer of the head and neck. *J. Clin. Med.* 8:2131. doi: 10.3390/jcm8122131

Satpute, P. S., Hazarey, V., Ahmed, R., and Yadav, L. (2013). Cancer stem cells in head and neck squamous cell carcinoma: a review. *Asian Pac. J. Cancer Prev.* 14, 5579–5587.

Sawant, S., Dongre, H., Singh, A. K., Joshi, S., Costea, D. E., Mahadik, S., et al. (2016). Establishment of 3D co-culture models from different stages of human tongue tumorigenesis: utility in understanding neoplastic progression. *PLoS One* 11:e0160615. doi: 10.1371/journal.pone.0160615

Schaal, C. M., Bora-Singhal, N., Kumar, D. M., and Chellappan, S. P. (2018). Regulation of Sox2 and stemness by nicotine and electronic-cigarettes in non-small cell lung cancer. *Mol. Cancer* 17:149.

Schirrmacher, V. (1985). Cancer metastasis: experimental approaches, theoretical concepts, and impacts for treatment strategies. *Adv. Cancer Res.* 43, 1–73. doi: 10.1016/s0065-230x(08)60942-2

Schmitz, S., Kaminsky-Forrett, M. C., Henry, S., Zanetta, S., Geoffrois, L., Bompas, E., et al. (2012). Phase II study of figitumumab in patients with recurrent and/or metastatic squamous cell carcinoma of the head and neck: clinical activity and molecular response (GORTEC 2008-02). *Ann. Oncol.* 23, 2153–2161. doi: 10.1093/annonc/mdr574

Schvartsman, G., Peng, S. A., Bis, G., Lee, J. J., Benveniste, M. F. K., Zhang, J., et al. (2017). Response rates to single-agent chemotherapy after exposure to immune checkpoint inhibitors in advanced non-small cell lung cancer. *Lung Cancer* 112, 90–95. doi: 10.1016/j.lungcan.2017.07.034

Scott, J. G., Berglund, A., Schell, M. J., Mihaylov, I., Fulp, W. J., Yue, B., et al. (2017). A genome-based model for adjusting radiotherapy dose (GARD): a retrospective, cohort-based study. *Lancet Oncol.* 18, 202–211. doi: 10.1016/s1470-2045(16)30648-9

Screaton, G. R., Bell, M. V., Bell, J. I., and Jackson, D. G. (1993). The identification of a new alternative exon with highly restricted tissue expression in transcripts encoding the mouse Pgp-1 (CD44) homing receptor. Comparison of all 10 variable exons between mouse, human, and rat. *J. Biol. Chem.* 268, 12235–12238. doi: 10.1016/s0021-9258(18)31376-0

Segrelles, C., Paramio, J. M., and Lorz, C. (2018). The transcriptional co-activator YAP: a new player in head and neck cancer. *Oral Oncol.* 86, 25–32. doi: 10.1016/j.oraloncology.2018.08.020

Seiwert, T. Y., Burtness, B., Mehra, R., Weiss, J., Berger, R., Eder, J. P., et al. (2016). Safety and clinical activity of pembrolizumab for treatment of recurrent or metastatic squamous cell carcinoma of the head and neck (KEYNOTE-012): an open-label, multicentre, phase 1b trial. *Lancet Oncol.* 17, 956–965. doi: 10.1016/s1470-2045(16)30066-3

Seiwert, T. Y., Kochanny, S., Wood, K., Worden, F. P., Adkins, D., Wade, J. L., et al. (2020). A randomized phase 2 study of temsirolimus and cetuximab versus temsirolimus alone in recurrent/metastatic, cetuximab-resistant head and neck cancer: the MAESTRO study. *Cancer* 126, 3237–3243. doi: 10.1002/cncr.32929

Seliger, B. (2019). Combinatorial approaches with checkpoint inhibitors to enhance anti-tumor immunity. *Front. Immunol.* 10:999. doi: 10.3389/fimmu.2019.00999

Shin, E., and Kim, J. (2020). The potential role of YAP in head and neck squamous cell carcinoma. *Exp. Mol. Med.* 52, 1264–1274. doi: 10.1038/s12276-020-00492-9

Shinohara, S., Funabiki, K., Kikuchi, M., Takebayashi, S., Hamaguchi, K., Hara, S., et al. (2020). Real-time imaging of head and neck squamous cell carcinomas using confocal micro-endoscopy and applicable dye: a preliminary study. *Auris. Nasus Larynx* 47, 668–675. doi: 10.1016/j.anl.2020.02.001

Simple, M., Suresh, A., Das, D., and Kuriakose, M. A. (2015). Cancer stem cells and field cancerization of oral squamous cell carcinoma. *Oral Oncol.* 51, 643–651. doi: 10.1016/j.oraloncology.2015.04.006

Singh, B., Li, R., Xu, L., Poluri, A., Patel, S., Shaha, A. R., et al. (2002). Prediction of survival in patients with head and neck cancer using the histoculture drug response assay. *Head Neck* 24, 437–442. doi: 10.1002/hed.10066

Skardal, A., Murphy, S. V., Devarasetty, M., Mead, I., Kang, H. W., Seol, Y. J., et al. (2017). Multi-tissue interactions in an integrated three-tissue organ-on-a-chip platform. *Sci. Rep.* 7:8837.

Slaughter, D. P., Southwick, H. W., and Smejkal, W. (1953). Field cancerization in oral stratified squamous epithelium; clinical implications of multicentric origin. *Cancer* 6, 963–968. doi: 10.1002/1097-0142(195309)6:5<963::aid-cncr2820060515>3.0.co;2-q

Song, J. I., and Grandis, J. R. (2000). STAT signaling in head and neck cancer. *Oncogene* 19, 2489–2495. doi: 10.1038/sj.onc.1203483

Sontheimer-Phelps, A., Hassell, B. A., and Ingber, D. E. (2019). Modelling cancer in microfluidic human organs-on-chips. *Nat. Rev. Cancer* 19, 65–81. doi: 10.1038/s41568-018-0104-6

Stamenkovic, I., Amiot, M., Pesando, J. M., and Seed, B. (1989). A lymphocyte molecule implicated in lymph node homing is a member of the cartilage link protein family. *Cell* 56, 1057–1062. doi: 10.1016/0092-8674(89)90638-7

Stecklum, M., Klinghammer, K., Wulf-Goldenberg, A., Brzezicha, B., Jöhrens, K., and Hoffmann, J. (2020). P03.14 Preclinical case study: patient-derived head and neck cancer xenograft on mice humanized with autologous immune cells, a model for personalized immuno-oncology research. *J. ImmunoTher. Cancer* 8, A27–A28.

Stine, R. R., and Matunis, E. L. (2013). JAK-STAT signaling in stem cells. *Adv. Exp. Med. Biol.* 786, 247–267.

Storch, K., Eke, I., Borgmann, K., Krause, M., Richter, C., Becker, K., et al. (2010). Three-dimensional cell growth confers radioresistance by chromatin density modification. *Cancer Res.* 70, 3925–3934. doi: 10.1158/0008-5472.can-09-3848

Su, Z., Liu, D., Chen, L., Zhang, J., Ru, L., Chen, Z., et al. (2019). CD44-targeted magnetic nanoparticles kill head and neck squamous cell carcinoma stem cells in an alternating magnetic field. *Int. J. Nanomedicine* 14, 7549–7560. doi: 10.2147/ijn.s215087

Sun, S., and Wang, Z. (2011). Head neck squamous cell carcinoma c-Met? cells display cancer stem cell properties and are responsible for cisplatin-resistance and metastasis. *Int. J. Cancer* 129, 2337–2348. doi: 10.1002/ijc.25927

Suresh, A., Vannan, M., Kumaran, D., Gümüs, Z. H., Sivadas, P., Murugaian, E. E., et al. (2012). Resistance/response molecular signature for oral tongue squamous cell carcinoma. *Dis. Markers* 32, 51–64. doi: 10.1155/2012/926703

Suzuki, H., Nishio, M., Hanai, N., Hirakawa, H., Tamaki, T., and Hasegawa, Y. (2015). Correlation between 18F-FDG-uptake and in vitro chemosensitivity of cisplatin in head and neck cancer. *Anticancer Res.* 35, 1009–1016.

Sylvester, D., Hattersley, S., Stafford, N., Haswell, S., and Greenman, J. (2013). Development of microfluidic-based analytical methodology for studying the effects of chemotherapy agents on cancer tissue. *Curr. Anal. Chem.* 9, 2–8. doi: 10.2174/1573411011309010002

Szabados, B., Van Dijk, N., Tang, Y. Z., Van Der Heijden, M. S., Wimalasingham, A., Gomez De Liano, A., et al. (2018). Response rate to chemotherapy after immune checkpoint inhibition in metastatic urothelial cancer. *Eur. Urol.* 73, 149–152. doi: 10.1016/j.eururo.2017.08.022

Tabassum, S., Rosli, N. B., and Mazalan, M. S. A. B. (2019). Mathematical modeling of cancer growth process: a review. *J. Phys. Conf. Ser.* 1366:012018. doi: 10.1088/1742-6596/1366/1/012018

Taccioli, C., Sorrentino, G., Zannini, A., Caroli, J., Beneventano, D., Anderlucci, L., et al. (2015). MDP, a database linking drug response data to genomic information, identifies dasatinib and statins as a combinatorial strategy to inhibit YAP/TAZ in cancer cells. *Oncotarget* 6, 38854–38865. doi: 10.18632/oncotarget.5749

Takahashi, H., Sakakura, K., Kudo, T., Toyoda, M., Kaira, K., Oyama, T., et al. (2016). Cancer-associated fibroblasts promote an immunosuppressive microenvironment through the induction and accumulation of protumoral macrophages. *Oncotarget* 8, 8633–8647. doi: 10.18632/oncotarget.14374

Takahashi-Yanaga, F., and Kahn, M. (2010). Targeting Wnt signaling: can we safely eradicate cancer stem cells? *Clin. Cancer Res.* 16, 3153–3162. doi: 10.1158/1078-0432.ccr-09-2943

Tan, L. H., Sykes, P. H., Alkaisi, M. M., and Evans, J. J. (2015). The characteristics of Ishikawa endometrial cancer cells are modified by substrate topography with cell-like features and the polymer surface. *Int. J. Nanomedicine* 10, 4883–4895. doi: 10.2147/ijn.s86336

Tang, K. H., Dai, Y. D., Tong, M., Chan, Y. P., Kwan, P. S., Fu, L., et al. (2013). A CD90(+) tumor-initiating cell population with an aggressive signature and metastatic capacity in esophageal cancer. *Cancer Res.* 73, 2322–2332. doi: 10.1158/0008-5472.can-12-2991

Tentler, J. J., Tan, A. C., Weekes, C. D., Jimeno, A., Leong, S., Pitts, T. M., et al. (2012). Patient-derived tumour xenografts as models for oncology drug development. *Nat. Rev. Clin. Oncol.* 9, 338–350. doi: 10.1038/nrclinonc.2012.61

Thenappan, A., Li, Y., Shetty, K., Johnson, L., Reddy, E. P., and Mishra, L. (2009). New therapeutics targeting colon cancer stem cells. *Curr. Colorectal. Cancer Rep.* 5:209. doi: 10.1007/s11888-009-0029-2

Tinhofer, I., Braunholz, D., and Klinghammer, K. (2020). Preclinical models of head and neck squamous cell carcinoma for a basic understanding of cancer biology and its translation into efficient therapies. *Cancers Head Neck* 5:9.

Topalian, S. L., Hodi, F. S., Brahmer, J. R., Gettinger, S. N., Smith, D. C., McDermott, D. F., et al. (2012). Safety, activity, and immune correlates of anti-PD-1 antibody in cancer. *N. Engl. J. Med.* 366, 2443–2454.

Townsend, E. C., Murakami, M. A., Christodoulou, A., Christie, A. L., Köster, J., Desouza, T. A., et al. (2016). The public repository of xenografts enables discovery and randomized phase ii-like trials in mice. *Cancer Cell* 30:183.

Trujillo-de Santiago, G., Flores-Garza, B. G., Tavares-Negrete, J. A., Lara-Mayorga, I. M., González-Gamboa, I., Zhang, Y. S., et al. (2019). The tumor-on-chip: recent advances in the development of microfluidic systems to recapitulate the physiology of solid tumors. *Materials* 12:2945. doi: 10.3390/ma12182945

Tsimberidou, A.-M., Hong, D. S., Ye, Y., Cartwright, C., Wheler, J. J., Falchook, G. S., et al. (2017). Initiative for molecular profiling and advanced cancer therapy (IMPACT): an MD Anderson precision medicine study. *JCO Precision Oncol.* 1, 1–18. doi: 10.1200/po.17.00002

Tsimberidou, A.-M., Iskander, N. G., Hong, D. S., Wheler, J. J., Falchook, G. S., Fu, S., et al. (2012). Personalized medicine in a phase I clinical trials program: the MD anderson cancer center initiative. *Clin. Cancer Res.* 18, 6373–6383. doi: 10.1158/1078-0432.ccr-12-1627

Valkenburg, K. C., De Groot, A. E., and Pienta, K. J. (2018). Targeting the tumour stroma to improve cancer therapy. *Nat. Rev. Clin. Oncol.* 15, 366–381. doi: 10.1038/s41571-018-0007-1

Vaupel, P., and Mayer, A. (2007). Hypoxia in cancer: significance and impact on clinical outcome. *Cancer Metastasis Rev.* 26, 225–239. doi: 10.1007/s10555-007-9055-1

Vaupel, P., Mayer, A., and Höckel, M. (2004). "Tumor hypoxia and malignant progression," in *Methods in Enzymology*, eds J. Abelson, M. Simon, G. Verdine, and A. Pyle (Amsterdam: Elsevier), 335–354. doi: 10.1016/s0076-6879(04)81023-1

Vermeulen, L., and Snippert, H. J. (2014). Stem cell dynamics in homeostasis and cancer of the intestine. *Nat. Rev. Cancer* 14, 468–480. doi: 10.1038/nrc3744

Vermorken, J. B., Trigo, J., Hitt, R., Koralewski, P., Diaz-Rubio, E., Rolland, F., et al. (2007). Open-label, uncontrolled, multicenter phase II study to evaluate the efficacy and toxicity of cetuximab as a single agent in patients with recurrent and/or metastatic squamous cell carcinoma of the head and neck who failed to respond to platinum-based therapy. *J. Clin. Oncol.* 25, 2171–2177. doi: 10.1200/jco.2006.06.7447

Voest, E. E., and Bernards, R. (2016). DNA-guided precision medicine for cancer: a case of irrational exuberance? *Cancer Discov.* 6, 130–132. doi: 10.1158/2159-8290.cd-15-1321

Vokes, E. E., Worden, F. P., Adkins, D., Bauman, J. E., Lim, D., Sukari, A., et al. (2015). A randomized phase II trial of the MET inhibitor tivantinib + cetuximab versus cetuximab alone in patients with recurrent/metastatic head and neck cancer. *Cancer* 33, 6060–6060. doi: 10.1200/jco.2015.33.15_suppl.6060

Von Hoff, D. D., Stephenson, J. J. Jr., Rosen, P., Loesch, D. M., Borad, M. J., Anthony, S., et al. (2010). Pilot study using molecular profiling of patients tumors to find potential targets and select treatments for their refractory cancers. *J. Clin. Oncol.* 28, 4877–4883. doi: 10.1200/jco.2009.26.5983

Vučičević Boras, V., Fučić, A., Baranović, S., Blivajs, I., Milenović, M., Bišof, V., et al. (2019). Environmental and behavioural head and neck cancer risk factors. *Cent. Eur. J. Public Health* 27, 106–109.

Wang, C. H., Chiou, S. H., Chou, C. P., Chen, Y. C., Huang, Y. J., and Peng, C. A. (2011). Photothermolysis of glioblastoma stem-like cells targeted by carbon nanotubes conjugated with CD133 monoclonal antibody. *Nanomedicine* 7, 69–79. doi: 10.1016/j.nano.2010.06.010

Wang, J., Sun, H., Zeng, Q., Guo, X. J., Wang, H., Liu, H. H., et al. (2019). HPV-positive status associated with inflamed immune microenvironment and improved response to anti-PD-1 therapy in head and neck squamous cell carcinoma. *Sci. Rep.* 9:13404.

Wang, Z., Li, Y., Banerjee, S., and Sarkar, F. H. (2008). Exploitation of the Notch signaling pathway as a novel target for cancer therapy. *Anticancer Res.* 28, 3621–3630.

Weiss, A., and Attisano, L. (2013). The TGFbeta superfamily signaling pathway. *Wiley Interdiscip. Rev. Dev. Biol.* 2, 47–63. doi: 10.1002/wdev.86

Weiswald, L. B., Bellet, D., and Dangles-Marie, V. (2015). Spherical cancer models in tumor biology. *Neoplasia* 17, 1–15. doi: 10.1016/j.neo.2014.12.004

Willenbrink, T. J., Ruiz, E. S., Cornejo, C. M., Schmults, C. D., Arron, S. T., and Jambusaria-Pahlajani, A. (2020). Field cancerization: definition, epidemiology,

risk factors, and outcomes. *J. Am. Acad. Dermatol.* 83, 709–717. doi: 10.1016/j.jaad.2020.03.126

Wu, L., Han, L., Zhou, C., Wei, W., Chen, X., Yi, H., et al. (2017). TGF-β1-induced CK17 enhances cancer stem cell-like properties rather than EMT in promoting cervical cancer metastasis via the ERK1/2-MZF1 signaling pathway. *FEBS J.* 284, 3000–3017. doi: 10.1111/febs.14162

Xu, M., and Luo, J. (2017). Alcohol and cancer stem cells. *Cancers* 9:158. doi: 10.3390/cancers9110158

Xu, X., Farach-Carson, M. C., and Jia, X. (2014). Three-dimensional in vitro tumor models for cancer research and drug evaluation. *Biotechnol. Adv.* 32, 1256–1268. doi: 10.1016/j.biotechadv.2014.07.009

Yang, L., Ren, Y., Yu, X., Qian, F., Bian, B. S., Xiao, H. L., et al. (2014). ALDH1A1 defines invasive cancer stem-like cells and predicts poor prognosis in patients with esophageal squamous cell carcinoma. *Mod. Pathol.* 27, 775–783. doi: 10.1038/modpathol.2013.189

Yauch, R. L., Gould, S. E., Scales, S. J., Tang, T., Tian, H., Ahn, C. P., et al. (2008). A paracrine requirement for hedgehog signalling in cancer. *Nature* 455, 406–410. doi: 10.1038/nature07275

Young, M., Rodenhizer, D., Dean, T., D'arcangelo, E., Xu, B., Ailles, L., et al. (2018). A TRACER 3D Co-Culture tumour model for head and neck cancer. *Biomaterials* 164, 54–69. doi: 10.1016/j.biomaterials.2018.01.038

Yu, M. A., Kiang, A., Wang-Rodriguez, J., Rahimy, E., Haas, M., Yu, V., et al. (2012). Nicotine promotes acquisition of stem cell and epithelial-to-mesenchymal properties in head and neck squamous cell carcinoma. *PLoS One* 7:e51967. doi: 10.1371/journal.pone.0051967

Yu, S. S., and Cirillo, N. (2020). The molecular markers of cancer stem cells in head and neck tumors. *J. Cell Physiol.* 235, 65–73. doi: 10.1002/jcp.28963

Zhang, R., Lahens, N. F., Ballance, H. I., Hughes, M. E., and Hogenesch, J. B. (2014). A circadian gene expression atlas in mammals: implications for biology and medicine. *Proc. Natl. Acad. Sci. U.S.A.* 111, 16219–16224. doi: 10.1073/pnas.1408886111

Zhang, Y. S., Duchamp, M., Oklu, R., Ellisen, L. W., Langer, R., and Khademhosseini, A. (2016). Bioprinting the cancer microenvironment. *ACS Biomater. Sci. Eng.* 2, 1710–1721. doi: 10.1021/acsbiomaterials.6b00246

Zhang, Z., Filho, M. S., and Nör, J. E. (2012). The biology of head and neck cancer stem cells. *Oral Oncol.* 48, 1–9.

Zhao, B., Tumaneng, K., and Guan, K. L. (2011). The Hippo pathway in organ size control, tissue regeneration and stem cell self-renewal. *Nat. Cell Biol.* 13, 877–883. doi: 10.1038/ncb2303

Zhao, Y., and Yang, X. (2015). The Hippo pathway in chemotherapeutic drug resistance. *Int. J. Cancer* 137, 2767–2773. doi: 10.1002/ijc.29293

Zhao, Z. L., Zhang, L., Huang, C. F., Ma, S. R., Bu, L. L., Liu, J. F., et al. (2016). NOTCH1 inhibition enhances the efficacy of conventional chemotherapeutic agents by targeting head neck cancer stem cell. *Sci. Rep.* 6:24704.

Zhou, C., and Sun, B. (2014). The prognostic role of the cancer stem cell marker aldehyde dehydrogenase 1 in head and neck squamous cell carcinomas: a meta-analysis. *Oral Oncol.* 50, 1144–1148. doi: 10.1016/j.oraloncology.2014.08.018

Zhou, J., Wulfkuhle, J., Zhang, H., Gu, P., Yang, Y., Deng, J., et al. (2007). Activation of the PTEN/mTOR/STAT3 pathway in breast cancer stem-like cells is required for viability and maintenance. *Proc. Natl. Acad. Sci. U.S.A.* 104, 16158–16163. doi: 10.1073/pnas.0702596104

Conflict of Interest: The authors declare that the research was conducted in the absence of any commercial or financial relationships that could be construed as a potential conflict of interest.

frontiers in Cell and Developmental Biology

REVIEW
published: 22 July 2021
doi: 10.3389/fcell.2021.691410

Emerging Regulatory Mechanisms Involved in Liver Cancer Stem Cell Properties in Hepatocellular Carcinoma

Duoduo Lv[1†], Liyu Chen[1†], Lingyao Du[1], Lingyun Zhou[1] and Hong Tang[1,2*]*

[1] Center of Infectious Diseases, West China Hospital of Sichuan University, Chengdu, China, [2] State Key Laboratory of Biotherapy and Center of Infectious Diseases, Division of Infectious Diseases, West China Hospital of Sichuan University, Chengdu, China

OPEN ACCESS

Edited by:
Vicky Yamamoto, University of Southern California, United States

Reviewed by:
Louis Charles Penning, Utrecht University, Netherlands
Bela Ozsvari, University of Salford, United Kingdom

***Correspondence:**
Lingyun Zhou
4423925@qq.com
Hong Tang
htang6198@hotmail.com

[†] These authors have contributed equally to this work and share first authorship

Specialty section:
This article was submitted to Stem Cell Research, a section of the journal Frontiers in Cell and Developmental Biology

Received: *06 April 2021*
Accepted: *01 July 2021*
Published: *22 July 2021*

Citation:
Lv D, Chen L, Du L, Zhou L and Tang H (2021) Emerging Regulatory Mechanisms Involved in Liver Cancer Stem Cell Properties in Hepatocellular Carcinoma. Front. Cell Dev. Biol. 9:691410. doi: 10.3389/fcell.2021.691410

Hepatocellular carcinoma (HCC) is the predominant form of primary liver cancer and one of the leading causes of cancer-related deaths worldwide. A growing body of evidence supports the hypothesis that HCC is driven by a population of cells called liver cancer stem cells (LCSCs). LCSCs have been proposed to contribute to malignant HCC progression, including promoting tumor occurrence and growth, mediating tumor metastasis, and treatment resistance, but the regulatory mechanism of LCSCs in HCC remains unclear. Understanding the signaling pathways responsible for LCSC maintenance and survival may provide opportunities to improve patient outcomes. Here, we review the current literature about the origin of LCSCs and the niche composition, describe the current evidence of signaling pathways that mediate LCSC stemness, then highlight several mechanisms that modulate LCSC properties in HCC progression, and finally, summarize the new developments in therapeutic strategies targeting LCSCs markers and regulatory pathways.

Keywords: liver cancer stem cells, niche, signaling pathways, stemness, hepatocellular carcinoma

INTRODUCTION

Hepatocellular carcinoma (HCC) is now the second most common cause of cancer mortality due to its resistance to chemotherapy, high rates of recurrence and metastasis, and poor prognosis (Bray et al., 2013; Torre et al., 2015; Sia et al., 2017). Although curative resection and liver transplantation are potential cures and there are new emerging medicines, the overall therapeutic effects of these strategies have limited efficacy in patients (El-Khoueiry et al., 2017; Zhu et al., 2018). One of the major reasons is that HCC has proved to be a heterogeneous disease (Anfuso et al., 2015). The situation was recently complicated by the discovery of cancer stem cells (CSCs) with highly dynamic characteristics that underlie cancer development and evolution (Iyer et al., 2019). Indeed, it is assumed that these contributors affect heterogeneity within tumors, leading to treatment resistance and tumor progression by affecting the stemness of cancer cells (Kreso and Dick, 2014).

CSCs have "stemness" characteristics similar to normal stem cells, including self-renewal capacity and differentiation and proliferation potential (Molofsky et al., 2004). CSCs and normal stem cells also share several important stemness signaling pathways such as Wnt/β-Catenin, Notch, nuclear factor (NF)-κB, Hedgehog (HH), and Janus kinase/signal transducer and activator of

transcription proteins (JAK/STAT) (Chen et al., 2013). These signaling pathways have crucial roles in maintaining the characteristics of stem cells or regulating their differentiation during many developmental processes. However, the stemness properties of CSCs are lost during differentiation and are controlled by multiple signaling pathways that are highly dysregulated in CSCs (Lathia and Liu, 2017). Evidence indicates that aberrant interactions between different signaling pathways may represent key events involved in CSC pathogenesis (Yang et al., 2018). Intracellular signaling pathway dysregulation plays a significant role in enabling CSCs to retain stem cell properties.

The discovery of liver cancer stem cells (LCSCs) greatly enhanced our understanding of HCC development and progression. Despite these new developments, the mechanisms associated with CSC features are not clear, and the link between how CSCs maintain stemness and contribute to HCC malignancy is not known. Several studies have demonstrated how LCSCs can be differentiated from liver cancer cells by targeting the cluster of differentiation markers CD13 (Haraguchi et al., 2010), CD44 (Zhu et al., 2010), CD90 (Yang Z. F. et al., 2008), CD133 (You et al., 2010); epithelial cell adhesion molecule (EpCAM) (Jin et al., 2011); and keratin 19 (Van Haele et al., 2019). Here we review the latest findings of the LCSC niche and their stemness, further clarify the signaling pathways that maintain LCSC stemness, and discuss the relationship between these mechanisms and HCC progression.

THE CONCEPT AND ORIGIN OF LCSCs

Stem cells are defined a specific cell type with the characteristics of self-renewal, multi-directional differentiation potential, and high proliferative potential under certain circumstances (Molofsky et al., 2004). Stemness refers to the extent to which cells have these functional features. As stem cells differentiate, they gradually lose their "stemness." Studying tumor origins has always been a topic of great interest, because the results may provide clues to improve anti-cancer treatments. In the past few decades, investigations have shown that only a few cancer cell subsets with tumor-initiating ability are the core source of tumorigenesis; these subsets were termed CSCs (Pierce, 1967; Eun et al., 2017). The concept of cancer as an abnormal stem cell disease was proposed based on the similar self-renewal abilities of cancer cells and normal stem cells (Wicha et al., 2006; Kreso and Dick, 2014).

Numerous studies have reported that CSCs exist in the context of multiple human cancers including HCC (Ma et al., 2007). Although the existence of LCSCs in HCC has been widely accepted, their origin remains controversial. One possibility is that liver cancer cells are the result of abnormal differentiation of undifferentiated stem cells or oval cells (OVCs) in the liver. There is evidence that these OVCs can abnormally differentiate into cancer cells under the actions of carcinogens. Many researchers believe that intrahepatic OVCs are the initiating cell of HCC (Baumann et al., 1999; Knight et al., 2000). Another possible source of LCSCs is adult hepatocytes/cholangiocytes transformed by mutations and dedifferentiation. He et al. (2013) successfully induced mature hepatocytes to dedifferentiate into HCC progenitor cells in a mouse liver cancer model by stimulating damaged liver cells with interleukin (IL-6). Nikolaou et al. (2015) used a PR-SET7-deleted experimental mouse model of liver cancer to show that promoting hepatocyte microtubule expansion can facilitate the transformation of normal liver cells into liver cancer cells. These results strongly suggest that it is entirely possible for differentiated cells to regain their stem cell status.

To better understand LCSCs, distinct markers have been reported such as CD133, CD90, CD44, CD24, CD13, OV6, Delta-like 1 homolog, and EpCAM, as well as measuring Hoechst dye efflux or aldehyde dehydrogenase activities; some of these may functionally support the LCSC phenotype including highly aggressive properties and chemoresistance (Yamashita and Wang, 2013; Xiao et al., 2017). For example, studies have indicated that EpCAM is involved in the Wnt/β-catenin signaling pathway, in which activated proto-oncogenic proteins cyclin A/E and c-Myc lead to tumorigenesis (Maetzel et al., 2009). Yang et al. (Maetzel et al., 2009; Sukowati et al., 2013) found high CD90 expression during tumor formation and reported that CD90 + cells have strong proliferation and drug resistance. Additionally, CD133 + EpCAM + Huh7 cells have powerful self-renewal, multi-directional differentiation, and clonal colony-forming capabilities (Sukowati et al., 2013). OV6 + HCC cells are more carcinogenic and resistant to chemotherapy than OV6- cells. Therefore, most LCSC makers can facilitate CSC functions in the liver and continuously maintain CSC stemness. LCSCs are highly heterogeneous and may exhibit different phenotypes in terms of carcinogenic/metastatic characteristics and chemosensitivity when purified utilizing distinct CSC markers (Yamashita et al., 2013). LCSCs were shown to be responsible for HCC metastasis and tumor recurrence, and they have innate resistance to multiple chemotherapeutic agents (Wicha et al., 2006; Adorno-Cruz et al., 2015).

THE LCSC NICHE

The tumor niche consists of numerous extracellular matrix (ECM) components; cytokines; and many cell types including fibroblasts, endothelial cells, immune cells and cancer cells that can regulate the CSC fate during tumor development. Great progress has been made in the identification of potential LCSCs niches over the past few years. Various components in the microenvironment can maintain LCSC stemness through altering signaling pathways or disrupting the master transcriptional regulation factors that maintain embryonic stem cell self-renewal, such as Nanog, Oct4, and Sox2 (Shan et al., 2012; Yamashita and Wang, 2013). The ECM plays a key role in cancer progression by providing structural and biochemical support for CSCs and binds with many kinds of growth factors that interact with CSCs. For instance, one study used hyaluronic acid-based multilayer film mimic niche to select and enrich LCSCs, which showed excellent colony forming ability, and the number of CD133/CD44 double-positive LCSCs was significantly increased (Lee et al., 2015).

Many groups have demonstrated that CSCs release a variety of factors into the niche that stimulate the stemness of CSCs themselves and also induce cancer angiogenesis and the recruitment of immune cells (e.g., macrophages, dendritic cells, and T cells) and other tumor stromal cells that secrete additional factors to promote tumor progression and chemotherapy resistance (Cheng et al., 2016). Tumor-associated macrophages (TAMs) have been reported to accumulate in hypoxic areas and support angiogenesis by releasing angiogenic factors isolated from the ECM, or they can promote revascularization by releasing metalloproteinase (Carmans et al., 2010). TAMs can also enhance CSC plasticity by inducing NF-κB or the transforming growth factor (TGF)-β-dependent epithelial-mesenchymal transition (EMT) process to produce tumor necrosis factor (TNF)-α or TGF-β. In HCC, TAMs have been shown to interact with CSCs (Muramatsu et al., 2013). A subsequent study found that TAMs can secrete TGF-β to enhance CSC-like characteristics and increase their invasive capability in Hepa1-6 cells (Fan et al., 2014).

SIGNALING PATHWAYS REGULATING LCSCs STEMNESS

Many signaling pathways have been demonstrated to control normal stem cell self-renewal and participated embryonic development and differentiation, including Wnt/β-catenin, Notch, and HH; however, persistent abnormal activation of these highly conserved pathways may underlie the characteristics of LCSCs. **Table 1** presents the signaling pathways related to LCSC features, which are also described in the following questions.

Wnt/β-Catenin Signaling

The activation of signaling pathways is responsible for embryogenesis, liver specification, and liver regeneration in a strictly controlled manner. Dysregulation of certain signaling pathways has been implicated in maintaining LCSC stemness. With regard to the Wnt/β-catenin pathway, Chen et al. (2016) found that the rapid generation of tumor spheres and high invasiveness of side population (SP) cells isolated from HCC samples depended on this signal transduction. They also showed that increased β-catenin expression results in a marked activation of Wnt/β-catenin target genes including AXIN2, DKK1, and CCND (Chen et al., 2016). Mokkapati et al. (2014) reported that β-catenin activation in LCSCs caused HCC development with spontaneous lung metastases. Wnt/β-catenin signaling is activated following nuclear translocation of the β-catenin components Shp2 (Xiang et al., 2017), c-Myc (He et al., 1998), and EpCAM (Yamashita et al., 2007). This also leads to the enrichment of CD133 + (Ma et al., 2007), EpCAM + (Yamashita et al., 2009) and OV6 + (Yang W. et al., 2008) LCSCs that contribute to tumor growth and chemoresistance.

STAT3 Signaling

STAT3 is a transcription factor that is constitutively activated in many malignancies and plays a key role in cancer growth and metastasis (Yuan et al., 2015). The STAT3 signaling pathway of CSCs is involved in the development of HCC. The functional LCSC marker CD24 was found to drive liver CSC genesis through STAT3-mediated Nanog regulation (Lee et al., 2011). The IL-6/STAT3 signaling pathway was proposed to be related to liver inflammation and liver regeneration (Schneller and Angel, 2019), and the mechanism is to maintain the liver CSC population through interaction with the TGF-β signaling pathway (Tang et al., 2008). A recent study demonstrated that the IL6/STAT3 signaling cascade mainly causes CD133 + enrichment in liver cancer (Won et al., 2015). Emerging evidence has implicated the aberrant expression of long non-coding RNAs (lncRNAs) in various malignancies including HCC. One lncRNA downregulated in LCSCs (lnc-DILC) mediates crosstalk between TNF-α/NF-κB signaling and the autocrine IL-6/STAT3 cascade and connects hepatic inflammation with LCSC expansion (Wang X. et al., 2016). Thus, the STAT3 signaling pathway could be a mechanism regulating LCSC stemness, as well as a possible therapeutic target.

TGF-β Signaling

TGF-β is a central regulator in chronic liver diseases including HCC (Dooley and ten Dijke, 2012). In HCC cells, TGF-β induces EMT by increasing the expression of mesenchymal genes and CD44, which enhances their stemness potential and migratory and invasive capacities (Malfettone et al., 2017). TGF-β signals can activate differentiation programs and inhibit cell cycle progression during early carcinogenesis through intermediary Smad proteins (Fausto et al., 1990). TGFβ signaling has also been related to the malignant transformation of LCSCs. Cyclin D1-mediated activation of TGF-β/Smad signaling is an important regulatory mechanism in LCSC self-renewal and stemness. The downregulation of Socs1 attenuates the effects of TGFβ signaling, leading to oncogenic STAT3 activation and malignant cell transformation (Bagnyukova et al., 2008). Recent reports pointed out that micro (mi)RNA-mediated regulation of LCSCs is related to TGF-β signaling (Chen et al., 2021). TGF-β/Smad2 signaling can attenuate CSC-like features because miR-148a inhibits this signaling pathway in several HCC cell lines including HepG2, Huh7, and MHCC97H (Jiang et al., 2014).

Notch Signaling

The Notch signaling pathway plays an important role in stem cell self-renewal and differentiation (Reya et al., 2001). Aberrant Notch expression may influence CSC regulation and induce tumorigenesis (Patil et al., 2006). One study demonstrated that the Notch pathway stimulated the CSC characteristics of CD90 + cells (Luo et al., 2016). The underlying mechanisms are facilitation of the G1-S transition of the cell cycle and inhibition of cell apoptosis, which promote CSC properties such as self-renewal, invasion, migration, and stem cell-related gene expression (Luo et al., 2016). Another study reported that restoring expression of the tumor suppressor gene runt-related transcription factor 3 can reduce LCSCs in HCC by inhibiting Jagged1-Notch signaling (Nishina et al., 2011). Collectively, the evidence supports exploring targeting the Notch signaling pathway in tumors.

TABLE 1 | Signaling pathways activated in LCSCs.

Wnt/β-catenin	Increased invasiveness	Chen et al., 2016
	Resulted in HCC with spontaneous lung metastases	Mokkapati et al., 2014
	Lead to tumor growth and chemoresistance	Ma et al., 2007; Yang W. et al., 2008; Yamashita et al., 2009
STAT3	CD24 was found to drive LCSC genesis	Lee et al., 2011
	Maintain the LCSC population	Tang et al., 2008
	Causes CD133 + enrichment in HCC	Won et al., 2015
	Connects hepatic inflammation with LCSC expansion	Wang X. et al., 2016
TGF-β	Induces EMT to increase stemness potential and migratory and invasive capacities	Malfettone et al., 2017
	Regulate LCSC self-renewal	Bagnyukova et al., 2008
	Attenuate CSC-like features	Jiang et al., 2014
Hedgehog	Increase stemness of self-renewal and tumorigenicity	Wang R. et al., 2016
	Contributes to hepatocarcinogenesis CD133 + Hepa 1–6 cells	Jeng et al., 2013
Notch	Inhibited apoptosis to facilitate the stemness characteristics of CD90 + cells	Luo et al., 2016
BMI1	Self-renewal	Luo et al., 2016
	Proliferation of LCSCs	Chiba et al., 2010; Zhang et al., 2013

Hedgehog Signaling

The HH pathway has a central role in embryonic development and adult tissue homeostasis, but mutations and/or aberrant activation of the pathway involved in malignancies (McMahon et al., 2003; Bai et al., 2008). Recent evidence has indicated that HH signaling significantly facilitates liver development and regeneration, and activation of the pathway may contribute to HCC growth (Eichenmuller et al., 2009). One group proposed that HH signaling facilitates hepatocarcinogenesis, primarily in CD133 + Hepa 1–6 cells that have significantly higher colony proliferation and clonogenicity (Jeng et al., 2013). Others suggested that HH signal transduction is related to tumor chemoresistance and aggressiveness. Chen et al. (2011) found that compared with well-differentiated CD133(+)/ALDH (high) or CD133(+)/EpCAM (+) cells, enhanced HH signaling activity in poorly differentiated HCC cells may be responsible for their chemical resistance and invasiveness.

BMI1 Signaling

B cell-specific Moloney murine leukemia virus integration site 1 (BMI1) acts as an epigenetic chromatin modifier (Park et al., 2003) and plays a central role in the self-renewal of somatic stem cells including CSCs. Aberrant BMI1 expression is associated with malignant transformation and acquisition of the malignant phenotype in HCC (Sasaki et al., 2008). SP cell analysis and sorting have been successfully applied to HCC cell lines to identify a minor cell population with CSC properties and isolate stem cells (Shimano et al., 2003). BMI1 contributes to the maintenance of tumor-initiating SP cells in HCC (Chiba et al., 2008). BMI1 repression inhibits HCC growth both *in vitro* and *in vivo* and reduces LCSC proliferation (Chiba et al., 2010; Zhang et al., 2013), suggesting that it could be a novel therapeutic target for LCSC eradication.

The Hippo pathway, along with its downstream transcriptional co-activator Yes-associated protein and transcriptional co-activator with PDZ-binding motif, has a decisive role in the pathogenesis of primary liver cancer (Van Haele et al., 2019; Nguyen-Lefebvre et al., 2021). Other signaling pathways involved in liver CSC include the Ras/Raf/mitogen-activated protein kinase (MAPK), phosphoinositide 3-kinase (PI3K)/protein kinase B (Akt)/mammalian target of rapamycin (mTOR), and NF-κB signaling pathways. Deregulation of these cascades has been shown to enrich CSCs. Notably, each individual cell line usually exhibits unique activation of oncogenic pathways, and HCC is known to be associated with aberrant stemness regulation mechanisms in LCSCs. Therefore, the mechanism of regulating the dryness of LCSCs still needs to be further studied.

MECHANISMS MODULATING LCSC FUNCTION IN HCC

The difference between CSCs and normal stem cells lies in their ability to change their pluripotency and lineage-dependent differentiation. CSCs that are resistant to radiotherapy and chemotherapy can regenerate tumors after treatment ends. The current CSC theory that heterogeneous populations of HCC cells are dictated and maintained at least partially by LCSCs may help explain the process of HCC formation (Andersen et al., 2010; Lu et al., 2010). LCSCs have important roles in the initiation, maintenance, recurrence, metastasis, and resistance of HCC. Here we describe the complex mechanisms that maintain the malignant functions of LCSCs, including the ECM, EMT, exosomes, autophagy, reactive oxygen species (ROS), hypoxia, and epigenetic alterations (**Figure 1**).

Extracellular Matrix-Mediated Regulation of LCSCs Properties

Accumulating evidence indicates that stem cells lose the possibility for continued self-renewal when removed from their niche, which implies an essential microenvironmental role in directing stem cell fate (Lathia and Liu, 2017). The highly dynamic ECM is a major structural component of the tumor microenvironment, and increasing evidence suggests that ECM proteins establish a physical and biochemical niche for CSCs

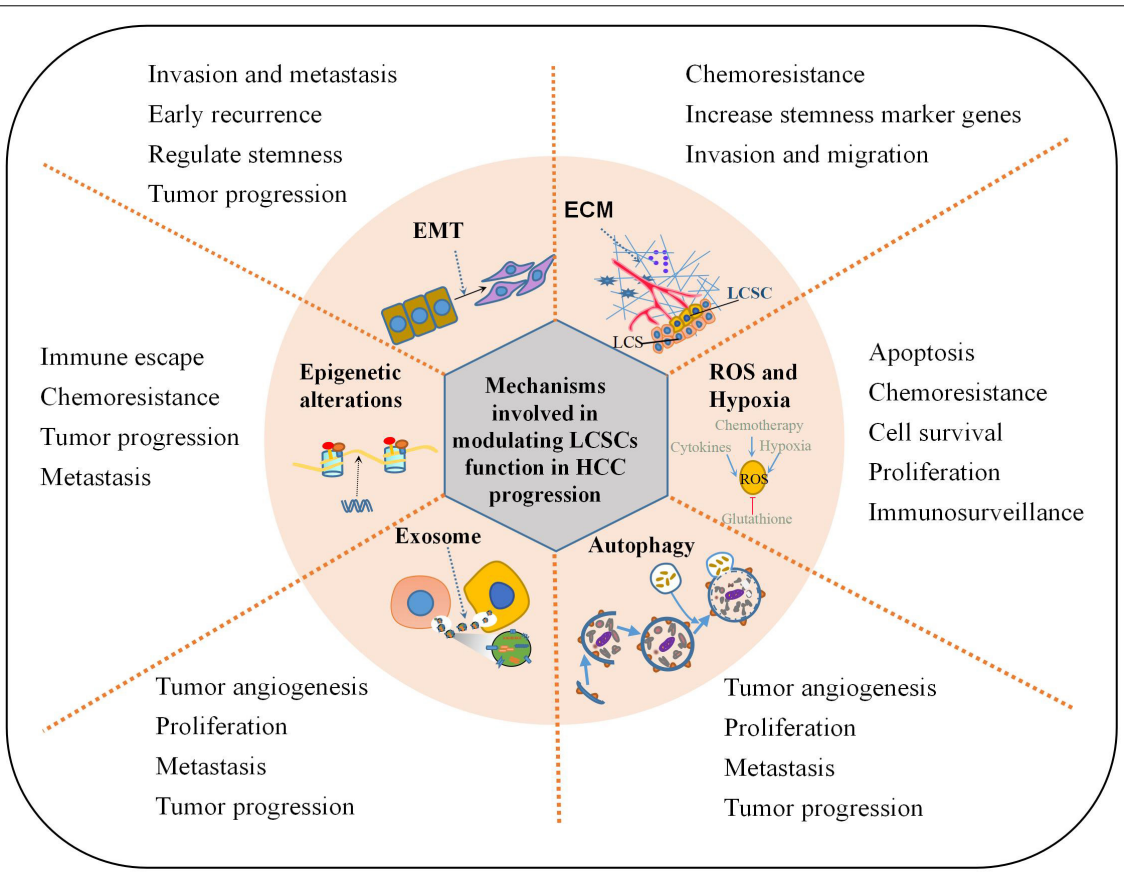

FIGURE 1 | Mechanisms involved in modulating LCSCs function in HCC progression. This illustration encompasses the key mechanisms involved in regulating LCSCs properties in HCC progression: ECM alteration, EMT program induction, oxidative stress resistance, epigenetic control, autophagy modulation, secretion of extracellular vesicles or exosomes.

(Nallanthighal et al., 2019). In HCC, hepatic stellate cells (HSCs) are the main source of ECM proteins in tumor stroma and greatly influence biological behaviors. For instance, HSCs may decrease hepatoma cell sensitization to chemotherapeutic agents by promoting EMT and CSC-like features *via* hepatocyte growth factor/Met signaling (Yu et al., 2013). In addition, NEDD9 is one of four members of a family of protein scaffolds that is crucial for HCC metastasis; it has been confirmed that NEDD9 downregulates Smad7 to activate Smad signaling and bind the FAK-Src-Crk complex to promote EMT and LCSC stemness (Wang et al., 2017). Furthermore, the pericellular matrix formed by hyaluronic acid and its interaction with tumor cell receptors can exacerbate malignancy and treatment resistance and aggravate the CSC phenotype by enhancing stem-cell marker genes and facilitating invasion and migration (Avnet and Cortini, 2016).

LCSC Acquisition of Malignant Function by EMT

The EMT plays crucial roles in developmental processes and tumor invasion and metastasis (Thiery et al., 2009). E-cadherin loss and upregulation of mesenchymal markers are hallmarks of the EMT process that have been associated with invasiveness, metastatic potential, and poor clinical outcomes in several cancers including HCC (Thiery and Sleeman, 2006; van Zijl et al., 2009). Initial work showed that EMT program activation in epithelial cells induces the acquisition of stem cell characteristics that may be conducive to CSC emergence in the context of cancer (Fabregat et al., 2016). For example, an *in vitro* study demonstrated that EMT activation could induce CSC characteristics, which is mediated by hypoxia-inducible factor 1 alpha (HIF-1α)-upregulated Notch intracellular domain expression (Jing et al., 2019). Notably, tumor cells that express EMT-related proteins also express stemness-related proteins in HCC (Kim et al., 2011). According to a study by Yamanaka et al. (2018), enrichment of the functional LCSC marker CD13 was correlated with early recurrence and shorter survival in patients with HCC. In the process of EMT, the switch from CD44v to CD44s expression is very important for the regulation of CSC stemness in cancer progression (Skandalis et al., 2019). Specifically, CSC expression of epithelial splicing regulatory protein 1, a key transcription factor required to control the transition from CD44v to CD44s in EMT, can be inhibited by Zinc finger E-box binding homeobox 1 (ZEB1) (Preca et al., 2015); CD44s in turn induces ZEB1 expression to form a

self-sustaining loop that further facilitates the EMT process, enabling cancer cells to acquire stemness without external stimuli (Park et al., 2016). In addition, EMT caused by the synergistic effect of CD44 and TGF-β1 is more likely show enhanced migration and lead to aggressive HCC progression (Park et al., 2016). CD44 has emerged as an LCSC marker that strongly induces EMT together with TGF-β1. Park et al. (2016) recently reported synergistic interactions between CD44 and TGF-β1 in EMT induction and CSC properties through the AKT/GSK-3β/β-catenin pathway in HCC cells. Moreover, Hu et al. (2017) found that overexpression of mammalian-enabled protein in HCC cells facilitated stem cell markers, EMT markers, and tumorigenicity through the extracellular signal-regulated kinase (ERK) and β-catenin signaling pathways. In addition, it was confirmed that Aurora Kinase A (AURKA), an oncogene involved in tumor development, can induce the EMT process and CSC properties through the PI3K/Akt pathway; silencing AURKA inhibits radiation-enhanced cell invasiveness of HCC (Chen et al., 2017). Therefore, EMT programs may be involved in the acquisition of malignant LCSC function during cancer progression.

Effect of Oxidative Stress and Hypoxia on the Role of LCSCs in HCC Progression

One of the striking characteristics of CSCs is their ability to form a specialized niche to adapt to changing microenvironmental conditions and exploit the characteristics of self-renewal and differentiation to drive tumor growth and progression (Baumann et al., 2008). Due to their heterogeneity, CSCs exhibit distinct metabolic phenotypes in different tumor types in terms of stemness features (Baumann et al., 2008). In particular, ROS levels are intimately tied to cellular metabolic phenotype (Yeo et al., 2013). Continuous ROS accumulation can induce apoptosis of both normal cells and cancer cells (Wiseman and Halliwell, 1996; Yamamori et al., 2012). Interestingly, CSCs can limit ROS production to maintain stem cell characteristics, inducing dormancy and enhancing drug resistance (Carnero et al., 2016; Clark and Palle, 2016). Several studies suggest that CSCs preferentially depend on glycolytic pathways, which have low or absent rates of oxidative phosphorylation and high lactate production (Wong et al., 2017; Chang et al., 2018). CSCs can also increase ATP production rates and reduce ROS production due to the Warburg effect in response to stressful environmental conditions characterized by low oxygen (hypoxia) (Wong et al., 2017; Chang et al., 2018). Interestingly, Chang et al. (2018) found that ROS-independent endoplasmic reticulum stress mediates nuclear factor erythroid 2-related factor 2 (NRF2) activation to promotes the Warburg effect and maintain CSC stemness-associated properties. Another study suggested that the hyaluronan-CD44 axis can upregulate p62 to deactivate KEAP1, which promotes NRF2 activation and the subsequent transcription of antioxidant response genes to inhibit ROS accumulation and induce drug resistance in cancer cells. In addition, CD44v9 has been reported to be associated with NRF2 activation and poor overall survival of HCC patients (Kakehashi et al., 2016).

Under hypoxic conditions, cells suppress energy-intensive mRNA translation by modulating the mTOR and pancreatic eIF2alpha kinase (PERK) pathways. Skandalis et al. (2019) found that hypoxic ROS regulate mTOR and PERK to control mRNA translation and cell survival. A recent study demonstrated that hypoxic CSCs impede CD8 + T cell proliferation and activation and inhibit immunosurveillance (Wei et al., 2011). Hypoxia also protects CSCs from chemo- and radiotherapy, and oxidative stress plays a central role in maintaining CSC stemness under hypoxia. Remarkably, hypoxia can promote CSC survival and EMT through ROS-activated stress response pathways (Liu et al., 2008) and ROS-induced TGF-β and TNF-α signaling pathways (Pavlides et al., 2010).

Epigenetic Alterations Provide LCSCs With a Survival Advantage

Epigenetic mechanisms including DNA methylation, post-translational histone modifications, chromatin conformation changes, and miRNA expression are the keys to normal stem cell differentiation. Similar processes have been shown to enable cancer cells to restore stem cell-specific characteristics (Baumann et al., 2008). Dysregulation of epigenetic mechanisms such as DNA methylation leads to abnormal epigenetic alterations that can contribute to CSC progression (Lathia and Liu, 2017). Specifically, DDX3 reduction can inhibit tumor-suppressive miRNA expression, promote up-regulation of DNA methyltransferase 3A (DNMT3A), enrich DNMT3A binding on promoters of tumor-suppressive miRNAs, and cause hypermethylation (Lathia and Liu, 2017). In addition, arsenic trioxide can enhance sensitivity to chemotherapy *via* the NF-κB pathway, which modulates de-methylation of miR-148a and inhibits LCSC properties (Wang et al., 2020). Assessing DNA methylation patterns also could provide a new approach to determining the origin of recurrent HCC (Zhang et al., 2015). Histone acetylation is another epigenetic mechanism that plays an important role in CSC regulation. NF-κB-mediated inhibition of histone deacetylases (HDACs), which are chromatin-remodeling enzymes, can facilitate an effective IKK inhibitor that targets a selected subgroup of CSCs in human HCC cell lines (Marquardt et al., 2015). HDAC inhibitors are useful for eradicating Spalt-like transcription factor 4 (SALL4)-positive HCC cells through their inhibitory effects on histone deacetylation *via* the nucleosome remodeling and deacetylation complex (Marquardt and Thorgeirsson, 2013). Encouragingly, a recent study demonstrated that SALL4 plays a role in controlling HDAC activity and contributing to the maintenance of HCC with stem cell features (Zeng et al., 2014). Moreover, BORIS, a testes-specific CTCF paralog (CCCTC-binding factor-like), up-regulates Oct4 *via* histone methylation to facilitate CSC-like characteristics in HCC cells (Zeng et al., 2014). miRNAs are another epigenetic mechanism responsible for regulating CSCs. For example, DDX3, a member of the DEAD-box RNA helicase family (Schroder, 2010), represses stemness in HCC by epigenetically modulating tumor-suppressive miRNAs

(including miR-200b, miR-200c, miR-122, and miR-145) (Li H. K. et al., 2016). Jiang et al. discovered that miR-500a-3p promotes LCSC characteristics including enhanced spheroid formation, increased SP fraction (purified from HCC cells harbors CSC-like properties), and upregulated expression of CSC factors (Zhang et al., 2017). Whole transcriptomic analyses of SP cells can generate common SP-gene expression profiles for predicting the clinical outcome (survival and recurrence) of in-patients with HCC (Marquardt et al., 2010). Epigenetic modification of miR-429 can manipulate LCSCs by targeting the RBBP4/E2F1/Oct4 axis, suggesting that targeting miR-429 might inactivate LCSCs, thus providing a novel strategy for HCC prevention and treatment (Li et al., 2015).

HCC Tumorigenesis and Progression Regulated by LCSC-Derived Extracellular Vesicles

Extracellular vectors (EVs) derived from CSCs (including exosomes, microvesicles, and apoptotic bodies) are important mediators that modulate communication between CSCs and their niches. EVs are rich in enzymes, miRNAs, transcription factors, heat shock proteins, major histocompatibility complexes, cytoskeleton components, signal transducers, and ECM effectors (Milane et al., 2015) that mediate the exchange of intracellular components and affect tumor aggressiveness. Emerging evidence indicates that CSCs and TAMs promote HCC tumorigenesis and progression. A functional study revealed that treating HCC cells with TAM exosomes or transfecting them with miR-125a/b suppressed cell proliferation and stem cell properties by targeting CD90, a marker of HCC stem cells (Wang et al., 2019a). Tumor angiogenesis has also been associated with exosomal export of specific RNA species in CSCs. For example, CD90 + liver CSC-released exosomes stimulated angiogenesis *via* the lncRNA H19, which mediated increased expression of vascular endothelial growth factor (VEGF) receptor 1 in endothelial cells (Conigliaro et al., 2015). Mechanically, Cheng et al. (2019a) showed that p120ctn in exosomes secreted from liver cancer cells suppresses HCC cell proliferation and metastasis and LCSC expansion *via* the STAT3 pathway. Another publication described the impact of CSC-derived exosomes on HCC progression *in vivo*. Specifically, CSC-exosomes can reduce apoptosis (marked by downregulation of Bax and p53, upregulation of Bcl2, and increased proliferating cell nuclear antigen immunostaining), increase angiogenic activity (shown by up-regulation of VEGF), enhance metastasis and invasiveness (indicated by upregulation of PI3K and ERK proteins and their downstream target matrix metalloproteinase 9 and downregulation of tissue inhibitor of metalloproteinase-1), and induce EMT (marked by increased serum and hepatic levels of TGFβ1 mRNA and protein) (Alzahrani et al., 2018).

Autophagy in LCSCs Maintenance

Following the establishment of the CSC theory and the discovery of LCSCs in HCC, autophagy was proposed as a vital mechanism driving cell fate (Nazio et al., 2019). Remarkably, in addition to maintaining cellular homeostasis, autophagy also affects cellular processes such as EMT and migration, both of which drive tumor progression and metastasis (Kiyono et al., 2009; Qiang et al., 2014; Sharifi et al., 2016). Indeed, the accelerated carcinogenesis observed in autophagy-deficient murine models strongly supports the hypothesis that autophagy prevents malignant transformation (Cianfanelli et al., 2015; Mainz and Rosenfeldt, 2018). Hypoxia-induced autophagy has been shown to be essential for survival of hepatic CD133 + CSCs, which is mediated by HIF-1α (Nazio et al., 2019). Notably, Li et al. found that CD133 + LCSCs could resist interferon-γ-induced autophagy, which might also be a mechanism through which CSCs resist immune eradication (Li J. et al., 2016). Lai et al. discovered that homeobox-containing protein 1 expression in hepatocytes could protect against HCC progression, and the underlying mechanisms may include promoting autophagy, inhibiting CSC phenotype, and increasing the sensitivity of tumor cells to natural killer cell cytolysis (Zhao et al., 2018). Autophagy can also regulate CSC resistance to chemotherapy drugs. For example, transactivation response element RNA-binding protein 2 is destabilized through autophagic-lysosomal proteolysis, thereby stabilizing the protein expression of the CSC marker Nanog to facilitate multikinase inhibitor sorafenib resistance in HCC cells (Lai et al., 2019).

Hepatitis Virus and LCSCs

Chronic infection with hepatitis B virus (HBV) has long been linked to HCC development. Studies have found that the C-terminally truncated HBx (HBx-ΔC) plays an important hepatocarcinogenesis by conferring enhanced invasiveness and reducing the apoptotic response in HCC cells (Ma et al., 2008; Yip et al., 2011; Zhu et al., 2015). Ng et al. (2016) recently found that HBx-ΔC—in particular at the 140 aa and 119 aa breakpoints—enhances stemness properties *in vitro* and induces a CD133 + LCSC subpopulation in HCC by modulating an altered genomic profile involving the FXR pathway and possibly drug metabolism. It was also previously reported that hepatitis C virus (HCV) infection of primary human hepatocytes (PHH) can induce an EMT state and extend cell lifespan (Bose et al., 2012). Compelling evidence has suggested that HCV infection of PHH induced a significant increase in the number of spheres on ultralow binding plates, and it enhanced EMT and CSC markers and tumor growth in immunodeficient mice (Kwon et al., 2015). These data support the hypothesis that hepatitis virus infection plays a crucial role in conferring stemness properties that contribute to HCC initiation and growth.

Non-coding RNA and LCSCs

A variety of non-coding RNAs play an important role in LCSC self-renewal and promote tumor propagation. For example, a recent study showed that lncHDAC2 drives the self-renewal of LCSCs *via* activation of HH signaling (Wu et al., 2019). Another lncRNA termed HAND2-AS1 promotes LCSC self-renewal and drives liver oncogenesis (Wang et al., 2019b). The novel lncRNA THOR (testis-associated highly conserved oncogenic lncRNA) was also

TABLE 2 | Summary of various agents in research development to target LCSCs pathways.

Target	Agent	Population	Results	References
Wnt/β-catenin	Salinomycin	Human HCC cell lines	Reduces the tumorigenicity of LCSCs	Liu et al., 2020
Wnt	IC-2	Human HCC cell lines	Suppresses liver CSC properties	Seto et al., 2017
Hedgehog	GDC-0449	Mouse hepatoma ML-1 cells	Mitigate the mice HCC growth	Jeng et al., 2015
Hedgehog	LDE225	Human HCC cell lines	Suppress EMT and migration of metastatic cells	Ding et al., 2017
Notch	RO4929097	Miouse liver progenitor cell	Reduces Tumor Growth, Tumor Malignancy and Liver Fibrosis *in vivo*	Jung et al., 2016
Notch	DAPT	Human HCC cell lines	Significantly reduced CD133/epcam positivity	Kahraman et al., 2019
TGF-β	LY2157299 (Galunisertib)	Human HCC cell lines	Suppresses the staminal phenotype in hepatocellular carcinoma by modulating CD44 expression	Rani et al., 2018
BMI1	RU-A1	Human HCC cell lines	Impair Self-Renewal and Tumorigenic Capability in HCC	Bartucci et al., 2017
NF-κB	Curcumin	Primary HCC cell line	Restrains stemness features in liver cancer	Marquardt et al., 2015
CD13	BC-02	Human HCC cell lines	Targeting CD13 and up-regulating intracellular ROS and DNA damage induced by ROS	Dou et al., 2017

upregulated in liver CSCs and could promote HCC cell dedifferentiation and liver CSC expansion by targeting β-catenin signaling (Cheng et al., 2019b). Ling Qi and colleagues demonstrated that lncCAMTA1 physically associates with the calmodulin-binding transcription activator 1 (CAMTA1) promoter, induces a repressive chromatin structure, and inhibits CAMTA1 transcription, thereby promoting HCC cell proliferation, CSC-like properties, and tumorigenesis. Furthermore, deregulation of miRNA expression in cancer cells (including HCC cells) is well documented, and the involvement of miRNAs in orchestrating tumor genesis and cancer progression has been recognized. miR-26b-5p imparts metastatic properties, helps maintain Ep + CSCs *via* HSC71/HSPA8, and augments malignant features in HCC (Khosla et al., 2019). Overexpression of miR-589-5p suppressed CD90 + CSC characteristics such as Oct4, Sox2, and Nanog expression; a high likelihood of forming cell spheres; high invasiveness; and high tumorigenicity (Zhang et al., 2016). MiR-491 attenuates CSC-like properties of HCC by inhibition of GIT-1/NF-κB-mediated EMT (Yang et al., 2016). MiR-452 directly acts on Sox7 that physically binds to β-catenin and TCF4 in the nucleus, then inhibits Wnt/β-catenin signaling and promotes the stem-like characteristics of HCC (Zheng et al., 2016). Given the significant contribution of non-coding RNA to LCSC properties, targeting specific non-coding RNA clusters might be an effective HCC treatment.

THERAPEUTIC STRATEGIES TO TARGET LCSCs PATHWAYS

Currently, targeting LCSCs and/or eradicating LCSCs brings hope of curing HCC. We have known that a variety of signaling pathways including STAT3, TGF-β, Hedgehog (Hh), Notch, Wnt and BMI1 are involved in the renewal of normal stem cells and the maintenance of tissue homeostasis. Dysregulation of these pathways is believed to be involved in driving CSC activity in a variety of cancers (including HCC) through different mechanisms (Gu et al., 2020; Huang et al., 2020; Babaei et al., 2021). More specific inhibitors of signaling pathways are currently under development and investigation, which may be potential therapeutic agent for eradicating liver CSCs and overcoming chemotherapy resistance of HCC. For example, A study demonstrated that Salinomycin significantly reduces the tumorigenicity of LCSCs *in vivo* by suppressing the Wnt/β-catenin signaling pathway 31971116. A novel small-molecule Wnt inhibitor, IC-2, has the potential to suppress LCSCs that may *via* inhibition of the CBP–β-catenin complex formation (Huang et al., 2020). Reportedly, aminopeptidase N (APN, also known as CD13) is a marker of semi-quiescent CSC. Hedgehog pathway molecules was altered, including upregulated S Hedgehog expression and downregulated smoothened expression in tumor fractions after GDC-0449 treatment, which effectively reduced tumor size and cell infiltration of the HCC in mice (Jeng et al., 2015). The CD13 inhibitor BC-02, a compound obtained by combining the CD13 inhibitor Battatin and Fluorouracil (5-FU), damages the properties of liver CSCs by targeting CD13 and up-regulating intracellular ROS and DNA damage induced by ROS (Dou et al., 2017). The treatment strategies for signaling pathways or mechanisms are summarized in **Table 2**.

CONCLUSION

There is a growing body of evidence indicating that CSCs are the root cause of cancers and are responsible for metastasis, resistance to conventional treatments, and tumor recurrence; however, the molecular mechanisms underlying the potential roles of LCSCs in HCC origin and progression have not been fully elucidated. LCSC status and survival are controlled by

multiple signaling pathways, and there are several mechanisms to maintain their malignant function. This overview presented findings suggesting that LCSCs drive HCC occurrence and development. In theory, if the LCSC subpopulation can be eliminated or have reduced stemness, it would be a way to control or even cure HCC. Although a great deal of effort is being made to reduce cancer stemness by targeting stemness signaling pathways, there are still many challenges given the complex biologic properties of CSCs. Perhaps the current focus should be on clarifying maintenance mechanisms involved in the malignant function of LCSCs. Since LCSCs must be eradicated to prevent HCC progression, recurrence, or metastasis, targeting the vital CSC signaling pathways is an attractive cancer treatment strategy. A comprehensive understanding of LCSC stemness and the mechanisms involved in cancer progression may help identify potential therapeutic targets and develop more effective therapies.

AUTHOR CONTRIBUTIONS

HT and LZ contributed to the conception of this study. DL and LC drafted the manuscript. HT, LZ, and LD revised the manuscript. All authors read and approved the final manuscript.

FUNDING

This work was supported by the National Natural Science Foundation of China (Nos. 81802468 and 81772193), the 1.3.5 project for disciplines of excellence, West China Hospital, Sichuan University (Nos. ZYGD20009 and ZYJC18008), the Sichuan Province Key Technologies R&D Program (19ZDYF), the Sichuan Science and Technology Program 2019YFS0207, and the China Postdoctoral Science Foundation 2020M670062ZX to LZ.

REFERENCES

Adorno-Cruz, V., Kibria, G., Liu, X., Doherty, M., Junk, D. J., Guan, D., et al. (2015). Cancer stem cells: targeting the roots of cancer, seeds of metastasis, and sources of therapy resistance. *Cancer Res.* 75, 924–929. doi: 10.1158/0008-5472.can-14-3225

Alzahrani, F. A., El-Magd, M. A., Abdelfattah-Hassan, A., Saleh, A. A., Saadeldin, I. M., El-Shetry, E. S., et al. (2018). Potential effect of exosomes derived from cancer stem cells and MSCs on progression of DEN-Induced HCC in rats. *Stem Cells Int.* 2018:8058979.

Andersen, J. B., Loi, R., Perra, A., Factor, V. M., Ledda-Columbano, G. M., Columbano, A., et al. (2010). Progenitor-derived hepatocellular carcinoma model in the rat. *Hepatology* 51, 1401–1409. doi: 10.1002/hep.23488

Anfuso, B., El-Khobar, K. E., Sukowati, C. H., and Tiribelli, C. (2015). The multiple origin of cancer stem cells in hepatocellular carcinoma. *Clin. Res. Hepatol. Gastroenterol.* 39(Suppl. 1), S92–S97.

Avnet, S., and Cortini, M. (2016). Role of pericellular matrix in the regulation of cancer stemness. *Stem Cell Rev. Rep.* 12, 464–475. doi: 10.1007/s12015-016-9660-x

Babaei, G., Aziz, S. G., and Jaghi, N. Z. Z. (2021). EMT, cancer stem cells and autophagy; The three main axes of metastasis. *Biomed. Pharmacother.* 133:110909. doi: 10.1016/j.biopha.2020.110909

Bagnyukova, T. V., Tryndyak, V. P., Muskhelishvili, L., Ross, S. A., Beland, F. A., and Pogribny, I. P. (2008). Epigenetic downregulation of the suppressor of cytokine signaling 1 (Socs1) gene is associated with the STAT3 activation and development of hepatocellular carcinoma induced by methyl-deficiency in rats. *Cell Cycle* 7, 3202–3210. doi: 10.4161/cc.7.20.6816

Bai, L. Y., Chiu, C. F., Lin, C. W., Hsu, N. Y., Lin, C. L., Lo, W. J., et al. (2008). Differential expression of Sonic hedgehog and Gli1 in hematological malignancies. *Leukemia* 22, 226–228. doi: 10.1038/sj.leu.2404978

Bartucci, M., Hussein, M. S., Huselid, E., Flaherty, K., Patrizii, M., Laddha, S. V., et al. (2017). Synthesis and characterization of novel BMI1 inhibitors targeting cellular self-renewal in hepatocellular carcinoma. *Target. Oncol.* 12, 449–462. doi: 10.1007/s11523-017-0501-x

Baumann, M., Krause, M., and Hill, R. (2008). Exploring the role of cancer stem cells in radioresistance. *Nat. Rev. Cancer* 8, 545–554. doi: 10.1038/nrc2419

Baumann, U., Crosby, H. A., Ramani, P., Kelly, D. A., and Strain, A. J. (1999). Expression of the stem cell factor receptor c-kit in normal and diseased pediatric liver: identification of a human hepatic progenitor cell? *Hepatology* 30, 112–117. doi: 10.1002/hep.510300140

Bose, S. K., Meyer, K., Di Bisceglie, A. M., Ray, R. B., and Ray, R. (2012). Hepatitis C virus induces epithelial-mesenchymal transition in primary human hepatocytes. *J. Virol.* 86, 13621–13628. doi: 10.1128/jvi.02016-12

Bray, F., Ren, J. S., Masuyer, E., and Ferlay, J. (2013). Global estimates of cancer prevalence for 27 sites in the adult population in 2008. *Int. J. Cancer* 132, 1133–1145. doi: 10.1002/ijc.27711

Carmans, S., Hendriks, J. J., Thewissen, K., Van Den Eynden, J., Stinissen, P., Rigo, J. M., et al. (2010). The inhibitory neurotransmitter glycine modulates macrophage activity by activation of neutral amino acid transporters. *J. Neurosci. Res.* 88, 2420–2430.

Carnero, A., Garcia-Mayea, Y., Mir, C., Lorente, J., Rubio, I. T., and Me, L. L. (2016). The cancer stem-cell signaling network and resistance to therapy. *Cancer Treat. Rev.* 49, 25–36. doi: 10.1016/j.ctrv.2016.07.001

Chang, C. W., Chen, Y. S., Tsay, Y. G., Han, C. L., Chen, Y. J., Yang, C. C., et al. (2018). ROS-independent ER stress-mediated NRF2 activation promotes warburg effect to maintain stemness-associated properties of cancer-initiating cells. *Cell Death Dis.* 9:194.

Chen, C., Song, G., Xiang, J., Zhang, H., Zhao, S., and Zhan, Y. (2017). AURKA promotes cancer metastasis by regulating epithelial-mesenchymal transition and cancer stem cell properties in hepatocellular carcinoma. *Biochem. Biophys. Res. Commun.* 486, 514–520. doi: 10.1016/j.bbrc.2017.03.075

Chen, H., Nio, K., Yamashita, T., Okada, H., Li, R., Suda, T., et al. (2021). BMP9-ID1 signaling promotes EpCAM-positive cancer stem cell properties in hepatocellular carcinoma. *Mol. Oncol.* doi: 10.1002/1878-0261.12963

Chen, K., Huang, Y. H., and Chen, J. L. (2013). Understanding and targeting cancer stem cells: therapeutic implications and challenges. *Acta Pharmacol. Sin.* 34, 732–740. doi: 10.1038/aps.2013.27

Chen, W., Zhang, Y. W., Li, Y., Zhang, J. W., Zhang, T., Fu, B. S., et al. (2016). Constitutive expression of Wnt/betacatenin target genes promotes proliferation and invasion of liver cancer stem cells. *Mol. Med. Rep.* 13, 3466–3474. doi: 10.3892/mmr.2016.4986

Chen, X., Lingala, S., Khoobyari, S., Nolta, J., Zern, M. A., and Wu, J. (2011). Epithelial mesenchymal transition and hedgehog signaling activation are associated with chemoresistance and invasion of hepatoma subpopulations. *J. Hepatol.* 55, 838–845. doi: 10.1016/j.jhep.2010.12.043

Cheng, Z., Lei, Z., Yang, P., Si, A., Xiang, D., Tang, X., et al. (2019a). Exosome-transmitted p120-catenin suppresses hepatocellular carcinoma progression via STAT3 pathways. *Mol. Carcinog.* 58, 1389–1399. doi: 10.1002/mc.23022

Cheng, Z., Lei, Z., Yang, P., Si, A., Xiang, D., Zhou, J., et al. (2019b). Long non-coding RNA THOR promotes liver cancer stem cells expansion via beta-catenin pathway. *Gene* 684, 95–103. doi: 10.1016/j.gene.2018.10.051

Cheng, Z., Li, X., and Ding, J. (2016). Characteristics of liver cancer stem cells and clinical correlations. *Cancer Lett.* 379, 230–238. doi: 10.1016/j.canlet.2015.07.041

Chiba, T., Miyagi, S., Saraya, A., Aoki, R., Seki, A., Morita, Y., et al. (2008). The polycomb gene product BMI1 contributes to the maintenance of tumor-initiating side population cells in hepatocellular carcinoma. *Cancer Res.* 68, 7742–7749. doi: 10.1158/0008-5472.can-07-5882

Chiba, T., Seki, A., Aoki, R., Ichikawa, H., Negishi, M., Miyagi, S., et al. (2010). Bmi1 promotes hepatic stem cell expansion and tumorigenicity in both Ink4a/Arf-dependent and -independent manners in mice. *Hepatology* 52, 1111–1123. doi: 10.1002/hep.23793

Cianfanelli, V., Fuoco, C., Lorente, M., Salazar, M., Quondamatteo, F., Gherardini, P. F., et al. (2015). AMBRA1 links autophagy to cell proliferation and tumorigenesis by promoting c-Myc dephosphorylation and degradation. *Nat. Cell Biol.* 17, 20–30. doi: 10.1038/ncb3072

Clark, D. W., and Palle, K. (2016). Aldehyde dehydrogenases in cancer stem cells: potential as therapeutic targets. *Ann. Transl. Med.* 4:518. doi: 10.21037/atm.2016.11.82

Conigliaro, A., Costa, V., Lo Dico, A., Saieva, L., Buccheri, S., Dieli, F., et al. (2015). CD90+ liver cancer cells modulate endothelial cell phenotype through the release of exosomes containing H19 lncRNA. *Mol. Cancer* 14:155.

Ding, J., Zhou, X. T., Zou, H. Y., and Wu, J. (2017). Hedgehog signaling pathway affects the sensitivity of hepatoma cells to drug therapy through the ABCC1 transporter. *Lab. Invest.* 97, 819–832. doi: 10.1038/labinvest.2017.34

Dooley, S., and ten Dijke, P. (2012). TGF-beta in progression of liver disease. *Cell Tissue Res.* 347, 245–256.

Dou, C., Fang, C., Zhao, Y., Fu, X., Zhang, Y., Zhu, D., et al. (2017). BC-02 eradicates liver cancer stem cells by upregulating the ROS-dependent DNA damage. *Int. J. Oncol.* 51, 1775–1784. doi: 10.3892/ijo.2017.4159

Eichenmuller, M., Gruner, I., Hagl, B., Haberle, B., Muller-Hocker, J., Von Schweinitz, D., et al. (2009). Blocking the hedgehog pathway inhibits hepatoblastoma growth. *Hepatology* 49, 482–490. doi: 10.1002/hep.22649

El-Khoueiry, A. B., Sangro, B., Yau, T., Crocenzi, T. S., Kudo, M., Hsu, C., et al. (2017). Nivolumab in patients with advanced hepatocellular carcinoma (CheckMate 040): an open-label, non-comparative, phase 1/2 dose escalation and expansion trial. *Lancet* 389, 2492–2502. doi: 10.1016/s0140-6736(17)31046-2

Eun, K., Ham, S. W., and Kim, H. (2017). Cancer stem cell heterogeneity: origin and new perspectives on CSC targeting. *BMB Rep.* 50, 117–125. doi: 10.5483/bmbrep.2017.50.3.222

Fabregat, I., Malfettone, A., and Soukupova, J. (2016). New insights into the crossroads between EMT and stemness in the context of cancer. *J. Clin. Med.* 5:37. doi: 10.3390/jcm5030037

Fan, Q. M., Jing, Y. Y., Yu, G. F., Kou, X. R., Ye, F., Gao, L., et al. (2014). Tumor-associated macrophages promote cancer stem cell-like properties via transforming growth factor-beta1-induced epithelial-mesenchymal transition in hepatocellular carcinoma. *Cancer Lett.* 352, 160–168. doi: 10.1016/j.canlet.2014.05.008

Fausto, N., Mead, J. E., Gruppuso, P. A., and Braun, L. (1990). TGF-beta in liver development, regeneration, and carcinogenesis. *Ann. N. Y. Acad. Sci.* 593, 231–242. doi: 10.1111/j.1749-6632.1990.tb16115.x

Gu, Y., Zheng, X., and Ji, J. (2020). Liver cancer stem cells as a hierarchical society: yes or no? *Acta Biochim. Biophys. Sin. (Shanghai)* 52, 723–735. doi: 10.1093/abbs/gmaa050

Haraguchi, N., Ishii, H., Mimori, K., Tanaka, F., Ohkuma, M., Kim, H. M., et al. (2010). CD13 is a therapeutic target in human liver cancer stem cells. *J. Clin. Invest.* 120, 3326–3339. doi: 10.1172/jci42550

He, G., Dhar, D., Nakagawa, H., Font-Burgada, J., Ogata, H., Jiang, Y., et al. (2013). Identification of liver cancer progenitors whose malignant progression depends on autocrine IL-6 signaling. *Cell* 155, 384–396. doi: 10.1016/j.cell.2013.09.031

He, T. C., Sparks, A. B., Rago, C., Hermeking, H., Zawel, L., Da Costa, L. T., et al. (1998). Identification of c-MYC as a target of the APC pathway. *Science* 281, 1509–1512. doi: 10.1126/science.281.5382.1509

Hu, K., Huang, P., Luo, H., Yao, Z., Wang, Q., Xiong, Z., et al. (2017). Mammalian-enabled (MENA) protein enhances oncogenic potential and cancer stem cell-like phenotype in hepatocellular carcinoma cells. *FEBS Open Bio* 7, 1144–1153. doi: 10.1002/2211-5463.12254

Huang, T., Song, X., Xu, D., Tiek, D., Goenka, A., Wu, B., et al. (2020). Stem cell programs in cancer initiation, progression, and therapy resistance. *Theranostics* 10, 8721–8743. doi: 10.7150/thno.41648

Iyer, D. N., Sin, W. Y., and Ng, L. (2019). Linking stemness with colorectal cancer initiation, progression, and therapy. *World J. Stem Cells* 11, 519–534. doi: 10.4252/wjsc.v11.i8.519

Jeng, K. S., Jeng, C. J., Jeng, W. J., Sheen, I. S., Chang, C. F., Hsiau, H. I., et al. (2015). Sonic hedgehog pathway inhibitor mitigates mouse hepatocellular carcinoma. *Am. J. Surg.* 210, 554–560. doi: 10.1016/j.amjsurg.2015.03.001

Jeng, K. S., Sheen, I. S., Jeng, W. J., Yu, M. C., Hsiau, H. I., Chang, F. Y., et al. (2013). Activation of the sonic hedgehog signaling pathway occurs in the CD133 positive cells of mouse liver cancer Hepa 1-6 cells. *Onco Targets Ther.* 6, 1047–1055. doi: 10.2147/ott.s44828

Jiang, F., Mu, J., Wang, X., Ye, X., Si, L., Ning, S., et al. (2014). The repressive effect of miR-148a on TGF beta-SMADs signal pathway is involved in the glabridin-induced inhibition of the cancer stem cells-like properties in hepatocellular carcinoma cells. *PLoS One* 9:e96698. doi: 10.1371/journal.pone.0096698

Jin, J., Joo, K. M., Lee, S. J., Jo, M. Y., Kim, Y., Jin, Y., et al. (2011). Synergistic therapeutic effects of cytokine-induced killer cells and temozolomide against glioblastoma. *Oncol. Rep.* 25, 33–39.

Jing, L., Ruan, Z., Sun, H., Li, Q., Han, L., Huang, L., et al. (2019). Epithelial-mesenchymal transition induced cancer-stem-cell-like characteristics in hepatocellular carcinoma. *J. Cell. Physiol.* 234, 18448–18458. doi: 10.1002/jcp.28480

Jung, K. H., Zhang, J., Zhou, C., Shen, H., Gagea, M., Rodriguez-Aguayo, C., et al. (2016). Differentiation therapy for hepatocellular carcinoma: multifaceted effects of miR-148a on tumor growth and phenotype and liver fibrosis. *Hepatology* 63, 864–879. doi: 10.1002/hep.28367

Kahraman, D. C., Kahraman, T., and Cetin-Atalay, R. (2019). Targeting PI3K/Akt/mTOR pathway identifies differential expression and functional role of IL8 in liver cancer stem cell enrichment. *Mol. Cancer Ther.* 18, 2146–2157.

Kakehashi, A., Ishii, N., Sugihara, E., Gi, M., Saya, H., and Wanibuchi, H. (2016). CD44 variant 9 is a potential biomarker of tumor initiating cells predicting survival outcome in hepatitis C virus-positive patients with resected hepatocellular carcinoma. *Cancer Sci.* 107, 609–618. doi: 10.1111/cas.12908

Khosla, R., Hemati, H., Rastogi, A., Ramakrishna, G., Sarin, S. K., and Trehanpati, N. (2019). miR-26b-5p helps in EpCAM+cancer stem cells maintenance via HSC71/HSPA8 and augments malignant features in HCC. *Liver Int.* 39, 1692–1703. doi: 10.1111/liv.14188

Kim, H., Choi, G. H., Na, D. C., Ahn, E. Y., Kim, G. I., Lee, J. E., et al. (2011). Human hepatocellular carcinomas with "Stemness"-related marker expression: keratin 19 expression and a poor prognosis. *Hepatology* 54, 1707–1717. doi: 10.1002/hep.24559

Kiyono, K., Suzuki, H. I., Matsuyama, H., Morishita, Y., Komuro, A., Kano, M. R., et al. (2009). Autophagy is activated by TGF-beta and potentiates TGF-beta-mediated growth inhibition in human hepatocellular carcinoma cells. *Cancer Res.* 69, 8844–8852. doi: 10.1158/0008-5472.can-08-4401

Knight, B., Yeoh, G. C., Husk, K. L., Ly, T., Abraham, L. J., Yu, C., et al. (2000). Impaired preneoplastic changes and liver tumor formation in tumor necrosis factor receptor type 1 knockout mice. *J. Exp. Med.* 192, 1809–1818. doi: 10.1084/jem.192.12.1809

Kreso, A., and Dick, J. E. (2014). Evolution of the cancer stem cell model. *Cell Stem Cell* 14, 275–291. doi: 10.1016/j.stem.2014.02.006

Kwon, Y. C., Bose, S. K., Steele, R., Meyer, K., Di Bisceglie, A. M., Ray, R. B., et al. (2015). Promotion of cancer stem-like cell properties in hepatitis C virus-infected hepatocytes. *J. Virol.* 89, 11549–11556. doi: 10.1128/jvi.01946-15

Lai, H. H., Li, C. W., Hong, C. C., Sun, H. Y., Chiu, C. F., Ou, D. L., et al. (2019). TARBP2-mediated destabilization of Nanog overcomes sorafenib resistance in hepatocellular carcinoma. *Mol. Oncol.* 13, 928–945. doi: 10.1002/1878-0261.12449

Lathia, J. D., and Liu, H. (2017). Overview of cancer stem cells and stemness for community oncologists. *Target Oncol.* 12, 387–399. doi: 10.1007/s11523-017-0508-3

Lee, I. C., Chuang, C. C., and Wu, Y. C. (2015). Niche mimicking for selection and enrichment of liver cancer stem cells by hyaluronic acid-based multilayer films. *ACS Appl. Mater. Interfaces* 7, 22188–22195. doi: 10.1021/acsami.5b04436

Lee, T. K., Castilho, A., Cheung, V. C., Tang, K. H., Ma, S., and Ng, I. O. (2011). CD24(+) liver tumor-initiating cells drive self-renewal and tumor initiation through STAT3-mediated NANOG regulation. *Cell Stem Cell* 9, 50–63. doi: 10.1016/j.stem.2011.06.005

Li, H. K., Mai, R. T., Huang, H. D., Chou, C. H., Chang, Y. A., Chang, Y. W., et al. (2016). DDX3 represses stemness by epigenetically modulating tumor-suppressive miRNAs in hepatocellular carcinoma. *Sci. Rep.* 6:28637.

Li, J., Chen, J. N., Zeng, T. T., He, F., Chen, S. P., Ma, S., et al. (2016). CD133+ liver cancer stem cells resist interferon-gamma-induced autophagy. *BMC Cancer* 16:15. doi: 10.1186/s12885-016-2050-6

Li, L., Tang, J., Zhang, B., Yang, W., Liugao, M., Wang, R., et al. (2015). Epigenetic modification of MiR-429 promotes liver tumour-initiating cell properties by targeting Rb binding protein 4. *Gut* 64, 156–167. doi: 10.1136/gutjnl-2013-305715

Liu, L., Wise, D. R., Diehl, J. A., and Simon, M. C. (2008). Hypoxic reactive oxygen species regulate the integrated stress response and cell survival. *J. Biol. Chem.* 283, 31153–31162. doi: 10.1074/jbc.m805056200

Liu, Q., Sun, J., Luo, Q., Ju, Y., and Song, G. (2020). Salinomycin suppresses tumorigenicity of liver cancer stem cells and Wnt/beta-catenin signaling. *Curr. Stem Cell Res. Ther.* 16, 630–637.

Lu, L., Li, Y., Kim, S. M., Bossuyt, W., Liu, P., Qiu, Q., et al. (2010). Hippo signaling is a potent in vivo growth and tumor suppressor pathway in the mammalian liver. *Proc. Natl. Acad. Sci. U.S.A.* 107, 1437–1442. doi: 10.1073/pnas.0911427107

Luo, J., Wang, P., Wang, R., Wang, J., Liu, M., Xiong, S., et al. (2016). The Notch pathway promotes the cancer stem cell characteristics of CD90+ cells in hepatocellular carcinoma. *Oncotarget* 7, 9525–9537. doi: 10.18632/oncotarget.6672

Ma, N. F., Lau, S. H., Hu, L., Xie, D., Wu, J., Yang, J., et al. (2008). COOH-terminal truncated HBV X protein plays key role in hepatocarcinogenesis. *Clin. Cancer Res.* 14, 5061–5068. doi: 10.1158/1078-0432.ccr-07-5082

Ma, S., Chan, K. W., Hu, L., Lee, T. K., Wo, J. Y., Ng, I. O., et al. (2007). Identification and characterization of tumorigenic liver cancer stem/progenitor cells. *Gastroenterology* 132, 2542–2556. doi: 10.1053/j.gastro.2007.04.025

Maetzel, D., Denzel, S., Mack, B., Canis, M., Went, P., Benk, M., et al. (2009). Nuclear signalling by tumour-associated antigen EpCAM. *Nat. Cell Biol.* 11, 162–171. doi: 10.1038/ncb1824

Mainz, L., and Rosenfeldt, M. T. (2018). Autophagy and cancer - insights from mouse models. *FEBS J.* 285, 792–808. doi: 10.1111/febs.14274

Malfettone, A., Soukupova, J., Bertran, E., Crosas-Molist, E., Lastra, R., Fernando, J., et al. (2017). Transforming growth factor-beta-induced plasticity causes a migratory stemness phenotype in hepatocellular carcinoma. *Cancer Lett.* 392, 39–50. doi: 10.1016/j.canlet.2017.01.037

Marquardt, J. U., and Thorgeirsson, S. S. (2013). Sall4 in "stemness"-driven hepatocarcinogenesis. *N. Engl. J. Med.* 368, 2316–2318. doi: 10.1056/nejme1303026

Marquardt, J. U., Factor, V. M., and Thorgeirsson, S. S. (2010). Epigenetic regulation of cancer stem cells in liver cancer: current concepts and clinical implications. *J. Hepatol.* 53, 568–577. doi: 10.1016/j.jhep.2010.05.003

Marquardt, J. U., Gomez-Quiroz, L., Arreguin Camacho, L. O., Pinna, F., Lee, Y. H., Kitade, M., et al. (2015). Curcumin effectively inhibits oncogenic NF-kappaB signaling and restrains stemness features in liver cancer. *J. Hepatol.* 63, 661–669. doi: 10.1016/j.jhep.2015.04.018

McMahon, A. P., Ingham, P. W., and Tabin, C. J. (2003). Developmental roles and clinical significance of hedgehog signaling. *Curr. Top. Dev. Biol.* 53, 1–114. doi: 10.1016/s0070-2153(03)53002-2

Milane, L., Singh, A., Mattheolabakis, G., Suresh, M., and Amiji, M. M. (2015). Exosome mediated communication within the tumor microenvironment. *J. Control. Release* 219, 278–294. doi: 10.1016/j.jconrel.2015.06.029

Mokkapati, S., Niopek, K., Huang, L., Cunniff, K. J., Ruteshouser, E. C., Decaestecker, M., et al. (2014). beta-catenin activation in a novel liver progenitor cell type is sufficient to cause hepatocellular carcinoma and hepatoblastoma. *Cancer Res.* 74, 4515–4525. doi: 10.1158/0008-5472.can-13-3275

Molofsky, A. V., Pardal, R., and Morrison, S. J. (2004). Diverse mechanisms regulate stem cell self-renewal. *Curr. Opin. Cell Biol.* 16, 700–707. doi: 10.1016/j.ceb.2004.09.004

Muramatsu, S., Tanaka, S., Mogushi, K., Adikrisna, R., Aihara, A., Ban, D., et al. (2013). Visualization of stem cell features in human hepatocellular carcinoma reveals in vivo significance of tumor-host interaction and clinical course. *Hepatology* 58, 218–228. doi: 10.1002/hep.26345

Nallanthighal, S., Heiserman, J. P., and Cheon, D. J. (2019). The role of the extracellular matrix in cancer stemness. *Front. Cell Dev. Biol.* 7:86. doi: 10.3389/fcell.2019.00086

Nazio, F., Bordi, M., Cianfanelli, V., Locatelli, F., and Cecconi, F. (2019). Autophagy and cancer stem cells: molecular mechanisms and therapeutic applications. *Cell Death Differ.* 26, 690–702. doi: 10.1038/s41418-019-0292-y

Ng, K. Y., Chai, S., Tong, M., Guan, X. Y., Lin, C. H., Ching, Y. P., et al. (2016). C-terminal truncated hepatitis B virus X protein promotes hepatocellular carcinogenesis through induction of cancer and stem cell-like properties. *Oncotarget* 7, 24005–24017. doi: 10.18632/oncotarget.8209

Nguyen-Lefebvre, A. T., Selzner, N., Wrana, J. L., and Bhat, M. (2021). The hippo pathway: a master regulator of liver metabolism, regeneration, and disease. *FASEB J.* 35:e21570.

Nikolaou, K. C., Moulos, P., Chalepakis, G., Hatzis, P., Oda, H., Reinberg, D., et al. (2015). Spontaneous development of hepatocellular carcinoma with cancer stem cell properties in PR-SET7-deficient livers. *EMBO J.* 34, 430–447. doi: 10.15252/embj.201489279

Nishina, S., Shiraha, H., Nakanishi, Y., Tanaka, S., Matsubara, M., Takaoka, N., et al. (2011). Restored expression of the tumor suppressor gene RUNX3 reduces cancer stem cells in hepatocellular carcinoma by suppressing Jagged1-Notch signaling. *Oncol. Rep.* 26, 523–531.

Park, I. K., Qian, D., Kiel, M., Becker, M. W., Pihalja, M., Weissman, I. L., et al. (2003). Bmi-1 is required for maintenance of adult self-renewing haematopoietic stem cells. *Nature* 423, 302–305. doi: 10.1038/nature01587

Park, N. R., Cha, J. H., Jang, J. W., Bae, S. H., Jang, B., Kim, J. H., et al. (2016). Synergistic effects of CD44 and TGF-beta1 through AKT/GSK-3beta/beta-catenin signaling during epithelial-mesenchymal transition in liver cancer cells. *Biochem. Biophys. Res. Commun.* 477, 568–574. doi: 10.1016/j.bbrc.2016.06.077

Patil, M. A., Zhang, J., Ho, C., Cheung, S. T., Fan, S. T., and Chen, X. (2006). Hedgehog signaling in human hepatocellular carcinoma. *Cancer Biol. Ther.* 5, 111–117. doi: 10.4161/cbt.5.1.2379

Pavlides, S., Tsirigos, A., Vera, I., Flomenberg, N., Frank, P. G., Casimiro, M. C., et al. (2010). Transcriptional evidence for the "Reverse Warburg Effect" in human breast cancer tumor stroma and metastasis: similarities with oxidative stress, inflammation, Alzheimer's disease, and "Neuron-Glia Metabolic Coupling". *Aging (Albany NY)* 2, 185–199. doi: 10.18632/aging.100134

Pierce, G. B. (1967). Teratocarcinoma: model for a developmental concept of cancer. *Curr. Top. Dev. Biol.* 2, 223–246. doi: 10.1016/s0070-2153(08)60289-6

Preca, B. T., Bajdak, K., Mock, K., Sundararajan, V., Pfannstiel, J., Maurer, J., et al. (2015). A self-enforcing CD44s/ZEB1 feedback loop maintains EMT and stemness properties in cancer cells. *Int. J. Cancer* 137, 2566–2577. doi: 10.1002/ijc.29642

Qiang, L., Zhao, B., Ming, M., Wang, N., He, T. C., Hwang, S., et al. (2014). Regulation of cell proliferation and migration by p62 through stabilization of Twist1. *Proc. Natl. Acad. Sci. U.S.A.* 111, 9241–9246. doi: 10.1073/pnas.1322913111

Rani, B., Malfettone, A., Dituri, F., Soukupova, J., Lupo, L., Mancarella, S., et al. (2018). Galunisertib suppresses the staminal phenotype in hepatocellular carcinoma by modulating CD44 expression. *Cell Death Dis.* 9:373.

Reya, T., Morrison, S. J., Clarke, M. F., and Weissman, I. L. (2001). Stem cells, cancer, and cancer stem cells. *Nature* 414, 105–111.

Sasaki, M., Ikeda, H., Itatsu, K., Yamaguchi, J., Sawada, S., Minato, H., et al. (2008). The overexpression of polycomb group proteins Bmi1 and EZH2 is associated with the progression and aggressive biological behavior of hepatocellular carcinoma. *Lab. Invest.* 88, 873–882. doi: 10.1038/labinvest.2008.52

Schneller, D., and Angel, P. (2019). "Cellular origin of hepatocellular carcinoma," in *Hepatocellular Carcinoma*, ed. J. E. E. Tirnitz-Parker (Brisbane, AU: Codon Publications).

Schroder, M. (2010). Human DEAD-box protein 3 has multiple functions in gene regulation and cell cycle control and is a prime target for viral manipulation. *Biochem. Pharmacol.* 79, 297–306. doi: 10.1016/j.bcp.2009.08.032

Seto, K., Sakabe, T., Itaba, N., Azumi, J., Oka, H., Morimoto, M., et al. (2017). A novel small-molecule WNT inhibitor, IC-2, has the potential to suppress liver cancer stem cells. *Anticancer Res.* 37, 3569–3579.

Shan, J., Shen, J., Liu, L., Xia, F., Xu, C., Duan, G., et al. (2012). Nanog regulates self-renewal of cancer stem cells through the insulin-like growth factor pathway in

human hepatocellular carcinoma. *Hepatology* 56, 1004–1014. doi: 10.1002/hep.25745

Sharifi, M. N., Mowers, E. E., Drake, L. E., Collier, C., Chen, H., Zamora, M., et al. (2016). Autophagy promotes focal adhesion disassembly and cell motility of metastatic tumor cells through the direct interaction of paxillin with LC3. *Cell Rep.* 15, 1660–1672. doi: 10.1016/j.celrep.2016.04.065

Shimano, K., Satake, M., Okaya, A., Kitanaka, J., Kitanaka, N., Takemura, M., et al. (2003). Hepatic oval cells have the side population phenotype defined by expression of ATP-binding cassette transporter ABCG2/BCRP1. *Am. J. Pathol.* 163, 3–9. doi: 10.1016/s0002-9440(10)63624-3

Sia, D., Villanueva, A., Friedman, S. L., and Llovet, J. M. (2017). Liver cancer cell of origin, molecular class, and effects on patient prognosis. *Gastroenterology* 152, 745–761. doi: 10.1053/j.gastro.2016.11.048

Skandalis, S. S., Karalis, T. T., Chatzopoulos, A., and Karamanos, N. K. (2019). Hyaluronan-CD44 axis orchestrates cancer stem cell functions. *Cell. Signal.* 63:109377. doi: 10.1016/j.cellsig.2019.109377

Sukowati, C. H., Anfuso, B., Torre, G., Francalanci, P., Croce, L. S., and Tiribelli, C. (2013). The expression of CD90/Thy-1 in hepatocellular carcinoma: an in vivo and in vitro study. *PLoS One* 8:e76830. doi: 10.1371/journal.pone.0076830

Tang, Y., Kitisin, K., Jogunoori, W., Li, C., Deng, C. X., Mueller, S. C., et al. (2008). Progenitor/stem cells give rise to liver cancer due to aberrant TGF-beta and IL-6 signaling. *Proc. Natl. Acad. Sci. U.S.A.* 105, 2445–2450. doi: 10.1073/pnas.0705395105

Thiery, J. P., Acloque, H., Huang, R. Y., and Nieto, M. A. (2009). Epithelial-mesenchymal transitions in development and disease. *Cell* 139, 871–890. doi: 10.1016/j.cell.2009.11.007

Thiery, J. P., and Sleeman, J. P. (2006). Complex networks orchestrate epithelial-mesenchymal transitions. *Nat. Rev. Mol. Cell Biol.* 7, 131–142. doi: 10.1038/nrm1835

Torre, L. A., Bray, F., Siegel, R. L., Ferlay, J., Lortet-Tieulent, J., and Jemal, A. (2015). Global cancer statistics, 2012. *CA Cancer J. Clin.* 65, 87–108. doi: 10.3322/caac.21262

Van Haele, M., Moya, I. M., Karaman, R., Rens, G., Snoeck, J., Govaere, O., et al. (2019). YAP and TAZ heterogeneity in primary liver cancer: an analysis of its prognostic and diagnostic role. *Int. J. Mol. Sci.* 20:638. doi: 10.3390/ijms20030638

van Zijl, F., Zulehner, G., Petz, M., Schneller, D., Kornauth, C., Hau, M., et al. (2009). Epithelial-mesenchymal transition in hepatocellular carcinoma. *Future Oncol.* 5, 1169–1179.

Wang, R., Sun, Q., Wang, P., Liu, M., Xiong, S., Luo, J., et al. (2016). Notch and Wnt/beta-catenin signaling pathway play important roles in activating liver cancer stem cells. *Oncotarget* 7, 5754–5768. doi: 10.18632/oncotarget.6805

Wang, X., Sun, W., Shen, W., Xia, M., Chen, C., Xiang, D., et al. (2016). Long non-coding RNA DILC regulates liver cancer stem cells via IL-6/STAT3 axis. *J. Hepatol.* 64, 1283–1294. doi: 10.1016/j.jhep.2016.01.019

Wang, Y., Jiang, F., Jiao, K., Ju, L., Liu, Q., Li, Y., et al. (2020). De-methylation of miR-148a by arsenic trioxide enhances sensitivity to chemotherapy via inhibiting the NF-kappaB pathway and CSC like properties. *Exp. Cell Res.* 386:111739. doi: 10.1016/j.yexcr.2019.111739

Wang, Y., Wang, B., Xiao, S., Li, Y., and Chen, Q. (2019a). miR-125a/b inhibits tumor-associated macrophages mediated in cancer stem cells of hepatocellular carcinoma by targeting CD90. *J. Cell. Biochem.* 120, 3046–3055. doi: 10.1002/jcb.27436

Wang, Y., Zhu, P., Luo, J., Wang, J., Liu, Z., Wu, W., et al. (2019b). LncRNA HAND2-AS1 promotes liver cancer stem cell self-renewal via BMP signaling. *EMBO J.* 38:e101110.

Wang, Z., Shen, M., Lu, P., Li, X., Zhu, S., and Yue, S. (2017). NEDD9 may regulate hepatocellular carcinoma cell metastasis by promoting epithelial-mesenchymal-transition and stemness via repressing Smad7. *Oncotarget* 8, 1714–1724. doi: 10.18632/oncotarget.13852

Wei, J., Wu, A., Kong, L. Y., Wang, Y., Fuller, G., Fokt, I., et al. (2011). Hypoxia potentiates glioma-mediated immunosuppression. *PLoS One* 6:e16195. doi: 10.1371/journal.pone.0016195

Wicha, M. S., Liu, S., and Dontu, G. (2006). Cancer stem cells: an old idea–a paradigm shift. *Cancer Res.* 66, 1883–1890; discussion 1895-1886.

Wiseman, H., and Halliwell, B. (1996). Damage to DNA by reactive oxygen and nitrogen species: role in inflammatory disease and progression to cancer. *Biochem. J.* 313(Pt 1), 17–29. doi: 10.1042/bj3130017

Won, C., Kim, B. H., Yi, E. H., Choi, K. J., Kim, E. K., Jeong, J. M., et al. (2015). Signal transducer and activator of transcription 3-mediated CD133 up-regulation contributes to promotion of hepatocellular carcinoma. *Hepatology* 62, 1160–1173. doi: 10.1002/hep.27968

Wong, T. L., Che, N., and Ma, S. (2017). Reprogramming of central carbon metabolism in cancer stem cells. *Biochim. Biophys. Acta Mol. Basis Dis.* 1863, 1728–1738. doi: 10.1016/j.bbadis.2017.05.012

Wu, J., Zhu, P., Lu, T., Du, Y., Wang, Y., He, L., et al. (2019). The long non-coding RNA LncHDAC2 drives the self-renewal of liver cancer stem cells via activation of Hedgehog signaling. *J. Hepatol.* 70, 918–929. doi: 10.1016/j.jhep.2018.12.015

Xiang, D., Cheng, Z., Liu, H., Wang, X., Han, T., Sun, W., et al. (2017). Shp2 promotes liver cancer stem cell expansion by augmenting beta-catenin signaling and predicts chemotherapeutic response of patients. *Hepatology* 65, 1566–1580. doi: 10.1002/hep.28919

Xiao, Y., Lin, M., Jiang, X., Ye, J., Guo, T., Shi, Y., et al. (2017). The recent advances on liver cancer stem cells: biomarkers, separation, and therapy. *Anal. Cell. Pathol. (Amst.)* 2017:5108653.

Yamamori, T., Yasui, H., Yamazumi, M., Wada, Y., Nakamura, Y., Nakamura, H., et al. (2012). Ionizing radiation induces mitochondrial reactive oxygen species production accompanied by upregulation of mitochondrial electron transport chain function and mitochondrial content under control of the cell cycle checkpoint. *Free Radic. Biol. Med.* 53, 260–270. doi: 10.1016/j.freeradbiomed.2012.04.033

Yamanaka, C., Wada, H., Eguchi, H., Hatano, H., Gotoh, K., Noda, T., et al. (2018). Clinical significance of CD13 and epithelial mesenchymal transition (EMT) markers in hepatocellular carcinoma. *Jpn. J. Clin. Oncol.* 48, 52–60. doi: 10.1093/jjco/hyx157

Yamashita, T., and Wang, X. W. (2013). Cancer stem cells in the development of liver cancer. *J. Clin. Invest.* 123, 1911–1918.

Yamashita, T., Budhu, A., Forgues, M., and Wang, X. W. (2007). Activation of hepatic stem cell marker EpCAM by Wnt-beta-catenin signaling in hepatocellular carcinoma. *Cancer Res.* 67, 10831–10839. doi: 10.1158/0008-5472.can-07-0908

Yamashita, T., Honda, M., Nakamoto, Y., Baba, M., Nio, K., Hara, Y., et al. (2013). Discrete nature of EpCAM+ and CD90+ cancer stem cells in human hepatocellular carcinoma. *Hepatology* 57, 1484–1497. doi: 10.1002/hep.26168

Yamashita, T., Ji, J., Budhu, A., Forgues, M., Yang, W., Wang, H. Y., et al. (2009). EpCAM-positive hepatocellular carcinoma cells are tumor-initiating cells with stem/progenitor cell features. *Gastroenterology* 136, 1012–1024. doi: 10.1053/j.gastro.2008.12.004

Yang, T., Zhang, W., Wang, L., Xiao, C., Wang, L., Gong, Y., et al. (2018). Co-culture of dendritic cells and cytokine-induced killer cells effectively suppresses liver cancer stem cell growth by inhibiting pathways in the immune system. *BMC Cancer* 18:984. doi: 10.1186/s12885-018-4871-y

Yang, W., Yan, H. X., Chen, L., Liu, Q., He, Y. Q., Yu, L. X., et al. (2008). Wnt/beta-catenin signaling contributes to activation of normal and tumorigenic liver progenitor cells. *Cancer Res.* 68, 4287–4295. doi: 10.1158/0008-5472.can-07-6691

Yang, X., Ye, J., Yan, H., Tang, Z., Shen, J., Zhang, J., et al. (2016). MiR-491 attenuates cancer stem cells-like properties of hepatocellular carcinoma by inhibition of GIT-1/NF-kappaB-mediated EMT. *Tumour Biol.* 37, 201–209. doi: 10.1007/s13277-015-3687-5

Yang, Z. F., Ho, D. W., Ng, M. N., Lau, C. K., Yu, W. C., Ngai, P., et al. (2008). Significance of CD90+ cancer stem cells in human liver cancer. *Cancer Cell* 13, 153–166. doi: 10.1016/j.ccr.2008.01.013

Yeo, H., Lyssiotis, C. A., Zhang, Y., Ying, H., Asara, J. M., Cantley, L. C., et al. (2013). FoxO3 coordinates metabolic pathways to maintain redox balance in neural stem cells. *EMBO J.* 32, 2589–2602. doi: 10.1038/emboj.2013.186

Yip, W. K., Cheng, A. S., Zhu, R., Lung, R. W., Tsang, D. P., Lau, S. S., et al. (2011). Carboxyl-terminal truncated HBx regulates a distinct microRNA transcription program in hepatocellular carcinoma development. *PLoS One* 6:e22888. doi: 10.1371/journal.pone.0022888

You, H., Ding, W., and Rountree, C. B. (2010). Epigenetic regulation of cancer stem cell marker CD133 by transforming growth factor-beta. *Hepatology* 51, 1635–1644. doi: 10.1002/hep.23544

Yu, G., Jing, Y., Kou, X., Ye, F., Gao, L., Fan, Q., et al. (2013). Hepatic stellate cells secreted hepatocyte growth factor contributes to the chemoresistance of hepatocellular carcinoma. *PLoS One* 8:e73312. doi: 10.1371/journal.pone.0073312

Yuan, J., Zhang, F., and Niu, R. (2015). Multiple regulation pathways and pivotal biological functions of STAT3 in cancer. *Sci. Rep.* 5:17663.

Zeng, S. S., Yamashita, T., Kondo, M., Nio, K., Hayashi, T., Hara, Y., et al. (2014). The transcription factor SALL4 regulates stemness of EpCAM-positive hepatocellular carcinoma. *J. Hepatol.* 60, 127–134. doi: 10.1016/j.jhep.2013.08.024

Zhang, R., Xu, L. B., Yue, X. J., Yu, X. H., Wang, J., and Liu, C. (2013). Bmi1 gene silencing inhibits the proliferation and invasiveness of human hepatocellular carcinoma cells and increases their sensitivity to 5-fluorouracil. *Oncol. Rep.* 29, 967–974. doi: 10.3892/or.2012.2189

Zhang, X., Jiang, P., Shuai, L., Chen, K., Li, Z., Zhang, Y., et al. (2016). miR-589-5p inhibits MAP3K8 and suppresses CD90(+) cancer stem cells in hepatocellular carcinoma. *J. Exp. Clin. Cancer Res.* 35:176.

Zhang, X., Liu, S., Shen, C., Wu, Y., Zhang, L., Chen, X., et al. (2015). DNA methylation consistency implicates the primary tumor cell origin of recurrent hepatocellular carcinoma. *Epigenomics* 7, 581–592. doi: 10.2217/epi.15.23

Zhang, Y., Wei, C., Guo, C. C., Bi, R. X., Xie, J., Guan, D. H., et al. (2017). Prognostic value of microRNAs in hepatocellular carcinoma: a meta-analysis. *Oncotarget* 8, 107237–107257.

Zhao, H., Jia, H., Han, Q., and Zhang, J. (2018). Homeobox containing 1 inhibits liver cancer progression by promoting autophagy as well as inhibiting stemness and immune escape. *Oncol. Rep.* 40, 1657–1665.

Zheng, Z., Liu, J., Yang, Z., Wu, L., Xie, H., Jiang, C., et al. (2016). MicroRNA-452 promotes stem-like cells of hepatocellular carcinoma by inhibiting Sox7 involving Wnt/beta-catenin signaling pathway. *Oncotarget* 7, 28000–28012. doi: 10.18632/oncotarget.8584

Zhu, A. X., Finn, R. S., Edeline, J., Cattan, S., Ogasawara, S., Palmer, D., et al. (2018). Pembrolizumab in patients with advanced hepatocellular carcinoma previously treated with sorafenib (KEYNOTE-224): a non-randomised, open-label phase 2 trial. *Lancet Oncol.* 19, 940–952.

Zhu, R., Mok, M. T., Kang, W., Lau, S. S., Yip, W. K., Chen, Y., et al. (2015). Truncated HBx-dependent silencing of GAS2 promotes hepatocarcinogenesis through deregulation of cell cycle, senescence and p53-mediated apoptosis. *J. Pathol.* 237, 38–49. doi: 10.1002/path.4554

Zhu, Z., Hao, X., Yan, M., Yao, M., Ge, C., Gu, J., et al. (2010). Cancer stem/progenitor cells are highly enriched in CD133+CD44+ population in hepatocellular carcinoma. *Int. J. Cancer* 126, 2067–2078.

Conflict of Interest: The authors declare that the research was conducted in the absence of any commercial or financial relationships that could be construed as a potential conflict of interest.

frontiers in Genetics

ORIGINAL RESEARCH
published: 16 August 2021
doi: 10.3389/fgene.2021.666561

Integrative Analysis of Gene Expression Through One-Class Logistic Regression Machine Learning Identifies Stemness Features in Multiple Myeloma

*Chunmei Ban†, Feiyan Yang†, Min Wei, Qin Liu, Jiankun Wang, Lei Chen, Liuting Lu, Dongmei Xie, Lie Liu and Jinxiong Huang**

Department of Hematology, Liuzhou People's Hospital, Liuzhou, China

OPEN ACCESS

Edited by:
Vicky Yamamoto, University of Southern California, United States

Reviewed by:
Elisa Cimetta, University of Padua, Italy
Akram Mohammed, University of Tennessee Health Science Center, United States
Travis Steele Johnson, Indiana University Bloomington, United States
Yuqi Tan, Stanford University, United States

***Correspondence:**
Jinxiong Huang
jxhuang66@hotmail.com

† These authors have contributed equally to this work

Specialty section:
This article was submitted to Stem Cell Research, a section of the journal Frontiers in Genetics

Received: *10 February 2021*
Accepted: *19 July 2021*
Published: *16 August 2021*

Citation:
Ban C, Yang F, Wei M, Liu Q, Wang J, Chen L, Lu L, Xie D, Liu L and Huang J (2021) Integrative Analysis of Gene Expression Through One-Class Logistic Regression Machine Learning Identifies Stemness Features in Multiple Myeloma. Front. Genet. 12:666561. doi: 10.3389/fgene.2021.666561

Tumor progression includes the obtainment of progenitor and stem cell-like features and the gradual loss of a differentiated phenotype. Stemness was defined as the potential for differentiation and self-renewal from the cell of origin. Previous studies have confirmed the effective application of stemness in a number of malignancies. However, the mechanisms underlying the growth and maintenance of multiple myeloma (MM) stem cells remain unclear. We calculated the stemness index for samples of MM by utilizing a novel one-class logistic regression (OCLR) machine learning algorithm and found that mRNA expression-based stemness index (mRNAsi) was an independent prognostic factor of MM. Based on the same cutoff value, mRNAsi could stratify MM patients into low and high groups with different outcomes. We identified 127 stemness-related signatures using weighted gene co-expression network analysis (WGCNA) and differential expression analysis. Functional annotation and pathway enrichment analysis indicated that these genes were mainly involved in the cell cycle, cell differentiation, and DNA replication and repair. Using the molecular complex detection (MCODE) algorithm, we identified 34 pivotal signatures. Meanwhile, we conducted unsupervised clustering and classified the MM cohorts into three MM stemness (MMS) clusters with distinct prognoses. Samples in MMS-cluster3 possessed the highest stemness fractions and the worst prognosis. Additionally, we applied the ESTIMATE algorithm to infer differential immune infiltration among the three MMS clusters. The immune core and stromal score were significantly lower in MMS-cluster3 than in the other clusters, supporting the negative relation between stemness and anticancer immunity. Finally, we proposed a prognostic nomogram that allows for individualized assessment of the 3- and 5-year overall survival (OS) probabilities among patients with MM. Our study comprehensively assessed the MM stemness index based on large cohorts and built a 34-gene based classifier for predicting prognosis and potential strategies for stemness treatment.

Keywords: stemness index, mRNAsi, multiple myeloma, OCLR, prognosis, WGCNA

INTRODUCTION

Multiple myeloma (MM), a clonal B-cell malignancy (Bataille and Harousseau, 1997), is characterized by the aberrant proliferation of bone marrow plasma cells and the overproduction of light-chain or monoclonal immunoglobulin (Röllig et al., 2015; Dhakal et al., 2016). Among the diseases with abnormal plasma cells, MM is the second most common hematologic malignancy (Röllig et al., 2015). Owing to the development of immunomodulators and proteasome inhibitors, patients with MM have significantly improved survival over the past decade. However, progressive disease remains a common cause of fatal outcomes (Martinez-Lopez et al., 2011). As a result, it is essential to understand the underlying mechanisms that contribute to disease relapse and progression in MM, as well as novel targets for therapeutic improvements or prognostic prediction.

Stemness was defined as the potential for differentiation and self-renewal from the cell of origin (Seguin et al., 2015; Prasetyanti and Medema, 2017). It has been reported that the gradual loss of differentiation capacity and acquisition of stem cell-like characteristics are important factors that promote tumor progression (Seguin et al., 2015). A growing body of research has confirmed the existence of cancer stem cells in multiple tumors, including hematological malignancies (Lapidot et al., 1994; Singh et al., 2004; O'Brien et al., 2007). Cancer stem cells play a key role in tumorigenesis, progression, metastasis, and drug resistance. Therapies targeting cancer stem cells are of great value for tumor prevention and treatment. For example, the use of retinoic acid to induce the maturation and differentiation of malignant proliferating cells has achieved great success in the clinical treatment of promyelocytic leukemia (Nowak et al., 2009). With the application of serial transplantation models and clonogenic *in vitro* assays, MM stem cells have been suggested to be part of a subset of $CD38^{-}CD19^{+}CD27^{+}$ B-cell precursors that do not express the classic MM markers *CD38* or CD138 (Matsui et al., 2008). These cells with clonogenic potential could mediate tumor regrowth and chemoresistance. The one-class logistic regression (OCLR) machine learning algorithm is an effective method of quantifying the cancer stemness index using two independent indices (Malta et al., 2018; Lian et al., 2019). One is the stemness index [mRNA expression-based stemness index (mRNAsi)] based on gene expression that reflects mRNA expression, and the other is mDNAsi, which reflects epigenetic characteristics (Sokolov et al., 2016). Previous studies have proven the effective application of stemness indices calculated by the OCLR algorithm in a variety of malignant tumors. However, there are few studies on the role and prognostic value of MM stemness (MMS); hence,it is an urgent need to develop prognostic or predictive biomarkers associated with stemness index.

In this study, we collected a total of 1,095 newly diagnosed or pre-treatment MM patients with expression data and clinical information and systematically evaluated the MM stemness index (mRNAsi) using the OCLR algorithm. By combining weighted gene co-expression network analysis (WGCNA) with MM mRNAsi, we searched for key genes related to stemness in 1,095 MM patients. The analysis of gene and module functions showed significance in MM. We classified MM patients into different subgroups based on the expression of stemness-related genes. Finally, mRNAsi was integrated with other clinicopathological characteristics to construct a nomogram to predict the prognosis of patients with MM.

MATERIALS AND METHODS

Data Collection and Pre-processing

The workflow of this study is shown in **Figure 1**. In this study, two MM cohorts were downloaded from the Gene Expression Omnibus (GEO)[1] database. The related information contained clinical, molecular, and microarray datasets. Samples in the GSE4204 cohort (N = 538) were pre-treated with bone marrow aspirates from MM patients (Driscoll et al., 2010). The GSE24080 cohort consisted of 559 newly diagnosed MM patients (Shi et al., 2010).

The gene expression values in the two cohorts were analyzed using the robust multi-array average algorithm for background correction, quantile normalization, and final summarization. After excluding samples without survival information, a total of 1,095 samples were selected for subsequent analysis (558 cases from the GSE24080 cohort and 537 cases from the GSE4204 cohort).

Calculation and Prognosis Evaluation of mRNAsi

Malta et al. (2018) provided a novel OCLR machine learning algorithm to assess oncogenic dedifferentiation that considered mRNAsi. We utilized the method to calculate the mRNAsi for each MM patient. The gene expression-based stemness index was mapped from zero to one. We assessed the prognostic value of mRNAsi and its relationship with other clinical features in different cohorts. First, we utilized univariate and multivariable Cox proportional hazard regression to calculate the hazard ratios (HRs) for overall survival (OS). Second, each cohort of MM patients was divided into low and high mRNAsi groups based on the same cutoff value of mRNAsi (0.4124166, identified by the *Survminer* package), and the Kaplan–Meier method and log-rank tests were used to determine the significance of survival differences.

Identification of Key Modules and Genes Associated With mRNAsi by WGCNA

The WGCNA was developed to discover correlations among genes by constructing significant modules (Langfelder and Horvath, 2008). The mRNAsi and expression modules were calculated using WGCNA to identify key modules and genes associated with mRNAsi. Module eigengenes (MEs) were defined as the first principal component of each gene module and were adopted as the representative of all genes in each module. Gene significance (GS), as the mediator p-value (GS = lgP) for each gene, represented the degree of linear correlation between gene expression of module and mRNAsi or other clinical features.

[1] https://www.ncbi.nlm.nih.gov/geo/

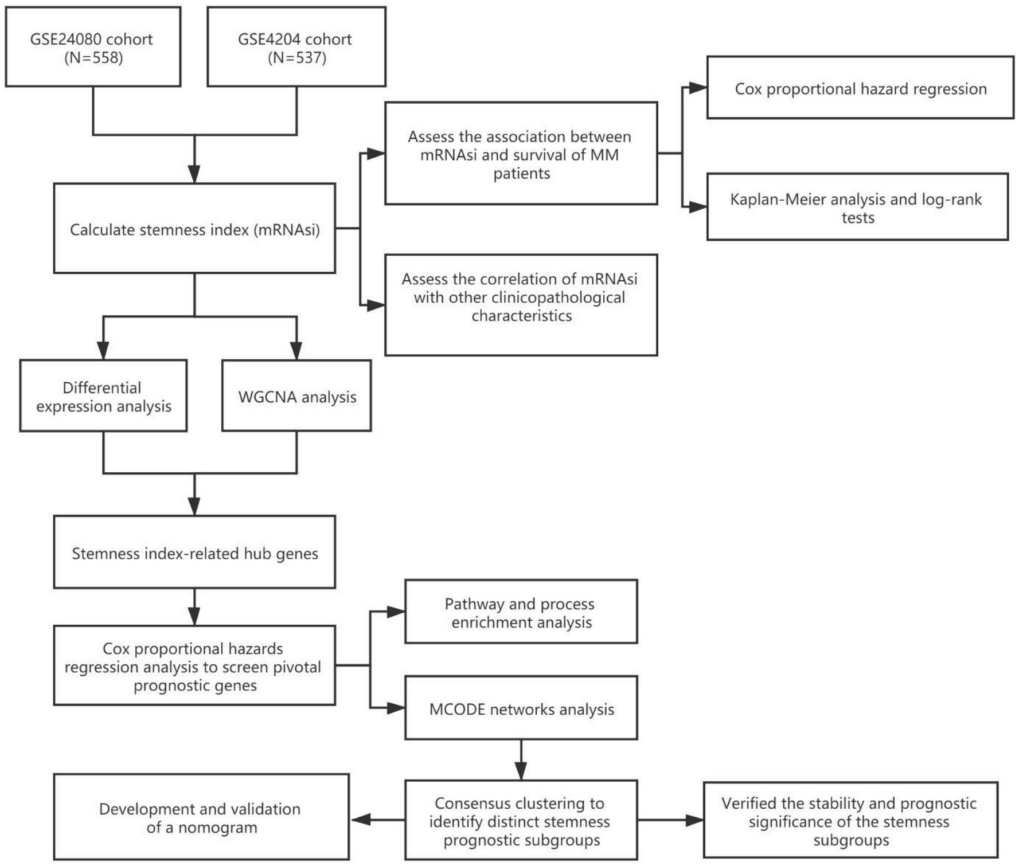

FIGURE 1 | Workflow of this research.

MRNAsi-related modules were defined according to $P < 0.01$, and a higher GS value was used for further analysis. Finally, we selected the intersection of the key genes identified in different data sets.

Screened Differentially Expressed Genes

The *limma* R package was used to screen differentially expressed genes (DEGs) between the high and low mRNAsi groups (Ritchie et al., 2015). The selection criteria were as follows: adjusted P-value < 0.0001 and $|\log2 \text{ fold change}| > 0.5$.

Functional Annotation and Pathway Enrichment Analysis

We first selected the intersection between the modular genes identified by WGCNA and the DEGs identified by differential expression analysis and then adopted a univariate Cox regression model to assess the prognostic significance of the overlapping genes. Only genes with a P-value < 0.05 were considered as prognosis-related hub genes. Functional annotation and pathway enrichment analysis of these hub genes was performed using Metascape (Zhou et al., 2019).[2]

[2]https://metascape.org/gp/index.html#/main/step1

Consensus Clustering and Prognostic Analysis Based on mRNAsi-Related Hub Genes

Protein-protein interaction enrichment analysis was conducted, and the molecular complex detection (MCODE) algorithm (Bader and Hogue, 2003) was used to identify densely connected network components. Based on the 34 mRNAsi-related hub genes identified by the MCODE algorithm, we subsequently performed unsupervised clustering on MM patients. The R package *ConsensusClusterPlus* was used to conduct unsupervised clustering (1,000 iterations, 80% resampling), and k-means and Euclidean distances were used as the clustering algorithm and distance metric, respectively (Wilkerson and Hayes, 2010). We then assessed the prognosis in each MMS-cluster via Kaplan–Meier analysis. Meanwhile, mRNAsi was also compared in distinct MMS clusters.

Development and Validation of a Nomogram for Prognosis Prediction of MM Patients

To develop a clinically applicable method of predicting MM prognosis, we integrated mRNAsi and other clinicopathological covariates to build a nomogram. Predictive factors included

mRNAsi, cytogenetic abnormalities, albumin (ALB), beta-2 microglobulin (B2M), and lactate dehydrogenase (LDH). The nomogram was verified using receiver operating characteristic (ROC) curves and calibration curves.

Statistical Analyses

The Wilcoxon rank-sum test was used to compare two groups with non-normally distributed variables, while Student's *t*-test was conducted to compare groups with normally distributed variables. The one-way analysis of variance or Kruskal–Wallis tests were used to compare differences between three or more groups. Based on the correlation between mRNAsi and patient survival, the cutoff point of mRNAsi was determined using the *Survminer* R package. The "surv-cutpoint" function, which repeatedly tested all potential cut points to find the maximum rank statistic, was applied to dichotomize mRNAsi, and the patients were then divided into high and low mRNAsi groups based on the maximally selected log-rank statistics to decrease the batch effect of calculation. The survival curves for the prognostic analysis were generated using the Kaplan–Meier method, and log-rank tests were used to determine the significance of differences. Independent prognostic factors were ascertained using the multivariable Cox regression model.

RESULTS

The Association Between mRNAsi and Patient Survival

We collected 1,095 MM samples with clinical information and corresponding expression data to systematically characterize the stemness features of MM. The overall characteristics of the MM cohort are listed in **Table 1**. MM samples were sorted according to their mRNAsi values (from low to high stemness index) and examined whether any clinical characteristic/molecular/demographic was associated with either a low or high stemness index (**Figures 2A**, **3A**). We did not find significant differences in mRNAsi in terms of gender and race, but we found that patients who died and patients who experienced adverse events occurred often showed a higher mRNAsi.

Correlations of mRNAsi With Clinical Prognosis in MM

We further explored the prognostic value of mRNAsi in patients with MM. First, the multivariate Cox regression model analysis in different cohorts confirmed mRNAsi as an independent and robust prognostic biomarker for evaluating MM patient outcomes (**Table 2** and **Supplementary Tables 1, 2**). Second, based on the cutoff point (0.4124166) identified by the *Survminer* R package, each MM cohort was separated into low and high mRNAsi groups. The Kaplan–Meier analysis confirmed that the high-mRNAsi group had shorter OS and event-free survival (EFS) than the low mRNAsi group in the GSE24080 cohort (**Figures 2B,C**). Consistent with this, in the GSE4204 cohort, the Kaplan–Meier analysis indicated that the high-mRNAsi group had shorter OS than the low mRNAsi group (**Figure 3B**).

TABLE 1 | Baseline characteristics of multiple myeloma (MM) patients.

Characteristic	Overall	GSE24080	GSE4204
Project (%)	1,095	558	537
GSE24080	558 (51.0)	558 (100.0)	0 (0.0)
GSE4204	537 (49.0)	0 (0.0)	537 (100.0)
OS CENSOR (%)			
Alive	832 (76.0)	387 (69.4)	445 (82.9)
Dead	263 (24.0)	171 (30.6)	92 (17.1)
OS TIME (median [IQR])	37.10 [19.06,53.55]	48.23 [34.63,64.07]	23.97 [12.07,39.67]
Treatment (%)			
TT2	688 (62.8)	344 (61.6)	344 (64.1)
TT3	407 (37.2)	214 (38.4)	193 (35.9)
SUBGRP7 (%)	127 (23.6)	0 (NaN)	127 (23.6)
CD1	28 (5.2)	0 (NaN)	28 (5.2)
CD2	59 (11.0)	0 (NaN)	59 (11.0)
HY	114 (21.2)	0 (NaN)	114 (21.2)
LB	58 (10.8)	0 (NaN)	58 (10.8)
MF	37 (6.9)	0 (NaN)	37 (6.9)
MS	67 (12.5)	0 (NaN)	67 (12.5)
PR	47 (8.8)	0 (NaN)	47 (8.8)
AGE (%)			
<60	317 (56.8)	317 (56.8)	0 (NaN)
≥60	241 (43.2)	241 (43.2)	0 (NaN)
Gender (%)			
Female	222 (39.8)	222 (39.8)	0 (NaN)
Male	336 (60.2)	336 (60.2)	0 (NaN)
RACE (%)			
White	496 (88.9)	496 (88.9)	0 (NaN)
Other	62 (11.1)	62 (11.1)	0 (NaN)
EFS CENSOR (%)			
No	310 (55.6)	310 (55.6)	0 (NaN)
Yes	248 (44.4)	248 (44.4)	0 (NaN)
EFS TIME (median [IQR])	42.40 [29.23,56.66]	42.40 [29.23,56.66]	NA [NA,NA]
ISOTYPE (%)	15 (2.7)	15 (2.7)	0 (NaN)
FLC	84 (15.1)	84 (15.1)	0 (NaN)
IgA	133 (23.8)	133 (23.8)	0 (NaN)
IgD	3 (0.5)	3 (0.5)	0 (NaN)
IgG	312 (55.9)	312 (55.9)	0 (NaN)
Non-secretory	6 (1.1)	6 (1.1)	0 (NaN)
NSE	2 (0.4)	2 (0.4)	0 (NaN)
NA	3 (0.5)	3 (0.5)	0 (NaN)
B2M (%)	1 (0.2)	1 (0.2)	0 (NaN)
<3.5	319 (57.2)	319 (57.2)	0 (NaN)
≥5.5	118 (21.1)	118 (21.1)	0 (NaN)
3.5-5.5	120 (21.5)	120 (21.5)	0 (NaN)
CRP (median [IQR])	4.40 [1.20, 11.00]	4.40 [1.20, 11.00]	NA [NA, NA]
CREAT (median [IQR])	1.00 [0.80, 1.20]	1.00 [0.80, 1.20]	NA [NA, NA]
LDH (median [IQR])	156.50 [127.00, 199.00]	156.50 [127.00, 199.00]	NA [NA, NA]
ALB (median [IQR])	4.10 [3.70, 4.40]	4.10 [3.70, 4.40]	NA [NA, NA]

(Continued)

TABLE 1 | Continued

Characteristic	Overall	GSE24080	GSE4204
HGB (median [IQR])	11.30 [9.80, 12.60]	11.30 [9.80, 12.60]	NA [NA, NA]
ASPC (median [IQR])	40.00 [23.00, 60.00]	40.00 [23.00, 60.00]	NA [NA, NA]
BMPC (median [IQR])	45.00 [21.25, 70.00]	45.00 [21.25, 70.00]	NA [NA, NA]
MRI (median [IQR])	5.00 [0.00, 16.00]	5.00 [0.00, 16.00]	NA [NA, NA]
Cyto_Abn (%)			
No	352 (63.1)	352 (63.1)	0 (NaN)
Yes	206 (36.9)	206 (36.9)	0 (NaN)

OS CENSOR, (dead = event) overall survival censor (dead); EFS CENSOR, (yes = event) event-free survival censor (disease relapse or progression); AGE, age at registration (years); B2M, beta-2 microglobulin (mg/l); CRP, C-reactive protein (mg/l); CREAT, creatinine (mg/dl); LDH, lactate dehydrogenase (U/l); ALB, albumin (35 g/l); HGB, hemoglobin (g/dl); ASPC, aspirate plasma cells (%); BMPC, bone marrow biopsy plasma cells (%); MRI, number of magnetic resonance imaging (MRI)-defined focal lesions (skull, spine, pelvis). Cytogenetic abnormality an indicator of the detection of cytogenetic abnormalities. Yes = abnormalities were detected, No = were not detected or were absent.

Surprisingly, we found that in both the GSE24080 and GSE4204 cohorts, the treatment regimen (TT2 or TT3) did not improve the survival of MM patients (**Figures 2D**, **3C**). Regardless of the treatment plan (TT2 or TT3), it failed to improve the survival disadvantages of patients in the high-mRNAsi group (**Figures 2E,F**, **3D,E**). Consistently with previous reports (Zhan et al., 2006), our analysis found that among the seven subgroups of MM, the PR subgroup had the worst prognosis, followed by the MS and MF subgroups (**Figure 3F**). Finally, we investigated the association between mRNAsi and other clinical characteristics. We found that the difference in mRNAsi among the groups was statistically significant when comparing groups of patients with B2M $\geq$ 3.5 and those with B2M $<$ 3.5 (**Figure 4A**). There was no significant difference in mRNAsi between the different isotype groups (**Figure 4B**). However, for the seven subgroups of MM, consistent with poor survival, patients in the PR subgroups possessed the highest mRNAsi (**Figure 4C**). In terms of cytogenetic abnormalities, patients with cytogenetic abnormalities tended to have higher mRNA levels (**Figure 4D**). Since different therapies (TT2 or TT3) failed to improve the survival of MM patients, we further investigated whether there were any differences in mRNAsi among MM patients who received different therapies. Consistent with our conjecture, different treatment regimens failed to effectively affect mRNAsi (**Figures 4E,F**). Based on the ESTIMATE algorithm, we calculated the individual stromal and immune scores to evaluate the level of infiltrating stromal and immune cells in any given MM sample (Yoshihara et al., 2013). We found that

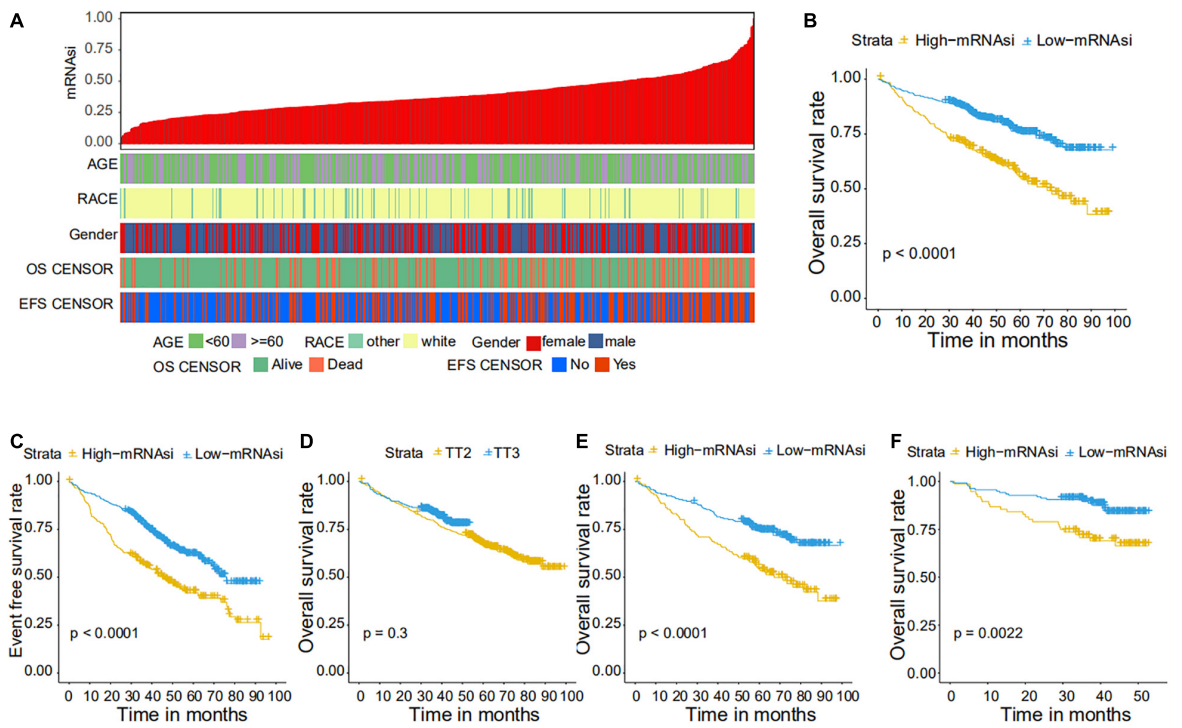

FIGURE 2 | Clinical characteristics related to the mRNA expression-based stemness index (mRNAsi) in the GSE24080 cohort. **(A)** Overview of the association between demographic characteristics and mRNAsi in MM. Columns represent samples sorted by mRNAsi from low to high (top row), and rows represent the demographic factors associated with mRNAsi. **(B,C)** The Kaplan–Meier curve was used to determine the overall survival (OS) **(B)** and event-free survival (EFS) **(C)** of patients in the multiple myeloma (MM) group with high and low mRNAsi. **(D)** The Kaplan–Meier curve was used to determine the OS of patients treated with the TT2 or TT3 regimen. **(E)** The Kaplan–Meier curve was used to determine the OS of high and low mRNAsi patients treated with the TT2 regimen. **(F)** The Kaplan–Meier curve was used to determine the OS of high and low mRNAsi patients treated with the TT3 regimen.

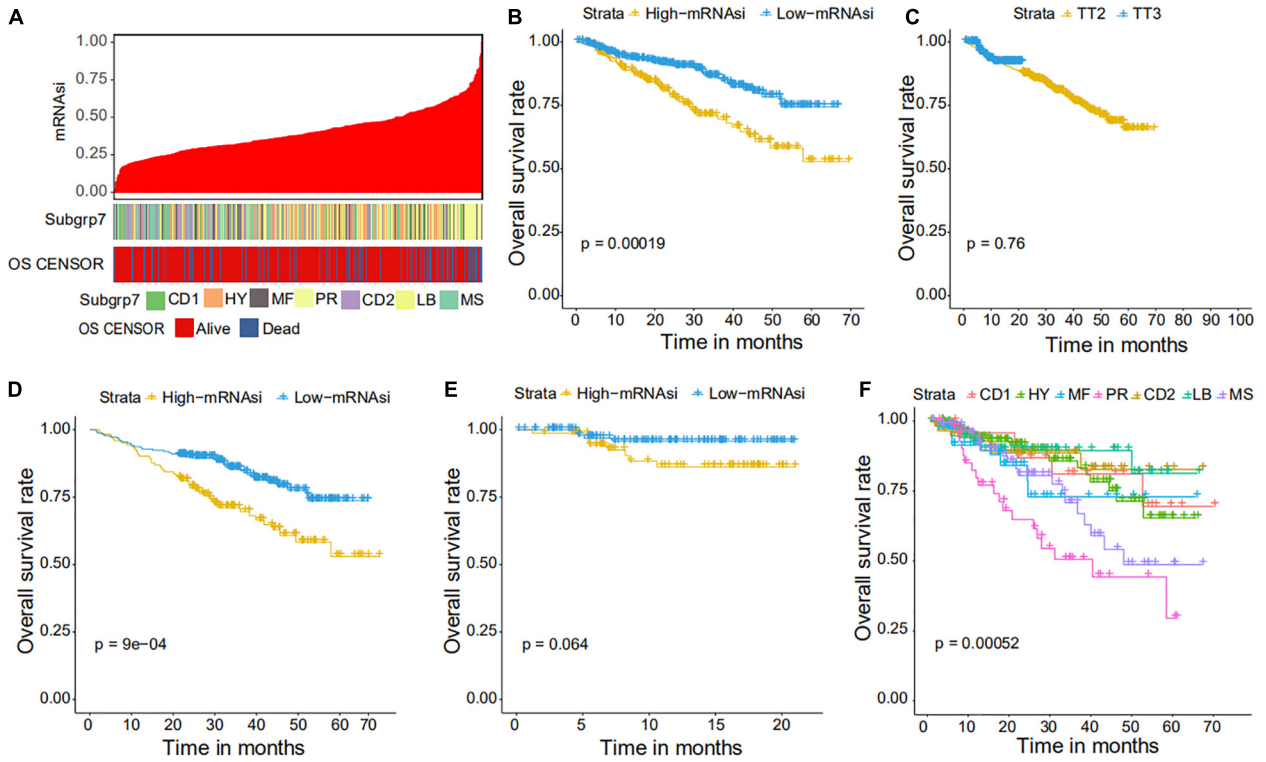

FIGURE 3 | Clinical characteristics related to the mRNAsi in the GSE4204 cohort. **(A)** Overview of the association between subtype and mRNAsi in MM. The columns represent samples sorted by mRNAsi from low to high (top row), while the rows represent the demographic factors associated with mRNAsi. **(B)** The Kaplan–Meier curve was used to determine the OS of patients in the MM group with high and low mRNAsi. **(C)** The Kaplan–Meier curve was used to determine the OS of patients treated with the TT2 or TT3 regimen. **(D)** The Kaplan–Meier curve was used to determine the OS of high and low mRNAsi patients treated with the TT2 regimen. **(E)** The Kaplan–Meier curve was used to determine the OS of high and low mRNAsi patients treated with the TT3 regimen. **(F)** The Kaplan–Meier curve was used to determine the OS of patients of different MM subtypes.

the high-mRNAsi group had lower immune and stromal scores than the low mRNAsi group, which suggested that MM patients with high mRNAsi had a lower level of infiltration of tumor microenvironment (TME) cells (**Figures 4G,H**).

Weighted Gene Co-expression Network Analysis: Identification of the Most Significant Modules and Genes

Weighted gene co-expression network analysis was used to build a gene co-expression network to classify all genes into biological gene modules based on average linkage hierarchical clustering and further identify genes strongly associated with MM stemness (**Figures 5A,D**, **6A,D**). The soft-thresholding powers in the WGCNA were determined based on scale-free R2 (**Figures 5B,C**, **6B,C**). The pink module had the highest correlation with mRNAsi in the GSE24080 cohort (**Figures 5E,F**). Additionally, the tan and green modules were highly associated with mRNAsi in the GSE4204 cohort (**Figures 6E–G**). The pink module contained 643 genes (**Figure 5F**), and tan and green contained 313 and 623 genes, respectively (**Figures 6F,G**). There were 379 overlapping genes in the three modules (**Figure 7A**). A total of 379 overlapping genes were retained for further analysis.

Differentially Expressed Genes Between Low and High mRNAsi Groups of MM Patients

Since the prognosis of MM patients in the high and low mRNAsi groups differed significantly, we conducted a differential expression analysis between high and low mRNAsi groups to identify the differentially expressed key genes that regulate stemness. We identified 370 DEGs, of which 326 were upregulated and 44 were downregulated in the high-mRNAsi group. After merging the 370 DEGs with the 379 co-expressed genes identified by WGCNA, 128 hub genes were retained for further analysis (**Figure 7B**).

Pathway and Process Enrichment Analysis of Hub Prognostic Genes

The prognostic evaluation of the 128 hub genes was performed using the Cox proportional hazards regression analysis in the GSE24080 cohort dataset. In total, 127 hub genes were identified as significantly prognostic of the outcome (**Supplementary Table 3**, $P < 0.05$). Functional enrichment analysis was performed using Metascape to elucidate the biological functions of the 127 hub prognostic genes (**Figure 7C**).

TABLE 2 | Univariate and multivariable cox regression analysis of clinical features and OS in the GSE24080 cohort of MM patients.

	Univariate Cox regression analysis		Multivariable Cox regression analysis	
	HR (95%CI)	***p* value**	**HR (95%CI)**	***p* value**
Treatment	0.82431 (0.57344–1.1849)	0.29671	0.85959 (0.56569–1.3062)	0.4785
Age	1.4345 (1.0616–1.9385)	0.018833	1.2299 (0.88208–1.715)	0.22238
Gender	0.95881 (0.70659–1.301)	0.78707	1.1181 (0.7849–1.5929)	0.53626
Race	1.0527 (0.65329–1.6965)	0.83276	0.98993 (0.58153–1.6851)	0.97025
B2M	1.0834 (1.0647–1.1025)	2.21E-19	1.1043 (1.0627–1.1475)	4.20E-07
CRP	1.0032 (0.99834–1.0081)	0.19614	0.99659 (0.98718–1.0061)	0.47955
CREAT	1.2329 (1.1382–1.3354)	2.79E-07	0.92317 (0.79575–1.071)	0.29151
LDH	1.0062 (1.0046–1.0079)	3.84E-13	1.0044 (1.0022–1.0065)	5.47E-05
ALB	0.58079 (0.471–0.71618)	3.73E-07	0.73108 (0.54743–0.97634)	0.033821
HGB	0.87091 (0.80301–0.94456)	0.00084631	1.0076 (0.90369–1.1235)	0.89144
ASPC	1.0102 (1.004–1.0164)	0.0011275	0.99881 (0.98875–1.009)	0.81831
BMPC	1.0096 (1.0038–1.0155)	0.0012532	1.0003 (0.99088–1.0099)	0.94347
MRI	1.0172 (1.0083–1.0261)	0.00012887	1.0089 (0.99865–1.0193)	0.088955
Cyto_Abn	2.2708 (1.6805–3.0685)	9.32E-08	1.7924 (1.2669–2.5358)	0.00098068
mRNAsi	28.219 (10.696–74.45)	1.50E-11	5.0703 (1.3013–19.756)	0.019312
StromalScore	0.9994 (0.99881–0.99998)	0.04337	1.0003 (0.99956–1.0011)	0.39522
ImmuneScore	0.99958 (0.99906–1.0001)	0.12077	1.0002 (0.99946–1.0009)	0.64608

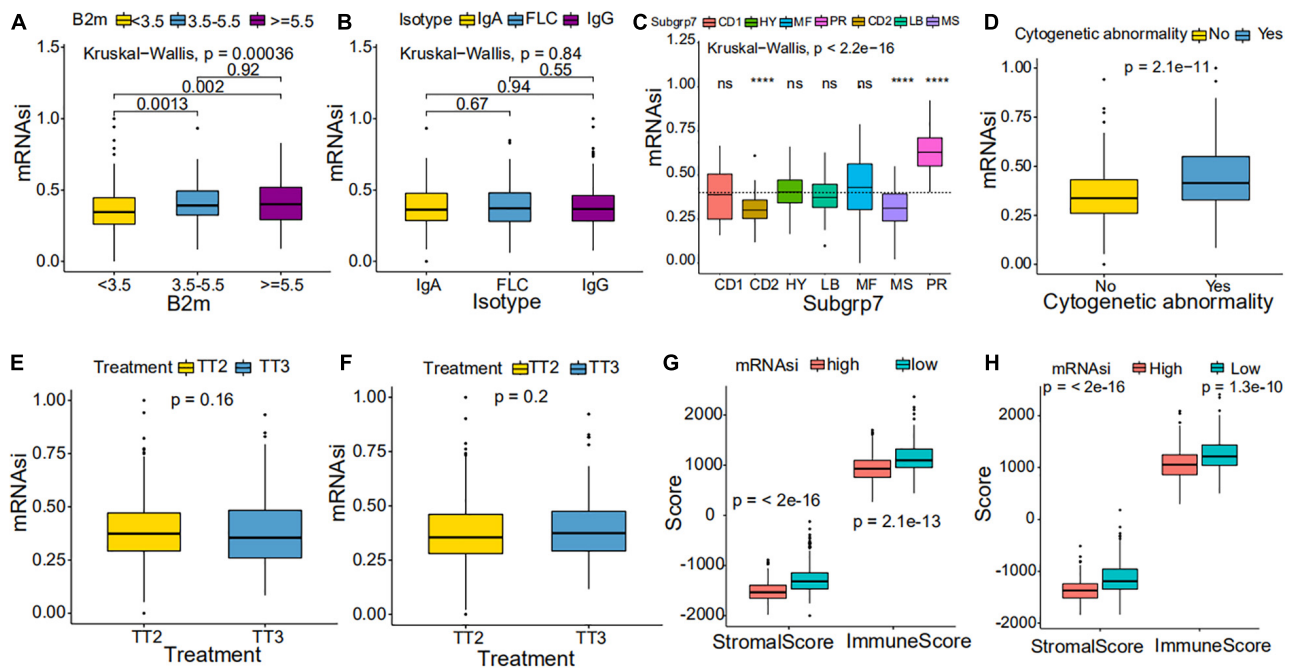

FIGURE 4 | Clinical characteristics in low mRNAsi and high mRNAsi MM patients. **(A,B)** Differences in mRNAsi between distinct B2M groups **(A)** and isotype groups **(B)** in patients with MM. The upper and lower ends of the boxes represent the interquartile range of values. The lines in the boxes represent median values. **(C,D)** Difference in mRNAsi between distinct subgroups **(C)** and cytogenetic abnormalities groups **(D)** in patients with MM. **(E,F)** Difference in mRNAsi between distinct treatment regimen groups in patients of the GSE24080 cohort **(E)** or the GSE4204 cohort **(F)**. **(G,H)** Difference in stromalscore and immunescore between high and low mRNAsi samples of the GSE24080 cohort **(G)** or the GSE4204 cohort **(H)**. ****$p < 0.0001$.

The enrichment analysis suggested that these genes were significantly enriched in pathways and processes related to cell cycle, cell differentiation, and DNA replication and repair (**Figure 7D**, hypergeometric test $P < 0.01$). Finally, based on the MCODE algorithm, the 127 hub prognostic genes were divided into four densely connected network components. The MCODE networks identified for the individual gene lists are shown in **Figure 7E**. A total of four major gene modules (MCODE 1–4) were identified, including 34 hub prognostic genes (**Supplementary Table 4**).

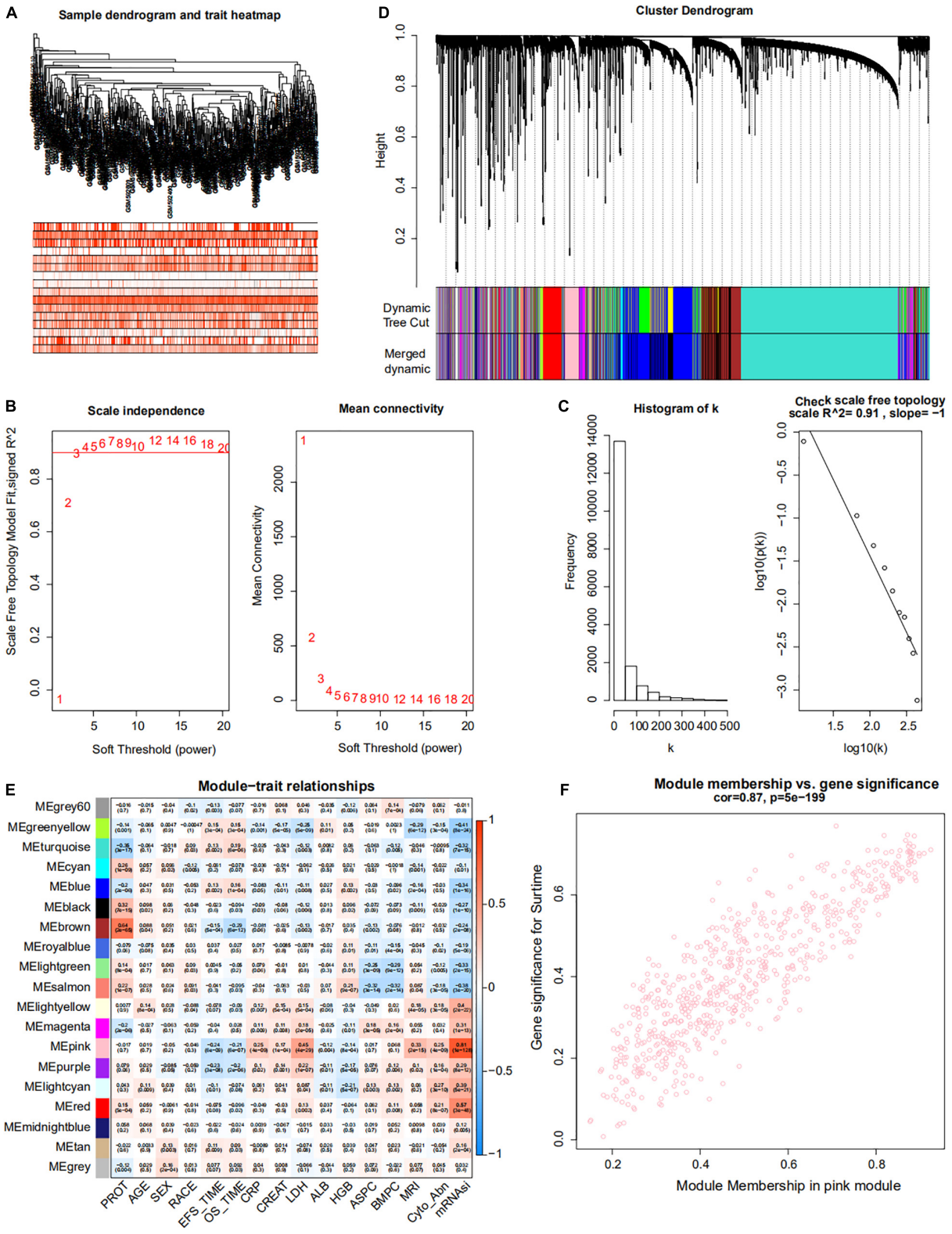

FIGURE 5 | Weighted gene co-expression network of MM of the GSE24080 cohort. **(A)** Sample dendrogram and trait heatmap. The colors represent the proportion of clinical traits. **(B)** Left panel: the scale-free topology fit index for soft-thresholding powers. Right panel: mean connectivity for soft-thresholding powers. **(C)** Scale-free *R*2 (*R*2 = 0.91). **(D)** Clustering dendrogram of genes in patients with MM. **(E)** Pertinence between clinical traits and gene modules. **(F)** Scatter plots of gene significance (GS) for mRNAsi corresponding to module membership in the pink module, with their correlation coefficients and *P*-values.

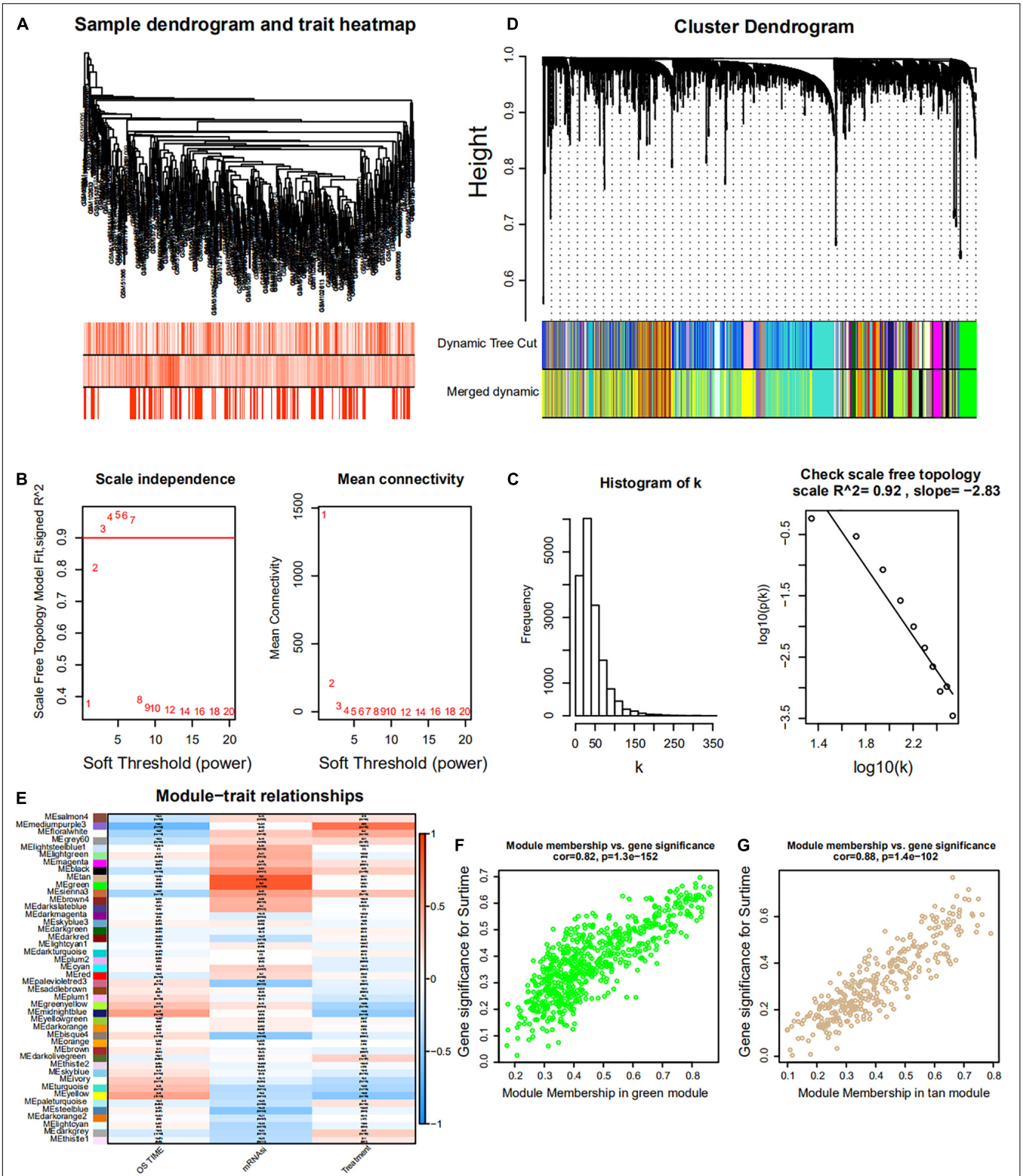

FIGURE 6 | Weighted gene co-expression network of MM of the GSE4204 cohort. **(A)** Sample dendrogram and trait heatmap. The colors represent the proportion to clinical traits. **(B)** Left panel: the scale-free topology fit index for soft-thresholding powers. Right panel: mean connectivity for soft-thresholding powers. **(C)** Scale-free *R2* (*R2* = 0.92). **(D)** Clustering dendrogram of gene in patients with MM. **(E)** Pertinence between clinical traits and gene modules. **(F,G)** Scatter plots of GS for mRNAsi corresponding to module membership in green and tan modules, with their correlation coefficients and *P*-values.

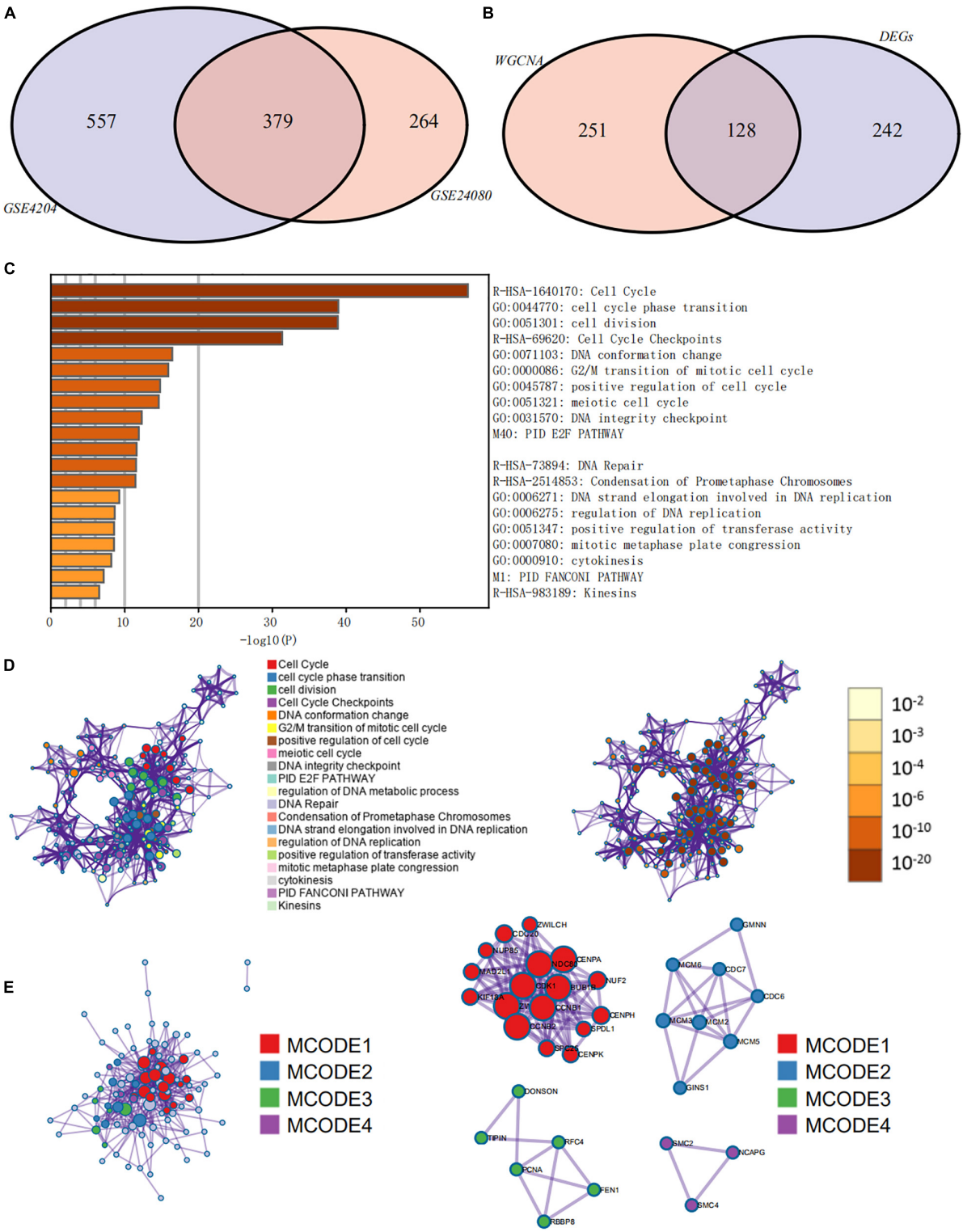

FIGURE 7 | Functional annotation and pathway enrichment analysis of key prognostic genes that were identified by weighted gene co-expression network analysis (WGCNA) and differential expression analysis. **(A)** Venn diagram of genes identified by WGCNA in the GSE24080 and GSE4204 cohorts. **(B)** Venn diagram of genes identified by WGCNA and differential expression analysis. **(C)** Bar graph of enriched terms of stemness-related genes, colored by *P*-values. **(D)** Network of enriched terms: (left panel) colored by cluster ID, where nodes that share the same cluster ID are typically close to each other; (right panel) colored by *P*-value, where terms containing more genes tend to have more significant *P*-values. **(E)** Protein–protein interaction network and molecular complex detection components identified in the gene lists of the 127 stemness-related signatures.

Consensus Clustering to Distinguish Different Stemness Prognostic Subtypes

First, we identified different stemness prognostic subgroups in the GSE24080 cohort. We utilized the 34 stemness-related signatures of MCODE 1–4 to conduct unsupervised clustering and identified the stemness molecular subtypes of MM for prognostic analysis. The R package of *ConsensusClusterPlus* was used to iterate 1,000 times for the stabilization of classification categories (parameters: pItem = 0.8, reps = 1,000, pFeature = 1), and three distinct stemness molecular subgroups were eventually identified using unsupervised clustering (**Figures 8A,B**). Unsupervised clustering is a useful technique in tumor research, where intrinsic groups sharing biological characteristics may exist but are unknown. A Kaplan–Meier analysis was conducted across the three clusters, where MMS-cluster3 had the worst OS prognosis and MMS-cluster2 had the most favorable prognosis (**Figure 8C**, log-rank test $P < 0.0001$). In agreement with these results, MMS-cluster3 had the highest mRNAsi, and MMS-cluster2 had the lowest mRNAsi (**Figure 8D**). In addition, to verify our stemness prognostic subgroups, based on the 34 stemness-related signatures, we also performed unsupervised clustering and prognostic analysis on the GSE4204 cohort. Consistent with the above results, the MM samples could be classified into three clusters with different prognoses (**Figure 8F**); MMS-cluster3 had the worst prognosis with the highest mRNAsi, while MMS-cluster2 had the most favorable prognosis with the lowest mRNAsi (**Figure 8G**). We also investigated whether there were any differences in immune and stromal scores among the three clusters. The results showed that MMS-cluster2 had higher stromal and immune scores, while MMS-cluster3 had lower stromal and immune scores (**Figures 8E,H**). In total, these analyses indicated that the 34 MMS-related signature could guide molecular classifications, by which the MMS clusters possessed different immune infiltration and had different prognostic outcomes.

Development and Validation of a Nomogram

Based on the multivariate Cox regression analysis, a nomogram was built to determine MM prognosis (**Figure 9A**), and a time-dependent ROC curve was used to evaluate the effect of the nomogram. As the data with complete clinical information was limited, we used the GSE24080 cohort as the whole dataset (training set) to construct the nomogram. To verify our nomogram, we set the random seed to 123 and used the *caret* R package to randomly cut the whole set and divided the samples into two different data sets (50%/50%) to verify the nomogram. In the whole dataset, the area under the curve was 0.759 and 0.740 for the 3- and 5-year survival, respectively (**Figures 9B,C**). The performance of the nomogram was far superior to that of mRNAsi, cytogenetic abnormalities, ALB, B2M, and LDH alone for assessing patient prognosis (**Figures 9B,C**). In addition, the nomogram showed good prediction performance in the verification cohorts, and the 3- and 5-year ROC curves of test sets 1 and 2, respectively, are shown in **Figures 9D–G** (**Figures 9D,E**, test set 1; **Figures 9F,G**, test set 2). A calibration curve was constructed to assess the accuracy of the nomogram. As shown in **Figures 9H,I** (training set) and **Figures 9J–M** (**Figures 9J,K**, test set 1; **Figures 9L,M**, test set 2), the combined nomogram showed good performance in predicting the 3- and 5-year survival rates of patients, and the prediction probability was close to the actual observed situation.

DISCUSSION

Cancer stem cells are commonly considered to be responsible for tumor persistence and progression, tumor recurrence, and resistance to traditional therapies (Seguin et al., 2015; Prasetyanti and Medema, 2017; Saygin et al., 2019). We comprehensively analyzed data from large cohorts to determine the cancer stemness of MM and found that mRNAsi was tightly associated with OS and EFS, possessing good fitness and quantification of stemness in MM. In addition, low- and high-mRNAsi groups had different features, including B2M, cytogenetic abnormalities, ALB, subgroups, and immune infiltration. This evidence indicates that stemness, as a yardstick to assess the degree of gradual loss of a differentiated phenotype and gain of progenitor and stem cell-like characteristics, strongly affects the prognosis of MM. Our researches showed that mRNAsi could effectively classify patients with MM into groups with low and high risks of poor prognosis. Additionally, the proposed mRNAsi provided additional prognostic value to existing clinicopathological prognosticators for MM. Of particular importance, this is the first study to demonstrate the clinical utility of the stemness signature as a prognostic tool in patients with MM. We observed that the prognoses of patients with MM who received different therapies (TT2 or TT3) were not significantly different. Similarly, mRNAsi did not differ significantly; however, in both the TT2 and TT3 groups, patients with high mRNAsi had shorter OS than patients with low mRNAsi. This suggests that the TT3 regimen did not significantly improve the prognosis of patients compared with the TT2 regimen. This might be because the TT3 regimen failed to remove the stemness, thus failing to influence the degree of oncogenic dedifferentiation, which might provide valuable insights for targeted therapies aimed at tumor differentiation of MM. Moreover, the stemness index-related modules and genes were identified using WGCNA and differential expression analysis. A total of 127 hub prognostic genes were found to be most significantly associated with stemness index. Pathway and process enrichment analysis revealed that these hub prognostic genes were involved in various biological functions related to the initiation and progression of MM, including the cell cycle, cell differentiation, and DNA replication and repair. Interestingly, these hub prognostic genes allowed for the discovery of innovative targets and possible targeted therapies aimed at tumor differentiation. Based on the MCODE algorithm, the most important connected network components were identified from these hub prognostic genes. We considered tumor heterogeneity and classified the MM cohorts into three MMS clusters based on the 34 stemness-related signatures. We observed distinct survival outcomes across the three MMS clusters and compared

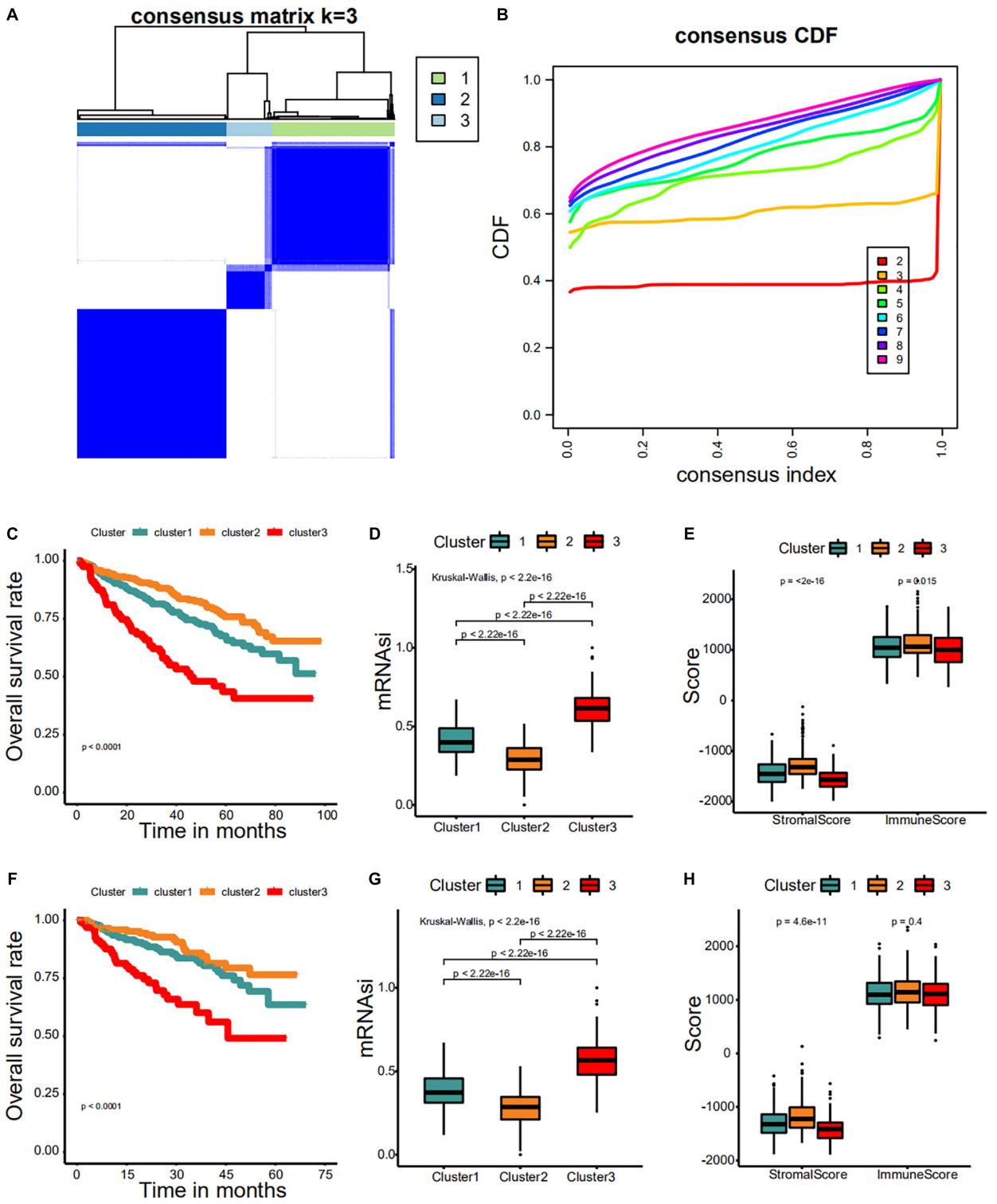

FIGURE 8 | Consensus clustering identified distinct multiple myeloma stemness (MMS) clusters with different prognoses. **(A)** Consensus score matrix for MM samples when $k = 3$. **(B)** The cumulative distribution function (CDF) describes a real random variable of its probability distribution based on consensus scores for different subtype numbers ($k = 2$–9). **(C)** The Kaplan–Meier curve was used to determine the OS of patients of different MMS clusters in the GSE24080 cohort. **(D)** Difference in mRNAsi among distinct MMS clusters in patients of the GSE24080 cohort. **(E)** Difference in stromalscore and immunescore among distinct MMS clusters in patients of the GSE24080 cohort. **(F)** The Kaplan–Meier curve was used to determine the OS of patients of different MMS clusters in the GSE4204 cohort. **(G)** Difference in mRNAsi among distinct MMS clusters in patients of the GSE4204 cohort. **(H)** Difference in stromalscore and immunescore among distinct MMS clusters in patients of the GSE4204 cohort.

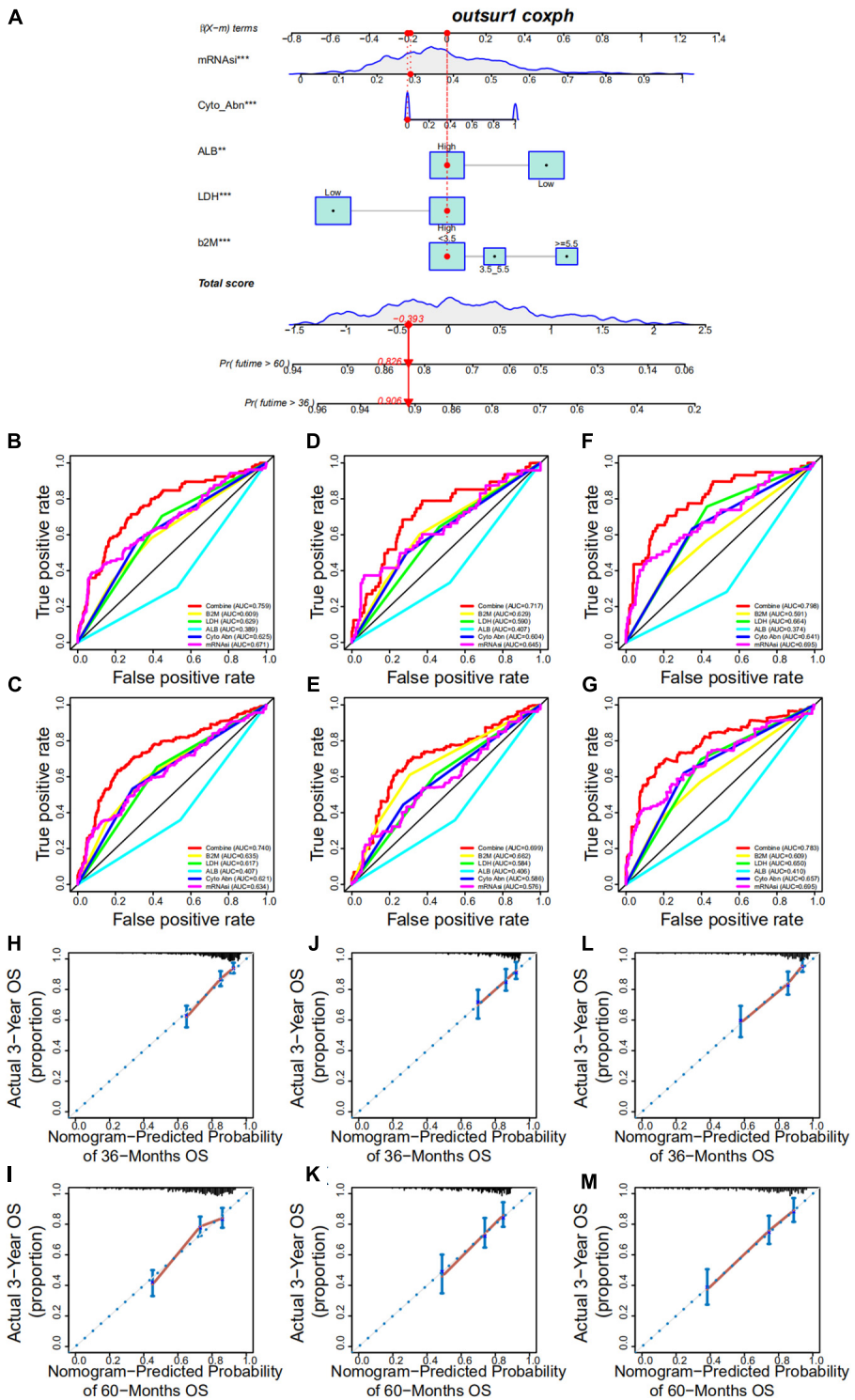

FIGURE 9 | Development and validation of a nomogram. **(A)** A nomogram combining mRNAsi and other clinicopathologic covariates. **(B,C)** Receiver operating characteristic (ROC) curve to evaluate the accuracy of the 3-year **(B)** and 5-year **(C)** OS nomogram in the training cohort. **(D,E)** ROC curve to evaluate the accuracy of the 3-year **(D)** and 5-year **(E)** OS nomogram in test set 1. **(F,G)** ROC curve to evaluate the accuracy of the 3-year **(F)** and 5-year **(G)** OS nomogram in test set 2. **(H,I)** Calibration plots indicating that nomogram-predicted 3- **(H)** and 5-year **(I)** survival probabilities of the training set corresponded closely to the observed proportions. **(J,K)** Calibration plots indicating that nomogram-predicted 3- **(J)** and 5-year **(K)** survival probabilities of test set 1 corresponded closely to the observed proportions. **(L,M)** Calibration plots indicating that nomogram-predicted 3- **(L)** and 5-year **(M)** survival probabilities of test set 2 corresponded closely to the observed proportions.

the differential mRNAsi among the three MMS clusters. In particular, MMS-cluster3 samples possessed the highest mRNAsi and had the worst OS outcomes compared with other clusters. We also applied the ESTIMATE method to evaluate the level of immune infiltrating cells in the TME of MM and found different infiltration patterns across the three clusters. These findings revealed the patterns of intra-tumor molecular heterogeneity and the different patterns of TME infiltration within MM and supported the negative regulation of the stemness index and anticancer immunity. Lastly, by integrating mRNAsi and other clinical characteristics, we proposed a prognostic nomogram that allows for individualized estimations of the 3- and 5-year OS probabilities among MM patients.

Stemness signatures have been identified in many malignancies and have different prognostic values in gastric cancer, acute myeloid leukemia, prostate cancer, and breast cancer (Ng et al., 2016; Malta et al., 2018; Wang et al., 2018; Miranda et al., 2019; Chang et al., 2020; Zhang et al., 2020). However, there are few studies on the stemness of MM and its prognostic value in MM patients. In our study, mRNAsi could stratify MM patients into two groups with notably different prognoses, which was convenient for risk stratification of MM in clinical practice. Integrated analyses also confirmed that mRNAsi is an independent prognostic biomarker in MM. In our screening in multiple cohorts, some of the stemness-related genes have never been reported in other previous researches that could predict the outcomes of MM, which was convenient to implement in clinical practice. BUB1B encodes a kinase involved in spindle checkpoint function. The protein is localized to the kinetochore and plays a role in the inhibition of the anaphase-promoting complex/cyclosome. An increasing body of literature has verified that aberrant expression of BUB1B is highly involved in the tumorigenesis and the development of various tumors (Wan et al., 2012; Qiu et al., 2020). A previous study revealed that BUB1B could promote MM cell proliferation through the CDC20/CCNB axis (Yang et al., 2015). MCM2, MCM3, MCM5, and MCM6, members of the minichromosome maintenance (MCM) family, are highly involved in DNA replication and are vital in limiting replication in the cell cycle (Freeman et al., 1999; Forsburg, 2004). Some investigations have shown that the expression of MCM family plays an important role in the prognosis of MM, and MCM2 is an independent risk factor for MM (Quan et al., 2020). Additionally, MCM2 is associated with many types of cancer, including acute lymphocytic leukemia, gallbladder cancer, and glioma (Hua et al., 2014; Liu et al., 2016; Li et al., 2018). Trichostatin A, a classical histone deacetylase inhibitor, could downregulate the expression of MCM2, and the silencing of MCM2 in colon cancer cells could induce cell cycle arrest and apoptosis as reported in a previous study (Liu et al., 2013). Therefore, MCM2 could be a potential therapeutic target for the treatment of MM. ZWILCH kinetochore protein is an essential part of the Rod–Zw10–Zwilch complex and is important in maintaining the normal function of mitotic checkpoints (Karess, 2005; Gama et al., 2017). The abnormal function of mitotic checkpoints is related to the appearance of chromosomal instability, a consensus sign of many human cancers. In MM, chromosomal instability contributes to the acquisition of tumor heterogeneity and thereby to drug resistance, disease progression, and eventual treatment failure (Fujibayashi et al., 2020; Neuse et al., 2020). Aberrant BUB1 overexpression promotes mitotic segregation errors and chromosomal instability in MM (Fujibayashi et al., 2020), and the synergistic mechanism of BUB1B and ZWILCH in the occurrence and development of MM requires further investigation.

Moreover, we proposed prognostic nomogram that contribute to individualized evaluations of the 3- and 5-year OS probabilities among patients with MM. Taken together, mRNAsi and the associated nomogram might serve as a clinically helpful tool to improve surveillance and guide decision-making regarding the administration of adjuvant chemotherapy.

Collectively, mRNAsi could effectively classify patients with MM into groups with different risks of outcomes, thereby raising the possibility that stemness might be supplementary to the conventional clinicopathological risk factors as a prognostic scheme. The 34-gene based MMS-related signature could be a good molecular classifier for uncovering distinct stemness clusters. Additionally, the proposed nomogram incorporating mRNAsi and existing clinical prognosticators might facilitate personalized surveillance and management of patients with MM.

DATA AVAILABILITY STATEMENT

The original contributions presented in the study are included in the article/**Supplementary Material**, further inquiries can be directed to the corresponding author/s.

AUTHOR CONTRIBUTIONS

JH designed the study, interpreted the data, and revised the manuscript. CB and FY performed the statistical analysis, interpreted the data, and wrote the manuscript. MW, QL, and JW provided the bioinformatic data and contributed to the manuscript revision. LC, LTL, DX, and LL provided the key scientific insights and contributed to the manuscript revision. All authors have read and approved the final version of the manuscript.

FUNDING

This work was financially supported by grants from the Self-funded Scientific Research Project of the Guangxi Zhuang Autonomous Region Health Commission (contract number: Z20200114) and the "The role and mechanism of quercetin in acute myeloid leukemia" project (contract number: lryjj201909).

SUPPLEMENTARY MATERIAL

The Supplementary Material for this article can be found online at: https://www.frontiersin.org/articles/10.3389/fgene.2021.666561/full#supplementary-material

REFERENCES

Bader, G. D., and Hogue, C. W. (2003). An automated method for finding molecular complexes in large protein interaction networks. *BMC Bioinform.* 4:2. doi: 10.1186/1471-2105-4-2

Bataille, R., and Harousseau, J. L. (1997). Multiple myeloma. *N. Engl. J. Med.* 336, 1657–1664. doi: 10.1056/nejm199706053362307

Chang, W., Wang, H., Kim, W., Liu, Y., Deng, H., Liu, H., et al. (2020). Hormonal suppression of stem cells inhibits symmetric cell division and gastric tumorigenesis. *Cell Stem Cell* 26, 739–54.e738. doi: 10.1016/j.stem.2020.01.020

Dhakal, B., Girnius, S., and Hari, P. (2016). Recent advances in understanding multiple myeloma. *F1000Res* 5:F1000FacultyRev–2053. doi: 10.12688/f1000research.8777.1

Driscoll, J. J., Pelluru, D., Lefkimmiatis, K., Fulciniti, M., Prabhala, R. H., Greipp, P. R., et al. (2010). The sumoylation pathway is dysregulated in multiple myeloma and is associated with adverse patient outcome. *Blood* 115, 2827–2834. doi: 10.1182/blood-2009-03-211045

Forsburg, S. L. (2004). Eukaryotic MCM proteins: beyond replication initiation. *Microbiol. Mol. Biol. Rev.* 68, 109–131. doi: 10.1128/mmbr.68.1.109-131.2004

Freeman, A., Morris, L. S., Mills, A. D., Stoeber, K., Laskey, R. A., Williams, G. H., et al. (1999). Minichromosome maintenance proteins as biological markers of dysplasia and malignancy. *Clin. Cancer Res.* 5, 2121–2132.

Fujibayashi, Y., Isa, R., Nishiyama, D., Sakamoto-Inada, N., Kawasumi, N., Yamaguchi, J., et al. (2020). Aberrant BUB1 overexpression promotes mitotic segregation errors and chromosomal instability in multiple myeloma. *Cancers* 12:2206. doi: 10.3390/cancers12082206

Gama, J. B., Pereira, C., Simões, P. A., Celestino, R., Reis, R. M., Barbosa, D. J., et al. (2017). Molecular mechanism of dynein recruitment to kinetochores by the Rod-Zw10-Zwilch complex and Spindly. *J. Cell Biol.* 216, 943–960. doi: 10.1083/jcb.201610108

Hua, C., Zhao, G., Li, Y., and Bie, L. (2014). Minichromosome maintenance (MCM) family as potential diagnostic and prognostic tumor markers for human gliomas. *BMC Cancer* 14:526. doi: 10.1186/1471-2407-14-526

Karess, R. (2005). Rod-Zw10-Zwilch: a key player in the spindle checkpoint. *Trends Cell Biol.* 15, 386–392. doi: 10.1016/j.tcb.2005.05.003

Langfelder, P., and Horvath, S. (2008). WGCNA: an R package for weighted correlation network analysis. *BMC Bioinform.* 9:559. doi: 10.1186/1471-2105-9-559

Lapidot, T., Sirard, C., Vormoor, J., Murdoch, B., Hoang, T., Caceres-Cortes, J., et al. (1994). A cell initiating human acute myeloid leukaemia after transplantation into SCID mice. *Nature* 367, 645–648. doi: 10.1038/367645a0

Li, S., Wang, C., Wang, W., Liu, W., and Zhang, G. (2018). Abnormally high expression of POLD1, MCM2, and PLK4 promotes relapse of acute lymphoblastic leukemia. *Medicine* 97:e10734. doi: 10.1097/md.0000000000010734

Lian, H., Han, Y. P., Zhang, Y. C., Zhao, Y., Yan, S., Li, Q. F., et al. (2019). Integrative analysis of gene expression and DNA methylation through one-class logistic regression machine learning identifies stemness features in medulloblastoma. *Mol. Oncol.* 13, 2227–2245. doi: 10.1002/1878-0261.12557

Liu, Y., He, G., Wang, Y., Guan, X., Pang, X., and Zhang, B. (2013). MCM-2 is a therapeutic target of Trichostatin A in colon cancer cells. *Toxicol. Lett.* 221, 23–30. doi: 10.1016/j.toxlet.2013.05.643

Liu, Z., Yang, Z., Jiang, S., Zou, Q., Yuan, Y., Li, J., et al. (2016). MCM2 and TIP30 are prognostic markers in squamous cell/adenosquamous carcinoma and adenocarcinoma of the gallbladder. *Mol. Med. Rep.* 14, 4581–4592. doi: 10.3892/mmr.2016.5851

Malta, T. M., Sokolov, A., Gentles, A. J., Burzykowski, T., Poisson, L., Weinstein, J. N., et al. (2018). Machine learning identifies stemness features associated with oncogenic dedifferentiation. *Cell* 173:338–354.e315. doi: 10.1016/j.cell.2018.03.034

Martinez-Lopez, J., Blade, J., Mateos, M. V., Grande, C., Alegre, A., García-Laraña, J., et al. (2011). Long-term prognostic significance of response in multiple myeloma after stem cell transplantation. *Blood* 118, 529–534. doi: 10.1182/blood-2011-01-332320

Matsui, W., Wang, Q., Barber, J. P., Brennan, S., Smith, B. D., Borrello, I., et al. (2008). Clonogenic multiple myeloma progenitors, stem cell properties, and drug resistance. *Cancer Res.* 68, 190–197. doi: 10.1158/0008-5472.Can-07-3096

Miranda, A., Hamilton, P. T., Zhang, A. W., Pattnaik, S., Becht, E., Mezheyeuski, A., et al. (2019). Cancer stemness, intratumoral heterogeneity, and immune response across cancers. *Proc. Natl. Acad. Sci. U.S.A.* 116, 9020–9029. doi: 10.1073/pnas.1818210116

Neuse, C. J., Lomas, O. C., Schliemann, C., Shen, Y. J., Manier, S., Bustoros, M., et al. (2020). Genome instability in multiple myeloma. *Leukemia* 34, 2887–2897. doi: 10.1038/s41375-020-0921-y

Ng, S. W., Mitchell, A., Kennedy, J. A., Chen, W. C., McLeod, J., Ibrahimova, N., et al. (2016). A 17-gene stemness score for rapid determination of risk in acute leukaemia. *Nature* 540, 433–437. doi: 10.1038/nature20598

Nowak, D., Stewart, D., and Koeffler, H. P. (2009). Differentiation therapy of leukemia: 3 decades of development. *Blood* 113, 3655–3665. doi: 10.1182/blood-2009-01-198911

O'Brien, C. A., Pollett, A., Gallinger, S., and Dick, J. E. (2007). A human colon cancer cell capable of initiating tumour growth in immunodeficient mice. *Nature* 445, 106–110. doi: 10.1038/nature05372

Prasetyanti, P. R., and Medema, J. P. (2017). Intra-tumor heterogeneity from a cancer stem cell perspective. *Mol. Cancer* 16:41. doi: 10.1186/s12943-017-0600-4

Qiu, J., Zhang, S., Wang, P., Wang, H., Sha, B., Peng, H., et al. (2020). BUB1B promotes hepatocellular carcinoma progression via activation of the mTORC1 signaling pathway. *Cancer Med.* 9, 8159–8172. doi: 10.1002/cam4.3411

Quan, L., Qian, T., Cui, L., Liu, Y., Fu, L., and Si, C. (2020). Prognostic role of minichromosome maintenance family in multiple myeloma. *Cancer Gene Ther.* 27, 819–829. doi: 10.1038/s41417-020-0162-2

Ritchie, M. E., Phipson, B., Wu, D., Hu, Y., Law, C. W., Shi, W., et al. (2015). limma powers differential expression analyses for RNA-sequencing and microarray studies. *Nucleic Acids Res.* 43:e47. doi: 10.1093/nar/gkv007

Röllig, C., Knop, S., and Bornhäuser, M. (2015). Multiple myeloma. *Lancet* 385, 2197–2208. doi: 10.1016/s0140-6736(14)60493-1

Saygin, C., Matei, D., Majeti, R., Reizes, O., and Lathia, J. D. (2019). Targeting cancer stemness in the clinic: from hype to hope. *Cell Stem Cell* 24, 25–40. doi: 10.1016/j.stem.2018.11.017

Seguin, L., Desgrosellier, J. S., Weis, S. M., and Cheresh, D. A. (2015). Integrins and cancer: regulators of cancer stemness, metastasis, and drug resistance. *Trends Cell Biol.* 25, 234–240. doi: 10.1016/j.tcb.2014.12.006

Shi, L., Campbell, G., Jones, W. D., Campagne, F., Wen, Z., Walker, S. J., et al. (2010). The MicroArray Quality Control (MAQC)-II study of common practices for the development and validation of microarray-based predictive models. *Nat. Biotechnol.* 28, 827–838. doi: 10.1038/nbt.1665

Singh, S. K., Hawkins, C., Clarke, I. D., Squire, J. A., Bayani, J., Hide, T., et al. (2004). Identification of human brain tumour initiating cells. *Nature* 432, 396–401. doi: 10.1038/nature03128

Sokolov, A., Paull, E. O., and Stuart, J. M. (2016). ONE-CLASS DETECTION OF CELL STATES IN TUMOR SUBTYPES. *Pac. Symp. Biocomput.* 21, 405–416.

Wan, X., Yeung, C., Kim, S. Y., Dolan, J. G., Ngo, V. N., Burkett, S., et al. (2012). Identification of FoxM1/Bub1b signaling pathway as a required component for growth and survival of rhabdomyosarcoma. *Cancer Res.* 72, 5889–5899. doi: 10.1158/0008-5472.Can-12-1991

Wang, T., Fahrmann, J. F., Lee, H., Li, Y. J., Tripathi, S. C., Yue, C., et al. (2018). JAK/STAT3-regulated fatty acid β-oxidation is critical for breast cancer stem cell self-renewal and chemoresistance. *Cell Metab.* 27, 136–150.e135. doi: 10.1016/j.cmet.2017.11.001

Wilkerson, M. D., and Hayes, D. N. (2010). ConsensusClusterPlus: a class discovery tool with confidence assessments and item tracking. *Bioinformatics* 26, 1572–1573. doi: 10.1093/bioinformatics/btq170

Yang, Y., Gu, C., Luo, C., Li, F., and Wang, M. (2015). BUB1B promotes multiple myeloma cell proliferation through CDC20/CCNB axis. *Med .Oncol.* 32:81. doi: 10.1007/s12032-015-0542-x

Yoshihara, K., Shahmoradgoli, M., Martínez, E., Vegesna, R., Kim, H., Torres-Garcia, W., et al. (2013). Inferring tumour purity and stromal and immune cell admixture from expression data. *Nat. Commun.* 4:2612. doi: 10.1038/ncomms3612

Zhan, F., Huang, Y., Colla, S., Stewart, J. P., Hanamura, I., Gupta, S., et al. (2006). The molecular classification of multiple myeloma. *Blood* 108, 2020–2028. doi: 10.1182/blood-2005-11-013458

Zhang, C., Chen, T., Li, Z., Liu, A., Xu, Y., Gao, Y., et al. (2020). Depiction of tumor stemlike features and underlying relationships with hazard immune infiltrations based on large prostate cancer cohorts. *Brief Bioinform.* 22:bbaa211. doi: 10.1093/bib/bbaa211

Zhou, Y., Zhou, B., Pache, L., Chang, M., Khodabakhshi, A. H., Tanaseichuk, O., et al. (2019). Metascape provides a biologist-oriented resource for the analysis of systems-level datasets. *Nat. Commun.* 10:1523.

Conflict of Interest: The authors declare that the research was conducted in the absence of any commercial or financial relationships that could be construed as a potential conflict of interest.

Publisher's Note: All claims expressed in this article are solely those of the authors and do not necessarily represent those of their affiliated organizations, or those of the publisher, the editors and the reviewers. Any product that may be evaluated in this article, or claim that may be made by its manufacturer, is not guaranteed or endorsed by the publisher.

frontiers in Cell and Developmental Biology

ORIGINAL RESEARCH
published: 29 October 2021
doi: 10.3389/fcell.2021.744969

Preclinical Application of Conditional Reprogramming Culture System for Laryngeal and Hypopharyngeal Carcinoma

Yanbo Dong[1†], Jian Wang[2†], Wei Ji[1], Mengzhu Zheng[2], Peng Wang[2], Liangfa Liu[1‡] and Shanhu Li[2*‡]*

[1] Department of Otolaryngology Head and Neck Surgery, Beijing Friendship Hospital, Capital Medical University, Beijing, China, [2] Department of Cell Engineering, Beijing Institute of Biotechnology, Beijing, China

OPEN ACCESS

Edited by:
Nikhil Baban Ghate,
University of Southern California,
United States

Reviewed by:
Xuefeng Liu,
Georgetown University, United States
Sourav Panja,
Vanderbilt University Medical Center,
United States

***Correspondence:**
Liangfa Liu
liuliangfa301@163.com
Shanhu Li
lishanhu6@163.com

[†] These authors have contributed equally to this work and share first authorship

[‡] These authors have contributed equally to this work

Specialty section:
This article was submitted to Stem Cell Research, a section of the journal Frontiers in Cell and Developmental Biology

Received: 21 July 2021
Accepted: 11 October 2021
Published: 29 October 2021

Citation:
Dong Y, Wang J, Ji W, Zheng M, Wang P, Liu L and Li S (2021) Preclinical Application of Conditional Reprogramming Culture System for Laryngeal and Hypopharyngeal Carcinoma. Front. Cell Dev. Biol. 9:744969. doi: 10.3389/fcell.2021.744969

Management of laryngeal and hypopharyngeal squamous cell carcinoma (LHSCC) remains highly challenging due to highly variable therapeutic responses. By establishing an *in vitro* model for LHSCC based on conditional reprogramming (CR), a cell-culture technique, we aim to investigate its potential value on personalized cancer therapies. Herein, a panel of 28 human LHSCC CR cells were established from 50 tumor tissues using the CR method. They retained tumorigenic potential upon xenotransplantation and recapitulated molecular characteristics of LHSCC. Differential responses to anticancer drugs and radiotherapy were detected *in vitro*. CR cells could be transformed to xenograft and organoid, and they shared comparable drug responses. The clinical drug responses were consistent with *in vitro* drug responses. Collectively, the patient-derived CR cell model could promisingly be utilized in clinical decision-making and assisted in the selection of personalized therapies for LHSCC.

Keywords: conditional reprogramming, head and neck squamous cell carcinoma, *in vitro* model, drug sensitivity, personalized treatment

INTRODUCTION

Malignant tumors arising from the epithelium of the larynx and hypopharynx are predominantly squamous cell carcinomas, constituting the most frequent malignancies of head and neck squamous cell carcinomas (HNSCC). The management of LHSCC remains very challenging due to highly variable treatment response to radiotherapy and chemoradiation therapy. Insensitive to radiotherapy or chemotherapy frequently occurs, one of the significant causes of tumor recurrence, and is associated with poor outcome. Thus, identifying a precise and optimal treatment strategy for individual patients is highly desirable.

Conditional reprogramming (CR) system is a platform to establish a long-term culture of primary epithelium cells derived from normal and tumor tissues (Liu et al., 2012, 2017). The reported advantages of CR include high success rate, exponential growth, genotype stability, and ease of manipulation. These characteristics enabled CR as an exceptional *in vitro* model compared with the others, such as patient-derived xenotransplantation (PDX) and organoids. Owing to these advantages, CR has been documented by two American National Cancer Institute programs: patient-derived cancer model repository (PDMR) and human cancer model initiatives (HCMI)

(Palechor-Ceron et al., 2019). Potential applications of the CR system in clinical settings have been investigated in breast (Mahajan et al., 2017), lung (Gao et al., 2017), prostate (Saeed et al., 2017), bladder (Kettunen et al., 2019), gastric (Zhao et al., 2021), and liver (Su et al., 2019) cancers. Recently, Liu et al., have also established one primary cell line using CR system derived from tongue squamous cell carcinoma, a type of head and neck cancer (Palechor-Ceron et al., 2019). However, long-term culture of laryngeal and hypopharyngeal tissues using CR system has not been reported. Although the CR system is robust, the application of CR cell lines was lack of evidence since much focus was on the establishment methods. Moreover, the clinical relationship of CR has not been completely validated.

The present study established a primary culture system that enabled the rapid amplification of genetically stable LHSCC cells with a high success rate. As a versatile *in vitro* model, CR could be transformed into organoids and be used to produce CR-derived xenografts. Both systems share comparable drug responses. This study aims to provide a preliminary investigation into the relationship between *in vitro* CR cell responses and clinical responses, which may contribute to its potential clinical implications.

MATERIALS AND METHODS

Experimental Design

This prospective observational study was conducted on patients with laryngeal or hypopharyngeal cancer who received treatment at the Beijing Friendship Hospital, Capital Medical University, between September 2018 and November 2020. This study was approved by the human research Ethics Committee of Beijing Friendship Hospital, Capital Medical University (Batch number: 2018-P2-198-01). The study was conducted in accordance with the Declaration of Helsinki and Chinese Law provisions and adhered to Good Clinical Practice guidelines. According to the Response Evaluation Criteria in Solid Tumors (RECIST) criteria, patients' clinical responses were assessed by experienced radiologists and physicians. Written informed consent was obtained from the patients and/or their authorized representatives. Inclusion criteria were as follows: primary or recurrent histologically confirmed LHSCC patients; aged above 18 years old; and fresh tissue available through either biopsy or surgical resection of the primary tumor site. Patients with cognitive impairment, mental health disorders, poor compliance, or allergic to chemotherapeutic agents were excluded. The CR cell viability and the clinical response were evaluated by technicians and clinicians double-blinded, respectively. All human tissue samples were obtained from diagnostic biopsies or therapeutic resections. Prior to surgery or biopsy, each patient signed written informed consent, allowing the excess tissue to be used for research studies.

Tissue Processing

Upon receipt of fresh tissue, the tissue sample was into three parts for cryopreservation, fixation, and digestion for primary cell derivation. For histology, a piece was removed and immediately fixed in formalin. The fixed tissue was processed and embedded in paraffin as described previously (Driehuis et al., 2019). For primary cell culture, tissue samples were minced and incubated at 37°C in 0.125% Trypsin (Sigma, catalog no. T1426) with high glucose DMEM (Life Technologies, catalog no. 12430-054) until digested. The tissue suspension was frequently agitated and monitored for up to 60 min. The suspension was strained through a 100 μm filter, centrifuged at 300 × *g* and lysed with blood cell lysis buffer for 5 min. After washing twice with PBS, the resulting pellet was resuspended in Complete F medium and seeded in the CR culture system.

Conditional Reprogramming Culture

Mouse embryonic fibroblast cell line 3T3-J2 (RRID:CVCL_W667; purchased from Otwo Biotech, Shenzhen, China) was cultured in complete DMEM with high glucose supplemented with 10% (v/v) FBS (Life Technologies) and 100 IU/ml penicillin, and 100 mg/ml streptomycin. In the CR system, 3T3-J2 were mitotically inactivated either by irradiation or by mitomycin C-treatment (2.5 h, 4 mg/ml final concentration, Sigma-Aldrich). Primary LHSCC cells were cultured in Complete F medium (**Table 1**) at 37°C in a 5% CO_2 humidified incubator. The medium was renewed every 2 days. The cell numbers of every passage were checked by a cell counter plate.

Conditionally Reprogrammed Cell Derived Organoid Culture

The primary cells were collected from the CR culture system when the cells reached 70–80% confluence; the feeder cells were removed following trypsinization for 1-min. The cells at an indicated count were mixed with ice-cold Matrigel and then were loaded in the center of the well of the culture plate. After polymerization by incubating at 37°C for 30 min, a prewarmed organoid medium was added to the plate. The medium was changed every alternate day. The main organoid culture methods and composition of the organoid medium were as previously described (Driehuis et al., 2019).

TABLE 1 | Formulation of complete F media.

Component	≈200 mL
Complete DMEM[1]	146 mL
F12 nutrient mixture	49 mL
Primocin	0.2 mL
EGF (10 μg/ml in PBS)	0.2 mL
Insulin (5 mg/ml in PBS)	0.2 mL
Rock inhibitor Y-27632 (10 mM in DMSO)	0.2 mL
Hydrocortisone (0.5 mg/ml in DMSO)	10 uL
Cholera toxin (8.4 μg/ml in distilled water)	0.2 mL
Adenine (2.4 mg/mL in 0.05M HCl)	2 mL
Glutamax (100×)	2 mL

[1]*Complete DMEM contains DMEM with 10% fetal bovine serum, 100 μg/ml penicillin and 100 μg/ml streptomycin.*

Immunofluorescence Staining

For histological examination, excised patient tissues or heterotransplanted tumors from nude mice were fixed overnight in 4% formaldehyde, dehydrated, and embedded in paraffin and followed with deparaffinization and standard hematoxylin & eosin (H&E) staining. Images were acquired on an inverted microscope (TH4-200, Olympus Optical Co., Ltd., Tokyo, Japan). Cells slides were used for indirect immunofluorescence. Briefly, cells were seeded into a 24-well plate with round cover slides (a diameter of 1 cm) in the well. After reaching 60–80% confluence, cell slides were fixed in paraformaldehyde for 15 min and acetone successively. After fixation, heat-induced antigen retrieval was performed using either citric acid solution or a microwave. The slides were then permeabilized with 0.1% Triton X-100 (Sigma) for 10 min and blocked with 1% (w/v) bovine serum albumin (BSA) for 1 h at room temperature. Following incubation overnight at 4°C with a primary antibody (anti-pan-keratin, proteintech, 26411-1-AP; anti-CD44, proteintech, 15675-1-AP), the cells were washed with PBS and incubated with secondary antibodies (Invitrogen) at room temperature for 1 h. The cells were then incubated with indicated additional stains (DAPI, life technologies D1306) for 5 min at room temperature. The samples were analyzed using a confocal microscope (LSM 880; Carl Zeiss, Germany). For immunofluorescence staining of the organoids, the whole mount staining method was performed as described previously (Hu et al., 2018). Primary antibodies used for organoids included anti-KRT5 (Santa Cruz Biotechnology; sc-32721) and anti-p63 (Abcam; ab124762). Secondary antibodies included goat anti-rabbit IgG (Alexa Fluor 594; Invitrogen; CA11012s) and goat anti-mouse IgG (Alexa Fluor 488; Invitrogen, CA11001).

Short Tandem Repeat Amplification

Genomic DNA was extracted from cells at different passages using a DNA extraction kit (AP-MN-MS-GDNA-50; Axygen, Union City, CA, United States). A total of 21 short tandem repeat (STR) loci, including D5S818, D13S317, D7S820, D16S539, VWA, TH01, TPOX, CSF1PO, D12S391, FGA, D2S1338, D21S11, D18S51, D8S1179, D3S1358, D6S1043, PENTAE, D19S433, PENTAD, D1S1656, and Amelogenin were amplified. The fragments were amplified using PCR and separated by capillary electrophoresis using Applied Biosystems® (ABI) 3730xl Genetic Analyzer (Applied Biosystems, Foster City, CA, United States), and data were automatically analyzed with the GeneMapper Software v3.2 (Applied Biosystems, Foster City, CA, United States).

In vitro Drug Screening

The cells at a density of 2,000 cells/well were seeded into 96-well culture plates. After 24 h, the cells were treated with different concentrations of the drugs. Control cultures received an equal amount of DMSO (0.01 to 0.1%). 72 h after treatment. The number of viable cells was estimated by using the CCK8 assay with a slight modification. Specifically, cells treated with different concentrations of the drugs were washed twice with PBS, and then CCK8 solution (100 μL, 10 mg/mL) (Dojindo) was added into each well at 37°C for 2 h. Following incubation, the absorbance (optical density) was measured at 450 nm using a microplate reader (Thermo Scientific Multiskan FC). The values were normalized to the vehicle (100%) and baseline control (0%). For each test, if the calculated cell viability was higher than 70% or lower than 30%, an additional screen was performed for that particular drug with an adjusted dose of the drug for the cell line. *Z* factor score was used as the parameter for screen quality assessment using the following equation:

$$Z\ score = 1 - \frac{3 \times \mathrm{SD(sample)} + 3 \times \mathrm{SD(negative\ control)}}{\left|Average(\mathrm{sample}) - Average(\mathrm{negative\ control})\right|}$$

Drug screens with a Z score of less than 0.3 were not used and repeated. Kill curves were generated using GraphPad® PRISM version 9.0 (Graph Pad Software, Inc., La Jolla, CA, United States), and the curves were fitted using the log (Inhibitor) vs. response – Variable slope (four parameters). The half-maximal inhibitory concentration (IC50), which is an essential indicator for drug sensitivity assay, was calculated by non-linear regression of the log of concentration versus the percentage of survival, implemented in GraphPad.

Radiation Sensitivity

The cells at a density of 2,000 cells/well were seeded in 96-well culture plates. After 24 h, cells were irradiated. The γ-ray irradiation was performed from a cobalt-60 source at a dose rate of 0.59 Gy/min at room temperature. A separate plate was used for each radiation dose. Plates were sealed air-tight and irradiated with a single fraction of 2, 4, 6, 8, and 10 Gy. After radiation, the medium was changed. Six days later, cell viability was measured using CCK8 assay. Kill curves were graphed following the method described above.

Colony Formation Assay

The cells were seeded into six-well culture plates immediately after exposure to 0 Gy and 4 Gy of γ-ray irradiation. After 7 days of incubation, the colonies were fixed in paraformaldehyde and stained with crystal violet solution. Colonies containing more than 50 cells were counted; the relative colony-forming efficiency was calculated and plotted.

Whole-Exome Sequencing and Bioinformatics Analysis

Whole-exome sequencing data were mapped against human reference genome GRCh37, and variants were called using the IAP pipeline[1]. To identify somatic genomic variants associated with laryngeal and hypopharyngeal cancer, WES was conducted on three paired normal/tumor CR cell lines following the protocol previously described (Li et al., 2019). We filtered out somatic single-nucleotide variations (SNVs), somatic InDels and copy number variants of tumor cells with evidence in their corresponding normal controls. The following genes were detected as cancer-associated genes and screened for all detected somatic genomic variants including, ABL1,

[1]https://github.com/UMCUGenetics/IAP

ADAMTS12, AKT1, ALK, APC, ATM, ATR, BRAF, CASP8, CCND1, CDH1, CDH12, CDKN2A, COL1A2, COL22A1, CSF1R, CSMD3, CTNNB1, DICER1, EGFR, ERBB2, ERBB4, ESR1, EZH2, FAT1, FBXW7, FGFR1, FGFR2, FGFR3, FLT3, GNA11, GNAQ, GNAS, GRM8, HNF1A, HRAS, IDH1, IDH2, IRF6, JAK2, JAK3, KDR, KIT, KRAS, MDM2, MED1, MET, MLH1, MLL2, MPL, NAV3, NOTCH1, NOTCH2, NOTCH3, NPM1, NRAS, OR4C15, PDGFRA, PIK3CA, PKHD1L1, PRB4, PRDM9, PTEN, PTPN11, RB1, RET, RIMS2, RIPK4, SI, SLC2A13, SMAD4, SMARCB1, SMO, SRC, STK11, SYNE1, SYNE2, TP53, TP63, USH2A, and VHL.

Heterotransplantation in Nude Mice and *in vivo* Treatment Studies

Animal experiments were approved by the Institutional Animal Care and Use Committee of Beijing Institute of Biotechnology (Ethics approval code IACUC-DWZX-2019-517, approved in May 2019). Four to 5-week-old female BALB/C-nude mice were procured from SPF (Beijing) Biotechnology Co., Ltd. Mice were cared for in accordance with the National Institute of Health (NIH) Guide for the Care and Use of Laboratory Animals. The mice were housed under specific pathogen-free conditions, at a temperature of 24°C with a relative humidity of 50–60%, under a 12-h-light/12-h-dark schedule. Animals were provided *ad libitum* access to standard rodent food and tap water. Mice were subcutaneously injected with 5 × 106 of primary cancer cells in the right flank (0.2 mL cell suspension per mouse). Six weeks after tumor cell inoculation, tumors were removed, and tumor tissues were fixed in 4% formaldehyde, embedded in paraffin, and subjected to an H&E staining procedure.

For *in vivo* treatment assay, tumor-bearing mice were established following the above-mentioned method. When tumors reached approximately 200 mm^3, the mice were randomized into three groups ($n \geq 3$/group) according to tumor volumes and body weights. The treatments included vehicle control, 4 mg/kg cisplatin by intraperitoneal (i.p.) injection twice a week, 5FU (100 mg/kg/week; i.p.), and paclitaxel (30 mg/kg/week; i.p.). Tumor volumes were measured using an electronic Vernier caliper and calculated with the formula $V = \pi(\text{length} \times \text{width}^2)/6$. On the 28th day after the first treatments, mice were weighed and then euthanized with CO_2 asphyxia. Subsequently, the tumors were harvested, weighed, and photographed.

Statistical Analysis

Statistical analysis was performed using GraphPad Prism 9.0 (GraphPad Software, Inc). All *in vitro* experiments were performed in triplicate and repeated three times. Data were expressed as mean ± standard deviation (SD). A two-tailed Student *t*-test was used to analyze differences between two groups. One-way analysis of variance (ANOVA) with Bonferroni correction was used to analyze multiple groups. The mean ± standard deviation was presented in all graphs, and raw data points were indicated. *P*-values of < 0.05 were considered statistically significant.

RESULTS

Establishment of Patient-Derived Matched Primary Normal and Laryngeal and Hypopharyngeal Squamous Cell Carcinoma Conditional Reprogramming Cells

We obtained normal and tumor samples from patients with a histopathologically confirmed diagnosis of laryngeal or hypopharyngeal squamous cell carcinoma. The media compositions were optimized to propagate primary cells based on the published protocols for CR (Liu et al., 2017). Conditions that were successful in growing breast and prostate epithelium were refined on head and neck tissues. Briefly, the epithelial layer from the surgical specimen was microdissected to eliminate fat and muscle, digested in trypsin, and filtered. The resulting cell suspension was then seeded onto an NIH-3T3 fibroblast feeder layer in Complete F Medium (**Figure 1A**). The detailed composition of Complete F Medium was listed in **Table 1**. Within the first few days after inoculation, the adherent LHSCC cells exhibited small colonies and progressed into cell islands. As illustrated in **Figure 1B**, the normal conditionally reprogrammed cells (CRCs) formed tight colonies surrounded by feeder cells, similar to the previously established CR cell lines (Liu et al., 2012; Palechor-Ceron et al., 2013). CRCs were organized in a regular arrangement and exhibited a heterogeneous cell population composed of small, dark, hexagonal cells and some large and flat cells (Palechor-Ceron et al., 2019). In contrast, malignant cells displayed a unique phenotype consisting of larger individual cells with prominent intercellular junctions and a highly homogenous population of dark, hexagonal cells (Palechor-Ceron et al., 2019). **Supplementary Figure 1** depicted the phase-contrast images of the six CRCs at different passages.

We received biopsy or surgical samples from 50 patients with LHSCC, intending to establish matched normal and tumor CRCs. Patient clinical characteristic data corresponding to established LHSCC CR cell lines was summarized in **Supplementary Table 1**. The median age of the patients was 63.7 years. Clinically, 74% (37/50) of patients exhibited T3/T4 grade tumors, according to the American Joint Committee on Cancer (AJCC, 8th edition, 2017). Additionally, 44% (22/50) of patients had lymph node metastasis. Tumor and normal CRCs were established from 56% (28/50) and 71.4% (30/42) patients, respectively (**Table 2**). The established criteria for CRC were long-term (>10 passages) proliferation and successful cryopreservation and recovery. These tumor CRCs were designated as T1, T2, T3, and so on, and the corresponding normal epithelium-derived CRCs were indicated by N1, N2, N3, and so on.

The histological features were compared between CRCs and original tumors using H&E sections. CRCs exhibited similar histological patterns to their original tumors (**Figure 1B**). In consideration of the heterogeneity of tumor tissues, the purity of epithelial-derived cells in CRCs was evaluated using immunofluorescence. Pan-keratin was used as an epithelial marker. Positive staining of pan-keratin was found in all

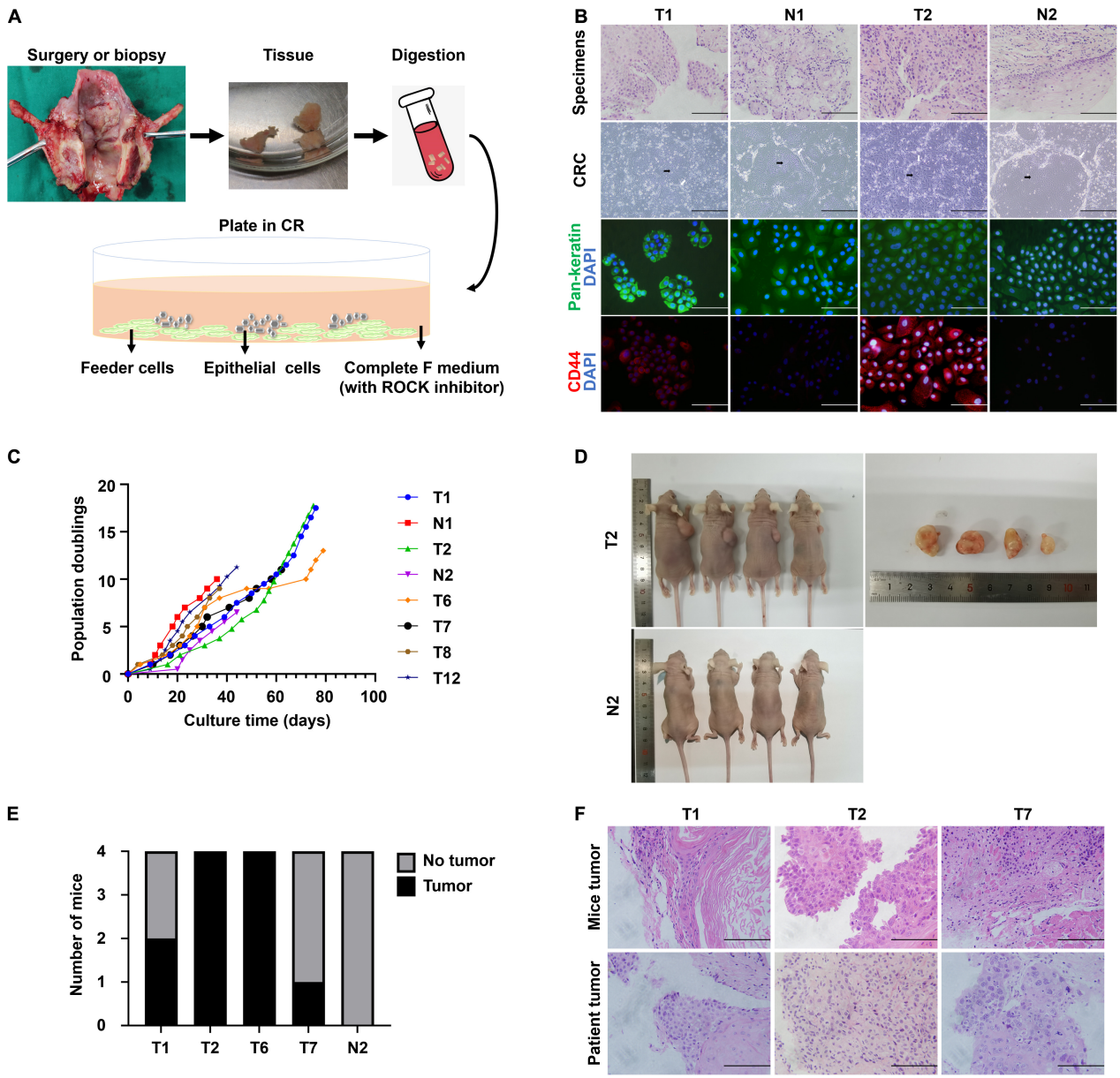

FIGURE 1 | The establishment of CR system from patient-derived tissues and the characteristics of CRC lines. **(A)** Schematic representation of the digestion and initial culture condition of CRCs. Tissue obtained via biopsy or resection was collected, minced, digested using trypsin, and subsequently inoculated. **(B)** Hematoxylin and eosin (H&E) staining of primary tissue of T1, N1, T2, and N2, bright-field microscopic images of the corresponding CRCs, and immunofluorescence for pan-keratin and CD44 markers of corresponding cell slides. Black arrow, conditionally reprogrammed cells. White arrow, feeder cells. Scale bars for HE staining and immunofluorescence images, 125 μm. Scale bars for bright-field microscopy images, 500 μm. **(C)** The CRC lines were passaged repeatedly and continued to proliferate with a steady growth rate. The cell number was recorded at each passage, and a plot of population doublings versus time (days) was constructed. **(D)** Representative images of mice bearing tumors and the dissected tumors were shown. **(E)** Four independent mice were injected subcutaneously with 4 tumor CRC lines and 1 normal CRC line, and the number of mice developing tumors was depicted. **(F)** Hematoxylin and eosin (H&E) stained images of mice tumors resembled those of the corresponding patient tumors.

cells (**Figure 1B**). The expression of CD44, a well-known stem cell marker for head and neck cancer (Leinung et al., 2015), was higher in tumor CRCs than in its matched normal CRCs (**Figure 1B**).

Conditional reprogramming method conditionally induces long-term and stable proliferation. On average, CRC could form small colonies within 2–5 days and be passaged within 5–7 days. After the first passage, CRC typically proliferated at a stable rate, being passaged every 2–5 days with a split ratio of 1:2. For instance, as shown in **Figure 1C**, primary cells were growing at different rates, which were passaged every 2–7 days after reaching confluence in CR co-culture and continued to proliferate at a steady rate for at least 40 days with 10 population doublings till the end of the experiment. STR analysis confirmed that the

TABLE 2 | Success rate of CRC culture.

Specimen	Growth (%)
Tumor tissue	28/50 (56%)
Larynx	20/32 (62.5%)
Hypopharynx	8/18 (44.4%)
Normal tissue	30/42 (71.4%)
Total	58/92 (63.0%)

primary cells were genetically stable up to a span of around 10 passages (**Table 3**).

The tumorigenic potential of the cultured LHSCC cells was evaluated by subcutaneous transplantation of the tumor CSCs into nude mice. Transplantation in all four tumor lines yielded macroscopically visible tumors after 6 weeks in at least 1 of 4 mice (n = 4 for each CRC line; **Figures 1D,E**), while injection with the normal CSCs did not result in outgrowth. H&E staining of the tumors revealed stratification and keratinization characteristics of LHSCC (**Figure 1F**). The tumor cells exhibited atypia, as observed in cancerous cells. Nuclear pleomorphism was also observed. Besides, muscle invasion was detected in one case. Together, LHSCC CRC lines retain tumorigenic potential and form xenografts with similar characteristics to the parental tumor.

Conditionally Reprogrammed Cell as a Platform for Chemotherapy and Radiotherapy Sensitive Assay

We exposed multiple CRC lines to cisplatin, 5FU, paclitaxel, and cetuximab, drugs currently used to treat patients with LHSCC. The *in vitro* concentration was based on the peak exposures observed at the highest clinically recommended doses delivered as a single administration (Liston and Davis, 2017). We observed differential sensitivity of the CRC lines to these compounds (**Figures 2A–D**). Based on the measured IC50 values, we ranked the CRC lines tested for cisplatin, 5FU, and paclitaxel (**Figures 2A–C**). For the sensitivity of cetuximab, the area under the curve (AUC) was applied as an alternative to IC50 values because the curvature of the kill curve was not suitable to calculate IC50 (**Figure 2D**). To assure the quality of the drug screening experiments, a Z-score, a parameter of assay quality (Zhang et al., 1999), was implemented and calculated for each drug screen (**Figure 2E**). The average Z-score was 0.84 (0.61–0.98), indicating an experimentally robust assay. To ensure the consistency of drug response between cells of different passages, 4 CRC lines in different passages were treated with cisplatin. Kill curves of the same CRC line in different passages resembled each other very well (**Figure 2F**).

Radiotherapy is another major treatment modality for LHSCC. Thus, we investigated the sensitivity of CRCs to ionizing radiation. Kill curves of radiotherapy were drawn, and AUC values were calculated and ranked among the five tested CRC lines (**Figure 2G**). Differential radiotherapy responses were observed among the CRC lines. The findings suggested that CRCs had the potential to reflect patients' clinical responses to radiotherapy.

Tumor Conditionally Reprogrammed Cells Recapitulate Genetic Alterations Identified in Laryngeal and Hypopharyngeal Squamous Cell Carcinoma

To determine whether the CRCs recapitulated genetic alterations found in LHSCC, whole-exome sequencing was conducted on matched tumor and normal CRCs from 3 patients with LHSCC. In general, the mean sequencing depth was 96.34×, and a mean of 90.99% of the target sequence was covered to a depth of at least 20× (**Table 4**). The somatic mutation load per subject varied significantly in LHSCC (mean 208, range 187–248; **Figure 3A**). The spectrum of mutations was also illustrated in **Figure 3B**.

A mutation lists were filtered for those genes that are most commonly affected in LHSCC (Stransky et al., 2011). We scrutinized all single nucleotide variants (SNV) and small insertions or deletions (Indels) throughout the genome in the tumor and normal CRC lines. Using this criterion, we detected pathogenic mutations in 2, 5, and 7 LHSCC cancer-associated genes, in T1, T2, and T7 lines, respectively (**Figure 3C**). The tumor CRC lines also revealed SNVs and Indels that were absent from the normal CRC lines. The most commonly mutated gene in LHSCC, TP53, was genetically altered in 2 of the 3 tumor lines. The other tumor line, though without TP53 mutation, exhibited the mutation of MDM2, an oncogene encoding protein MDM2 binding and inhibiting P53. Thus, all the 3 tumor lines suffered from the functional alteration of P53. NOTCH1 was

TABLE 3 | STR analysis of three representative CRCs at different passages.

Cell lines	STR alleles									AMEL
	D5S818	D13S317	D7S820	D16S539	VWA	TH01	D21S11	TPOX	CSF1PO	
T1 P5	10 13	9 12	8 12	9 9	16 19	9 9	29 29	8 8	9 11	X Y
T1 P15	10 13	9 12	8 12	9 9	16 19	9 9	29 29	8 8	9 11	X Y
T3 P3	11 12	8 12	9 10	9 12	16 18	6 8	28 31.2	8 11	11 11	X Y
T3 P12	11 12	8 12	9 10	9 12	16 18	6 8	28 31.2	8 11	11 11	X Y
T12 P2	13 13	9 10	8 9	9 12	18 18	7 9	30 30	11 12	11 12	X Y
T12 P12	13 13	9 10	8 9	9 12	18 18	7 9	30 30	11 12	11 12	X Y

P, passage.

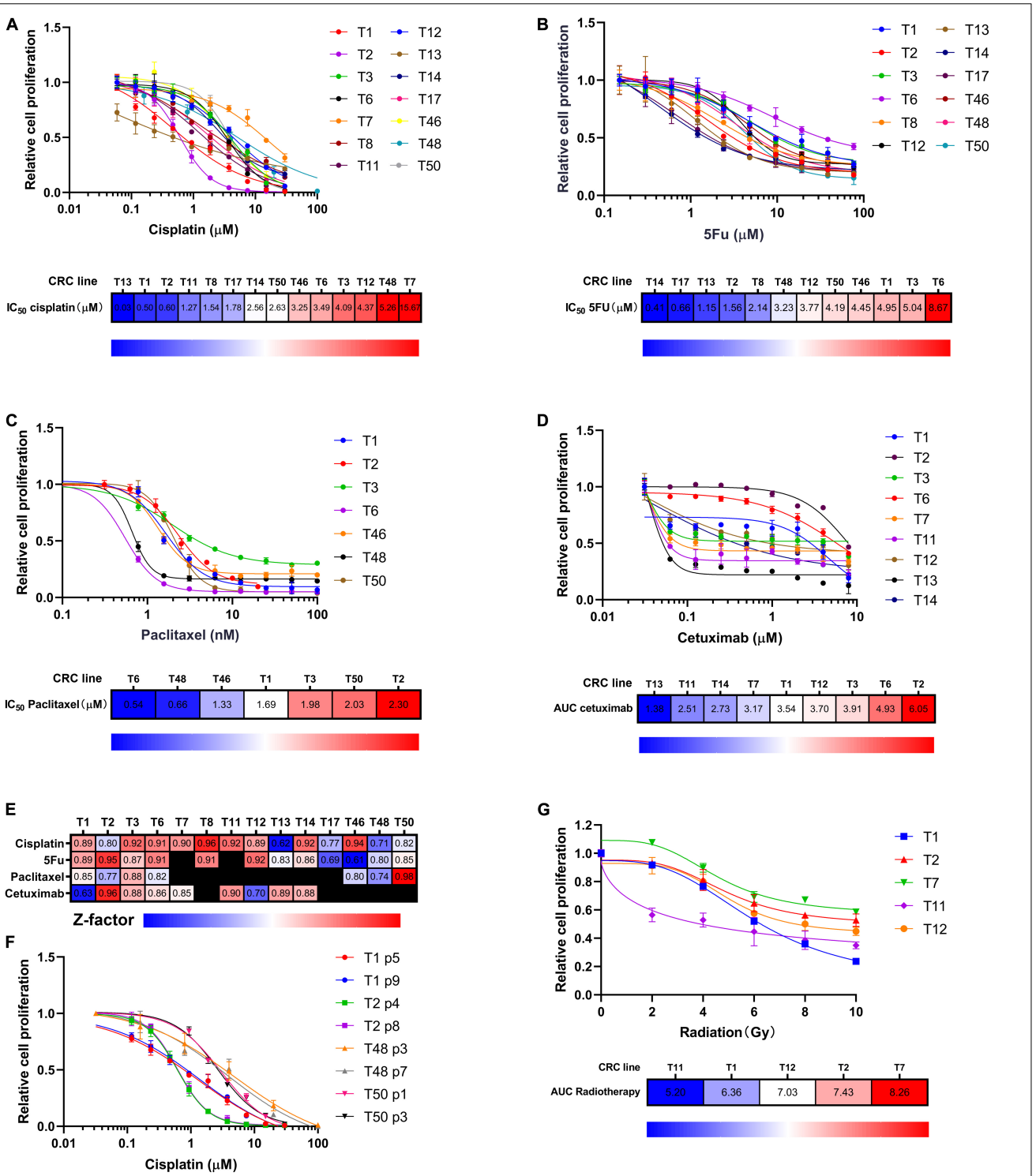

FIGURE 2 | CRC lines as a platform for chemotherapy and radiotherapy sensitivity assay. **(A–C)** CRC lines revealed variable sensitivity to cisplatin, 5FU, and paclitaxel. Relative cell proliferation was plotted on the *y*-axis for different concentrations of drugs (*x*-axis). Heat maps indicated the CRCs ranking according to drug IC50. Red indicated high IC50 values; blue indicated low IC50 values. **(D)** CRC lines exhibited variable sensitivity to cetuximab. Relative cell proliferation was plotted on the *y*-axis for different concentrations of cetuximab (*x*-axis). Heat map showing the CRC lines ranked based on cetuximab sensitivity as measured by AUC. Red indicated high AUC values; blue indicated low AUC values. **(E)** Heat map showing Z factor scores of the performed drug screens for all drugs and all CRC lines presented in this study. **(F)** The consistency of cisplatin killing effects among different-passage CRC lines. 4 CRC lines were used to compare. **(G)** CRC lines revealed differential sensitivity to radiation. Relative cell proliferation was plotted on the *y*-axis for different amounts of radiation, ranging from 0 to 10 Gy (*x*-axis). Heat map showing the CRC lines ranked according to radiotherapy sensitivity as measured by AUC. Red indicated high AUC values; blue indicated low AUC values.

TABLE 4 | Summary of whole-exome sequencing data of six CR cell lines.

Sample	Average sequencing depth on target	Mapping rate on genome[1] (%)	Fraction of target covered ≥ 10x (%)	Fraction of target covered ≥ 20x (%)
N1	93.08	99.84	96.45	91.28
T1	113.06	99.89	96.86	92.43
N2	92.59	99.85	96.25	90.79
T2	101.48	99.88	96.26	90.81
N6	79.18	99.8	95.76	89.27
T6	98.67	99.88	96.38	91.35
Average	96.34	99.86	96.33	90.99

[1]*Based on NCBI human reference genome GRC Build 37 (hg19).*

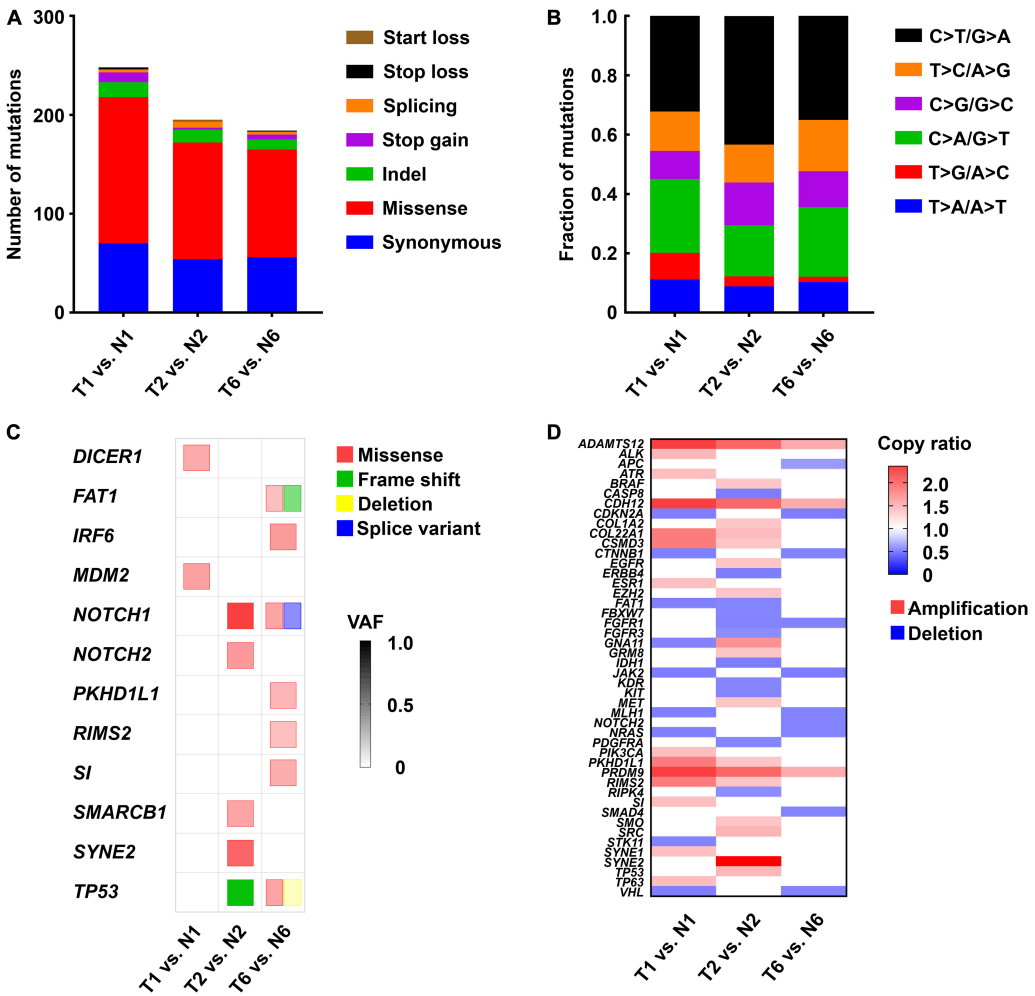

FIGURE 3 | Genetic alterations identified by whole-exome sequencing in 3 paired tumor and normal CRC lines. **(A)** The number and type of somatic mutations. **(B)** The spectrum of mutations in LHSCC. **(C)** Mutations detected in LHSCC-derived CRCs that were sequenced using whole-exome sequencing. The color of the square indicated the type of mutation detected: missense (red), frameshift (green), deletion (yellow), splice variant (blue). Color intensities indicated the variant allele frequency (VAF) of the detected genetic alteration. **(D)** Heat map of copy number variant (CNV) of tumor-associated genes. Red indicated amplification with copy ratio > 1; blue indicated deletion with copy ratio < 1.

altered in 2 of the 3 CRC lines. Genes affected in one case include DICER1, FAT1, IRF6, MDM2, NOTCH2, PKHD1L1, RIMS2, SI, SMARCB1, and SYNE2. In the T6 line, we sequenced different mutation types in FAT1, NOTCH1, and TP53, such as missense, frameshift, deletion, or splice variant. Normal CRC lines lacked these genetic alterations, confirming they consisted of non-tumor cells. The copy number variants of cancer-associated genes were also represented in **Figure 3D**.

TP53 gene loci of the above CRC lines were sequenced. In detail, T1 exhibited no TP53 mutation. T2 harbored TP53 exon deletion mutation; T6 harbored TP53 exon deletion mutation and a distinct SNV, Pro72Arg, which was a defined bad mutational status indicating cisplatin-resistance (Bergamaschi et al., 2003). According to previous studies, resistance to cisplatin-based chemotherapy was positively correlated with the TP53 mutation burden (Bergamaschi et al., 2003). T1, T2, and T6 CRC lines were used to test the cisplatin treatment sensitivity. We found that CRC line T1 had the lowest IC50 than the others. Notably, T6 with two TP53 mutations propagated better than T2 with a single TP53 mutation under the same concentration of cisplatin, indicating that T6 was resistant to cisplatin treatment, and T2 was relatively sensitive to cisplatin (**Figure 2A**). These findings suggested that whole-exome sequencing and CRC lines derived from patient samples could predict response or resistance to individual therapy and could be used to evaluate target therapy based on gene mutation.

Relationship of Drug Responses Between *in vitro* Conditionally Reprogrammed Cells and Xenografts in Nude Mice

Following *in vitro* findings of the routine chemotherapy agents against LHSCC, we then validated their efficacy in suppressing the growth of xenograft tumors *in vivo*. As confirmed *in vitro*, T2 was relatively sensitive to cisplatin and 5FU, while T6 was relatively resistant to the two drugs (**Figures 2A,B**). Hence, the same doses of cisplatin (DDT) or 5FU were administered to nude mice bearing xenografts of T2 or T6 and compared with their corresponding vehicles (**Figures 4A,D**). The tumor weight and mouse body weight at the endpoint were also measured (**Figures 4B,C,E,F**). Under the same treatment, the growth of T2 xenografts was inhibited evidently, while the growth of T6 xenografts was not hampered significantly compared with normal controls. Moreover, T6 was relatively sensitive to paclitaxel (PTX) compared to the others according to the previous *in vitro* drug response test (**Figure 2C**). The growth of xenografts was markedly suppressed with PTX administration, rather than DDT or 5FU (**Figure 4D**). Hence, the CRCs and xenografts exhibited consistent drug responses.

Conditionally Reprogrammed Cell Derived Organoids and the Application for Drug Testing

Traditionally, 3D cultures have represented a widespread system to recapitulate the structural organization of primary tissues. CRCs could be transformed into organoids using the embedded method. In brief, the feeder cells were removed by first trypsinization from the CR culture system, and then the primary cells were collected by second trypsinization. Next, cells were mixed with Matrigel, and the Matrigel-cell mixture seeded into the well of the culture plate. After solidifying the gel, a dome-like structure was formed to provide the cells with a 3D growing environment. The viable cells could proliferate into spheres under this condition: CRC derived organoids (**Figure 5A**). Consistent with previous studies performed on head and neck cancers (Driehuis et al., 2019), CRCs successfully formed spheres that resembled the morphology of head and neck cancer organoids. The non-malignant cells expanded and re-associated to spheres of approximately 100 μm with a mass-like morphology and polarized growth (**Figure 5B**), while smaller spheres distinguished their malignant counterpart and a relatively slow growth rate. Immunofluorescence (IF) analysis revealed that the organoids were composed of basal cells expressing KRT5 and p63 in the outer cell layer. In contrast, keratinized and differentiated cells with enlarged nuclei were inside the organoids (**Figure 5B**). Furthermore, cisplatin was used to treat tumor organoid T1, T6, and T7. Bright-field images of the organoids under different drug concentrations were shown in **Figure 5C**. Organoids treated with 1 μM cisplatin were smaller and sparsely distributed than those treated with 0.1 μM cisplatin. Kill curves were plotted (**Figure 5D**). The IC50 values to cisplatin of T1, T6 and T7 were 0.50 μM, 3.6 μM and 11.6 μM, respectively. Hence, the sensitivity of the three tumor organoids to cisplatin ranked as T1 > T6 > T7. This rank was consistent with the *in vitro* CRCs responses (**Figure 2A**).

Relationship Between *in vitro* Conditionally Reprogrammed Cells Responses and Clinical Responses: Special Cases

To demonstrate the relationship between *in vitro* and clinical responses, four special cases were selected. Their corresponding CRC lines were derived from their biopsy tissues. After diagnosed with LHSCC, they received chemo/radiotherapy prior to surgery. Before and after the chemo/radiotherapy, imaging examinations were conducted twice to evaluate their clinical responses to the treatment according to the RECIST criterion (Eisenhauer et al., 2009). The timeline of diagnosis and treatment procedure was depicted in **Figure 6A**. An overview table of therapy responses of 6 representative tumors and corresponding *in vitro* models was also provided (**Table 5**).

The patient from whom T11 was derived had hypopharyngeal carcinoma (stage T3N0M0). The patient was treated with chemoradiotherapy (two sessions of cisplatin and radiotherapy dose of 40 Gy) prior to surgery because of the strong personal willingness of the laryngeal preservation approach. The tumor partially responded to the treatment as assessed from imaging examination (**Figure 6B**), and a laryngeal preservation surgery was conducted later. Fortunately, a pathologic complete response (pCR) was achieved after postoperative pathologic examination of the resected tissue (**Figure 6B**). This indicated that T11 was sensitive to the treatment of cisplatin and radiotherapy *in vivo*. Indeed, CRC line T11 was relatively sensitive to cisplatin from our *in vitro* drug screening assay. Similarly, patient T13, who exhibited the highest sensitivity to cisplatin, was diagnosed with hypopharyngeal carcinoma (stage T4N1M0) and was also treated with 2 sessions of cisplatin and a radiotherapy dose of 40 Gy prior to surgery. After the removal of the residual primary tumor, the pathologic examination demonstrated a pCR (**Figure 6C**).

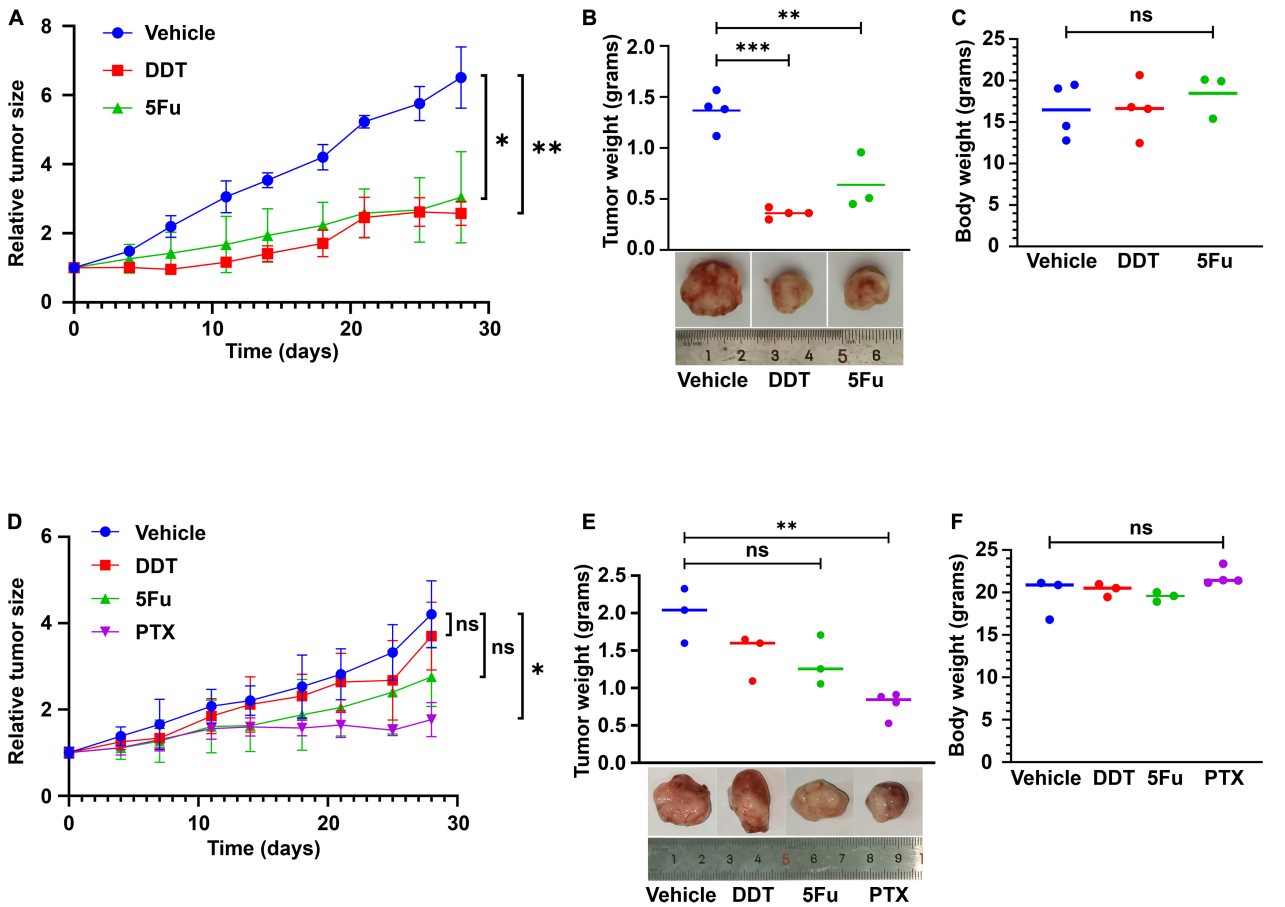

FIGURE 4 | CR cell-derived xenografts used for drug testing. **(A)** T2 cell-derived xenografts were treated with vehicle control, cisplatin (DDT), and 5FU beginning from the same day after grouping for 4 weeks. Tumor sizes were measured as indicated. Mean ± SEM ($n \geq 3$) was measured. **(B)** The tumor weight at the end of the treatment was plotted. Representative images of the tumor were presented. **(C)** Mouse body weights were also compared, with no significant difference. **(D)** T6 cell-derived xenografts were treated with vehicle control, DDT, 5FU, and paclitaxel (PTX) beginning from the same day after grouping for 4 weeks. Tumor sizes were measured as indicated. Mean ± SEM ($n \geq 3$) was measured. **(E)** The values of tumor weight at the end of the treatment were plotted. Representative images of the tumor were presented. **(F)** Mouse body weights were also compared, with no significant difference. $^{*}P < 0.05$, $^{**}P < 0.01$, $^{***}P < 0.001$.

The patient of T2 presented with laryngeal squamous cell carcinoma (stage T4N2M0) was treated with preoperative radiotherapy. However, the patient showed progressive disease status shortly after radiotherapy of 40 Gy, and a total laryngectomy was performed. Postoperative radiotherapy of a dose of 26 Gy was administered because of lymph node metastasis. Unfortunately, the patient succumbed to locoregional recurrence 4 months later. Patient T7 was diagnosed with hypopharyngeal carcinoma (stage T4N2M0). Progressive disease status was observed after preoperative radiotherapy of 40 Gy, hence partial hypopharyngectomy and total laryngectomy were performed on the patient. Postoperative radiotherapy of a dose of 26 Gy was given because of positive margins. The patient was last followed up 1 year after the end of treatment. There were no signs of recurrence to this point. Further, follow-up would be conducted to observe any remission. The *in vitro* sensitivity to radiation, colony formation assay, and cell proliferation assay were performed on the CRCs. After exposing to 4 Gy radiation, T1 exhibited a significant inhibition in colony formation efficiency, while T2 did not (**Figure 6D**). Besides, CRCs T1, T2, T7, and T11 were treated with 4 Gy radiation. After 3 days' culture, their relative cell proliferation was detected. The result indicated that relative cell proliferation of T2 and T7 was significantly higher than that of T1 and T11 after radiation (**Figure 6E**). Based on these findings, T2 and T7 presented resistant to radiotherapy. Consistently, the clinical history showed concordance with the *in vitro* findings.

DISCUSSION

Management of LHSCC is highly complicated and mandates multidisciplinary care (Ringash, 2015). Precision oncology aims to identify and target tumor-specific aberrations with effective therapeutic strategies for individual cancer patients. Currently, in precision oncology, the recommendation of molecularly targeted drugs is primarily based on the genomic profile of a drug-target gene as a therapeutic indicator (Bailey et al., 2018).

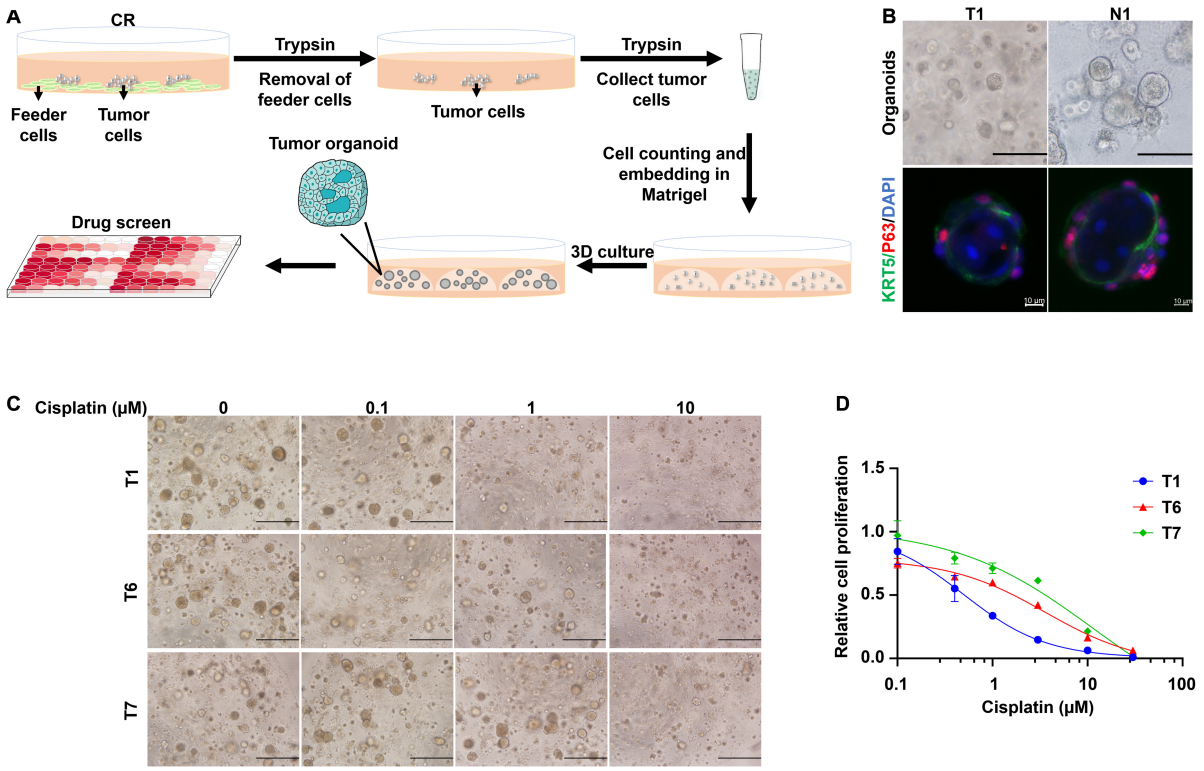

FIGURE 5 | CRCs could form organoids, which could be further used for drug testing. **(A)** Schematic representation of the culture of CRC-derived organoids and further application for drug testing. **(B)** Bright-field microscopic images of CRC derived organoids (scale bar, 125 μm) and immunofluorescence analysis (scale bar, 10 μm) for the basal cell marker KRT5 (green) and p63 (red). Nuclei were counterstained with DAPI (blue). **(C)** Bright-field microscopic images of CRC derived organoids treated with different concentrations of cisplatin. Scale bar, 500 μm. **(D)** Kill curves of cisplatin to T1, T6, and T7 organoids.

The drive toward precision oncology has significantly increased attention in adapting *in vitro* tumor models for patient-specific therapies, drug response assessment, and clinical management. Various *in vitro* models for LHSCC were developed to guide patient-specific therapies in the past decades, including patient-derived primary tumor cells, 3D culture spheres, patient-derived xenotransplantation, and tumor organoids (Seshadri et al., 2009; Dohmen et al., 2015; Méry et al., 2017; Karamboulas et al., 2018; Tanaka et al., 2018). Although promising, those models had numerous limitations for further clinical practice (Dohmen et al., 2015). Success rate, time window, accuracy, and cost-effectiveness are considered essential criteria to the establishment of *in vitro* tumor models. Herein, using CR technology, we established patient-derived LHSCC cells and investigated the clinical implications of them.

In this study, the primary cells were successfully established from 56% tumor samples and 71.4% normal epithelial samples under CR system conditions. We confirmed that the primary cells were epithelial-derived cells expressing pan-keratin, and tumor cells exhibited stemness expressing tumor marker CD44. STR results of the CRCs differed from each other and did not match any cell lines in the database of DSMZ (Deutsche Sammlung von Mikroorganismen und Zellkulturen)[2], German Collection of Microorganisms and Cell Cultures GmbH. STR results of each cell lines remained stable at different passages. Through tissue dissociation and cells' amplification in the CR culture system, we were able to obtain 10^6 cells from each individual endoscopic biopsy or tumor sample within 2 weeks. The cells could be cultured for more than 40 days and 10 passages, with a stable proliferation rate during the extended period. Moreover, the proliferation of cells was not affected by repeated cycles of cryopreservation and resuscitation. Collectively, the CR system contented the criteria for continuous cell culture from LHSCC tumor samples. Besides, sufficient cell numbers could be acquired for further assays such as drug screening, sequencing, or xenografts.

In the present study, the drug and radiation sensitivity of some established CRC lines were tested. Four mostly used drugs in treating LHSCC patients were used in the drug screening. Various drug response was observed. We ranked the CRC lines by their IC50 values for each drug. The CRC lines with higher IC50 values were considered to be more resistant to the specific drug than those with lower IC50 values. There was no obviously regular pattern of the sensitivity to each drug among the CRC lines. These findings motivated to explore the clinical responses using CR techniques. These results were robust due to reliable Z-scores and biological duplication, and they were applied further in the comparison to the drug responses of other *in vitro* models.

[2]www.dsmz.de

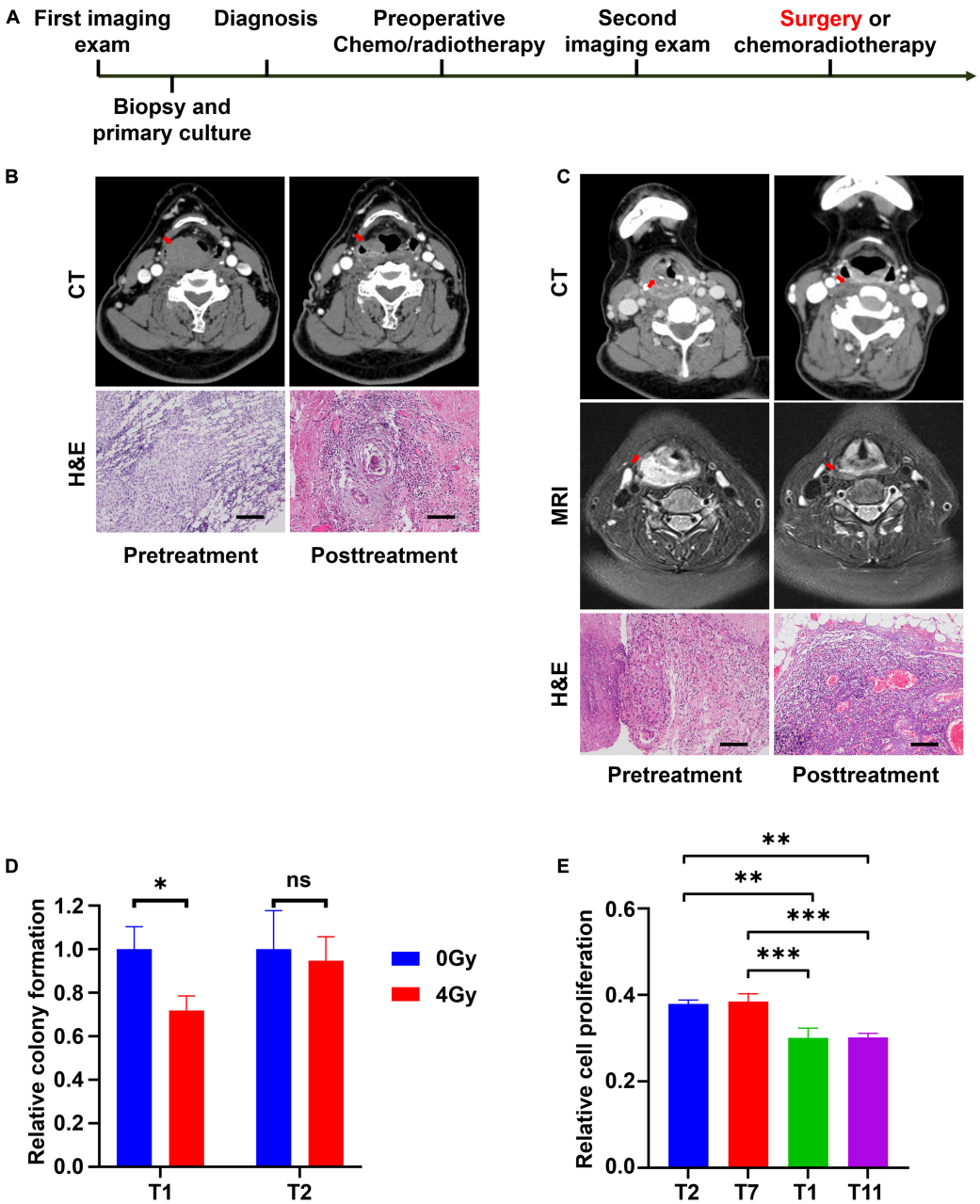

FIGURE 6 | CRCs reflect the clinical outcomes of representative patients with LHSCC. **(A)** The timeline of diagnosis and treatment procedure for patients receiving preoperative chemotherapy or radiotherapy before surgery. **(B)** CT images and microscopic images of tumor tissues of patient T11 before and after chemotherapy. The size of the primary tumor, indicated by a red arrow, decreased more than 50%. Microscopic morphologies indicated pathologic complete response after chemotherapy. Scale bar, 250 μm. **(C)** CT and MRI images and microscopic images of tumor tissues of patient T13 before and after chemotherapy. The size of the primary tumor (red arrow) decreased. Microscopic morphologies indicated pathologic complete response after chemotherapy. Scale bar, 250 μm. **(D)** Relative colony formation of T1 and T2, 7 days after treatment with 0 Gy or 4 Gy radiation. $^{*}P < 0.05$. **(E)** Relative cell proliferation of T1, T2, T7, and T11, 3 days' culture after treatment with 4 Gy radiation. $^{**}P < 0.01$, $^{***}P < 0.001$.

As a milestone for the CR technique, Liu et al., successfully generated continuous cell cultures from tumor samples in a patient with recurrent respiratory papillomatosis and identified Vorinostat as a therapeutic agent using *in vitro* chemosensitivity testing (Yuan et al., 2012). CR technique played a crucial role in guiding clinical administration, though only 1 case was involved. Most of the patients included in this study received surgical resection of the tumor as primary treatment, making it impossible to assess their chemoradiotherapy response outcomes by RECIST criterion (Eisenhauer et al., 2009). Only 4 cases treated with preoperative chemo/radiotherapy were selected to validate the relationship between *in vitro* and clinical responses. And closely

TABLE 5 | Overview of therapy responses of six representative tumors and corresponding *in vitro* models.

Sample	CR	Xenograft	Organoid	Clinical response
T1	S: DDT	NA	S: DDT	NA
T2	S: DDT and 5FU R: RT	S: DDT and 5FU	NA	R: RT
T6	S: PTX R: DDT and 5FU	S: PTX R: DDT and 5FU	R: DDT	NA
T7	R: DDT and RT	NA	R: DDT	R: RT
T11	S: DDT and RT	NA	NA	S: DDT and RT
T13	S: DDT	NA	NA	S: DDT and RT

S, sensitivity; R, resistance; DDT, cisplatin; RT, radiotherapy; PTX, paclitaxel; NA, not applicable.

matched responses were observed. However, more cases are required to validate this relationship robustly. These results implied that CR cultured LHSCC could predict patients' clinical responses to chemotherapy or radiotherapy and might serve as an excellent preclinical model for precision oncology.

Based on the whole-exome sequencing of the three pairs of CRC lines, resistance to cisplatin-based chemotherapy was also positively correlated with TP53 mutation burden, consistent with a previous study (Bergamaschi et al., 2003). Epidermal growth factor receptor (EGFR) was overexpressed in 50%∼90% of the tumors (Bossi et al., 2016), and about 15% of patients carry gene amplification of EGFR (Network, 2015). None of the sequenced cells carried EGFR mutation in this study, and only one of them (T2) had EGFR gene amplification. Cetuximab, a monoclonal antibody targeting EGFR, was used in drug screening. However, the cetuximab sensitivity of the CRC lines could not be reflected by their EGFR expression levels. Although conflicting, the result agreed with previous studies (Bossi et al., 2016).

After being heterotransplanted subcutaneously in nude mice, the primary tumor CRC lines could form tumors successfully, while the normal paired ones could not. This demonstrated the malignant potential of the tumor cells. These CR cell-derived xenografts retained the primary tumors' histopathologic characteristics and could be used for personalized treatment just as patient-derived xenografts (PDX) did (Karamboulas et al., 2018). Moreover, CRC lines could be expanded, cryopreserved, and resuscitated *in vitro* and are repeatedly used for xenografts, which made it much more flexible and convenient than the PDX model.

Patient-derived organoids (PDOs), recapitulating the primary tissues' genetic and molecular characteristics, have been applied to conduct high-throughput drug screening and predict the treatment responses of HNSCC (Driehuis et al., 2019). We could not ignore its disadvantage as aiming at potential clinical application. Firstly, the success rate of LHSCC organoids culture was relatively low, according to the previously published literature (Driehuis et al., 2019). We also tried to culture tumor organoids following previously described methods, but a dissatisfying success rate of 12.5% (2/16) was achieved. Secondly, a clinically significant time window was not available as required for personalized treatment decision-making, which is generally less than 2–3 weeks for preoperative and postoperative chemotherapy. It is not sufficient time for tumor organoids to proliferate to optimal cell number for drug testing. Thirdly, the organoid culture system relied on multiple expensive growth factors in the culture medium and extracellular matrix substitutes. The high expense hampered its extensive application for a less supported institute. Finally, organoid associated processes, unlike classical monolayer cell culture techniques, were special and too complicated to get started. Furthermore, to demonstrate the stemness of CRC lines, we embedded the dissociated CR primary cells in Matrigel and cultured them under the media of organoid culture (Driehuis et al., 2019). Sphere-shaped organoids could be cultured from the primary cells. A polarized growth was observed as the basal cells stratified the outer layer of the organoids while the differentiated and keratinized cells located inside the organoids. Furthermore, these CR derived organoids could also be used to test drug sensitivity.

The success rate of culturing LHSCC cells using CR system was not among the highest (Dohmen et al., 2015), though superior to PDX and organoid. This was partly due to the nature of LHSCC as follows. Most patients were aged ones with poor cell activity. Too many necrotic or fibrotic tissues which were unable to proliferate. And the primary tumor was exposed to numerous microbes that increased the probability of contamination.

In summary, we established LHSCC primary cell lines using the CR technique. The CR cell lines had retained histological and molecular characteristics and heterogeneity of the parental LHSCC. CR cell lines could be transformed into xenografts and organoids, serving as versatile *in vitro* models. Collectively, patient-derived cell model system using CR technology could be promisingly utilized in clinical decision-making and help identify personalized therapies for LHSCC.

DATA AVAILABILITY STATEMENT

The datasets presented in this study can be found in online repositories. The names of the repository/repositories and accession number(s) can be found below: https://www.ncbi.nlm.nih.gov/sra/?term=PRJNA758159.

ETHICS STATEMENT

The studies involving human participants were reviewed and approved by the human research Ethics Committee of Beijing Friendship Hospital, Capital Medical University. The patients/participants provided their written informed consent to participate in this study. The animal study was reviewed and

approved by Institutional Animal Care and Use Committee of Beijing Institute of Biotechnology.

AUTHOR CONTRIBUTIONS

SL and LL designed the study and experiments. YD analyzed the data. YD, JW, WJ, and MZ performed molecular and cell biological experiments. YD, JW, and MZ performed animal studies. YD and WJ collected the patients' clinical data. YD, WJ, and LL analyzed the clinical manifestations and responses. YD, JW, and SL drafted the manuscript. All authors commented on the manuscript.

FUNDING

This work was supported by grants from the National Natural Science Foundation of China (81772750 and 81672640), Beijing Municipal Commission of Education (KZ202110025035), and Major Research Program of China (AWS17J009).

ACKNOWLEDGMENTS

We would like to thank all the patients and clinicians for their involvement and participation. We would also like to thank MogoEdit (www.mogoedit.com) for English language editing.

SUPPLEMENTARY MATERIAL

The Supplementary Material for this article can be found online at: https://www.frontiersin.org/articles/10.3389/fcell.2021.744969/full#supplementary-material

REFERENCES

Bailey, M. H., Tokheim, C., Porta-Pardo, E., Sengupta, S., Bertrand, D., Weerasinghe, A., et al. (2018). Comprehensive characterization of cancer driver genes and mutations. *Cell* 173, 371–385.e318. doi: 10.1016/j.cell.2018.02.060

Bergamaschi, D., Gasco, M., Hiller, L., Sullivan, A., Syed, N., Trigiante, G., et al. (2003). p53 polymorphism influences response in cancer chemotherapy via modulation of p73-dependent apoptosis. *Cancer Cell* 3, 387–402. doi: 10.1016/s1535-6108(03)00079-5

Bossi, P., Resteghini, C., Paielli, N., Licitra, L., Pilotti, S., and Perrone, F. (2016). Prognostic and predictive value of EGFR in head and neck squamous cell carcinoma. *Oncotarget* 7, 74362–74379. doi: 10.18632/oncotarget.11413

Dohmen, A. J., Swartz, J. E., Van Den Brekel, M. W., Willems, S. M., Spijker, R., Neefjes, J., et al. (2015). Feasibility of primary tumor culture models and preclinical prediction assays for head and neck cancer: a narrative review. *Cancers (Basel)* 7, 1716–1742. doi: 10.3390/cancers7030858

Driehuis, E., Kolders, S., Spelier, S., Lõhmussaar, K., Willems, S. M., Devriese, L. A., et al. (2019). Oral mucosal organoids as a potential platform for personalized cancer therapy. *Cancer Discov.* 9, 852–871. doi: 10.1158/2159-8290.Cd-18-1522

Eisenhauer, E. A., Therasse, P., Bogaerts, J., Schwartz, L. H., Sargent, D., Ford, R., et al. (2009). New response evaluation criteria in solid tumours: revised RECIST guideline (version 1.1). *Eur. J. Cancer* 45, 228–247. doi: 10.1016/j.ejca.2008.10.026

Gao, B., Huang, C., Kernstine, K., Pelekanou, V., Kluger, Y., Jiang, T., et al. (2017). Non-malignant respiratory epithelial cells preferentially proliferate from resected non-small cell lung cancer specimens cultured under conditionally reprogrammed conditions. *Oncotarget* 8, 11114–11126. doi: 10.18632/oncotarget.14366

Hu, H., Gehart, H., Artegiani, B., LÖpez-Iglesias, C., Dekkers, F., Basak, O., et al. (2018).). Long-term expansion of functional mouse and human hepatocytes as 3d organoids. *Cell* 175, 1591–1606.e1519. doi: 10.1016/j.cell.2018.11.013

Karamboulas, C., Bruce, J. P., Hope, A. J., Meens, J., Huang, S. H., Erdmann, N., et al. (2018). Patient-derived xenografts for prognostication and personalized treatment for head and neck squamous cell carcinoma. *Cell Rep.* 25, 1318–1331.e1314. doi: 10.1016/j.celrep.2018.10.004

Kettunen, K., Boström, P. J., Lamminen, T., Heinosalo, T., West, G., Saarinen, I., et al. (2019). Personalized drug sensitivity screening for bladder cancer using conditionally reprogrammed patient-derived cells. *Eur. Urol.* 76, 430–434. doi: 10.1016/j.eururo.2019.06.016

Leinung, M., Ernst, B., Doring, C., Wagenblast, J., Tahtali, A., Diensthuber, M., et al. (2015). Expression of ALDH1A1 and CD44 in primary head and neck squamous cell carcinoma and their value for carcinogenesis, tumor progression and cancer stem cell identification. *Oncol. Lett.* 10, 2289–2294. doi: 10.3892/ol.2015.3542

Li, Z., Zhang, X., Xue, W., Zhang, Y., Li, C., Song, Y., et al. (2019). Recurrent GNAQ mutation encoding T96S in natural killer/T cell lymphoma. *Nat. Commun.* 10:4209. doi: 10.1038/s41467-019-12032-9

Liston, D. R., and Davis, M. (2017). Clinically relevant concentrations of anticancer drugs: a guide for nonclinical studies. *Clin. Cancer Res.* 23, 3489–3498. doi: 10.1158/1078-0432.Ccr-16-3083

Liu, X., Krawczyk, E., Suprynowicz, F. A., Palechor-Ceron, N., Yuan, H., Dakic, A., et al. (2017). Conditional reprogramming and long-term expansion of normal and tumor cells from human biospecimens. *Nat. Protoc.* 12, 439–451. doi: 10.1038/nprot.2016.174

Liu, X., Ory, V., Chapman, S., Yuan, H., Albanese, C., Kallakury, B., et al. (2012). ROCK inhibitor and feeder cells induce the conditional reprogramming of epithelial cells. *Am. J. Pathol.* 180, 599–607. doi: 10.1016/j.ajpath.2011.10.036

Mahajan, A. S., Sugita, B. M., Duttargi, A. N., Saenz, F., Krawczyk, E., McCutcheon, J. N., et al. (2017). Genomic comparison of early-passage conditionally reprogrammed breast cancer cells to their corresponding primary tumors. *PLoS One* 12:e0186190. doi: 10.1371/journal.pone.0186190

Méry, B., Rancoule, C., Guy, J. B., Espenel, S., Wozny, A. S., Battiston-Montagne, P., et al. (2017). Preclinical models in HNSCC: a comprehensive review. *Oral. Oncol.* 65, 51–56. doi: 10.1016/j.oraloncology.2016.12.010

Network, T. C. G. A. (2015). Comprehensive genomic characterization of head and neck squamous cell carcinomas. *Nature* 517, 576–582. doi: 10.1038/nature14129

Palechor-Ceron, N., Krawczyk, E., Dakic, A., Simic, V., Yuan, H., Blancato, J., et al. (2019). Conditional reprogramming for patient-derived cancer models and next-generation living biobanks. *Cells* 8:1327. doi: 10.3390/cells8111327

Palechor-Ceron, N., Suprynowicz, F. A., Upadhyay, G., Dakic, A., Minas, T., Simic, V., et al. (2013). Radiation induces diffusible feeder cell factor(s) that cooperate with ROCK inhibitor to conditionally reprogram and immortalize epithelial cells. *Am. J. Pathol.* 183, 1862–1870. doi: 10.1016/j.ajpath.2013.08.009

Ringash, J. (2015). Survivorship and quality of life in head and neck cancer. *J. Clin. Oncol.* 33, 3322–3327. doi: 10.1200/jco.2015.61.4115

Saeed, K., Rahkama, V., Eldfors, S., Bychkov, D., Mpindi, J. P., Yadav, B., et al. (2017). Comprehensive drug testing of patient-derived conditionally reprogrammed cells from castration-resistant prostate cancer. *Eur. Urol.* 71, 319–327. doi: 10.1016/j.eururo.2016.04.019

Seshadri, M., Merzianu, M., Tang, H., Rigual, N. R., Sullivan, M., Loree, T. R., et al. (2009). Establishment and characterization of patient tumor-derived head and neck squamous cell carcinoma xenografts. *Cancer Biol. Ther.* 8, 2275–2283. doi: 10.4161/cbt.8.23.10137

Stransky, N., Egloff, A. M., Tward, A. D., Kostic, A. D., Cibulskis, K., Sivachenko, A., et al. (2011). The mutational landscape of head and neck squamous cell carcinoma. *Science* 333, 1157–1160. doi: 10.1126/science.1208130

Su, S., Di Poto, C., Roy, R., Liu, X., Cui, W., Kroemer, A., et al. (2019). Highlight article: long-term culture and characterization of patient-derived primary hepatocytes using conditional reprogramming. *Exp. Biol. Med. (Maywood)* 244, 857–864. doi: 10.1177/1535370219855398

Tanaka, N., Osman, A. A., Takahashi, Y., Lindemann, A., Patel, A. A., Zhao, M., et al. (2018). Head and neck cancer organoids established by modification of the CTOS method can be used to predict in vivo drug sensitivity. *Oral Oncol.* 87, 49–57. doi: 10.1016/j.oraloncology.2018.10.018

Yuan, H., Myers, S., Wang, J., Zhou, D., Woo, J. A., Kallakury, B., et al. (2012). Use of reprogrammed cells to identify therapy for respiratory papillomatosis. *N. Engl. J. Med.* 367, 1220–1227. doi: 10.1056/NEJMoa1203055

Zhang, J. H., Chung, T. D., and Oldenburg, K. R. (1999). A simple statistical parameter for use in evaluation and validation of high throughput screening assays. *J. Biomol. Screen.* 4, 67–73. doi: 10.1177/108705719900400206

Zhao, W., Liu, K., Sun, Z., Wang, L., Liu, B., Liu, L., et al. (2021). Application research of individualized conditional reprogramming system to guide treatment of gastric cancer. *Front. Oncol.* 11:709511. doi: 10.3389/fonc.2021.709511

Conflict of Interest: The authors declare that the research was conducted in the absence of any commercial or financial relationships that could be construed as a potential conflict of interest.

Publisher's Note: All claims expressed in this article are solely those of the authors and do not necessarily represent those of their affiliated organizations, or those of the publisher, the editors and the reviewers. Any product that may be evaluated in this article, or claim that may be made by its manufacturer, is not guaranteed or endorsed by the publisher.

frontiers in Cell and Developmental Biology

REVIEW
published: 03 January 2022
doi: 10.3389/fcell.2021.660210

Advancement in Cancer Stem Cell Biology and Precision Medicine—Review Article Head and Neck Cancer Stem Cell Plasticity and the Tumor Microenvironment

Molly E. Heft Neal[1], *J. Chad Brenner*[1,2], *Mark E. P. Prince*[1*†] *and Steven B. Chinn*[1,2*†]

[1]*Department of Otolaryngology-Head and Neck Surgery, University of Michigan, Ann Arbor, MI, United States,* [2]*Rogel Cancer Center, University of Michigan, Ann Arbor, MI, United States*

Head and Neck cancer survival has continued to remain around 50% despite treatment advances. It is thought that cancer stem cells play a key role in promoting tumor heterogeneity, treatment resistance, metastasis, and recurrence in solid malignancies including head and neck cancer. Initial studies identified cancer stem cell markers including CD44 and ALDH in head and neck malignancies and found that these cells show aggressive features in both *in vitro* and *in vivo* studies. Recent evidence has now revealed a key role of the tumor microenvironment in maintaining a cancer stem cell niche and promoting cancer stem cell plasticity. There is an increasing focus on identifying and targeting the crosstalk between cancer stem cells and surrounding cells within the tumor microenvironment (TME) as new therapeutic potential, however understanding how CSC maintain a stem-like state is critical to understanding how to therapeutically alter their function. Here we review the current evidence for cancer stem cell plasticity and discuss how interactions with the TME promote the cancer stem cell niche, increase tumor heterogeneity, and play a role in treatment resistance.

Keywords: head and neck cancer, cancer stem cell, tumor microenvironment, niche, heterogeneity

OPEN ACCESS

Edited by:
Vicky Yamamoto,
University of Southern California, United States

Reviewed by:
Chunying Li,
Georgia State University, United States
Cornelis Johannes Forrendinis Van Noorden,
Academic Medical Center, Netherlands
Shankargouda Patil,
Jazan University, Saudi Arabia
Kursad Turksen,
Retired, Ottawa, ON, Canada

***Correspondence:**
Mark E. P. Prince
mepp@med.umich.edu
Steven B. Chinn
schinn@med.umich.edu

†These authors have contributed equally to this work

Specialty section:
This article was submitted to Stem Cell Research, a section of the journal Frontiers in Cell and Developmental Biology

Received: *29 January 2021*
Accepted: *01 December 2021*
Published: *03 January 2022*

Citation:
Heft Neal ME, Brenner J, Prince MEP and Chinn SB (2022) Advancement in Cancer Stem Cell Biology and Precision Medicine—Review Article Head and Neck Cancer Stem Cell Plasticity and the Tumor Microenvironment. Front. Cell Dev. Biol. 9:660210. doi: 10.3389/fcell.2021.660210

INTRODUCTION

Head and neck cancer accounts for approximately 60,000 new cancer diagnoses and 13,000 cancer related deaths in the United States each year. Overall survival for head and neck cancer averages around 50%. Despite advances in treatment modalities these statistics have remained relatively unchanged over the past 30 years (Siegel et al., 2015). Regional and distant metastases remain the leading cause of treatment failure in head and neck cancer patients (Chinn et al., 2015). Cancer stem cells (CSCs) have been theorized to be a leading cause of treatment failure and recurrence. In head and neck tumors, CSCs have been associated with advanced T stage, regional and distant metastases, perineural invasion, radiation failure, and shorter disease-free survival (Wang et al., 2009; Joshua et al., 2012; Chinn et al., 2015).

There are two contrasting, although not mutually exclusive, models of tumorigenesis (Reya et al., 2001; Shackleton et al., 2009). In the clonal model a population of cells gain a proliferative advantage through various mutations and environmental factors that drives tumor growth. In this model the tumor is made up of heterogenous cells that are all capable of creating a new tumor. In contrast, the

cancer stem cell model proposes that there exists a limited subset of cells that are capable of regenerating various cell types that make up the tumor and that these progenitor cells are unable to create a *de novo* tumor (Wang and Dick 2005; Dick 2008). Proponents of the cancer stem cell model argue that because CSCs are thought to be relatively resistant to radiation and chemotherapy; they evade initial treatment modalities and subsequently are able to recreate the heterogeneous tumor. As such it is this small subset of cells that needs to be targeted in order to eradicate the tumor (Bao et al., 2006; Dick 2008; Al-Assar et al., 2009; Mroz et al., 2013; Dionne et al., 2015; Subramanian et al., 2017; Zonga et al., 2018; Hu et al., 2019; Shibata and Hoque 2019; Keysar et al., 2020; Saito et al., 2021). More recently there has been an evolution in this model that suggests an inherent plasticity to CSCs that is mediated through the TME, arguing against the unidirectionality of the CSCs models (Chaffer et al., 2013; Sancho et al., 2015; Shimokawa et al., 2017; Ahmed et al., 2018; Yao et al., 2019; Heise and Sommer 2021). This highlights the importance of a deeper understanding of the plasticity and interactions with the TME to identify new ways to target cancer stem cells to move the field forward.

While CSCs were initially characterized in hematologic malignancies, the evidence for their role in solid tumors, including head and neck cancer (HNC), remains robust (Reya et al., 2001; Prince et al., 2007; Chinn et al., 2015; Prince et al., 2016). Multiple cell markers have been identified and utilized to isolate CSCs in HNC. One of the first and most widely cited surface markers for CSCs identified in HNC is CD44 (Škerlová et al., 2015). Initial studies by Prince et al. found that CD44 positive but not CD44 negative cells were capable of regenerating tumors in mouse xenograft models, maintained the ability to be further passaged, and histologically mirrored primitive cells. Additional work by Prince and Chinn et al. revealed increased rates of tumorigenesis, decreased time to regional metastasis, increased rate of metastatic growth, and a higher likelihood of distant metastases in mice with CD44 high tumors verses CD44 low tumors (Prince et al., 2007; Davis et al., 2010; Chinn et al., 2015). Based on work done in other cancers, additional stem cell markers have been identified in HNC (Zhou et al., 2007; Wei et al., 2009; Chen et al., 2011; Martens-de Kemp et al., 2013; Yan et al., 2013; Prince et al., 2016; Fukusumi et al., 2018). Of these, aldehyde dehydrogenase (ALDH) has been a highly specific cancer stem cell marker, specifically when co-analyzed with CD44. It is CD44's role as a surface protein involved in cell-cell interactions, adhesion, and migration that further supports the mechanistic study of CD44+ stem cells in interaction with the tumor microenvironment (Škerlová et al., 2015; Ferreira et al., 2018; Choi et al., 2021). These data support the clinical importance of CSCs in tumorigenesis, metastasis, and treatment failure.

There is mounting evidence that CSCs require close interactions with neighboring cells within the tumor microenvironment in order to survive and in order to allow for the plasticity inherent to CSCs (Medema and Vermeulen 2011). It is within this ecosystem that the CSC niche is maintained (Borovski et al., 2011; Marusyk et al., 2012; Plaks et al., 2015). A thorough understanding of the crosstalk between CSCs and the tumor microenvironment (TME) that allows for CSC maintenance is a critical step towards the discovery of therapeutic targets in head and neck cancer.

Here we discuss the plasticity of cancer stem cells and impact of the TME, metabolic reprogramming, and potential translational strategies to target head and neck CSCs plasticity as a means for novel therapeutic strategies.

CANCER STEM CELL PLASTICITY

As described previously, in contrast to the clonal model, the cancer stem cell model suggests a unidirectional hierarchical process by which CSCs can give rise to progenitor cells, but progenitor cells cannot give rise to CSCs. Recent evidence suggests that there is a fluid state by which CSCs and non-stem cancer cells can interconvert between stem and non-stem like states; thus integrating both the CSC and clonal models (Medema 2013). The work by Chaffer et al. were the first group to demonstrate this "bidirectional interconversion" of breast CSCs and non-CSCs. Here they demonstrated that differentiated transformed and non-transformed human mammary epithelial cells can convert into a "stem-like state" and that this occurs in the absence of new genetic alterations. Furthermore, this ability to interconvert between a non-stem-like and stem-like state in transformed cells occurred at a significantly higher rate than seen in non-transformed cells, further suggesting a unique mechanism for CSC plasticity in cancer (Chaffer et al., 2011). The mechanism of this plasticity in breast CSCs was found to be dependent on activation of ZEB1, a critical mediator of epithelial-mesenchymal transition. Here the non-stem state is maintained by inactivation of ZEB1 through a bivalent chromatin state. Various stimuli then convert the bivalent chromatin into an active form with increased ZEB1 expression in the stem-like state (Chaffer et al., 2013). Several studies have looked at ZEB1 and its interaction with maintenance of a stem state (Yuan et al., 2019; Nong et al., 2021; Pérez et al., 2021). Within head and neck cancer, ZEB1 overexpression was found in cells enriched for CD133 and was associated with increased tumor initiation, again suggesting the importance of ZEB1 and the EMT in the CSC phenotype (Chu et al., 2013). Given an EMT regulator was found to mediate interconversion and maintenance of a stem-like state, this offers a critical area of study to target CSC maintenance and plasticity. Additional work evaluating the impact of CSC interconversion by Gupta et al. further examined the plasticity model using in silico gene set enrichment analysis and mathematical modeling. Here they found breast cancer cells fluctuate between luminal, basal, and stem cell phenotypes to reach an equilibrium state, even after sorting, thus suggesting that breast CSC can arise *de novo* from non-CSC. This study further demonstrated that sensitivity to systemic chemotherapy is dependent upon the phenotypic state of the tumor cells, further illustrating the critical need to understand plasticity for therapeutic use (Gupta et al., 2011).

Despite this seminal work, only a few studies have explored CSC plasticity, mechanism, and potential targeting for therapy: with even fewer in head and neck cancer. A recent study by Leong

et al. suggests that HNC cell lines also share a similar propensity to return to an equilibrium state. HNC cell lines enriched for ALDH showed that ALDH+ and ALDH- populations would return to a steady state of admixed CSCs and non-stem CSC (Leong et al., 2014). This interconversion was found to be driven in part by EGFR and IGF-1R pathway activation. Xie et al. evaluated targeting differentiation pathways in nasopharyngeal cancer as a means of altering stem transitions and impacting cell survival (Xie et al., 2021). These studies suggest that the rigid unidirectional aspect of the initial CSC theory may not be the whole story. This has important implications in treatment paradigms, as the goal of targeting CSCs may yield initial eradication of the CSCs however if progenitor cells possess the ability to convert into CSCs this may lead to ultimate treatment failure. Whether the conversion between CSCs and non-stem can cells is driven by environmental factors, genetic alteration, or a stochastic process is still debated (Morel et al., 2008; Medema 2013) however these results suggests that targeting the mediating factors that control the interconversion and maintenance of the CSC niche offers a potential therapeutic option.

CANCER STEM CELL REPROGRAMMING

Metabolic reprogramming is thought to play a role in both tumor formation by CSCs and in the plasticity of CSCs (Menendez et al., 2013). Metabolic signaling (whether it be epigenetic changes or environmental interactions) can affect the rate at which CSCs and non-stem cancer cells interconvert and can thereby dictate the tumorigenicity. As described by Menendez et al. these metabolic factors can be thought of as "facilitators" or "impediments" in this interconversion. Initial advances in this area involved the discovery of metabolic signaling that induced pluripotent stem cells from somatic cells (Hanna et al., 2010), which involves expression of known CSC markers such as Oct4 and Sox2 (Carey et al., 2011). This idea was subsequently applied to development of stem cells in cancer. While not the only factor necessary for development of CSCs, certain metabolic environments will increase the likelihood of the epigenetic and ultimately stochastic events that lead to interconversion of non-stem cancer cells (Menendez et al., 2013). Proposed metabolic reprogramming events include the propensity for tumor cells to switch to anaerobic glycolysis, one of the initial tenants of cancer suggested by Warburg (Warburg 1956). This has been shown in breast, osteosarcoma and nasopharyngeal CSCs (Cioce et al., 2014; Palorini et al., 2014; Shen et al., 2015), and inhibition of this metabolic reprogramming reduced stemness in nasopharyngeal cancer cells. Anaerobic glycolysis is further supported by CSCs dependency on HIF-1α (Gammon et al., 2013; Nam et al., 2016). Liu et al. looked at the mechanism of tumor associated fibroblasts (TAFs) on maintenance of a stem-like state and increased glycolysis through regulation of HIF-1α (Liu Y. et al., 2021). Here, they identified a specific microRNA (miR-7641) that could silence HIF-1a expression and alter breast cancer cells glycolysis ability and stem cell gene expression. This alteration of the metabolic pathway through paracrine interaction of the supporting stromal cells further supports the critical impact of the TME on stem cell maintenance. This interaction of an oxidative state and metabolic reprogramming for CSC maintenance is further supported based on the shift towards hypoxia and increased reactive oxygen species (further elucidated below), or by overexpression of inflammatory markers such as cyclooxygenase-2 (COX-2) (Tian et al., 2017). Epigenetic and post-translational alterations provide additional mechanisms for cancer stem cell reprogramming. Dong et al. demonstrated the importance of super enhancers in promoting cancer stem cells (Dong et al., 2021) and there is mounting evidence for the role of microRNAs in cancer stem call regulation (Bourguignon et al., 2012; Barlak et al., 2020; Fitriana et al., 2021). These necessary metabolic and other perturbations are often driven by interactions with neighboring cells in the tumor microenvironment. However, despite burgeoning research in this area, only a single study to date has evaluated the role of metabolic reprogramming in head and neck CSC and this was solely in nasopharyngeal cancer (Shen et al., 2015), thus representing a novel area of study. Despite limited data in metabolic reprogramming, there has been significant data evaluating the stromal maintenance of CSC.

THE PERIVASCULAR NICHE

Evidence has shown that endothelial cells are influenced by neighboring cancer cells to create a perivascular niche. Initially discovered in neural tumors (Shen et al., 2004; Calabrese et al., 2007), this idea of a perivascular niche has more recently been described in head and neck tumors as well as other solid malignancies. Studies have shown that cancer stem cells reside within these specialized areas (Krishnamurthy et al., 2010; Ghajar et al., 2013). Krishnamurthy et al. utilized patient derived HNC cells implanted into xenograft mouse models to demonstrate the tumor generating potential of CD44+/ALDH+ tumor cells compared to CD44-/ALDH- tumor cells. In this experiment they also implanted human endothelial cells to allow for neovascularization surrounding the tumors. As expected the CD44+/ALDH+ cells resulted in a significantly higher number of tumors after implantation compared to the CD44−/ALDH− tumors cells. Histologic analysis of these tumors revealed that the majority of ALDH+ stem like tumor cells were localized within 100 um of blood vessels. Subsequent histologic analysis of primary head and neck oral cavity tumors revealed that approximately 80% of stem like cancer cells (defined as ALDH+) were located within 100 um of blood vessels. To further evaluate the role of endothelial cells in creating a perivascular niche, CSCs and non-stem cancer cells were grown in the presence of endothelial cell conditioned medium. There was a significant increase in sphere formation in the CD44+/ALDH+ cells in the presence of the conditioned media. Further, conditioned media resulted in increased expression of BMI -1 suggesting a role of endothelial cells in promoting CSCs potential for epithelial-to-mesenchymal transition (EMT) and metastasis. Validation experiments also demonstrated that ablation of endothelial vessels resulted in a decreased number of CSCs in xenograft models. A second study

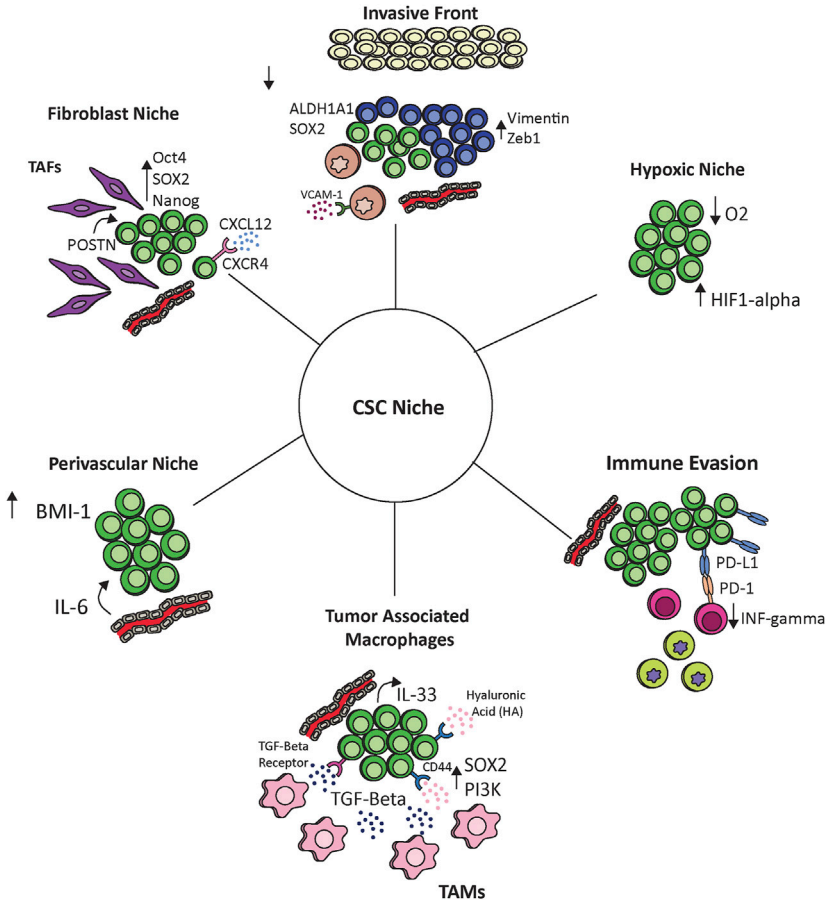

FIGURE 1 | The interaction of cancer stem cells with the tumor microenvironment. Cancer stem cells communicate with and react to the tumor ecosystem including endothelial cells, hypoxic environments, tumor associated fibroblasts (TAFs), tumor associated macrophages (TAMs), monocytes, and other immune cells. These interactions maintain the cancer stem cell niche and provide potential therapeutic options.

by this same group further evaluated the role of endothelial cells on maintenance of CSCs and aimed to identify the factors that regulate the CSCs niche. This study identified that IL-6 secreted by endothelial cells promoted tumorigenesis and survival of CSCs, and that inhibition of IL-6 through shRNA or treatment with an anti-IL-6 antibody (tocilizumab) reduced this effect (Krishnamurthy et al., 2014). These two studies support the role of endothelial cells in maintaining CSCs in head and neck tumors and suggest that targeting endothelial cells within the tumor may also affect CSCs residing within the perivascular niche.

In contrast to the perivascular niche, which remains a well-oxygenated environment due to its proximity to blood vessels, there is also evidence that CSCs are maintained through hypoxic conditions (Ritchie and Nor 2013). Alluding back to the idea of metabolic reprograming, A study by Wu et al. demonstrated increased percentages of CSCs (defined by CD133) and increased expression of stem cell markers including NANOG, SOX2, and OCT4 in laryngeal tumor cell lines exposed to hypoxic conditions (Wu et al., 2014). Whether hypoxia promotes CSCs growth through direct mechanisms or selects for CSCs due to death of non-stem cancer cells is less clear. A study by Duarte et al. demonstrates that hypoxic conditions resulted in an overall decrease in growth of HNC cell line models and that the proportion of CSCs in the surviving group increased potentially suggesting that hypoxia selects for CSCs as a survival mechanism in adverse conditions (Duarte et al., 2012). Furthermore, a study by Marcu et al. utilizing in silica models suggests that there is increased resistance of CSCs to radiation therapy when exposed to hypoxic conditions (Marcu et al., 2016). Cancer stem cells residing within hypoxic niches contribute to the overall resistance of HNC to radiation therapy and additional evidence suggests this may be mediated through a Hif-1 alpha mediated mechanism (Wozny et al., 2017). Together these studies demonstrate the plasticity of CSCs in their ability for survival and tumor maintenance in varying conditions (**Figure 1**).

STROMAL NICHE AND TUMOR ASSOCIATED FIBROBLASTS

Fibroblasts residing within the tumor stroma are also thought to play a critical role in maintenance of the tumor microenvironment and in tumorigenesis (Xing et al., 2010; Wheeler et al., 2014). These tumor associated fibroblasts (TAFs) are characterized by high levels of smooth muscle actin (alpha SMA), fibroblast activation protein (FAP), Thy-1, desmin, and S100A4 protein expression (Garin-Chesa et al., 1990). In head and neck squamous cell carcinoma, TAFs have been shown to promote tumor invasion and are associated with disease progression and worse survival outcomes (Lin et al., 2011; Wheeler et al., 2014). Studies have aimed to identify pathways by which TAFs promote tumor growth. Select pathways have been identified including TGF-Beta1 and EGFR mediated mechanisms (Marsh et al., 2011; Magan et al., 2020). More recent studies have now discovered significant crosstalk between cancer stem cells and TAFs within the TME and data suggests this may play a previously unrecognized role in CSCs maintenance and tumor progression (Yu et al., 2018; Liu et al., 2020). One of these mechanistic studies by Yu et al. which evaluated the effect of TAF secreted periostin (POSTN) on HNC, and found that HNC tumor cells treated with POSTN showed increased expression of stem cell markers including CD166, SALL4, CD271, CD90, CD133, OCT-4, ALDH, SOX2, and NANOG as well as increased spheroid formation (Yu et al., 2018). They also showed that knockdown of protein tyrosine kinase 7 (PTK7) dampened this response, suggesting a mechanistic dependence on the POSTN-PKT7 axis. Further experiments using both *in vitro* and *in vivo* models demonstrated that activation of this axis not only increased tumorigenicity but also increased activation of the wnt/B-Catenin pathway. This study is one of the first to define a mechanistic pathway by which TAFs maintain the CSCs niche. The CXCR4-CXCL12 axis has also been implicated as a stromal mediator of the CSC niche. Best described in hematologic malignancies, this axis has been shown to play a key role in numerous solid malignancies such as breast, esophageal, and pancreatic cancer among others and is of particular interest as there are multiple small molecule inhibitors of CXCR4 and CXCL12 that are under investigation (Hermann et al., 2007; Popple et al., 2012; Wang et al., 2017; López-Gil et al., 2021). In head and neck cancer there are mixed studies investigating this pathway. Faber et al. found that CXCR4 expressing cells were highly expressed in tumor nests but did not co-localize to the stroma with the CD44 expressing cells (Faber et al., 2013a). In contrast to these results, the same group also demonstrated that in the head and neck cancer cell line UMSCC-11A CD44+/CXCR4+ cells showed increased podia formation with the additional of CXCL12 suggesting a role of this axis in the regulation of CD44+ CSC (Faber et al., 2013b). A study by Jungbauer et al. further evaluated the role of CXCL12 on HPV+ and HPV− head and neck cancer cell lines and found that only HPV− cells lines showed increased podia formation in response to CXCL12 (Jungbauer et al., 2017). Together these results suggest the CXCR4/CXCL12 axis as a promising area of further research.

CSCS AND TUMOR ASSOCIATED MACROPHAGES

Immune cells additionally play a key role in maintaining the TME and creating an immunosuppressive milieu. Tumor associated macrophages (TAMs) are thought to closely mirror the subset of M2 macrophages which promote wound healing and have pro-tumorigenic properties (Chanmee et al., 2014; Aras and Zaidi 2017; Mantovani et al., 2017). Associations between TAMs and CSCs has been demonstrated in other solid malignancies such as breast, lung, and colorectal (Rao et al., 2013; Yang et al., 2019). Zhang et al. found that polarized M2 macrophages when co-cultured with lung adenocarcinoma cell lines lead to increased proliferation and stemness. While some evidence in HNC suggests an association between TAMs and CSC in HNC, there is a gap in understanding a clear mechanistic pathway (He et al., 2014; Hu et al., 2016). A recent study by Gomez et al. utilized *in vitro* and *in vivo* models to demonstrate the intricate interactions between TAMs and head and neck CSCs (Gomez et al., 2020). In this study head and neck cancer cells were co-cultured with macrophages to mimic an established TME which resulted in increased levels of PI3K-4EBP1 phosphorylation, SOX2, and ALDH1A1, compared to HNC cells cultured alone. There was also a higher proportion of CD44+/ALDH high cells in the co-culture group indicating increased stemness of the population. Conversely when HNC cells were co-cultured with immature monocytes, mimicking the leading edge of tumors, there was downregulation of PI3K-4EBP1 phosphorylation, SOX2 and ALDH1A1 and a decreased proportion of CD44+/ALDH high cells. Co-culture with monocytes leads to increased levels of vimentin and Zeb1, both of which are involved in EMT. The authors also found that binding of CD44 to hyaluronic acid (a protein expressed in high levels in the extracellular matrix) resulted in a positive feedback loop that promoted expression of PI3K and SOX2. These results support similar findings from previous studies (Liu and Cheng 2017; Passi et al., 2019). These data also suggest that this positive feedback loop was promoted in the presence of TAMs. Finally, in the models of the invasive front the authors showed that monocyte binding to VCAM-1 increased invasion with associated decrease in CSCs population. Overall this study supports an intimate interaction between TAMs and CSCs and demonstrates how macrophages and monocytes promote a transition between the invasive verses growth phenotypes in CSCs. These results further reflect the role of the TME and CSCs in maintaining tumor heterogeneity. An additional study by Taniguchi et al. also supports the role of TAMs in cancer stem cell maintenance (Taniguchi et al., 2020). In this study authors leveraged a mouse model of squamous cell carcinoma and human squamous cell tumor samples to demonstrate that TAMs create a TGF-Beta rich environment that stimulates CSCs to release IL-33. These paracrine signals then result in further differentiation of immature immune cells into FcεRIα+ tumor associated macrophages. These data support a method of cross-communication between CSCs and cells

within the microenvironment that stimulate ongoing tumor growth.

CSCS AND IMMUNE EVASION

In addition to interactions between CSCs and neighboring cells within the TME, there is also evidence that CSCs interact with host immune cells and play a key role in tumor immune evasion (Qi et al., 2012; Maccalli et al., 2018).

Numerous studies have aimed to further delineate the role of CSCs in immune escape. A study by Lee et al. utilizing PDX mouse models inoculated with human tumor cells found that CD44+ cells expressed higher levels of EMT markers and Programmed death-ligand 1 (PD-L1) compared to CD44− cells (Lee et al., 2016). The authors also examined 21 primary tumors and found that CD44+ cells expressed higher levels of PD-L1 at the RNA and protein level. CD44+ cells were also found to induce less INF-gamma expression in CD8+ tumor infiltrating lymphocytes (TILs) when co-cultured with these cells compared to the CD44− subgroups, suggesting lower immunogenicity of the CD44+ population. Interferon gamma expression in these CD44+ cells was rescued with inhibition of the PD-L1/PD1 axis. This effect was not observed in the CD44− subgroup further supporting the interaction between PD-L1 and CD44+ CSCs in the tumor microenvironment. Similar findings of increased PD-L1 expression has also been demonstrated in ALDH+ oropharynx tumor cells compared to ALDH− cells (Tsai et al., 2017). This difference in PD-L1 expression was enhanced after radiation therapy. This same study also correlated ALDH positive tumors with increased levels of peripheral myeloid-derived suppressor cell (MDSC), cells known to play a key role in immune escape.

While decreased major histocompatibility complex (MHC) class 1 expression is a well described mechanism of immune escape in head and neck cancer (Meissner et al., 2005), multiple studies have failed to show differences in MHC class I expression on CSCs compared to paired non-stem cancer cell (Chikamatsu et al., 2011; Liao et al., 2013). However, a study by Chikamatsu et al. did identify possible mechanism by which HNC CSCs exploit the antigen processing and presentation pathway to aid in immune evasion. Type 2 transporter associated with antigen processing (TAP2) is a protein critical for peptide translocation from the cytosol to the lumen of the endoplasmic reticulum, which is required for subsequent peptide loading onto MHC class I proteins. In this study the authors demonstrated a significant difference in expression between CD44+ and CD44− groups, with CD44+ cells having decreased expression of TAP2. Therefore, these data support a possible second mechanism of immune escape that involves suppression of the neoantigen presentation pathway. CD44+ cells also showed increased levels of immunosuppressive cytokines such as IL-8 G-CSF and TGF-Beta when compared to CD44− cells, and showed greater suppression of T cells in culture. Further peripheral blood mononuclear cells co-cultured with CD44+ cells showed increased levels of T regulatory cells and MDSCs, increased IL-10 secretion from peripheral blood monocytes, and increased inhibition of IFN-gamma and IL-2 compared to CD44− negative cells. Together these studies indicate that CD44+ cells promote immune suppression through interaction with host immune cells and suggest a role for immunotherapy as a target for CSCs in HNC (Canter et al., 2016). An important caveat to this, however, is that while inhibition of the PD-1/PD-L1 axis may inhibit one mechanism of immune escape, the secondary escape mechanism of reduced TAP2 protein may render CSCs resistant to monotherapy with anti-PD-1/PD-L1 treatments.

TARGETING CANCER STEM CELLS

Tumor heterogeneity remains one of the persistent challenges in developing novel cancer therapeutics. As discussed above, cancer stem cells are thought to play a critical role in development of tumor heterogeneity (Sottoriva et al., 2010) and is often cited as a primary mechanism of treatment failure (Greaves 2015). Cancer's ability to evade both intrinsic (immune response) and extrinsic (cancer therapies) pressures is based on clonal and sub-clonal evolution leading to highly adaptable cellular heterogeneity (McGranahan et al., 2016; Ayob and Ramasamy 2018). One of the challenges of current and novel targeted cancer therapy is the vast burden of molecular data and deciphering of the complex interaction of supporting cells within the tumor ecosystem (Agrawal et al., 2011; Stransky et al., 2011; TCGA 2015). As clonal mutations propagate, selective pressures force evolution of resistant genotypes and phenotypes (**Figure 2**). Despite significant advances in high-throughput sequencing, heterogeneity may cause critical data points to be missed or averaged out if they are not dominant (Shah et al., 2009; Ding et al., 2010). Recent work in single cell analyses of HNC further demonstrated the extreme diversity of molecular signatures amongst both malignant and non-malignant cells as well as inter- and intra-tumoral heterogeneity (Puram et al., 2017). Deciphering and narrowing the focus to only the critical mediators of tumor heterogeneity is critical to understanding and treating cancer resistance. Given their central importance in hierarchical tumor heterogeneity, CSCs are a highly attractive target for cancer therapy; they likely represent a conserved population that may be more homogenous than the general cancer milieu. However, given their rarity and plasticity, characterizing cancer stem cell signatures with high fidelity remains challenging, yet a crucial step to reduce tumor heterogeneity. Further, given recent advances in discovery of tumor plasticity and the challenges of standard therapeutics in eradicating a heterogenous tumor, targeting the metabolic and immune signals that promote conversion to CSCs may serve as opportunity for novel treatment development.

Recent studies have aimed to develop therapies targeting cancer stem cell plasticity and reprogramming by interfering with the interactions between CSCs and the TME. In head and neck cancer Leong et al. demonstrated that inhibition of

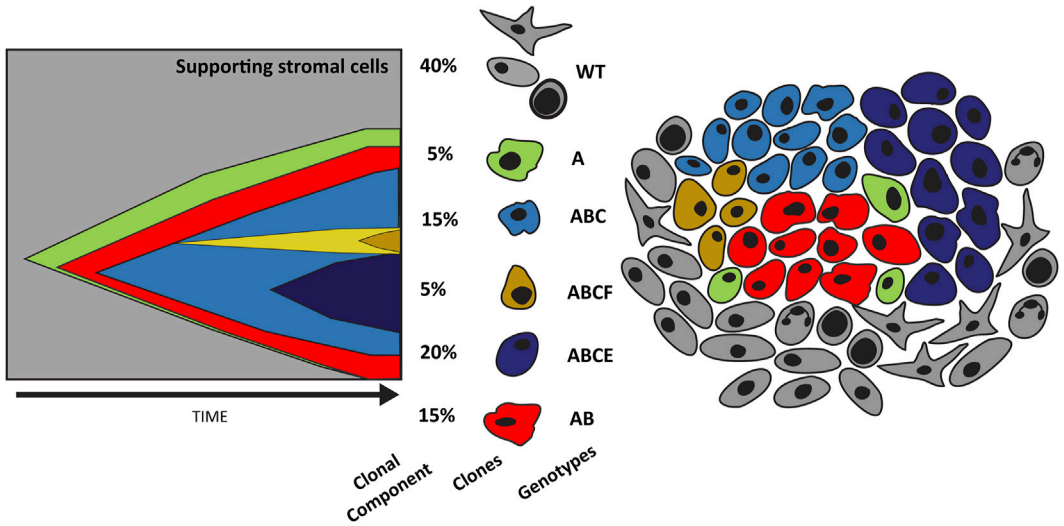

FIGURE 2 | Evolution of tumor heterogeneity. The graph on the left depicts the evolution of cancer cells as described by the original cancer stem cell theory. Here cancer stem cells (green) can replicate and differentiate into individual clones (red) that over time accumulate mutations secondary to selective pressures (blue and yellow). This results in significant tumor heterogeneity as depicted in the illustration on the right. Tumor heterogeneity increases treatment challenges and nominates a conserved population such as cancer stem cells as a potential therapeutic target.

EGFR and IGF-1R reduced levels of ALDH+ cells in the population. The authors postulated that this may prove to be an effective strategy for blunting CSC plasticity in the future (Leong et al., 2014). A study by Lee et al. discovered that isoorientin inhibits stemness in oral cavity cell lines through inhibition of the STAT3/Wnt/β-catenin axis and that these results were synergistic in combination with cisplatin (Liu S.-C. et al., 2021). As discussed above, COX-2 has been shown to promote maintenance of CSCs. A study investigating the effects of COX-2 inhibition in hypopharyngeal cancer resulted in deceased expression of genes associated with CSCs and reduced sphere formation. Tumor viability was also decreased and these results were improved by the addition of docetaxel (Saito et al., 2021). Dong et al. demonstrated that inhibition of Bromo- and Extra-Terminal domain (BET) results in an unanticipated impairment of super enhancers and reduced stemness in HNC (Dong et al., 2021). These results suggest that reduction in the cancer stem cell population may reduce tumor heterogeneity and serve as adjunctive therapy to enhance standard therapeutics. Despite the breadth of studies investigating potential interactions between the TME and CSCs, there remains a need for further therapeutic studies targeting CSC plasticity and interruption of the CSC niche.

CONCLUSION

There is increasing evidence for the role of CSCs in treatment resistance and recurrence in HNC as well as the role of the TME in maintaining the CSC niche. Here we review an updated model of CSC plasticity and identify potential therapeutic targets including ZEB1, EGFR, and IGF-1R. We also evaluate the evidence for the role of endothelial cells (per-vascular nice), TAFs, and TAMs in promoting CSC growth and maintenance, suggesting another area for therapeutic potential. We also review the critical relationship between CSCs and the host immune system that promotes tumor immune evasion suggesting a potential use of immunotherapy in modulating the CSC niche. Future studies to target these interactions and reduce CSCs plasticity may yield novel therapeutic combinations for HNC as well as other solid malignancies.

AUTHOR CONTRIBUTIONS

MEH, JCB, SBC, and MEPP contributed to conception and design of the study. MEH performed literature review and drafted of the manuscript. SBC wrote sections of the manuscript. All authors contributed to manuscript revision, read, and approved the submitted version.

FUNDING

MEH was funded by NIH T32 grant (T32 DC005356), SBC was funded by NIH/NCI Grant K08 17-PAF07511. JCB was supported by NIH/NCI grants U01DE02925501 and 1R01DE030691-01A1 as well as the American Cancer Society grant 132034-RSG-18-062-01-TBG. Institutional support for funding was provided through the NCI Cancer Center Support Grant-grant number P30CA046592.

REFERENCES

Agrawal, N., Frederick, M. J., Pickering, C. R., Bettegowda, C., Chang, K., Li, R. J., et al. (2011). Exome Sequencing of Head and Neck Squamous Cell Carcinoma Reveals Inactivating Mutations in NOTCH1. *Science* 333 (6046), 1154–1157. doi:10.1126/science.1206923

Ahmed, N., Escalona, R., Leung, D., Chan, E., and Kannourakis, G. (2018). Tumour Microenvironment and Metabolic Plasticity in Cancer and Cancer Stem Cells: Perspectives on Metabolic and Immune Regulatory Signatures in Chemoresistant Ovarian Cancer Stem Cells. *Semin. Cancer Biol.* 53, 265–281. doi:10.1016/j.semcancer.2018.10.002

Al-Assar, O., Muschel, R. J., Mantoni, T. S., McKenna, W. G., and Brunner, T. B. (2009). Radiation Response of Cancer Stem-like Cells from Established Human Cell Lines after Sorting for Surface Markers. *Int. J. Radiat. Oncology*Biology*Physics* 75 (4), 1216–1225. doi:10.1016/j.ijrobp.2009.07.001

Aras, S., and Zaidi, M. R. (2017). TAMeless Traitors: Macrophages in Cancer Progression and Metastasis. *Br. J. Cancer* 117 (11), 1583–1591. doi:10.1038/bjc.2017.356

Ayob, A. Z., and Ramasamy, T. S. (2018). Cancer Stem Cells as Key Drivers of Tumour Progression. *J. Biomed. Sci.* 25 (1), 20. doi:10.1186/s12929-018-0426-4

Bao, S., Wu, Q., McLendon, R. E., Hao, Y., Shi, Q., Hjelmeland, A. B., et al. (2006). Glioma Stem Cells Promote Radioresistance by Preferential Activation of the DNA Damage Response. *Nature* 444 (7120), 756–760. doi:10.1038/nature05236

Barlak, N., Capik, O., Sanli, F., and Karatas, O. F. (2020). The Roles of microRNAs in the Stemness of Oral Cancer Cells. *Oral Oncol.* 109, 104950. doi:10.1016/j.oraloncology.2020.104950

Borovski, T., De Sousa E Melo, F., Vermeulen, L., and Medema, J. P. (2011). Cancer Stem Cell Niche: The Place to Be: Figure 1. *Cancer Res.* 71 (3), 634–639. doi:10.1158/0008-5472.can-10-3220

Bourguignon, L. Y. W., Earle, C., Wong, G., Spevak, C. C., and Krueger, K. (2012). Stem Cell Marker (Nanog) and Stat-3 Signaling Promote MicroRNA-21 Expression and Chemoresistance in hyaluronan/CD44-Activated Head and Neck Squamous Cell Carcinoma Cells. *Oncogene* 31 (2), 149–160. doi:10.1038/onc.2011.222

Calabrese, C., Poppleton, H., Kocak, M., Hogg, T. L., Fuller, C., Hamner, B., et al. (2007). A Perivascular Niche for Brain Tumor Stem Cells. *Cancer Cell* 11 (1), 69–82. doi:10.1016/j.ccr.2006.11.020

Canter, R. J., Grossenbacher, S. K., Ames, E., and Murphy, W. J. (2016). Immune Targeting of Cancer Stem Cells in Gastrointestinal Oncology. *J. Gastrointest. Oncol.* 7 (Suppl. 1), S1–s10. doi:10.3978/j.issn.2078-6891.2015.066

Carey, B. W., Markoulaki, S., Hanna, J. H., Faddah, D. A., Buganim, Y., Kim, J., et al. (2011). Reprogramming Factor Stoichiometry Influences the Epigenetic State and Biological Properties of Induced Pluripotent Stem Cells. *Cell Stem Cell* 9 (6), 588–598. doi:10.1016/j.stem.2011.11.003

Chaffer, C. L., Brueckmann, I., Scheel, C., Kaestli, A. J., Wiggins, P. A., Rodrigues, L. O., et al. (2011). Normal and Neoplastic Nonstem Cells Can Spontaneously Convert to a Stem-like State. *Proc. Natl. Acad. Sci.* 108 (19), 7950–7955. doi:10.1073/pnas.1102454108

Chaffer, C. L., Marjanovic, N. D., Lee, T., Bell, G., Kleer, C. G., Reinhardt, F., et al. (2013). Poised Chromatin at the ZEB1 Promoter Enables Breast Cancer Cell Plasticity and Enhances Tumorigenicity. *Cell* 154 (1), 61–74. doi:10.1016/j.cell.2013.06.005

Chanmee, T., Ontong, P., Konno, K., and Itano, N. (2014). Tumor-associated Macrophages as Major Players in the Tumor Microenvironment. *Cancers* 6 (3), 1670–1690. doi:10.3390/cancers6031670

Chen, Y.-S., Wu, M.-J., Huang, C.-Y., Lin, S.-C., Chuang, T.-H., Yu, C.-C., et al. (2011). CD133/Src axis Mediates Tumor Initiating Property and Epithelial-Mesenchymal Transition of Head and Neck Cancer. *PLoS One* 6 (11), e28053. doi:10.1371/journal.pone.0028053

Chikamatsu, K., Takahashi, G., Sakakura, K., Ferrone, S., and Masuyama, K. (2011). Immunoregulatory Properties of CD44+ Cancer Stem-like Cells in Squamous Cell Carcinoma of the Head and Neck. *Head Neck* 33 (2), 208–215. doi:10.1002/hed.21420

Chinn, S. B., Darr, O. A., Owen, J. H., Bellile, E., McHugh, J. B., Spector, M. E., et al. (2015). Cancer Stem Cells: Mediators of Tumorigenesis and Metastasis in Head and Neck Squamous Cell Carcinoma. *Head Neck* 37 (3), 317–326. doi:10.1002/hed.23600

Choi, J.-I., Jang, S. I., Hong, J., Kim, C. H., Kwon, S. S., Park, J. S., et al. (2021). Cancer-initiating Cells in Human Pancreatic Cancer Organoids Are Maintained by Interactions with Endothelial Cells. *Cancer Lett.* 498, 42–53. doi:10.1016/j.canlet.2020.10.012

Chu, P.-Y., Hu, F.-W., Yu, C.-C., Tsai, L.-L., Yu, C.-H., Wu, B.-C., et al. (2013). Epithelial-mesenchymal Transition Transcription Factor ZEB1/ZEB2 Co-expression Predicts Poor Prognosis and Maintains Tumor-Initiating Properties in Head and Neck Cancer. *Oral Oncol.* 49 (1), 34–41. doi:10.1016/j.oraloncology.2012.07.012

Cioce, M., Valerio, M., Casadei, L., Pulito, C., Sacconi, A., Mori, F., et al. (2014). Metformin-induced Metabolic Reprogramming of Chemoresistant ALDHbright Breast Cancer Cells. *Oncotarget* 5 (12), 4129–4143. doi:10.18632/oncotarget.1864

Davis, S. J., Divi, V., Owen, J. H., Bradford, C. R., Carey, T. E., Papagerakis, S., et al. (2010). Metastatic Potential of Cancer Stem Cells in Head and Neck Squamous Cell Carcinoma. *Arch. Otolaryngol. Head Neck Surg.* 136 (12), 1260–1266. doi:10.1001/archoto.2010.219

Dick, J. E. (2008). Stem Cell Concepts Renew Cancer Research. *Blood* 112 (13), 4793–4807. doi:10.1182/blood-2008-08-077941

Ding, L., Ellis, M. J., Li, S., Larson, D. E., Chen, K., Wallis, J. W., et al. (2010). Genome Remodelling in a Basal-like Breast Cancer Metastasis and Xenograft. *Nature* 464 (7291), 999–1005. doi:10.1038/nature08989

Dionne, L. K., Driver, E. R., and Wang, X. J. (2015). Head and Neck Cancer Stem Cells. *J. Dent Res.* 94 (11), 1524–1531. doi:10.1177/0022034515599766

Dong, J., Li, J., Li, Y., Ma, Z., Yu, Y., and Wang, C.-Y. (2021). Transcriptional Super-enhancers Control Cancer Stemness and Metastasis Genes in Squamous Cell Carcinoma. *Nat. Commun.* 12 (1), 3974. doi:10.1038/s41467-021-24137-1

Duarte, S., Loubat, A., Momier, D., Topi, M., Faneca, H., Pedroso de Lima, M. C., et al. (2012). Isolation of Head and Neck Squamous Carcinoma Cancer Stem-like Cells in a Syngeneic Mouse Model and Analysis of Hypoxia Effect. *Oncol. Rep.* 28 (3), 1057–1062. doi:10.3892/or.2012.1904

Faber, A., Goessler, U. R., Hoermann, K., Schultz, J. D., Umbreit, C., and Stern-Straeter, J. (2013a). SDF-1-CXCR4 axis: Cell Trafficking in the Cancer Stem Cell Niche of Head and Neck Squamous Cell Carcinoma. *Oncol. Rep.* 29 (6), 2325–2331. doi:10.3892/or.2013.2380

Faber, A., Hoermann, K., Stern-Straeter, J., Schultz, D. J., and Goessler, U. R. (2013b). Functional Effects of SDF-1α on a CD44+ CXCR4+ Squamous Cell Carcinoma Cell Line as a Model for Interactions in the Cancer Stem Cell Niche. *Oncol. Rep.* 29 (2), 579–584. doi:10.3892/or.2012.2171

Ferreira, L. P., Gaspar, V. M., and Mano, J. F. (2018). Bioinstructive Microparticles for Self-Assembly of Mesenchymal Stem Cell-3D Tumor Spheroids. *Biomaterials* 185, 155–173. doi:10.1016/j.biomaterials.2018.09.007

Fitriana, M., Hwang, W. L., Chan, P. Y., Hsueh, T. Y., and Liao, T. T. (2021). Roles of microRNAs in Regulating Cancer Stemness in Head and Neck Cancers. *Cancers (Basel)* 13 (7). doi:10.3390/cancers13071742

Fukusumi, T., Guo, T. W., Sakai, A., Ando, M., Ren, S., Haft, S., et al. (2018). The NOTCH4-HEY1 Pathway Induces Epithelial-Mesenchymal Transition in Head and Neck Squamous Cell Carcinoma. *Clin. Cancer Res.* 24 (3), 619–633. doi:10.1158/1078-0432.ccr-17-1366

Gammon, L., Biddle, A., Heywood, H. K., Johannessen, A. C., and Mackenzie, I. C. (2013). Sub-sets of Cancer Stem Cells Differ Intrinsically in Their Patterns of Oxygen Metabolism. *PLoS One* 8 (4), e62493. doi:10.1371/journal.pone.0062493

Garin-Chesa, P., Old, L. J., and Rettig, W. J. (1990). Cell Surface Glycoprotein of Reactive Stromal Fibroblasts as a Potential Antibody Target in Human Epithelial Cancers. *Pnas* 87 (18), 7235–7239. doi:10.1073/pnas.87.18.7235

Ghajar, C. M., Peinado, H., Mori, H., Matei, I. R., Evason, K. J., Brazier, H., et al. (2013). The Perivascular Niche Regulates Breast Tumour Dormancy. *Nat. Cel Biol* 15 (7), 807–817. doi:10.1038/ncb2767

Gomez, K. E., Wu, F., Keysar, S. B., Morton, J. J., Miller, B., Chimed, T.-S., et al. (2020). Cancer Cell CD44 Mediates Macrophage/Monocyte-Driven Regulation of Head and Neck Cancer Stem Cells. *Cancer Res.* 80 (19), 4185–4198. doi:10.1158/0008-5472.can-20-1079

Greaves, M. (2015). Evolutionary Determinants of Cancer. *Cancer Discov.* 5 (8), 806–820. doi:10.1158/2159-8290.cd-15-0439

Gupta, P. B., Fillmore, C. M., Jiang, G., Shapira, S. D., Tao, K., Kuperwasser, C., et al. (2011). Stochastic State Transitions Give Rise to Phenotypic

Equilibrium in Populations of Cancer Cells. *Cell* 146 (4), 633–644. doi:10.1016/j.cell.2011.07.026

Hanna, J. H., Saha, K., and Jaenisch, R. (2010). Pluripotency and Cellular Reprogramming: Facts, Hypotheses, Unresolved Issues. *Cell* 143 (4), 508–525. doi:10.1016/j.cell.2010.10.008

He, K. F., Zhang, L., Huang, C. F., Ma, S. R., Wang, Y. F., Wang, W. M., et al. (20142014). CD163+ Tumor-Associated Macrophages Correlated with Poor Prognosis and Cancer Stem Cells in Oral Squamous Cell Carcinoma. *Biomed. Res. Int.* 2014, 838632. doi:10.1155/2014/838632

Heise, T., and Sommer, G. (2021). RNA-binding Protein La Mediates TGFβ-Induced Epithelial to Mesenchymal Transition and Cancer Stem Cell Properties. *Cancers* 13 (2), 343. doi:10.3390/cancers13020343

Hermann, P. C., Huber, S. L., Herrler, T., Aicher, A., Ellwart, J. W., Guba, M., et al. (2007). Distinct Populations of Cancer Stem Cells Determine Tumor Growth and Metastatic Activity in Human Pancreatic Cancer. *Cell Stem Cell* 1 (3), 313–323. doi:10.1016/j.stem.2007.06.002

Hu, J., Mirshahidi, S., Simental, A., Lee, S. C., De Andrade Filho, P. A., Peterson, N. R., et al. (2019). Cancer Stem Cell Self-Renewal as a Therapeutic Target in Human Oral Cancer. *Oncogene* 38 (27), 5440–5456. doi:10.1038/s41388-019-0800-z

Hu, Y., He, M. Y., Zhu, L. F., Yang, C. C., Zhou, M. L., Wang, Q., et al. (2016). Tumor-associated Macrophages Correlate with the Clinicopathological Features and Poor Outcomes via Inducing Epithelial to Mesenchymal Transition in Oral Squamous Cell Carcinoma. *J. Exp. Clin. Cancer Res.* 35 (1), 12. doi:10.1186/s13046-015-0281-z

Joshua, B., Kaplan, M. J., Doweck, I., Pai, R., Weissman, I. L., Prince, M. E., et al. (2012). Frequency of Cells Expressing CD44, a Head and Neck Cancer Stem Cell Marker: Correlation with Tumor Aggressiveness. *Head Neck* 34 (1), 42–49. doi:10.1002/hed.21699

Jungbauer, F., Aderhold, C., Birk, R., Hoermann, K., Kramer, B., Kuhlin, B., et al. (2017). Communicate or Die - A Model for HPV+ and HPV- CSCs and Their Interactions with SDF-1α. *Anticancer Res.* 37 (9), 4827–4836. doi:10.21873/anticanres.11890

Keysar, S. B., Gomes, N., Miller, B., Jackson, B. C., Le, P. N., Morton, J. J., et al. (2020). Inhibiting Translation Elongation with SVC112 Suppresses Cancer Stem Cells and Inhibits Growth in Head and Neck Squamous Carcinoma. *Cancer Res.* 80 (5), 1183–1198. doi:10.1158/0008-5472.can-19-3232

Krishnamurthy, S., Dong, Z., Vodopyanov, D., Imai, A., Helman, J. I., Prince, M. E., et al. (2010). Endothelial Cell-Initiated Signaling Promotes the Survival and Self-Renewal of Cancer Stem Cells. *Cancer Res.* 70 (23), 9969–9978. doi:10.1158/0008-5472.can-10-1712

Krishnamurthy, S., Warner, K. A., Dong, Z., Imai, A., Nör, C., Ward, B. B., et al. (2014). Endothelial Interleukin-6 Defines the Tumorigenic Potential of Primary Human Cancer Stem Cells. *Stem Cells* 32 (11), 2845–2857. doi:10.1002/stem.1793

Lee, Y., Shin, J. H., Longmire, M., Wang, H., Kohrt, H. E., Chang, H. Y., et al. (2016). CD44+ Cells in Head and Neck Squamous Cell Carcinoma Suppress T-Cell-Mediated Immunity by Selective Constitutive and Inducible Expression of PD-L1. *Clin. Cancer Res.* 22 (14), 3571–3581. doi:10.1158/1078-0432.ccr-15-2665

Leong, H. S., Chong, F. T., Sew, P. H., Lau, D. P., Wong, B. H., Teh, B.-T., et al. (2014). Targeting Cancer Stem Cell Plasticity through Modulation of Epidermal Growth Factor and Insulin-like Growth Factor Receptor Signaling in Head and Neck Squamous Cell Cancer. *Stem Cell Transl Med* 3 (9), 1055–1065. doi:10.5966/sctm.2013-0214

Liao, T., Kaufmann, A. M., Qian, X., Sangvatanakul, V., Chen, C., Kube, T., et al. (2013). Susceptibility to Cytotoxic T Cell Lysis of Cancer Stem Cells Derived from Cervical and Head and Neck Tumor Cell Lines. *J. Cancer Res. Clin. Oncol.* 139 (1), 159–170. doi:10.1007/s00432-012-1311-2

Lin, J., Liu, C., Ge, L., Gao, Q., He, X., Liu, Y., et al. (2011). Carcinoma-associated Fibroblasts Promotes the Proliferation of a Lingual Carcinoma Cell Line by Secreting Keratinocyte Growth Factor. *Tumor Biol.* 32 (3), 597–602. doi:10.1007/s13277-011-0158-5

Liu, L., Zhang, Z., Zhou, L., Hu, L., Yin, C., Qing, D., et al. (2020). Cancer Associated Fibroblasts-Derived Exosomes Contribute to Radioresistance through Promoting Colorectal Cancer Stem Cells Phenotype. *Exp. Cel Res.* 391 (2), 111956. doi:10.1016/j.yexcr.2020.111956

Liu, S.-C., Huang, C.-S., Huang, C.-M., Hsieh, M.-S., Huang, M.-S., Fong, I.-H., et al. (2021a). Isoorientin Inhibits Epithelial-To-Mesenchymal Properties and Cancer Stem-cell-like Features in Oral Squamous Cell Carcinoma by Blocking Wnt/β-catenin/STAT3 axis. *Toxicol. Appl. Pharmacol.* 424, 115581. doi:10.1016/j.taap.2021.115581

Liu, S., and Cheng, C. (2017). Akt Signaling Is Sustained by a CD44 Splice Isoform-Mediated Positive Feedback Loop. *Cancer Res.* 77 (14), 3791–3801. doi:10.1158/0008-5472.can-16-2545

Liu, Y., Sun, Y., Han, S., Guo, Y., Tian, Q., Ma, Q., et al. (2021b). CHIP Promotes the Activation of NF-Kb Signaling through Enhancing the K63-Linked Ubiquitination of TAK1. *Cell Death Discov.* 7 (1), 246. doi:10.1038/s41420-021-00637-3

López-Gil, J. C., Martin-Hijano, L., Hermann, P. C., and Sainz, B. (2021). The CXCL12 Crossroads in Cancer Stem Cells and Their Niche. *Cancers* 13 (3), 469. doi:10.3390/cancers13030469

Maccalli, C., Rasul, K. I., Elawad, M., and Ferrone, S. (2018). The Role of Cancer Stem Cells in the Modulation of Anti-tumor Immune Responses. *Semin. Cancer Biol.* 53, 189–200. doi:10.1016/j.semcancer.2018.09.006

Magan, M., Wiechec, E., and Roberg, K. (2020). CAFs Affect the Proliferation and Treatment Response of Head and Neck Cancer Spheroids during Co-culturing in a Unique *In Vitro* Model. *Cancer Cel Int* 20 (1), 599. doi:10.1186/s12935-020-01718-6

Mantovani, A., Marchesi, F., Malesci, A., Laghi, L., and Allavena, P. (2017). Tumour-associated Macrophages as Treatment Targets in Oncology. *Nat. Rev. Clin. Oncol.* 14 (7), 399–416. doi:10.1038/nrclinonc.2016.217

Marcu, L. G., Marcu, D., and Filip, S. M. (2016). In Silicostudy of the Impact of Cancer Stem Cell Dynamics and Radiobiological Hypoxia on Tumour Response to Hyperfractionated Radiotherapy. *Cell Prolif.* 49 (3), 304–314. doi:10.1111/cpr.12251

Marsh, D., Suchak, K., Moutasim, K. A., Vallath, S., Hopper, C., Jerjes, W., et al. (2011). Stromal Features Are Predictive of Disease Mortality in Oral Cancer Patients. *J. Pathol.* 223 (4), 470–481. doi:10.1002/path.2830

Martens-de Kemp, S. R., Brink, A., Stigter-van Walsum, M., Damen, J. M. A., Rustenburg, F., Wu, T., et al. (2013). CD98 marks a Subpopulation of Head and Neck Squamous Cell Carcinoma Cells with Stem Cell Properties. *Stem Cel Res.* 10 (3), 477–488. doi:10.1016/j.scr.2013.02.004

Marusyk, A., Almendro, V., and Polyak, K. (2012). Intra-tumour Heterogeneity: a Looking Glass for Cancer? *Nat. Rev. Cancer* 12 (5), 323–334. doi:10.1038/nrc3261

McGranahan, N., Furness, A. J. S., Rosenthal, R., Ramskov, S., Lyngaa, R., Saini, S. K., et al. (2016). Clonal Neoantigens Elicit T Cell Immunoreactivity and Sensitivity to Immune Checkpoint Blockade. *Science* 351 (6280), 1463–1469. doi:10.1126/science.aaf1490

Medema, J. P. (2013). Cancer Stem Cells: the Challenges Ahead. *Nat. Cel Biol* 15 (4), 338–344. doi:10.1038/ncb2717

Medema, J. P., and Vermeulen, L. (2011). Microenvironmental Regulation of Stem Cells in Intestinal Homeostasis and Cancer. *Nature* 474 (7351), 318–326. doi:10.1038/nature10212

Meissner, M., Reichert, T. E., Kunkel, M., Gooding, W., Whiteside, T. L., Ferrone, S., et al. (2005). Defects in the Human Leukocyte Antigen Class I Antigen Processing Machinery in Head and Neck Squamous Cell Carcinoma: Association with Clinical Outcome. *Clin. Cancer Res.* 11 (7), 2552–2560. doi:10.1158/1078-0432.ccr-04-2146

Menendez, J., Joven, J., Cufí, S., Corominas-Faja, B., Oliveras-Ferraros, C., Cuyàs, E., et al. (2013). The Warburg Effect Version 2.0: Metabolic Reprogramming of Cancer Stem Cells. *Cell Cycle* 12 (8), 1166–1179. doi:10.4161/cc.24479

Morel, A.-P., Lièvre, M., Thomas, C., Hinkal, G., Ansieau, S., and Puisieux, A. (2008). Generation of Breast Cancer Stem Cells through Epithelial-Mesenchymal Transition. *PLoS One* 3 (8), e2888. doi:10.1371/journal.pone.0002888

Mroz, E. A., Tward, A. D., Pickering, C. R., Myers, J. N., Ferris, R. L., and Rocco, J. W. (2013). High Intratumor Genetic Heterogeneity Is Related to Worse Outcome in Patients with Head and Neck Squamous Cell Carcinoma. *Cancer* 119 (16), 3034–3042. doi:10.1002/cncr.28150

Nam, K., Oh, S., and Shin, I. (2016). Ablation of CD44 Induces Glycolysis-To-Oxidative Phosphorylation Transition via Modulation of the C-Src-Akt-LKB1-Ampkα Pathway. *Biochem. J.* 473 (19), 3013–3030. doi:10.1042/bcj20160613

Nong, S., Wei, Z., Wang, Z., Ma, L., Guan, Y., and Ni, J. (2021). Reduced DAPK1 Expression Promotes Stem Cell-like Characteristics of Prostate Cancer Cells by Activating ZEB1 via Hippo/YAP Signaling Pathway. *Stem Cell Dev.* 30 (18), 934–945. doi:10.1089/scd.2021.0043

Palorini, R., Votta, G., Balestrieri, C., Monestiroli, A., Olivieri, S., Vento, R., et al. (2014). Energy Metabolism Characterization of a Novel Cancer Stem Cell-like Line 3AB-OS. *J. Cel. Biochem.* 115 (2), 368–379. doi:10.1002/jcb.24671

Passi, A., Vigetti, D., Buraschi, S., and Iozzo, R. V. (2019). Dissecting the Role of Hyaluronan Synthases in the Tumor Microenvironment. *Febs j* 286 (15), 2937–2949. doi:10.1111/febs.14847

Pérez, G., López-Moncada, F., Indo, S., Torres, M. J., Castellón, E. A., and Contreras, H. R. (2021). Knockdown of ZEB1 Reverses Cancer Stem Cell Properties in Prostate Cancer Cells. *Oncol. Rep.* 45 (5).

Plaks, V., Kong, N., and Werb, Z. (2015). The Cancer Stem Cell Niche: How Essential Is the Niche in Regulating Stemness of Tumor Cells? *Cell Stem Cell* 16 (3), 225–238. doi:10.1016/j.stem.2015.02.015

Popple, A., Durrant, L. G., Spendlove, I., Rolland, P., Scott, I. V., Deen, S., et al. (2012). The Chemokine, CXCL12, Is an Independent Predictor of Poor Survival in Ovarian Cancer. *Br. J. Cancer* 106 (7), 1306–1313. doi:10.1038/bjc.2012.49

Prince, M. E. P., Zhou, L., Moyer, J. S., Tao, H., Lu, L., Owen, J., et al. (2016). Evaluation of the Immunogenicity of ALDHhigh Human Head and Neck Squamous Cell Carcinoma Cancer Stem Cells *In Vitro*. *Oral Oncol.* 59, 30–42. doi:10.1016/j.oraloncology.2016.05.013

Prince, M. E., Sivanandan, R., Kaczorowski, A., Wolf, G. T., Kaplan, M. J., Dalerba, P., et al. (2007). Identification of a Subpopulation of Cells with Cancer Stem Cell Properties in Head and Neck Squamous Cell Carcinoma. *Pnas* 104 (3), 973–978. doi:10.1073/pnas.0610117104

Puram, S. V., Tirosh, I., Parikh, A. S., Patel, A. P., Yizhak, K., Gillespie, S., et al. (2017). Single-Cell Transcriptomic Analysis of Primary and Metastatic Tumor Ecosystems in Head and Neck Cancer. *Cell* 171 (7), 1611–1624. doi:10.1016/j.cell.2017.10.044

Qi, Y., Li, R.-M., Kong, F.-M., Li, H., Yu, J.-P., and Ren, X.-B. (2012). How Do Tumor Stem Cells Actively Escape from Host Immunosurveillance? *Biochem. Biophysical Res. Commun.* 420 (4), 699–703. doi:10.1016/j.bbrc.2012.03.086

Rao, G., Wang, H., Li, B., Huang, L., Xue, D., Wang, X., et al. (2013). Reciprocal Interactions between Tumor-Associated Macrophages and CD44-Positive Cancer Cells via osteopontin/CD44 Promote Tumorigenicity in Colorectal Cancer. *Clin. Cancer Res.* 19 (4), 785–797. doi:10.1158/1078-0432.ccr-12-2788

Reya, T., Morrison, S. J., Clarke, M. F., and Weissman, I. L. (2001). Stem Cells, Cancer, and Cancer Stem Cells. *Nature* 414 (6859), 105–111. doi:10.1038/35102167

Ritchie, K. E., and Nör, J. E. (2013). Perivascular Stem Cell Niche in Head and Neck Cancer. *Cancer Lett.* 338 (1), 41–46. doi:10.1016/j.canlet.2012.07.025

Saito, S., Ozawa, H., Imanishi, Y., Sekimizu, M., Watanabe, Y., Ito, F., et al. (2021). Cyclooxygenase-2 E-xpression I-s A-ssociated with C-hemoresistance through C-ancer S-temness P-roperty in H-ypopharyngeal C-arcinoma. *Oncol. Lett.* 22 (1), 533. doi:10.3892/ol.2021.12794

Sancho, P., Burgos-Ramos, E., Tavera, A., Bou Kheir, T., Jagust, P., Schoenhals, M., et al. (2015). MYC/PGC-1α Balance Determines the Metabolic Phenotype and Plasticity of Pancreatic Cancer Stem Cells. *Cel Metab.* 22 (4), 590–605. doi:10.1016/j.cmet.2015.08.015

Shackleton, M., Quintana, E., Fearon, E. R., and Morrison, S. J. (2009). Heterogeneity in Cancer: Cancer Stem Cells versus Clonal Evolution. *Cell* 138 (5), 822–829. doi:10.1016/j.cell.2009.08.017

Shah, S. P., Morin, R. D., Khattra, J., Prentice, L., Pugh, T., Burleigh, A., et al. (2009). Mutational Evolution in a Lobular Breast Tumour Profiled at Single Nucleotide Resolution. *Nature* 461 (7265), 809–813. doi:10.1038/nature08489

Shen, Q., Goderie, S. K., Jin, L., Karanth, N., Sun, Y., Abramova, N., et al. (2004). Endothelial Cells Stimulate Self-Renewal and Expand Neurogenesis of Neural Stem Cells. *Science* 304 (5675), 1338–1340. doi:10.1126/science.1095505

Shen, Y.-A., Wang, C.-Y., Hsieh, Y.-T., Chen, Y.-J., and Wei, Y.-H. (2015). Metabolic Reprogramming Orchestrates Cancer Stem Cell Properties in Nasopharyngeal Carcinoma. *Cell Cycle* 14 (1), 86–98. doi:10.4161/15384101.2014.974419

Shibata, M., and Hoque, M. O. (2019). Targeting Cancer Stem Cells: A Strategy for Effective Eradication of Cancer. *Cancers (Basel)* 11 (5). doi:10.3390/cancers11050732

Shimokawa, M., Ohta, Y., Nishikori, S., Matano, M., Takano, A., Fujii, M., et al. (2017). Visualization and Targeting of LGR5+ Human colon Cancer Stem Cells. *Nature* 545 (7653), 187–192. doi:10.1038/nature22081

Siegel, R. L., Miller, K. D., and Jemal, A. (20152015)., 65. CA, 5–29. doi:10.3322/caac.21254Cancer Statistics, 2015*CA: A Cancer J. Clinicians*1

Škerlová, J., Král, V., Kachala, M., Fábry, M., Bumba, L., Svergun, D. I., et al. (2015). Molecular Mechanism for the Action of the Anti-CD44 Monoclonal Antibody MEM-85. *J. Struct. Biol.* 191 (2), 214–223.

Sottoriva, A., Verhoeff, J. J. C., Borovski, T., McWeeney, S. K., Naumov, L., Medema, J. P., et al. (2010). Cancer Stem Cell Tumor Model Reveals Invasive Morphology and Increased Phenotypical Heterogeneity. *Cancer Res.* 70 (1), 46–56. doi:10.1158/0008-5472.can-09-3663

Stransky, N., Egloff, A. M., Tward, A. D., Kostic, A. D., Cibulskis, K., Sivachenko, A., et al. (2011). The Mutational Landscape of Head and Neck Squamous Cell Carcinoma. *Science* 333 (6046), 1157–1160. doi:10.1126/science.1208130

Subramanian, C., Kovatch, K. J., Sim, M. W., Wang, G., Prince, M. E., Carey, T. E., et al. (2017). Novel C-Terminal Heat Shock Protein 90 Inhibitors (KU711 and Ku757) Are Effective in Targeting Head and Neck Squamous Cell Carcinoma Cancer Stem Cells. *Neoplasia* 19 (12), 1003–1011. doi:10.1016/j.neo.2017.09.003

Taniguchi, S., Elhance, A., Van Duzer, A., Kumar, S., Leitenberger, J. J., and Oshimori, N. (2020). Tumor-initiating Cells Establish an IL-33-TGF-β Niche Signaling Loop to Promote Cancer Progression. *Science* 369 (6501). doi:10.1126/science.aay1813

Tcga, N. (2015). Comprehensive Genomic Characterization of Head and Neck Squamous Cell Carcinomas. *Nature* 517 (7536), 576–582. doi:10.1038/nature14129

Tian, J., Hachim, M. Y., Hachim, I. Y., Dai, M., Lo, C., Raffa, F. A., et al. (2017). Cyclooxygenase-2 Regulates TGFβ-Induced Cancer Stemness in Triple-Negative Breast Cancer. *Sci. Rep.* 7, 40258. doi:10.1038/srep40258

Tsai, M.-S., Chen, W.-C., Lai, C.-H., Chen, Y.-Y., and Chen, M.-F. (2017). Epigenetic Therapy Regulates the Expression of ALDH1 and Immunologic Response: Relevance to the Prognosis of Oral Cancer. *Oral Oncol.* 73, 88–96. doi:10.1016/j.oraloncology.2017.08.007

Wang, J. C. Y., and Dick, J. E. (2005). Cancer Stem Cells: Lessons from Leukemia. *Trends Cel Biol.* 15 (9), 494–501. doi:10.1016/j.tcb.2005.07.004

Wang, S. J., Wong, G., de Heer, A.-M., Xia, W., and Bourguignon, L. Y. W. (2009). CD44 Variant Isoforms in Head and Neck Squamous Cell Carcinoma Progression. *The Laryngoscope* 119 (8), 1518–1530. doi:10.1002/lary.20506

Wang, X., Cao, Y., Zhang, S., Chen, Z., Fan, L., Shen, X., et al. (2017). Stem Cell Autocrine CXCL12/CXCR4 Stimulates Invasion and Metastasis of Esophageal Cancer. *Oncotarget* 8 (22), 36149–36160. doi:10.18632/oncotarget.15254

Warburg, O. (1956). On the Origin of Cancer Cells. *Science* 123 (3191), 309–314. doi:10.1126/science.123.3191.309

Wei, X. D., Zhou, L., Cheng, L., Tian, J., Jiang, J. J., and Maccallum, J. (2009). *In Vivo* investigation of CD133 as a Putative Marker of Cancer Stem Cells in Hep-2 Cell Line. *Head Neck* 31 (1), 94–101. doi:10.1002/hed.20935

Wheeler, S. E., Shi, H., Lin, F., Dasari, S., Bednash, J., Thorne, S., et al. (2014). Enhancement of Head and Neck Squamous Cell Carcinoma Proliferation, Invasion, and Metastasis by Tumor-Associated Fibroblasts in Preclinical Models. *Head Neck* 36 (3), 385–392. doi:10.1002/hed.23312

Wozny, A.-S., Lauret, A., Battiston-Montagne, P., Guy, J.-B., Beuve, M., Cunha, M., et al. (2017). Differential Pattern of HIF-1α Expression in HNSCC Cancer Stem Cells after Carbon Ion or Photon Irradiation: One Molecular Explanation of the Oxygen Effect. *Br. J. Cancer* 116 (10), 1340–1349. doi:10.1038/bjc.2017.100

Wu, C.-P., Du, H.-D., Gong, H.-L., Li, D.-W., Tao, L., Tian, J., et al. (2014). Hypoxia Promotes Stem-like Properties of Laryngeal Cancer Cell Lines by Increasing the CD133+ Stem Cell Fraction. *Int. J. Oncol.* 44 (5), 1652–1660. doi:10.3892/ijo.2014.2307

Xie, J., Wang, Z., Fan, W., Liu, Y., Liu, F., Wan, X., et al. (2021). Targeting Cancer Cell Plasticity by HDAC Inhibition to Reverse EBV-Induced Dedifferentiation in Nasopharyngeal Carcinoma. *Sig Transduct Target. Ther.* 6 (1), 333. doi:10.1038/s41392-021-00702-4

Xing, F., Saidou, J., and Watabe, K. (2010). Cancer Associated Fibroblasts (CAFs) in Tumor Microenvironment. *Front. Biosci.* 15, 166–179. doi:10.2741/3613

Yan, M., Yang, X., Wang, L., Clark, D., Zuo, H., Ye, D., et al. (2013). Plasma Membrane Proteomics of Tumor Spheres Identify CD166 as a Novel Marker for

Cancer Stem-like Cells in Head and Neck Squamous Cell Carcinoma. *Mol. Cell Proteomics* 12 (11), 3271–3284. doi:10.1074/mcp.m112.025460

Yang, C., Cao, M., Liu, Y., He, Y., Du, Y., Zhang, G., et al. (2019). Inducible Formation of Leader Cells Driven by CD44 Switching Gives Rise to Collective Invasion and Metastases in Luminal Breast Carcinomas. *Oncogene* 38 (46), 7113–7132. doi:10.1038/s41388-019-0899-y

Yao, Z., Du, L., Xu, M., Li, K., Guo, H., Ye, G., et al. (2019). MTA3-SOX2 Module Regulates Cancer Stemness and Contributes to Clinical Outcomes of Tongue Carcinoma. *Front. Oncol.* 9 (816), 816. doi:10.3389/fonc.2019.00816

Yu, B., Wu, K., Wang, X., Zhang, J., Wang, L., Jiang, Y., et al. (2018). Periostin Secreted by Cancer-Associated Fibroblasts Promotes Cancer Stemness in Head and Neck Cancer by Activating Protein Tyrosine Kinase 7. *Cell Death Dis* 9 (11), 1082. doi:10.1038/s41419-018-1116-6

Yuan, W., Ji, J., Shu, Y., Chen, J., Liu, S., Wu, L., et al. (2019). Downregulation of DAPK1 Promotes the Stemness of Cancer Stem Cells and EMT Process by Activating ZEB1 in Colorectal Cancer. *J. Mol. Med.* 97 (1), 89–102. doi:10.1007/s00109-018-1716-8

Zhou, L., Wei, X., Cheng, L., Tian, J., and Jiang, J. J. (2007). CD133, One of the Markers of Cancer Stem Cells in Hep-2 Cell Line. *The Laryngoscope* 117 (3), 455–460. doi:10.1097/01.mlg.0000251586.15299.35

Zong, X., Ozes, A. R., and Nephew, K. P. (2018). Abstract B07: Targeting DAB2IP in Ovarian Cancer Stem Cells. *Clin. Cancer Res.* 24 (15 Suppl. ment), B07. doi:10.1158/1557-3265.ovca17-b07

Conflict of Interest: The authors declare that the research was conducted in the absence of any commercial or financial relationships that could be construed as a potential conflict of interest.

Publisher's Note: All claims expressed in this article are solely those of the authors and do not necessarily represent those of their affiliated organizations, or those of the publisher, the editors and the reviewers. Any product that may be evaluated in this article, or claim that may be made by its manufacturer, is not guaranteed or endorsed by the publisher.

frontiers in Cell and Developmental Biology

REVIEW
published: 16 February 2022
doi: 10.3389/fcell.2022.773038

The Roles of Noncoding RNAs in the Development of Osteosarcoma Stem Cells and Potential Therapeutic Targets

*Jinxin Liu and Guanning Shang**

Department of Orthopedic Surgery, Shengjing Hospital, China Medical University, Shenyang, China

Osteosarcoma (OS) is the common bone tumor in children and adolescents. Because of chemotherapy resistance, the OS patients have a poor prognosis. The one reason of chemotherapeutic resistance is the development of cancer stem cells (CSCs). CSCs represent a small portion of tumor cells with the capacity of self-renewal and multipotency, which are associated with tumor initiation, metastasis, recurrence and drug resistance. Recently, noncoding RNAs (ncRNAs) have been reported to critically regulate CSCs. Therefore, in this review article, we described the role of ncRNAs, especially miRNAs, lncRNAs and circRNAs, in regulating CSCs development and potential mechanisms. Specifically, we discussed the role of multiple miRNAs in targeting CSCs, including miR-26a, miR-29b, miR-34a, miR-133a, miR-143, miR-335, miR-382, miR-499a, miR-1247, and let-7days. Moreover, we highlighted the functions of lncRNAs in regulating CSCs in OS, such as B4GALT1-AS1, DANCR, DLX6-AS1, FER1L4, HIF2PUT, LINK-A, MALAT1, SOX2-OT, and THOR. Due to the critical roles of ncRNAs in regulation of OS CSCs, targeting ncRNAs might be a novel strategy for eliminating CSCs for OS therapy.

Keywords: noncoding RNA, miRNA, stem cell, osteosarcoma, lncRNAs

OPEN ACCESS

Edited by:
Eliza Chakraborty, University of California, Los Angeles, United States

Reviewed by:
Margherita Cortini, Rizzoli Orthopedic Institute (IRCCS), Italy
Sourav Panja, Vanderbilt University Medical Center, United States

****Correspondence:***
Guanning Shang
shangguanning@hotmail.com

Specialty section:
This article was submitted to Stem Cell Research, a section of the journal Frontiers in Cell and Developmental Biology

Received: *09 September 2021*
Accepted: *31 January 2022*
Published: *16 February 2022*

Citation:
Liu J and Shang G (2022) The Roles of Noncoding RNAs in the Development of Osteosarcoma Stem Cells and Potential Therapeutic Targets. Front. Cell Dev. Biol. 10:773038. doi: 10.3389/fcell.2022.773038

INTRODUCTION

Osteosarcoma (OS) is the common bone tumor in children and adolescents, which causes a huge healthy problem in childhood (Siegel et al., 2021; Sung et al., 2021). Because a majority of OS patients at diagnosis have micro-metastasis, chemotherapy is often the first strategy for OS treatment (Gill and Gorlick, 2021). However, the drug resistance causes poor outcomes of OS therapy and leads to lower survival rate (Hattinger et al., 2021; Yan and Xiang, 2021). Drug resistance could be due to the development of cancer stem cells (CSCs) in tumorigenesis and progression (Akbar Samadani et al., 2020). CSCs represent a small group of tumor cells with the capacity of self-renewal and multipotency (Izadpanah et al., 2020). It has been documented that CSCs are involved in tumor initiation, metastasis, recurrence and drug resistance. CSCs were identified in a variety of human cancers including OS (Brown et al., 2017; Schiavone et al., 2019). One study identified that CD-117 and Stro-1 might be CSC biomarkers for mouse and human OS, which is involved in tumor metastasis and doxorubicin resistance (Adhikari et al., 2010). Aldehyde dehydrogenase (ALDH) has been considered as a CSC biomarker in OS (Belayneh and Weiss, 2020; Izadpanah et al., 2020). In addition, CD44, CD105, CD199, CD133, CD271, ABCG2, and Sca-1 were repowered as biomarkers for OS CSCs (Yan et al., 2016). Three important pluripotent proteins Sox2, Nanog and Oct3/4 were also correlated with OS CSCs

TABLE 1 | miRNAs regulate CSCs in OS.

miRNAs	Expression	Genes and pathways	References
miR-26a	Down	Jagged-1	Lu et al. (2017)
miR-29b	Down	PI3K/Akt, STAT3	(Di Fiore et al., 2013; Di Fiore et al., 2014; Li et al., 2020b)
miR-34a	Down	DNMT1, Bcl-2	(Liang et al., 2019a; Liang et al., 2019b)
miR-133a	Up	SGMS2, UBA2, SNX30, ANXA2	Fujiwara et al. (2014)
miR-143	Down	KIAA1429, Notch-1	Han et al. (2020)
miR-335	Down	POU5F1	Guo et al. (2017)
miR-382	Down	YB-1	Xu et al. (2015)
miR-499a	Down	SHKBP1	Di Fiore et al. (2016)
miR-1247	Down	MAP3K9	Zhao et al. (2015)
let-7d	Down	CXCR4, MMP-9, VersicanV1, caspase-3, Bcl-2, E-cadherin, N-cadherin, Vimentin, E2F, CCND2, Lin28B, HMGA2	Di Fiore et al. (2016)

(Yan et al., 2016). Targeting CSCs could be useful for blockade of tumor metastasis and overcoming drug resistance in OS.

NONCODING RNAS IN OS

A number of studies have demonstrated that noncoding RNAs (ncRNAs) are involved in the development, diagnosis, prognosis and treatment of OS (Yang et al., 2021). It has been documented that ncRNAs cannot encode proteins but can regulate gene expression, which include microRNAs (miRNAs), long ncRNAs (lncRNAs) and circRNAs (Slack and Chinnaiyan, 2019). MiRNAs often have 18–25 nucleotides in length and target specific mRNAs via completely or partially complementary binding with 3′UTR of mRNAs (Gebert and Macrae, 2019). LncRNAs with >200 nucleotides exert their functions mainly via sponging miRNAs and targeting specific substrates. Emerging evidence has dissected that ncRNAs participate in OS tumorigenesis and progression (Ghafouri-Fard et al., 2021). For example, ncRNAs are involved in chemotherapeutic drug resistance in osteosarcoma (Ferretti and Leon, 2021; Lin et al., 2021). In recent years, ncRNAs were reported to critically participate in CSCs in a variety of cancers, including OS (Lei et al., 2020; Humphries et al., 2021; Melendez-Zajgla and Maldonado, 2021). Therefore, in the following paragraphs, we will discuss the role of ncRNAs, especially miRNAs, including miR-26a, miR-29b, miR-34a, miR-133a, miR-143, miR-335, miR-382, miR-499a, miR-1247, and let-7days, and lncRNAs, such as B4GALT1-AS1, DANCR, DLX6-AS1, FER1L4, HIF2PUT, LINK-A, MALAT1, SOX2-OT, and THOR, and circRNAs including circ_0001658, circ_0002052 and circPIP5K1A, in regulating CSCs development and potential mechanisms.

MIRNAS REGULATE OSTEOSARCOMA CSCS

It is clear that miRNAs participate in regulation of OS CSCs in various types of human cancers, including OS (**Table 1**). One study determined the genetic characterizations of 3AB-OS CSC line that was established from MG63 cells, and found that 189 differentially expressed miRNAs were existed in 3AB-OS CSCs compared with their parental MG63 cells (Di Fiore et al., 2013). Among these miRNAs, let-7, miR-98 and miR-29a, b, c were downregulated in 3AB-OS CSCs (Di Fiore et al., 2013). One group used DNA microarray and detected the miRNA expression profile in OS cells with CD117 and Stro-1 positive compared with CD117 and Stro-1 negative OS cells (Zhao et al., 2015). This study identified five downregulated miRNAs, including miR-15a, miR-212, miR-302a, miR-423-5p and miR-1247, and three upregulated miRNAs, such as miR-890, miR-518b and miR-1243 (Zhao et al., 2015), suggesting that miRNAs could participate in CSC regulation.

MIRNAS REGULATE PROLIFERATION OF OSTEOSARCOMA CSC CELLS

miR-26a

Evidence has revealed that miR-26a is critically involved in osteosarcoma progression via regulating several downstream targets (Song et al., 2014; Liu et al., 2018). Downregulation of miR-26a was observed and associated with poor prognosis in osteosarcoma patients (Song et al., 2014). For example, miR-26a blocked the migration and invasion of osteosarcoma cells via directly inhibiting HMGA1 (Liu et al., 2018). Similarly, miR-26a retarded the migratory and invasive capacity of osteosarcoma cells via repressing EZH2 expression (Song et al., 2014). Tan et al. reported that miR-26a attenuated cell proliferation via inhibiting IGF-1 expression in osteosarcoma cells (Tan et al., 2015). Li et al. found that miR-26a could reverse doxorubicin resistance via inhibiting MCL1 in osteosarcoma cells (Li and Ma, 2021). Surprisingly, one study reported that miR-26a might be an oncogene in osteosarcoma. Qu et al. found that miR-26a enhanced cell growth and tumor metastasis via regulating the Wnt/β-catenin pathway by inhibiting GSK-3β in osteosarcoma (Qu et al., 2016). Another study showed that miR-26a repressed stem cell-like properties via inhibition of Jagged-1 in osteosarcoma (Lu et al., 2017). Notably, decreased expression

of miR-26a was linked to lung metastasis and poor survival in patients with osteosarcoma (Lu et al., 2017). Moreover, lower expression of miR-26a existed in osteosarcoma CSCs, and lentivirus-mediated upregulation of miR-26a reduced the expression of stem cell biomarkers, including SOX2, CD133, OCT3/4, Nanog, and nucleostemin in osteosarcoma cells (Lu et al., 2017). ZOS and 143B cells formed smaller and fewer sarcosphere and had a reduction of the ALDH activity after infection with lentiviruses carrying miR-26a. Moreover, miR-26a suppressed the expression of Jagged-1, and led to inhibition of tumor cell growth *in vitro* and *in vivo* (Lu et al., 2017).

miR-34a

Zou et al. revealed that miR-34a expression was lower in osteosarcoma stem-like cells, and overexpression of miR-34a reduced the expression of the stem cell markers and retarded the osteosphere formation (Zou et al., 2017). Zhang et al. discovered that miR-34a worked as a suppressor in regulation of osteosarcoma dedifferentiation into CSCs via inhibition of Sox2 (Zhang et al., 2018). Liang et al. reported that miR-34a was increased after DNMT1 downregulation, leading to suppression of stemness markers expression, including CD133, CD44, Oct4, Sox2, Bmi1 and ABCG2 in osteosarcoma stem-like cells (Liang et al., 2019b). Consistently, overexpression of DNMT1 reduced the expression of miR-34a and promoted the expression of stemness markers in osteosarcoma stem-like cells (Liang et al., 2019b). Moreover, Liang et al. found that isovitexin, a natural flavonoid, reduced the expression of CD133, CD44, ALDH1 and ABCG2 at mRNA levels in osteosarcoma sphere cells, leading to suppression of tumor growth and induction of apoptosis. Mechanistic study showed that isovitexin reduced DNMT1 expression and activity, upregulated miR-34a and attenuated the expression of Bcl-2 in osteosarcoma sphere cells (Liang et al., 2019a).

miR-143

Evidence demonstrated that miR-143 is linked to the survival of OS cells with ALDH1+CD133+ and participated in drug resistance (Zhou et al., 2015). Loss of miR-143 expression was associated with poor survival of OS patients. Overexpression of miR-143 overcame drug resistance via inhibition of ATG2B, LC3-1 and Bcl-2 in U2OS- and SaOS-2-resistant cells (Zhou et al., 2015). In addition, miR-143-3p is involved in osteosarcoma development and progression. MiR-143-3p was identified as a potential marker for diagnosis and prognosis in osteosarcoma patients, because low expression of miR-143-3p was correlated with tumor size, stage and metastasis (Yang et al., 2020). Sun et al. showed that miR-143-3p repressed cell proliferation and invasion via suppression of FOSL2 in osteosarcoma (Sun et al., 2018). Hou et al. observed that miR-143-3p reduced cell growth, migratory and invasive capacity via attenuation of MAPK7 expression in osteosarcoma (Hou et al., 2019). Han et al. uncovered that ectopic expression of miR-143-3p blocked stemness features in osteosarcoma cells, including CD44, Oct4, Nanog and Notch1 (Han et al., 2020). Moreover, miR-143-3p inhibited KIAA1429 expression via binding with its 3′-UTR in U2OS and 143B cells (Han et al., 2020). Furthermore, miR-143-3p suppressed proliferation and invasiveness in a KIAA1429-dependent manner in osteosarcoma cells (Han et al., 2020).

miR-1247

Wei et al. reported that miR-1247 repressed cell viability and blocked tumor metastasis via inhibiting NRP1 expression and mediating Wnt/β-catenin pathway in OS (Wei et al., 2019). Evidence showed that miR-1247 was downregulated in OS cells with CD117+Stro-1+ (Zhao et al., 2015). Moreover, miR-1247 bound to MAP3K9 and inhibited its expression in OS cells. MAP3K9 facilitated proliferation of OS cells and stem cell sphere formation in CD117+Stro-1+ cells (Zhao et al., 2015). Restoration of miR-1247 reduced the clonogenic growth and suppressed tumor spheres in OS cells (Zhao et al., 2015). This study implied that miR-1247 could be involved in regulation of the self-renewal of OS CSCs.

MIRNAS REGULATE METASTASIS OF OSTEOSARCOMA CSC CELLS

miR-133a

One investigation revealed the association between miR-133a expression and osteosarcoma-initiating cells (Fujiwara et al., 2014). This study found that 20 miRNAs were upregulated in CD133 (high) OS cells, including miR-133a (Fujiwara et al., 2014). Moreover, miR-133a promoted cell invasion in CD133 (high) OS cells. Moreover, OS patients with poor prognosis have a high expression of miR-133a (Fujiwara et al., 2014). Chemotherapeutic treatment increased the expression of miR-133a in OS cells. Furthermore, miR-133a exerted its functions in part via inhibition of SGMS2, UBA2, SNX30 and ANXA2 in OS cells (Fujiwara et al., 2014). Therefore, miR-133a could be involved in development and metastasis of OS CSCs.

miR-382

miR-382 has been reported to regulate tumor growth and metastasis in osteosarcoma cells (Xu et al., 2014). Osteosarcoma patients with lower expression of miR-382 had a poor chemoresponse and poor survival (Xu et al., 2014). Ectopic expression of miR-382 reduced growth and chemoresistance of osteosarcoma cells via attenuating KLF12 and HIPK3 (Xu et al., 2014). miR-382-5p, a miRNA species of miR-382, was reported to govern hematopoietic stem cell differentiation via the inhibition of MXD1 (Zini et al., 2016). One study revealed that miR-382 was involved in regulation of CSC populations in colorectal cancer spheroid cells (Rengganaten et al., 2020). miR-382 reduced metastasis and relapse via suppression of YB-1 in osteosarcoma cells (Xu et al., 2015). The upregulation of miR-382 repressed EMT and lung metastasis as well as reduced the population of CSCs (CD133 high) in LM-5 and M132 osteosarcoma cells (Xu et al., 2015). In keeping with this result, knockdown of miR-382 induced EMT and metastasis and elevated the percentage of CSCs in SaOs-2 and HuO9 osteosarcoma cells (Xu et al., 2015). Consistently, the numbers of ALDH1-positive cells were changed after miR-382 modulation. Notably, miR-382 retarded the capacity of osteosarcoma cells to

form osteospheres (Xu et al., 2015). The clinical data demonstrated that lower expression of miR-382 was existed in highly metastatic osteosarcoma cells and relapsed osteosarcoma specimens. Moreover, miR-382 expression level was linked to relapse and survival in patients with osteosarcoma. Furthermore, ectopic expression of miR-382 blocked CSC-mediated tumor formation in mice (Xu et al., 2015). Notably, miR-382 in combination with doxorubicin blocked disease relapse in osteosarcoma in nude mice. Mechanistically, miR-382 controlled EMT, stemness and tumor metastasis and relapse via inhibiting YB-1 (Xu et al., 2015).

MIRNAS REGULATE DRUG RESISTANCE OF OSTEOSARCOMA CSC CELLS

miR-29b-1

Zhang et al. observed that miR-29b-1 decreased proliferation and migration of OS cells via blocking the expression of VEGF (Zhang et al., 2014). Zhu et al. found that miR-29b exerted antitumor activity in OS via modulation of CDK6 (Zhu et al., 2016). Xu and others reported that miR-29 family targeted COL3A1 and Mcl-1 and increased methotrexate sensitivity in OS cells (Xu et al., 2018). Moreover, miR-29b was reported to sensitize OS cells to doxorubicin via suppressing MMP-9 (Luo et al., 2019). Overexpression of miR-29b increased the radiosensitivity of OS cells via targeting PTEN/Akt/Sp1 pathway (Kim et al., 2020). One research dissected that miR-29b-1 repressed proliferation, self-renewal and overcame chemoresistance in 3AB-OS CSCs (Di Fiore et al., 2014). miR-29b expression was downregulated in 3AB-OS CSCs (Di Fiore et al., 2013), and overexpression of miR-29b-1 impaired proliferation, sarcosphere ability and colony formation ability (Di Fiore et al., 2014). Upregulation of miR-29b-1 sensitized chemotherapeutic drug efficacy in 3AB-OS cells. Moreover, miR-29b-1 reduced stemness properties via suppression of Oct3/4, Sox2 and Nanog in 3AB-OS CSCs (Di Fiore et al., 2014). Recently, soft substrate inhibited miR-29b expression and upregulated Spin one expression, leading to activation of PI3K/Akt and STAT3 pathways, which resulted in self-renewal, differentiation and drug resistance in OS cells (Li S. et al., 2020).

miR-335

Emerging evidence has revealed that miR-335 overexpression retarded invasion and migration of osteosarcoma cells via repressing ROCK1 and SNIP1 expression (Wang et al., 2013; Xie et al., 2019). LncRNA TUG1 enhanced invasion and migration of OS cells via sponging miR-335-5p and upregulating ROCK1 (Wang et al., 2017b). LncRNA DANCR enhanced ROCK-1-induced proliferation and motility of OS cells via sponging miR-335-5p and miR-1972 (Wang et al., 2018). LncRNA LOC100129620 increased proliferation and migration via interacting with miR-335-3p and regulating CDK6 in OS cells (Chen et al., 2021). LncRNA CRNDE elevated OS progression by suppression of miR-335-3p (Yu et al., 2021). Upregulation of miR-335 induced apoptosis and attenuated cell viability via inhibition of survivin expression in OS cells (Liu et al., 2016). Clinically, the expression of miR-335 was lower in OS tissues compared with normal control tissues (Wang et al., 2013; Liu et al., 2016). Notably, lower expression of miR-335 was positively correlated with advanced clinical stage and distant metastasis (Wang et al., 2017a). Guo et al. reported that the downregulation of miR-335 was reported in osteosarcoma stem cells (Guo et al., 2017). Furthermore, miR-335 inhibited stem cell-like properties via suppression of POU5F1 in osteosarcoma (Guo et al., 2017). miR-335 upregulation inhibited the expression of CD117, Stro-1, and Sox2 in osteosarcoma cells. Inhibition of miR-335 enhanced stem cell-like properties and increased invasion of osteosarcoma cells. Moreover, miR-335 overexpression increased sensitivity of cisplatin in osteosarcoma cells (Guo et al., 2017).

miR-499a

Wang et al. reported that TGF-β-triggered EMT reduced the expression of miR-499a because Snail1 and Zeb1 bound with miR-499a promoter (Wang et al., 2019). Upregulation of miR-499a reduced TGF-β-mediated erlotinib resistance via inhibition of SHKBP1 in CD166 + OS CSCs (Di Fiore et al., 2016). The high ratio of the SHKBP1 and miR-499a were associated with EMT and erlotinib resistance in OS samples (Di Fiore et al., 2016). This study indicated that miR-499a might be involved in drug resistance in OS CSCs.

Let-7d

One research showed that the expression of let-7days miRNA was decreased in the 3AB-OS CSCs (Di Fiore et al., 2013). Upregulation of let-7d inhibited cell proliferation via suppressing the expression of CCND2 and E2F2 and upregulating p21 and p27 expression in 3AB-OS CSCs (Di Fiore et al., 2016). Moreover, overexpression of let-7d reduced sarcosphere capacity and attenuated the expression of several stem markers, including Sox2, Lin28B, Oct3/4, Nanog, and HMGA2, in 3AB-OS CSCs (Di Fiore et al., 2016). Furthermore, overexpression of let-7d reduced vimentin expression and N-cadherin expression, but increased E-cadherin expression, leading to mesenchymal to epithelial transition (Di Fiore et al., 2016). Interestingly, overexpression of let-7days elevated the expression of CXCR4, MMP-9 and VersicanV1, resulting in promotion of migration and invasion in 3AB-OS CSCs (Di Fiore et al., 2016). Moreover, upregulation of let-7d increased resistance to chemotherapy drugs, which was associated with downregulation of caspase-3 and upregulation of Bcl-2 expression in 3AB-OS CSCs (Di Fiore et al., 2016).

LNCRNAS REGULATE OSTEOSARCOMA CSCS

Recently, multiple studies have suggested that lncRNAs could regulate properties of osteosarcoma. For example, lncRNA GClnc1 enhanced tumorigenesis via suppression of p53 signaling pathway in osteosarcoma (Sui et al., 2018).

TABLE 2 | LncRNAs regulate CSCs in OS.

LncRNAs	Expression	Genes and pathways	References
B4GALT1-AS1	Up	YAP	Li et al. (2018)
DANCR	Up	miR-33a-5p, AXL, PI3K/Akt	Jiang et al. (2017)
DLX6-AS1	Up	miR-129-5p, DLK1, Wnt	Zhang et al. (2018)
FER1L4	Down	PI3K/Akt	Ma et al. (2019b)
HIF2PUT	Down	HIF-2α	(Wang et al., 2015; Li et al., 2016a)
LINK-A	Up	TGF-β1	Kong et al. (2020)
MALAT1	Up	miR-129-5p, RET-Akt, PI3K	Chen et al. (2018a)
SOX2-OT	Up	SOX2	Wang et al. (2017d)
THOR	Up	SOX9	Wu et al. (2019b)

Knockdown of lncRNA 91H blocked the tumorigenesis via induction of methylation of CDK4 promoter in osteosarcoma (Cheng et al., 2021). Overexpression of lncRNA FGFR3-AS1 facilitated osteosarcoma growth via governing the antisense transcript FGFR3 (Sun et al., 2016). Several studies have revealed that lncRNA HOTTIP increased cell proliferation, migration, invasion, EMT, chemoresistance, in osteosarcoma (Li Z. et al., 2016; Tang and Ji, 2019; Liu et al., 2020; Yao et al., 2021). LncRNA HULC promoted the progression of osteosarcoma via targeting the miR-372-3p/HMGB1 (Li Y. et al., 2020). In addition, inhibition of lncRNA UCA1 reduced tumorigenesis and metastasis via targeting miR-513b-5p/E2F5 axis and CREB1-mediated EMT and PI3K/AKT/mTOR axis in osteosarcoma (Ma H. et al., 2019; Zhang et al., 2021). Here, we will briefly describe the functions and molecular insights of these lncRNAs in governing CSC features in osteosarcoma (**Table 2**).

LNCRNAS REGULATE PROLIFERATION OF OSTEOSARCOMA CSC CELLS

lncRNA DANCR

Recently, several studies identified that DANCR was increased in osteosarcoma tissues and tumor cell lines. High expression of DANCR was linked to tissue typing and TNM stage as well as metastasis in osteosarcoma patients (Jiang et al., 2017; Wang et al., 2018; Zhang W. et al., 2020). One study revealed that deficient of DANCR suppressed growth and autophagy, and triggered apoptosis via sponging miR-216a-5p and increasing the expression of SOX5 (Pan et al., 2020). Moreover, DANCR inhibited migration and invasion via targeting miR-149 and its downstream MSI2 in osteosarcoma (Zhang W. et al., 2020). In addition, DANCR acted as a ceRNA to sponge miR-335-5p and miR-1972, leading to inhibition of ROCK1 expression and depression of proliferation and motility of osteosarcoma cells (Wang et al., 2018). Jiang et al. reported that DANCR decoyed miR-33a-5p and upregulated AXL expression, contributing to tumor growth, migration, invasion and lung metastasis (Jiang et al., 2017). Mechanistically, DANCR stimulated tumor malignant phenotype via enhancement of CSCs features, which might be due to activation of PI3K/Akt signaling pathway in osteosarcoma (Jiang et al., 2017). Yuan et al. reported that DANCR promoted cell stemness property via derepressing CTNNB1 in hepatocellular carcinoma (HCC) cells (Yuan et al., 2016). DANCR expression was high in HCC cells with stem-like features (Yuan et al., 2016). DANCR depletion suppressed expression of several CSC markers, such as CD44, ABCG2, and ALDH1 in TNBC cells (Sha et al., 2017). In lung cancer cells, DANCR overexpression increased cell stemness via decoying miR-216a expression and subsequent activation of Wnt/β-catenin axis (Yu et al., 2020).

LncRNA DLX6-AS1

LncRNA DLX6-AS1 deficiency blocked tumor development due to inhibition of CADM1 promoter methylation and suppression of STAT3 pathway in liver CSCs (Wu D.-M. et al., 2019). Knockdown of DLX6-AS1 repressed spheroid formation and suppressed the expression of stem markers in liver CSCs, such as SOX2, Nanog, OCT4, CD13 and CD133 (Wu D.-M. et al., 2019). Similarly, DLX6-AS1 overexpression promoted stemness of osteosarcoma cells via interacting with miR-129-5p and activation of DLK1, leading to activating Wnt pathway (Zhang et al., 2018). Patients with high expression of DLX6-AS1 often had poor grade, advanced stage and poor overall survival (Zhang et al., 2018). Deficient of DLX6-AS1 decreased sphere size and number, and CD117+Stro-1+ cells were decreased in osteosarcoma cells after DLX6-AS1 silencing (Zhang et al., 2018).

LncRNA HIF2PUT

LncRNA HIF2PUT was reported to regulate the proliferation, invasion and migration in osteosarcoma cells (Zhao D. et al., 2019). One group reported that HIF2PUT overexpression attenuated cell growth and motility in U2OS and MG-63 cells (Zhao D. et al., 2019). HIF2PUT expression was correlated with clinical features of osteosarcoma patients, including tumor size, stage, distant metastasis, and OS and DFS (Li W. et al., 2016). Interestingly, HIF2PUT was also reported to be highly expressed in osteosarcoma, suggesting that the deeper investigation is necessary to dissect the role of HIF2PUT in osteosarcoma tumorigenesis. HIF2PUT has been revealed to control CSCs in several types of human malignancies. For instance, HIF2PUT overexpression repressed CSC properties via targeting HIF-2α in colon cancer (Yao et al., 2015). Downregulation of HIF2PUT decreased the expression of stemness biomarkers in colon cancer DLD-1 and HT29 cells, leading to blockade of spheroid formation (Yao et al., 2015). However,

downregulation of HIF2PUT elevated cell growth and migratory ability in MG63 cells, and elevation of HIF2PUT showed an opposite effect in osteosarcoma cells (Wang et al., 2015). Moreover, increased HIF2PUT led to a reduction of CD133 + MG63 cells and inhibition of sphere-forming ability, while decreased HIF2PUT resulted in an induction of CD133 positive cells and promotion of sphere-forming capacity (Wang et al., 2015). Another study validated that HIF2PUT upregulation inhibited sphere formation of osteosarcoma cells (Zhao D. et al., 2019). A mechanistical experiment showed that HIF2PUT could target HIF-2α expression and perform its biological function in osteosarcoma cells (Wang et al., 2015). Furthermore, the clinical data revealed that HIF2PUT expression was linked to HIF-2α levels in tumor tissues of osteosarcoma patients (Wang et al., 2015; Li W. et al., 2016).

LncRNA THOR

LncRNA THOR was found to involve in CSC maintenance in TNBC cells (Wang B. et al., 2020). THOR expression was higher in TNBC tissues than that in luminal A-type and luminal B-type breast cancer (Wang B. et al., 2020). Silencing of lncRNA THOR attenuated the expression of stemness regulatory factors, including CD44, Nanog, and Oct4, and reduced ALDH1 activity, leading to suppressing the sphere-formation ability, which is evidenced by reduced sphere size and number in MDA-MB-231 and MDA-MB-453 cells (Wang B. et al., 2020). Overexpression of THOR promoted CSC properties and increased stemness factor expression, indicating that THOR might promote stemness of TNBC cells. Moreover, THOR interacted with β-catenin mRNA and increased its mRNA stability and elevated its expression (Wang B. et al., 2020). In line with the role of THOR in regulating CSCs, Cheng et al. found that THOR promoted CSC expansion and stimulated the self-renewal ability via targeting β-catenin axis in hepatocellular carcinoma (Cheng et al., 2019). Similarly, THOR knockdown reduced the stemness via inhibition of multiple stemness markers, such as CD44, SOX2, SOX9, Nanog, Oct1/2/4, and ALDH, in MKN-45 and BGC-23 gastric cancer cells (Song et al., 2018). Silencing of THOR attenuated the spheroids size and number and reduced the ability of spheroid formation in gastric cancer (Song et al., 2018). Moreover, depletion of THOR reduced SOX9 expression via binding to and increasing SOX9 mRNA stability (Song et al., 2018). In nasopharyngeal carcinoma (NPC) cells, THOR decreased sensitivity of cisplatin via promoting CSC stemness (Gao et al., 2018). THOR interacted with YAP and blocked its translocation to cytoplasm from nuclear, leading to enhancement of YAP transcription activity in NPC cells (Gao et al., 2018). In osteosarcoma cells, THOR increased stemness and migratory capacity via increasing stability of SOX9 mRNA (Wu H. et al., 2019). THOR expression was higher in cell spheroids than that in adherent cells in osteosarcoma. Upregulation of THOR elevated the ALDH activity and enhanced spheroid formation in adherent cells of osteosarcoma, whereas downregulation of THOR showed an opposite function in spheroids (Wu H. et al., 2019). THOR promoted osteosarcoma CSC stemness via increasing SOX9 mRNA stability and upregulating its expression (Wu H. et al., 2019). Altogether, lncRNA THOR participate in controlling CSCs in osteosarcoma.

LNCRNAS REGULATE METASTASIS OF OSTEOSARCOMA CSC CELLS

LncRNA FER1L4

LncRNA FER1L4 plays an anti-tumor role in osteosarcoma development (Fei et al., 2018). The evidence is that lncRNA FER1L4 has a lower expression in tissues of osteosarcoma patients, which is linked to stage and metastasis (Chen ZX. et al., 2018; Ye et al., 2019). In addition, FER1L4 retarded osteosarcoma tumorigenesis via sponging miR-18a-5p and increasing PTEN expression (Fei et al., 2018). FER1L4 was reported to control PDLSCs under compressive stress (Huang et al., 2019). One study found that 72 lncRNAs were increased and 18 lncRNAs were decreased in PDLSCs after static compressive stress (Huang et al., 2019). These lncRNAs contained FER1L4, NEAT1, LUCAT1 and HIF1A-AS2 (Huang et al., 2019). Moreover, FER1L4 stimulated osteogenic differentiation of PDLSCs via binding with miR-874-3p and targeting VEGFA, suggesting that FER1L4 could enhance bone formation (Huang et al., 2020). Furthermore, FER1L4 triggered the autophagy via regulating Akt/FOXO3 signaling pathway in PDLSCs under orthodontic compressive strain (Huang et al., 2021). Ma et al. reported that ectopic expression of FER1L4 inhibited proliferation, induced apoptosis, blocked migration and invasion, suppressed EMT in osteosarcoma cells (Ma L. et al., 2019). Moreover, silencing of FER1L4 upregulated the expression of several stemness biomarkers, including CD44, Oct4, SOX9, Nanog, and ALDH1 (Ma L. et al., 2019). In mechanism, FER1L4 suppressed tumor progression via targeting PI3K/Akt pathway in osteosarcoma.

LncRNA LINK-A

One group showed that metastatic osteosarcoma patients had a higher level of LINK-A in plasma (Zhao B. et al., 2019). Elevation of LINK-A enlarged migratory and invasive capacity of osteosarcoma cells via induction of HIF-1α expression (Zhao B. et al., 2019). Another group also observed that LINK-A in plasma was highly expressed in osteosarcoma patients (Kong et al., 2020). LINK-A upregulation increased TGF-β1 expression in osteosarcoma cells. Deficient of LINK-A led to suppression of migration and invasion of osteosarcoma cells. Moreover, depletion of LINK-A decreased the percentage of CD133 + cells in osteosarcoma cell lines (Kong et al., 2020). This finding indicated that LINK-A might participate in governing stemness of osteosarcoma.

LncRNA MALAT1

LncRNA MALAT1 has been discovered to regulate stem cell expression in osteosarcoma (Chen Y. et al., 2018). Chen et al.

reported that MALAT1 expression level was increased in tumor tissues and linked to tumor size, metastasis and poor survival in osteosarcoma patients (Chen Y. et al., 2018). Ectopic expression of MALAT1 increased proliferation, migratory and invasive ability in osteosarcoma cells and promoted tumor growth in mice via sponging miR-129-5p and regulating the RET-Akt pathway (Chen Y. et al., 2018). It has been known that CD90, SOX2 and CD133 are well-characterized stemness markers. Moreover, MALAT1 upregulation elevated the expression of CD90, SOX2 and CD133 in SW1353 and SOSP-9607 cells. In consistent, depletion of MALAT1 reduced the expression of CD90, CD133 and SOX2 in osteosarcoma cells (Chen Y. et al., 2018). In line with this finding, MALAT1 overexpression in SW1353 and SOSP-9607 cells resulted in enhancement of CD133 + CD44 $^{+}$ cell proportion, while depletion of MALAT1 displayed the opposite effects (Chen Y. et al., 2018). This study suggested that MALAT1 enhanced stem cell-like features via promotion of RET expression via targeting miR-129-5p and subsequently activating the PI3K-Akt pathway in osteosarcoma. MALAT1 was highly expressed in patients with osteosarcoma (Wang et al., 2017c). MALAT1 promoted proliferation and metastasis via sponging miR-144-3p and blocking ROCK1/ROCK2 axis in osteosarcoma cells (Wang et al., 2017c).

LncRNA SOX2-OT

LncRNA SOX2-OT has been characterized as an oncogene and is highly expressed in various cancers (Li PY. et al., 2020). Higher level of lncRNA SOX2-OT was existed in several osteosarcoma cell lines and tumor specimens. Notably, osteosarcoma patients with high level of lncRNA SOX2-OT often have bigger tumor size, advanced stage, high grade and metastasis and poor OS (Wang Z. et al., 2017). An *in vitro* experiment showed that knockdown of lncRNA SOX2-OT attenuated proliferation and migration and invasion of U2OS cells. In consistent, elevation of lncRNA SOX2-OT enhanced proliferation and facilitated invasive and migratory capacity in SaOS-2 cells (Wang Z. et al., 2017). Moreover, SOX2 was confirmed as a downstream target of lncRNA SOX2-OT in osteosarcoma. Strikingly, the expression of stemness biomarkers was downregulated in osteosarcoma cells after lncRNA SOX2-OT knockdown, including ALDH1, Nanog, Oct4, CD44 and CD133 (Wang Z. et al., 2017). Taken together, lncRNA SOX2-OT might regulate CSCs via positively regulating SOX2 in osteosarcoma.

LNCRNAS REGULATE DRUG RESISTANCE OF OSTEOSARCOMA CSC CELLS

LncRNA B4GALT1-AS1

B4GALT1-AS1 has been reported to serve as a ceRNA to sequester the expression of miR-30e, resulting in the upregulation of SOX9 in NSCLC (Lin et al., 2020). B4GALT1-AS1 had an increased expression in NSCLC tissues and cells. Silencing of B4GALT1-AS1 blocked malignant phenotype in A549 and H1299 cells, including cell viability and colony-forming ability (Lin et al., 2020). Deficient of B4GALT1-AS1 reduced clone formation capacity in colon cancer cells, and attenuated the expression of the stemness biomarkers. B4GALT1-AS1 silencing also reduced ALDH1 activity and retarded spheroid formation in colon cancer cells (Wu D.-M. et al., 2019). Mechanistically, B4GALT1-AS1 might enhance the relocation of YAP into nucleus from cytoplasm and promote its transcription, leading to maintenance of CSCs in colon cancer (Wu D.-M. et al., 2019). Similarly, higher expression of B4GALT1-AS1 was observed in osteosarcoma tissues. Depletion of B4GALT1-AS1 decreased proliferation and migratory capacity of osteosarcoma cells, blocked EMT progression, evidenced by an increase of E-cadherin and a decrease of vimentin (Li et al., 2018). Knockdown of B4GALT1-AS1 attenuated the expression of Nanog and ALDH1 and reduced the capability of spheroid formation, suggesting that B4GALT1-AS1 is involved in regulation of osteosarcoma cell stemness (Li et al., 2018). *In vivo* data further confirmed that B4GALT1-AS1 silencing decreased tumor formation in mice. B4GALT1-AS1 promoted the translocation of HuR into cytoplasm from nuclear and led to upregulation of YAP transcription in osteosarcoma (Li et al., 2018). Notably, deficient of B4GALT1-AS1 reduced adriamycin resistance in a YAP-dependent manner in osteosarcoma cells. This study revealed that B4GALT1-AS1 shed light on the regulation of CSC features in osteosarcoma.

CIRCRNAS REGULATE OSTEOSARCOMA CSCS

Increasing evidence suggests that circRNAs play a pivotal role in osteosarcoma development and progression (Li et al., 2021). Wang et al. found that circ_0001658 increased cell proliferation and tumor metastasis via sponging miR-382-5p and increasing YB-1 axis in osteosarcoma cells (Wang L. et al., 2020). One group identified that miR-382 knockdown triggered EMT and promoted metastasis and increased the percentage of CSCs via suppressing YB-1 in osteosarcoma cells (Xu et al., 2015). Therefore, circ_0001658 could regulate CSCs and osteospheres via targeting miR-382-5p/YB-1 axis in osteosarcoma. Moreover, circ_0002052 knockdown inhibited cell growth, migration and invasion via sponging miR-382 in osteosarcoma, indicating that circ_0002052 might increase CSCs via inhibiting miR-382 (Zhang P.-r. et al., 2020). CircNRIP1 encapsulated by BMSC-EVs aggravated osteosarcoma via targeting miR-532-3p and PI3K/AKT axis (Shi Z. et al., 2021). Shi et al. reported that circPIP5K1A depletion reduced the sphere formation abilities in osteosarcoma cells and decreased the CD133 + CD44 $^{+}$ cell population (Shi P. et al., 2021). Knockdown of circPIP5K1A reduced the expression of Nanog ad ALDH1 in osteosarcoma cells. Moreover, circPIP5K1A increased YAP expression via regulating miR-515-5p, and miR-515-5p suppressed cancer stemness in osteosarcoma cells (Shi P. et al., 2021). Notably, circPIP5K1A depletion or miR-515-

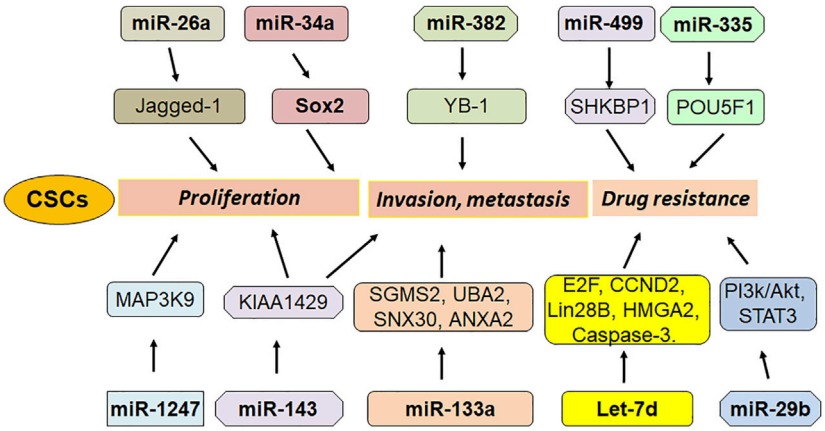

FIGURE 1 | The role of miRNAs in regulation of OS stem cells.

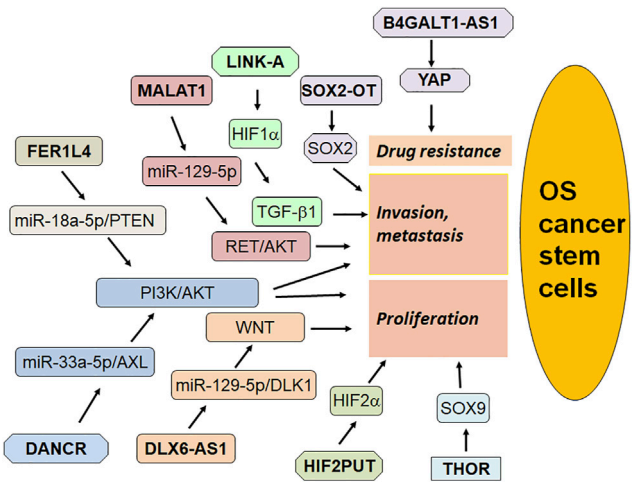

FIGURE 2 | The role of lncRNAs in regulation of OS stem cells.

5p mimic inhibited the CSC properties in osteosarcoma cells, suggesting that circPIP5K1A can control CSCs in osteosarcoma (Shi P. et al., 2021).

NCRNAS IN CHONDROSARCOMA

It is necessary to mention that ncRNAs have been uncovered to play an essential role in another primary bone sarcomas chondrosarcoma, including miR-30a, miR-125b, miR-126, miR-129-5p, miR-145, miR-181a, miR-150, miR-494, and miR-497 (Chang et al., 2015; Li et al., 2015; Lu et al., 2016; Pu et al., 2016; Palmini et al., 2017; Zhang et al., 2017). Several lncRNAs, such as SNHG6 (Pu et al., 2021), RAMP2-AS1 (Cheng et al., 2020), BCAR4 (Shui et al., 2017) and HOTAIR (Bao et al., 2017), have been reported to promote chondrosarcoma development and progression. However, the role of ncRNAs in regulation of chondrosarcoma CSCs is rarely investigated. One report showed that miR-34a in combination with carbon ions irradiation can control chondrosarcoma CSCs (Vares et al., 2020). Therefore, further studies are warranted to determine the functions of ncRNAs in governing chondrosarcoma CSCs.

CONCLUSION AND PERSPECTIVES

In conclusion, ncRNAs critically regulate CSCs via different mechanisms in osteosarcoma (**Figures 1**, **2**). Because CSCs are important in tumor initiation, reoccurrence, metastasis and drug resistance, modulating ncRNAs could be helpful for overcoming tumor progression and enhancing drug sensitivity via killing CSCs in osteosarcoma. It is important to mention that numerous ncRNAs are involved in regulating osteosarcoma CSCs. Whether ncRNAs are the most important factors to control CSCs compared with other transcript factors that were involved in CSCs? Among these ncRNAs, which ncRNA is most important factor to govern CSCs in osteosarcoma. It is known that ncRNAs have multiple downstream targets. How can we judge the key targets of ncRNAs in regulating CSCs? Answering these questions will provide the evidence for targeting CSCs via modulation of ncRNAs for osteosarcoma treatment. In addition, it is critical to discover a standardized approach to measure the ncRNAs expression. A useful and ideal deliver system to send ncRNAs to specific organs *in vivo* is also important to establish. LncRNAs have been evaluated for targeting critical cancer-associated genes and they are in different phases of clinical trials (Slaby, 2016). Since discover of possible biomarkers is important for diagnosis and treatment of osteosarcoma, it is essential to determine whether these ncRNAs could be potential biomarkers for detection of osteosarcoma CSCs. Lastly, further investigations are needed to validate whether targeting ncRNAs could control OS CSCs and overcome drug resistance in clinical management of OS in the future.

AUTHOR CONTRIBUTIONS

JL and GS wrote this manuscript. JL prepared the figures and tables. All authors approved the final version.

FUNDING

This work was supported by the grants from the Shenyang Key Technological project (21-173-9-74) and Shengjing 345 program.

REFERENCES

Adhikari, A. S., Agarwal, N., Wood, B. M., Porretta, C., Ruiz, B., Pochampally, R. R., et al. (2010). CD117 and Stro-1 Identify Osteosarcoma Tumor-Initiating Cells Associated with Metastasis and Drug Resistance. *Cancer Res.* 70, 4602–4612. doi:10.1158/0008-5472.can-09-3463

Akbar Samadani, A., Keymoradzdeh, A., Shams, S., Soleymanpour, A., Elham Norollahi, S., Vahidi, S., et al. (2020). Mechanisms of Cancer Stem Cell Therapy. *Clinica Chim. Acta* 510, 581–592. doi:10.1016/j.cca.2020.08.016

Bao, X., Ren, T., Huang, Y., Sun, K., Wang, S., Liu, K., et al. (2017). Knockdown of Long Non-coding RNA HOTAIR Increases miR-454-3p by Targeting Stat3 and Atg12 to Inhibit Chondrosarcoma Growth. *Cell Death Dis* 8–e2605. doi:10.1038/cddis.2017.31

Belayneh, R., and Weiss, K. (2020). The Role of ALDH in the Metastatic Potential of Osteosarcoma Cells and Potential ALDH Targets. *Adv. Exp. Med. Biol.* 1258, 157–166. doi:10.1007/978-3-030-43085-6_10

Brown, H. K., Tellez-Gabriel, M., and Heymann, D. (2017). Cancer Stem Cells in Osteosarcoma. *Cancer Lett.* 386, 189–195. doi:10.1016/j.canlet.2016.11.019

Chang, L., Shrestha, S., Lachaud, G., Scott, M. A., and James, A. W. (2015). Review of microRNA in Osteosarcoma and Chondrosarcoma. *Med. Oncol.* 32, 613. doi:10.1007/s12032-015-0613-z

Chen, Y., Huang, W., Sun, W., Zheng, B., Wang, C., Luo, Z., et al. (2018a). LncRNA MALAT1 Promotes Cancer Metastasis in Osteosarcoma via Activation of the PI3K-Akt Signaling Pathway. *Cell Physiol Biochem* 51, 1313–1326. doi:10.1159/000495550

Chen, Y., Tang, G., Qian, H., Chen, J., Cheng, B., Zhou, C., et al. (2021). LncRNA LOC100129620 Promotes Osteosarcoma Progression through Regulating CDK6 Expression, Tumor Angiogenesis, and Macrophage Polarization. *Aging* 13, 14258–14276. doi:10.18632/aging.203042

Chen, Z. X., Chen, C. P., Zhang, N., and Wang, T. X. (2018b). Low-expression of lncRNA FER1L4 Might Be a Prognostic Marker in Osteosarcoma. *Eur. Rev. Med. Pharmacol. Sci.* 22, 2310–2314. doi:10.26355/eurrev_201804_14820

Cheng, C., Zhang, Z., Cheng, F., and Shao, Z. (2020). Exosomal lncRNA RAMP2-AS1 Derived from Chondrosarcoma Cells Promotes Angiogenesis through miR-2355-5p/VEGFR2 Axis. *Ott* 13, 3291–3301. doi:10.2147/ott.s244652

Cheng, S., Zheng, J., Liu, X., Shi, J., Gong, F., Zhang, X., et al. (2021). Knockdown of 91 H Suppresses the Tumorigenesis of Osteosarcoma via Inducing Methylation of CDK4 Promoter. *Technol. Cancer Res. Treat.* 20, 1533033821990006. doi:10.1177/1533033821990006

Cheng, Z., Lei, Z., Yang, P., Si, A., Xiang, D., Zhou, J., et al. (2019). Long Non-coding RNA THOR Promotes Liver Cancer Stem Cells Expansion via β-catenin Pathway. *Gene* 684, 95–103. doi:10.1016/j.gene.2018.10.051

Di Fiore, R., Drago-Ferrante, R., Pentimalli, F., Di Marzo, D., Forte, I. M., Carlisi, D., et al. (2016). Let-7d miRNA Shows Both Antioncogenic and Oncogenic Functions in Osteosarcoma-Derived 3AB-OS Cancer Stem Cells. *J. Cel. Physiol.* 231, 1832–1841. doi:10.1002/jcp.25291

Di Fiore, R., Drago-Ferrante, R., Pentimalli, F., Di Marzo, D., Forte, I. M., D'Anneo, A., et al. (2014). MicroRNA-29b-1 Impairs *In Vitro* Cell Proliferation, Self-Renewal and Chemoresistance of Human Osteosarcoma 3AB-OS Cancer Stem Cells. *Int. J. Oncol.* 45, 2013–2023. doi:10.3892/ijo.2014.2618

Di Fiore, R., Fanale, D., Drago-Ferrante, R., Chiaradonna, F., Giuliano, M., De Blasio, A., et al. (2013). Genetic and Molecular Characterization of the Human Osteosarcoma 3AB-OS Cancer Stem Cell Line: a Possible Model for Studying Osteosarcoma Origin and Stemness. *J. Cel. Physiol.* 228, 1189–1201. doi:10.1002/jcp.24272

Fei, D., Zhang, X., Liu, J., Tan, L., Xing, J., Zhao, D., et al. (2018). Long Noncoding RNA FER1L4 Suppresses Tumorigenesis by Regulating the Expression of PTEN Targeting miR-18a-5p in Osteosarcoma. *Cel Physiol Biochem* 51, 1364–1375. doi:10.1159/000495554

Ferretti, V. A., and León, I. E. (2021). Long Non-coding RNAs in Cisplatin Resistance in Osteosarcoma. *Curr. Treat. Options. Oncol.* 22, 41. doi:10.1007/s11864-021-00839-y

Fujiwara, T., Katsuda, T., Hagiwara, K., Kosaka, N., Yoshioka, Y., Takahashi, R.-U., et al. (2014). Clinical Relevance and Therapeutic Significance of microRNA-133a Expression Profiles and Functions in Malignant Osteosarcoma-Initiating Cells. *Stem Cells* 32, 959–973. doi:10.1002/stem.1618

Gao, L., Cheng, X.-l., and Cao, H. (2018). LncRNA THOR Attenuates Cisplatin Sensitivity of Nasopharyngeal Carcinoma Cells via Enhancing Cells Stemness. *Biochimie* 152, 63–72. doi:10.1016/j.biochi.2018.06.015

Gebert, L. F. R., and Macrae, I. J. (2019). Regulation of microRNA Function in Animals. *Nat. Rev. Mol. Cel Biol* 20, 21–37. doi:10.1038/s41580-018-0045-7

Ghafouri-Fard, S., Shirvani-Farsani, Z., Hussen, B. M., and Taheri, M. (2021). The Critical Roles of lncRNAs in the Development of Osteosarcoma. *Biomed. Pharmacother.* 135, 111217. doi:10.1016/j.biopha.2021.111217

Gill, J., and Gorlick, R. (2021). Advancing Therapy for Osteosarcoma. *Nat. Rev. Clin. Oncol.* 18 (10), 609–624. doi:10.1038/s41571-021-00519-8

Guo, X., Yu, L., Zhang, Z., Dai, G., Gao, T., and Guo, W. (2017). miR-335 Negatively Regulates Osteosarcoma Stem Cell-like Properties by Targeting POU5F1. *Cancer Cel Int* 17, 29. doi:10.1186/s12935-017-0398-6

Han, Q., Yang, J., Yang, H., Li, C., Li, J., and Cao, Y. (2020). RETRACTED ARTICLE: KIAA1429 Promotes Osteosarcoma Progression by Promoting Stem Cell Properties and Is Regulated by miR-143-3p. *Cell Cycle* 19, 1172–1185. doi:10.1080/15384101.2020.1749465

Hattinger, C. M., Patrizio, M. P., Fantoni, L., Casotti, C., Riganti, C., and Serra, M. (2021). Drug Resistance in Osteosarcoma: Emerging Biomarkers, Therapeutic Targets and Treatment Strategies. *Cancers (Basel)* 13, 2878. doi:10.3390/cancers13122878

Hou, Y., Feng, H., Jiao, J., Qian, L., Sun, B., Chen, P., et al. (2019). Mechanism of miR-143-3p Inhibiting Proliferation, Migration and Invasion of Osteosarcoma Cells by Targeting MAPK7. *Artif. Cell Nanomedicine, Biotechnol.* 47, 2065–2071. doi:10.1080/21691401.2019.1620252

Huang, Y., Han, Y., Guo, R., Liu, H., Li, X., Jia, L., et al. (2020). Long Non-coding RNA FER1L4 Promotes Osteogenic Differentiation of Human Periodontal Ligament Stromal Cells via miR-874-3p and Vascular Endothelial Growth Factor A. *Stem Cel Res Ther* 11, 5. doi:10.1186/s13287-019-1519-z

Huang, Y., Liu, H., Guo, R., Han, Y., Yang, Y., Zhao, Y., et al. (2021). Long Non-coding RNA FER1L4 Mediates the Autophagy of Periodontal Ligament Stem Cells under Orthodontic Compressive Force via AKT/FOXO3 Pathway. *Front. Cel Dev. Biol.* 9, 631181. doi:10.3389/fcell.2021.631181

Huang, Y., Zhang, Y., Li, X., Liu, H., Yang, Q., Jia, L., et al. (2019). The Long Non-coding RNA Landscape of Periodontal Ligament Stem Cells Subjected to Compressive Force. *Eur. J. Orthod.* 41, 333–342. doi:10.1093/ejo/cjy057

Humphries, B., Wang, Z., and Yang, C. (2021). MicroRNA Regulation of Breast Cancer Stemness. *Int. J. Mol. Sci.* 22, 3756. doi:10.3390/ijms22073756

Izadpanah, S., Shabani, P., Aghebati-Maleki, A., Baghbanzadeh, A., Fotouhi, A., Bisadi, A., et al. (2020). Prospects for the Involvement of Cancer Stem Cells in the Pathogenesis of Osteosarcoma. *J. Cel Physiol* 235, 4167–4182. doi:10.1002/jcp.29344

Jiang, N., Wang, X., Xie, X., Liao, Y., Liu, N., Liu, J., et al. (2017). lncRNA DANCR Promotes Tumor Progression and Cancer Stemness Features in Osteosarcoma by Upregulating AXL via miR-33a-5p Inhibition. *Cancer Lett.* 405, 46–55. doi:10.1016/j.canlet.2017.06.009

Kim, E. H., Kim, J. Y., Kim, M. S., Vares, G., Ohno, T., Takahashi, A., et al. (2020). Molecular Mechanisms Underlying the Enhancement of Carbon Ion Beam Radiosensitivity of Osteosarcoma Cells by miR-29b. *Am. J. Cancer Res.* 10, 4357–4371.

Kong, Y., Nie, Z., Guo, H., and Ma, C. (2020). LINK-A lncRNA Is Upregulated in Osteosarcoma and Regulates Migration, Invasion and Stemness of Osteosarcoma Cells. *Oncol. Lett.* 19, 2832–2838. doi:10.3892/ol.2020.11367

Lei, Y., Junxin, C., Yongcan, H., Xiaoguang, L., and Binsheng, Y. (2020). Role of microRNAs in the Crosstalk between Osteosarcoma Cells and the Tumour Microenvironment. *J. Bone Oncol.* 25, 100322. doi:10.1016/j.jbo.2020.100322

Li, J., Wang, L., Liu, Z., Zu, C., Xing, F., Yang, P., et al. (2015). MicroRNA-494 Inhibits Cell Proliferation and Invasion of Chondrosarcoma Cellsin Vivoandin Vitroby Directly Targeting SOX9. *Oncotarget* 6, 26216–26229. doi:10.18632/oncotarget.4460

Li, M., and Ma, W. (2021). miR-26a Reverses Multidrug Resistance in Osteosarcoma by Targeting MCL1. *Front. Cel Dev. Biol.* 9, 645381. doi:10.3389/fcell.2021.645381

Li, P. Y., Wang, P., Gao, S. G., and Dong, D. Y. (2020a). Long Noncoding RNA SOX2-OT: Regulations, Functions, and Roles on Mental Illnesses, Cancers, and Diabetic Complications. *Biomed. Res. Int.* 2020, 2901589. doi:10.1155/2020/2901589

Li, S., Bai, H., Chen, X., Gong, S., Xiao, J., Li, D., et al. (2020b). Soft Substrate Promotes Osteosarcoma Cell Self-Renewal, Differentiation, and Drug Resistance through miR-29b and its Target Protein Spin 1. *ACS Biomater. Sci. Eng.* 6, 5588–5598. doi:10.1021/acsbiomaterials.0c00816

Li, W., He, X., Xue, R., Zhang, Y., Zhang, X., Lu, J., et al. (2016a). Combined Over-expression of the Hypoxia-Inducible Factor 2α Gene and its Long Non-coding RNA Predicts Unfavorable Prognosis of Patients with Osteosarcoma. *Pathol. - Res. Pract.* 212, 861–866. doi:10.1016/j.prp.2016.06.013

Li, Y., Liu, J.-J., Zhou, J.-H., Chen, R., and Cen, C.-Q. (2020c). LncRNA HULC Induces the Progression of Osteosarcoma by Regulating the miR-372-3p/HMGB1 Signalling axis. *Mol. Med.* 26, 26. doi:10.1186/s10020-020-00155-5

Li, Z., Zhao, L., and Wang, Q. (2016b). Overexpression of Long Non-coding RNA HOTTIP Increases Chemoresistance of Osteosarcoma Cell by Activating the Wnt/β-Catenin Pathway. *Am. J. Transl Res.* 8, 2385–2393.

Li, Z., Li, X., Xu, D., Chen, X., Li, S., Zhang, L., et al. (2021). An Update on the Roles of Circular RNAs in Osteosarcoma. *Cell Prolif* 54, e12936. doi:10.1111/cpr.12936

Li, Z., Wang, Y., Hu, R., Xu, R., and Xu, W. (2018). LncRNA B4GALT1-AS1 Recruits HuR to Promote Osteosarcoma Cells Stemness and Migration via Enhancing YAP Transcriptional Activity. *Cel Prolif* 51, e12504. doi:10.1111/cpr.12504

Liang, X., Xu, C., Wang, W., and Li, X. (2019b). The DNMT1/miR-34a Axis Is Involved in the Stemness of Human Osteosarcoma Cells and Derived Stem-like Cells. *Stem Cell Int* 2019, 7028901. doi:10.1155/2019/7028901

Liang, X., Xu, C., Cao, X., and Wang, W. (2019a). Isovitexin Suppresses Cancer Stemness Property and Induces Apoptosis of Osteosarcoma Cells by Disruption of the DNMT1/miR-34a/Bcl-2 Axis. *Cmar* 11, 8923–8936. doi:10.2147/cmar.s222708

Lin, J. H., Chen, F. N., Wu, C. X., Hu, S. Q., and Ma, J. (2020). Long non-coding RNA B4GALT1-Antisense RNA 1/microRNA-30e/SRY-box transcription factor 9 signaling axis contributes to non-small cell lung cancer cell growth. *Oncol. Lett.* 20, 284. doi:10.3892/ol.2020.12146

Lin, Z., Xie, X., Lu, S., and Liu, T. (2021). Noncoding RNAs in Osteosarcoma: Implications for Drug Resistance. *Cancer Lett.* 504, 91–103. doi:10.1016/j.canlet.2021.02.007

Liu, J., Mi, B., Wang, Y., Shi, C., Mi, X., Lu, Y., et al. (2018). miR-26a Suppresses Osteosarcoma Migration and Invasion by Directly Targeting HMGA1. *Oncol. Lett.* 15, 8303–8310. doi:10.3892/ol.2018.8359

Liu, K., Ni, J. D., Li, W. Z., Pan, B. Q., Yang, Y. T., Xia, Q., et al. (2020). The Sp1/FOXC1/HOTTIP/LATS2/YAP/β-catenin cascade Promotes Malignant and Metastatic Progression of Osteosarcoma. *Mol. Oncol.* 14, 2678–2695. doi:10.1002/1878-0261.12760

Liu, Z. F., Liang, Z. Q., Li, L., Zhou, Y. B., Wang, Z. B., Gu, W. F., et al. (2016). MiR-335 Functions as a Tumor Suppressor and Regulates Survivin Expression in Osteosarcoma. *Eur. Rev. Med. Pharmacol. Sci.* 20, 1251–1257.

Lu, J., Song, G., Tang, Q., Yin, J., Zou, C., Zhao, Z., et al. (2017). MiR-26a Inhibits Stem Cell-like Phenotype and Tumor Growth of Osteosarcoma by Targeting Jagged1. *Oncogene* 36, 231–241. doi:10.1038/onc.2016.194

Lu, Y., Li, F., Xu, T., and Sun, J. (2016). miRNA-497 Negatively Regulates the Growth and Motility of Chondrosarcoma Cells by Targeting Cdc25A. *Oncol. Res.* 23, 155–163. doi:10.3727/096504016x14519157902681

Luo, D. J., Li, L. J., Huo, H. F., Liu, X. Q., Cui, H. W., and Jiang, D. M. (2019). MicroRNA-29b Sensitizes Osteosarcoma Cells to Doxorubicin by Targeting Matrix Metalloproteinase 9 (MMP-9) in Osteosarcoma. *Eur. Rev. Med. Pharmacol. Sci.* 23, 1434–1442. doi:10.26355/eurrev_201902_17100

Ma, H., Su, R., Feng, H., Guo, Y., and Su, G. (2019a). Long Noncoding RNA UCA1 Promotes Osteosarcoma Metastasis through CREB1-Mediated Epithelial-Mesenchymal Transition and Activating PI3K/AKT/mTOR Pathway. *J. Bone Oncol.* 16, 100228. doi:10.1016/j.jbo.2019.100228

Ma, L., Zhang, L., Guo, A., Liu, L. C., Yu, F., Diao, N., et al. (2019b). Overexpression of FER1L4 Promotes the Apoptosis and Suppresses Epithelial-Mesenchymal Transition and Stemness Markers via Activating PI3K/AKT Signaling Pathway in Osteosarcoma Cells. *Pathol. - Res. Pract.* 215, 152412. doi:10.1016/j.prp.2019.04.004

Melendez-Zajgla, J., and Maldonado, V. (2021). The Role of lncRNAs in the Stem Phenotype of Pancreatic Ductal Adenocarcinoma. *Int. J. Mol. Sci.* 22, 6374. doi:10.3390/ijms22126374

Palmini, G., Marini, F., and Brandi, M. L. (2017). What Is New in the miRNA World Regarding Osteosarcoma and Chondrosarcoma? *Molecules* 22, 417. doi:10.3390/molecules22030417

Pan, Z., Wu, C., Li, Y., Li, H., An, Y., Wang, G., et al. (2020). LncRNA DANCR Silence Inhibits SOX5-Medicated Progression and Autophagy in Osteosarcoma via Regulating miR-216a-5p. *Biomed. Pharmacother.* 122, 109707. doi:10.1016/j.biopha.2019.109707

Pu, F.-F., Shi, D.-Y., Chen, T., Liu, Y.-X., Zhong, B.-L., Zhang, Z.-C., et al. (2021). SP1-induced Long Non-coding RNA SNHG6 Facilitates the Carcinogenesis of Chondrosarcoma through Inhibiting KLF6 by Recruiting EZH2. *Cel Death Dis* 12, 59. doi:10.1038/s41419-020-03352-6

Pu, F., Chen, F., and Shao, Z. (2016). MicroRNAs as Biomarkers in the Diagnosis and Treatment of Chondrosarcoma. *Tumour Biol.* doi:10.1007/s13277-016-5468-1

Qu, F., Li, C.-B., Yuan, B.-T., Qi, W., Li, H.-L., Shen, X.-Z., et al. (2016). MicroRNA-26a Induces Osteosarcoma Cell Growth and Metastasis via the Wnt/β-Catenin Pathway. *Oncol. Lett.* 11, 1592–1596. doi:10.3892/ol.2015.4073

Rengganaten, V., Huang, C. J., Tsai, P. H., Wang, M. L., Yang, Y. P., Lan, Y. T., et al. (2020). Mapping a Circular RNA-microRNA-mRNA-Signaling Regulatory Axis that Modulates Stemness Properties of Cancer Stem Cell Populations in Colorectal Cancer Spheroid Cells. *Int. J. Mol. Sci.* 21, 7864. doi:10.3390/ijms21217864

Schiavone, K., Garnier, D., Heymann, M.-F., and Heymann, D. (2019). The Heterogeneity of Osteosarcoma: The Role Played by Cancer Stem Cells. *Adv. Exp. Med. Biol.* 1139, 187–200. doi:10.1007/978-3-030-14366-4_11

Sha, S., Yuan, D., Liu, Y., Han, B., and Zhong, N. (2017). Targeting Long Non-coding RNA DANCR Inhibits Triple Negative Breast Cancer Progression. *Biol. Open* 6, 1310–1316. doi:10.1242/bio.023135

Shi, P., Li, Y., and Guo, Q. (2021a). Circular RNA circPIP5K1A Contributes to Cancer Stemness of Osteosarcoma by miR-515-5p/YAP axis. *J. Transl Med.* 19, 464. doi:10.1186/s12967-021-03124-6

Shi, Z., Wang, K., Xing, Y., and Yang, X. (2021b). CircNRIP1 Encapsulated by Bone Marrow Mesenchymal Stem Cell-Derived Extracellular Vesicles Aggravates Osteosarcoma by Modulating the miR-532-3p/AKT3/PI3K/AKT Axis. *Front. Oncol.* 11, 658139. doi:10.3389/fonc.2021.658139

Shui, X., Zhou, C., Lin, W., Yu, Y., Feng, Y., and Kong, J. (2017). Long Non-coding RNA BCAR4 Promotes Chondrosarcoma Cell Proliferation and Migration through Activation of mTOR Signaling Pathway. *Exp. Biol. Med. (Maywood)* 242, 1044–1050. doi:10.1177/1535370217700735

Siegel, R. L., Miller, K. D., Fuchs, H. E., and Jemal, A. (2021). Cancer Statistics, 2021. *CA A. Cancer J. Clin.* 71, 7–33. doi:10.3322/caac.21654

Slaby, O. (2016). Non-coding RNAs as Biomarkers for Colorectal Cancer Screening and Early Detection. *Adv. Exp. Med. Biol.* 937, 153–170. doi:10.1007/978-3-319-42059-2_8

Slack, F. J., and Chinnaiyan, A. M. (2019). The Role of Non-coding RNAs in Oncology. *Cell* 179, 1033–1055. doi:10.1016/j.cell.2019.10.017

Song, H., Xu, Y., Shi, L., Xu, T., Fan, R., Cao, M., et al. (2018). LncRNA THOR Increases the Stemness of Gastric Cancer Cells via Enhancing SOX9 mRNA Stability. *Biomed. Pharmacother.* 108, 338–346. doi:10.1016/j.biopha.2018.09.057

Song, Q.-C., Shi, Z.-B., Zhang, Y.-T., Ji, L., Wang, K.-Z., Duan, D.-P., et al. (2014). Downregulation of microRNA-26a Is Associated with Metastatic Potential and the Poor Prognosis of Osteosarcoma Patients. *Oncol. Rep.* 31, 1263–1270. doi:10.3892/or.2014.2989

Sui, Y., Han, Y., Zhao, X., Li, D., and Li, G. (2018). Long Non-coding RNA GClnc1 Promotes Tumorigenesis in Osteosarcoma by Inhibiting P53 Signaling. *Biochem. Biophysical Res. Commun.* 507, 36–42. doi:10.1016/j.bbrc.2018.10.135

Sun, J., Wang, X., Fu, C., Wang, X., Zou, J., Hua, H., et al. (2016). Long Noncoding RNA FGFR3-AS1 Promotes Osteosarcoma Growth through Regulating its Natural Antisense Transcript FGFR3. *Mol. Biol. Rep.* 43, 427–436. doi:10.1007/s11033-016-3975-1

Sun, X., Dai, G., Yu, L., Hu, Q., Chen, J., and Guo, W. (2018). miR-143-3p Inhibits the Proliferation, Migration and Invasion in Osteosarcoma by Targeting FOSL2. *Sci. Rep.* 8, 606. doi:10.1038/s41598-017-18739-3

Sung, H., Ferlay, J., Siegel, R. L., Laversanne, M., Soerjomataram, I., Jemal, A., et al. (2021). Global Cancer Statistics 2020: GLOBOCAN Estimates of Incidence and Mortality Worldwide for 36 Cancers in 185 Countries. *CA A. Cancer J. Clin.* 71, 209–249. doi:10.3322/caac.21660

Tan, X., Fan, S., Wu, W., and Zhang, Y. (2015). MicroRNA-26a Inhibits Osteosarcoma Cell Proliferation by Targeting IGF-1. *Bone Res.* 3, 15033. doi:10.1038/boneres.2015.33

Tang, Y., and Ji, F. (2019). lncRNA HOTTIP Facilitates Osteosarcoma Cell Migration, Invasion and Epithelial-Mesenchymal Transition by Forming a Positive Feedback Loop with C-Myc. *Oncol. Lett.* 18, 1649–1656. doi:10.3892/ol.2019.10463

Vares, G., Ahire, V., Sunada, S., Ho Kim, E., Sai, S., Chevalier, F., et al. (2020). A Multimodal Treatment of Carbon Ions Irradiation, miRNA-34 and mTOR Inhibitor Specifically Control High-Grade Chondrosarcoma Cancer Stem Cells. *Radiother. Oncol.* 150, 253–261. doi:10.1016/j.radonc.2020.07.034

Wang, B., Ye, Q., and Zou, C. (2020a). Long Non-coding RNA THOR Enhances the Stem Cell-like Traits of Triple-Negative Breast Cancer Cells through Activating β-Catenin Signaling. *Med. Sci. Monit.* 26, e923507. doi:10.12659/MSM.923507

Wang, L., Wang, P., Su, X., and Zhao, B. (2020b). Circ_0001658 Promotes the Proliferation and Metastasis of Osteosarcoma Cells via Regulating miR-382-5p/YB-1 axis. *Cell Biochem Funct* 38, 77–86. doi:10.1002/cbf.3452

Wang, T., Wang, D., Zhang, L., Yang, P., Wang, J., Liu, Q., et al. (2019). The TGFβ-miR-499a-SHKBP1 Pathway Induces Resistance to EGFR Inhibitors in Osteosarcoma Cancer Stem Cell-like Cells. *J. Exp. Clin. Cancer Res.* 38, 226. doi:10.1186/s13046-019-1195-y

Wang, Y., Wang, N., Zeng, X., Sun, J., Wang, G., Xu, H., et al. (2017a). MicroRNA-335 and its Target Rock1 Synergistically Influence Tumor Progression and Prognosis in Osteosarcoma. *Oncol. Lett.* 13, 3057–3065. doi:10.3892/ol.2017.5818

Wang, Y., Yang, T., Zhang, Z., Lu, M., Zhao, W., Zeng, X., et al. (2017b). Long Non-coding RNA TUG1 Promotes Migration and Invasion by Acting as a ceRNA of miR-335-5p in Osteosarcoma Cells. *Cancer Sci.* 108, 859–867. doi:10.1111/cas.13201

Wang, Y., Yao, J., Meng, H., Yu, Z., Wang, Z., Yuan, X., et al. (2015). A Novel Long Non-coding RNA, Hypoxia-Inducible Factor-2α Promoter Upstream Transcript, Functions as an Inhibitor of Osteosarcoma Stem Cells *In Vitro*. *Mol. Med. Rep.* 11, 2534–2540. doi:10.3892/mmr.2014.3024

Wang, Y., Zeng, X., Wang, N., Zhao, W., Zhang, X., Teng, S., et al. (2018). Long Noncoding RNA DANCR, Working as a Competitive Endogenous RNA, Promotes ROCK1-Mediated Proliferation and Metastasis via Decoying of miR-335-5p and miR-1972 in Osteosarcoma. *Mol. Cancer* 17, 89. doi:10.1186/s12943-018-0837-6

Wang, Y., Zhang, Y., Yang, T., Zhao, W., Wang, N., Li, P., et al. (2017c). Long Non-coding RNA MALAT1 for Promoting Metastasis and Proliferation by Acting as a ceRNA of miR-144-3p in Osteosarcoma Cells. *Oncotarget* 8, 59417–59434. doi:10.18632/oncotarget.19727

Wang, Y., Zhao, W., and Fu, Q. (2013). miR-335 Suppresses Migration and Invasion by Targeting ROCK1 in Osteosarcoma Cells. *Mol. Cel Biochem* 384, 105–111. doi:10.1007/s11010-013-1786-4

Wang, Z., Tan, M., Chen, G., Li, Z., and Lu, X. (2017d). LncRNA SOX2-OT Is a Novel Prognostic Biomarker for Osteosarcoma Patients and Regulates Osteosarcoma Cells Proliferation and Motility through Modulating SOX2. *IUBMB Life* 69, 867–876. doi:10.1002/iub.1681

Wei, Q. F., Yao, J. S., and Yang, Y. T. (2019). MicroRNA-1247 Inhibits the Viability and Metastasis of Osteosarcoma Cells via Targeting NRP1 and Mediating Wnt/β-Catenin Pathway. *Eur. Rev. Med. Pharmacol. Sci.* 23, 7266–7274. doi:10.26355/eurrev_201909_18831

Wu, D.-M., Zheng, Z.-H., Zhang, Y.-B., Fan, S.-H., Zhang, Z.-F., Wang, Y.-J., et al. (2019a). Down-regulated lncRNA DLX6-AS1 Inhibits Tumorigenesis through STAT3 Signaling Pathway by Suppressing CADM1 Promoter Methylation in Liver Cancer Stem Cells. *J. Exp. Clin. Cancer Res.* 38, 237. doi:10.1186/s13046-019-1239-3

Wu, H., He, Y., Chen, H., Liu, Y., Wei, B., Chen, G., et al. (2019b). Lnc RNA THOR Increases Osteosarcoma Cell Stemness and Migration by Enhancing SOX 9 mRNA Stability. *FEBS Open Bio* 9, 781–790. doi:10.1002/2211-5463.12620

Xie, Y., Deng, H., Wei, R., Sun, W., Qi, Y., Yao, S., et al. (2019). Overexpression of miR-335 Inhibits the Migration and Invasion of Osteosarcoma by Targeting SNIP1. *Int. J. Biol. Macromolecules* 133, 137–147. doi:10.1016/j.ijbiomac.2019.04.016

Xu, M., Jin, H., Xu, C.-X., Sun, B., Mao, Z., Bi, W.-Z., et al. (2014). miR-382 Inhibits Tumor Growth and Enhance Chemosensitivity in Osteosarcoma. *Oncotarget* 5, 9472–9483. doi:10.18632/oncotarget.2418

Xu, M., Jin, H., Xu, C.-X., Sun, B., Song, Z.-G., Bi, W.-Z., et al. (2015). miR-382 Inhibits Osteosarcoma Metastasis and Relapse by Targeting Y Box-Binding Protein 1. *Mol. Ther.* 23, 89–98. doi:10.1038/mt.2014.197

Xu, W., Li, Z., Zhu, X., Xu, R., and Xu, Y. (2018). miR-29 Family Inhibits Resistance to Methotrexate and Promotes Cell Apoptosis by Targeting COL3A1 and MCL1 in Osteosarcoma. *Med. Sci. Monit.* 24, 8812–8821. doi:10.12659/msm.911972

Yan, G.-N., Lv, Y.-F., and Guo, Q.-N. (2016). Advances in Osteosarcoma Stem Cell Research and Opportunities for Novel Therapeutic Targets. *Cancer Lett.* 370, 268–274. doi:10.1016/j.canlet.2015.11.003

Yan, J.-P., and Xiang, R.-M. (2021). Effect Assessment of Methotrexate in Combination with Other Chemotherapeutic Agents for Osteosarcoma in Children. *Medicine (Baltimore)* 100, e25534. doi:10.1097/md.0000000000025534

Yang, G., Wu, Y., Wan, R., Sang, H., Liu, H., and Huang, W. (2021). The Role of Non-coding RNAs in the R-egulation, D-iagnosis, P-rognosis and T-reatment of O-steosarcoma (Review). *Int. J. Oncol.* 59, 69. doi:10.3892/ijo.2021.5249

Yang, L., Li, H., and Huang, A. (2020). MiR-429 and MiR-143-3p Function as Diagnostic and Prognostic Markers for Osteosarcoma. *Clin. Lab.* 66. doi:10.7754/Clin.Lab.2020.191237

Yao, J., Geng, P., Li, Y., Chen, H., Li, J., and Zhu, Y. (2015). Knockdown of a HIF-2α Promoter Upstream Long Noncoding RNA Impairs Colorectal Cancer Stem Cell Properties *In Vitro* through HIF-2α Downregulation. *Ott* 8, 3467–3474. doi:10.2147/ott.s81393

Yao, X.-Y., Liu, J.-F., Luo, Y., Xu, X.-Z., and Bu, J. (2021). LncRNA HOTTIP Facilitates Cell Proliferation, Invasion, and Migration in Osteosarcoma by Interaction with PTBP1 to Promote KHSRP Level. *Cell Cycle* 20, 283–297. doi:10.1080/15384101.2020.1870820

Ye, F., Tian, L., Zhou, Q., and Feng, D. (2019). LncRNA FER1L4 Induces Apoptosis and Suppresses EMT and the Activation of PI3K/AKT Pathway in Osteosarcoma Cells via Inhibiting miR-18a-5p to Promote SOCS5. *Gene* 721, 144093. doi:10.1016/j.gene.2019.144093

Yu, J. E., Ju, J. A., Musacchio, N., Mathias, T. J., and Vitolo, M. I. (2020). Long Noncoding RNA DANCR Activates Wnt/β-Catenin Signaling through MiR-216a Inhibition in Non-small Cell Lung Cancer. *Biomolecules* 10, 1646. doi:10.3390/biom10121646

Yu, Y., Wang, L., Li, Z., Zheng, Y., Shi, Z., and Wang, G. (2021). Long Noncoding RNA CRNDE Functions as a Diagnostic and Prognostic Biomarker in Osteosarcoma, as Well as Promotes its Progression via Inhibition of miR-335-3p. *J. Biochem. Mol. Toxicol.* 35, e22734. doi:10.1002/jbt.22734

Yuan, S.-x., Wang, J., Yang, F., Tao, Q.-f., Zhang, J., Wang, L.-l., et al. (2016). Long Noncoding RNADANCRincreases Stemness Features of Hepatocellular Carcinoma by Derepression ofCTNNB1. *Hepatology* 63, 499–511. doi:10.1002/hep.27893

Zhang, K., Zhang, C., Liu, L., and Zhou, J. (2014). A Key Role of microRNA-29b in Suppression of Osteosarcoma Cell Proliferation and Migration via Modulation of VEGF. *Int. J. Clin. Exp. Pathol.* 7, 5701–5708.

Zhang, P.-r., Ren, J., Wan, J.-s., Sun, R., and Li, Y. (2020a). Circular RNA Hsa_circ_0002052 Promotes Osteosarcoma via Modulating miR-382/STX6 axis. *Hum. Cel* 33, 810–818. doi:10.1007/s13577-020-00335-9

Zhang, P., Li, J., Song, Y., and Wang, X. (2017). MiR-129-5p Inhibits Proliferation and Invasion of Chondrosarcoma Cells by Regulating

SOX4/Wnt/β-Catenin Signaling Pathway. *Cel Physiol Biochem* 42, 242–253. doi:10.1159/000477323

Zhang, W., Li, J. Z., Tai, Q. Y., Tang, J. J., Huang, Y. H., and Gao, S. B. (2020b). LncRNA DANCR Regulates Osteosarcoma Migration and Invasion by Targeting miR-149/MSI2 axis. *Eur. Rev. Med. Pharmacol. Sci.* 24, 6551–6560. doi:10.26355/eurrev_202006_21639

Zhang, Y., Pan, Y., Xie, C., and Zhang, Y. (2018). miR-34a Exerts as a Key Regulator in the Dedifferentiation of Osteosarcoma via PAI-1-Sox2 axis. *Cel Death Dis* 9, 777. doi:10.1038/s41419-018-0778-4

Zhang, Z., Wu, X., Han, Q., and Huang, Z. (2021). Downregulation of Long Non-coding RNA UCA1 Represses Tumorigenesis and Metastasis of Osteosarcoma via miR-513b-5p/E2F5 axis. *Anticancer Drugs* 32, 602–613. doi:10.1097/cad.0000000000001034

Zhao, B., Liu, K., and Cai, L. (2019a). LINK-A lncRNA Functions in the Metastasis of Osteosarcoma by Upregulating HIF1α. *Oncol. Lett.* 17, 5005–5011. doi:10.3892/ol.2019.10177

Zhao, D., Wang, S., Chu, X., and Han, D. (2019b). LncRNA HIF2PUT Inhibited Osteosarcoma Stem Cells Proliferation, Migration and Invasion by Regulating HIF2 Expression. *Artif. Cell Nanomedicine, Biotechnol.* 47, 1342–1348. doi:10.1080/21691401.2019.1596934

Zhao, F., Lv, J., Gan, H., Li, Y., Wang, R., Zhang, H., et al. (2015). MiRNA Profile of Osteosarcoma with CD117 and Stro-1 Expression: miR-1247 Functions as an Onco-miRNA by Targeting MAP3K9. *Int. J. Clin. Exp. Pathol.* 8, 1451–1458.

Zhou, J., Wu, S., Chen, Y., Zhao, J., Zhang, K., Wang, J., et al. (2015). microRNA-143 Is Associated with the Survival of ALDH1+CD133+ Osteosarcoma Cells and the Chemoresistance of Osteosarcoma. *Exp. Biol. Med. (Maywood)* 240, 867–875. doi:10.1177/1535370214563893

Zhu, K., Liu, L., Zhang, J., Wang, Y., Liang, H., Fan, G., et al. (2016). MiR-29b Suppresses the Proliferation and Migration of Osteosarcoma Cells by Targeting CDK6. *Protein Cell* 7, 434–444. doi:10.1007/s13238-016-0277-2

Zini, R., Rossi, C., Norfo, R., Pennucci, V., Barbieri, G., Ruberti, S., et al. (2016). miR-382-5p Controls Hematopoietic Stem Cell Differentiation through the Downregulation of MXD1. *Stem Cell Development* 25, 1433–1443. doi:10.1089/scd.2016.0150

Zou, Y., Huang, Y., Yang, J., Wu, J., and Luo, C. (2017). miR-34a Is Downregulated in Human Osteosarcoma Stem-like Cells and Promotes Invasion, Tumorigenic Ability and Self-Renewal Capacity. *Mol. Med. Rep.* 15, 1631–1637. doi:10.3892/mmr.2017.6187

Conflict of Interest: The authors declare that the research was conducted in the absence of any commercial or financial relationships that could be construed as a potential conflict of interest.

Publisher's Note: All claims expressed in this article are solely those of the authors and do not necessarily represent those of their affiliated organizations, or those of the publisher, the editors and the reviewers. Any product that may be evaluated in this article, or claim that may be made by its manufacturer, is not guaranteed or endorsed by the publisher.

Advantages of publishing in Frontiers

OPEN ACCESS
Articles are free to read for greatest visibility and readership

FAST PUBLICATION
Around 90 days from submission to decision

HIGH QUALITY PEER-REVIEW
Rigorous, collaborative, and constructive peer-review

TRANSPARENT PEER-REVIEW
Editors and reviewers acknowledged by name on published articles

Frontiers
Avenue du Tribunal-Fédéral 34
1005 Lausanne | Switzerland

Visit us: www.frontiersin.org
Contact us: frontiersin.org/about/contact

REPRODUCIBILITY OF RESEARCH
Support open data and methods to enhance research reproducibility

DIGITAL PUBLISHING
Articles designed for optimal readership across devices

FOLLOW US
@frontiersin

IMPACT METRICS
Advanced article metrics track visibility across digital media

EXTENSIVE PROMOTION
Marketing and promotion of impactful research

LOOP RESEARCH NETWORK
Our network increases your article's readership